Physical layer limitations on 4G MIMO handset Systems

Szini, Istvan Janos

Publication date:
2014

Document Version
Early version, also known as pre-print

Physical layer limitations on 4G MIMO handset Systems

Ph.D. Thesis

Istvan Szini

Aalborg University
Faculty of Engineering and Science
Department of Electronic Systems
DK-9220 Aalborg

Physical layer limitations on 4G MIMO handset systems
Ph.D. Thesis

ISBN: 978-87-7152-034-7
March 2014

Academic advisor:
Prof. Gert Frølund Pedersen
Head of APNet Section at the Department of Electronic Systems, Aalborg University,
DK-9220 Aalborg.

Para Luciana

CONTENTS

ACKNOWLEDGMENTS

I would like to start acknowledging my advisor Prof. Gert Frølund Pedersen for allowing me to join his selected group of PhD students. Despite the distance, I always felt welcome and part of the team when visiting Aalborg or working remotely.

Jesper Ødum Nielsen and Boyan Yanakiev for their support scrutinizing and reviewing my work, always pointing me to the right direction. My fellow students Alexandru Tatomirescu and Samatha Del Barrio for kindly presenting my work in conferences that I couldn't attend.

Karl Chin, Michael Frenzer and Eric Krenz, Motorola Mobility management that always support my journey through higher education financially sponsoring my course, and allowing me to use the available hardware and software resources during off business hours.

And for last but not least my wife Luciana, the love of my life who always believes and supports my dreams.

This work was supported and cleared for publication by Motorola Mobility LLC.

ABSTRACT

Abstract in English (Danish version following)

The new technologies adopted for high data rate mobile devices communications; i.e. Long Term Evolution (LTE) and LTE-advanced, relies on Multiple-Input-Multiple-Output (MIMO) radio channel to increase capacity. MIMO physical layer has been rigorously investigated and it is a reality today in fourth generation (4G) of mobile devices. The deployment of commercially capable MIMO devices is largely motivated by the increased demand for smart-phones replacing feature phones. In spite of the large demand and consequently deployment of these devices, the certification process didn't follow the industry needs, nowadays many cell-phone operators still defines MIMO compliance tests based on antenna figure of merit measured under uniform incoming power, and total isotropic sensitivity thus without the implementation of realistic spatial/temporal channel models.

This thesis is based on work done in multiple MIMO OTA standard and research groups (CTIA MOSG, 3GPP RAN4 and COST IC1004 TWGO), supporting the definition of the upcoming MIMO over the air conformance test that meet the industry needs, presenting test methodologies that emulate channel environments with realistic spatial and temporal characteristics, as well as demonstrating that the behavior of different MIMO antenna systems under spatial channel models can't be predicted while adopting isotropic channel models, neither can evaluate MIMO antenna design innovation.

This work is formed by a collection of papers addressing relevant topics in MIMO OTA, from the creation of MIMO antenna systems to aid certification activities, definition of frameworks to validate the current MIMO OTA test methodologies to the design of MIMO novel antenna system and test methodology. With track record of contribution to the MIMO OTA standardization process, this work provide an update view on the remaining challenges on MIMO OTA certification process and upcoming challenges designing MIMO adaptive antenna systems.

På Dansk

De nye teknologier, som er indført til kommunikation med mobile enheder med høj datahastighed, dvs. Long Term Evolution (LTE), og LTE - Advanced, er afhængige af Multiple- Input- Multiple- Output (MIMO) radiokanalen for at kunne øge kapaciteten. Det fysiske lag af MIMO kanalen er blevet grundigt undersøgt, og er i dag en realitet i fjerde generation (4G) mobile enheder. Udrulingen på markedet med kompetente MIMO enheder er i vid udstrækning motiveret af den øgede efterspørgsel efter smartphones, som erstatter feature-telefoner. På trods af den store efterspørgsel og dermed udbredelsen af disse enheder, så har certificeringsprocessen ikke fulgt industriens behov. Selv i dag definerer mange mobiloperatører stadig MIMO ud fra overensstemmelsestests baseret på antenne-ydelse målt under vinkelmssigt konstant indkommende effekt og den såkaldte totale isotrope følsomhed, og dermed uden realistiske rumlige / temporale kanalmodeller.
Denne afhandling er baseret på arbejde udført i flere MIMO OTA standardiserings- og forskergrupper (CTIA MOSG, 3GPP RAN4 og COST IC1004 TWGO), som støtter definitionen af den kommende OTA MIMO overensstemmelsestest, som opfylder industriens behov og som præsenterer testmetodikker, der emulerer kanalmiljøer med realistiske rumlige og tidsmæssige karakteristika, samt påviser at man ikke kan forudsige forskellige MIMO antennesystemers ydelser ved brug af isotrope kanalmodeller; ej heller kan man evaluere MIMO antennedesign innovation.
Denne afhandling er udarbejdet på baggrund af en samling af artikler, som omhandler relevante emner indenfor MIMO OTA, fra skabelsen af MIMO antennesystemer, som hjælper certificeringsaktiviteter, definition af rammer til at validere nuværende MIMO OTA testmetoder til design af nye MIMO antennesystemer og testmetoder. Med en referenceliste over bidrag til standardiseringsprocessen for MIMO OTA, giver dette arbejde en opdatering på de tilbageværende udfordringer, som vi har omkring MIMO OTA certificeringsprocessen og de kommende udfordringer vi står overfor, når vi skal designe MIMO tilpasningsdygtige antennesystemer.

THESIS DETAILS

Thesis title: Physical layer limitations on 4G MIMO handset Systems
Name of the PhD student: Istvan Janos Szini
Supervisor: Prof. Gert Frølund Pedersen

List of published papers:

[1] Szini, I.; Pedersen, G.F.; Scannavini, A.; Foged, L.J., "MIMO 2X2 Reference Antennas Concept," *Antennas and Propagation (EUCAP), 2012 6th European Conference on*, vol., no., pp.1540,1543, 26-30 March 2012

[2] Szini, I.; Pedersen, G. F.; Estrada, J.; Scannavini, A.; Foged, L.J., "Design and Verification of MIMO 2x2 Reference Antennas," *Antennas and Propagation Society International Symposium (APSURSI), 2012 IEEE*, vol., no., pp.1,2, 8-14 July 2012.

[3] Szini, I.; Pedersen, G. F.; Del Barrio, S.C.; Foegelle, M.D., "LTE Radiated Data Throughput Measurements Adopting, MIMO 2x2 Reference Antennas," *Vehicular Technology Conference (VTC Fall), 2012 IEEE*, vol., no., pp.1,5, 3-6 Sept. 2012.

[4] Szini, I.; Pedersen, G.; Tatomirescu, A.; Ioffe, A., "MIMO 22 absolute data throughput concept," *Antennas and Propagation (EuCAP), 2013 7th European Conference on*, vol., no., pp.299,302, 8-12 April 2013.

[5] Szini, I.; Yanakiev, B.; Pedersen, G. F., "MIMO Reference Antennas Performance in Anisotropic Channel Environments," *IEEE Transaction on Antenna and Propagation*, accepted May 2013.

[6] Szini, I.;Foegelle, M.D.; Reed, D.; Brown, T.; Pedersen, G. F. , "On antenna polarization discrimination, validating MIMO OTA test methodologies," *IEEE Antennas and Wireless Propagation Letters, February 2014*, vol., no., pp.265,268, 4 Feb. 2014.

[7] Szini, I.; Tatomirescu, A.; Pedersen, G., "On Small Terminal MIMO Antennas, harmonizing Characteristic Modes with Ground Plane Geometry," *IEEE Transaction on Antenna and Propagation*, accepted December 2013.

[8] Fan, W.; Szini, I.; Nielsen, J.; Pedersen, G., "Channel Spatial Correlation Reconstruction in Flexible Multi-Probe Setups," *Antennas and Wireless Propagation Letters, IEEE*, vol., no., pp.1724,1727, 11 Jan. 2014.

[9] Fan, W.; Szini, I.; Foegelle, M.; Nielsen, J.; Pedersen, G., "Measurement Uncertainty Investigation in the Multi-probe OTA Setups," *8th European Conference on Antennas and Propagation (EuCAP)*, accepted April 2014.

[10] Szini, I.; Tatomirescu, A.; Yanakiev, B.; Ioffe, A.; Pedersen, G., " Beam-Steered Adaptive Antenna System For MIMO OTA Test Methodology Validation".*IEEE Transaction on Antenna and Propagation*, to be submitted in March 2014.

In addition to the accepted and published peer reviewed papers, 80 technical documents were submitted and presented in several MIMO OTA standard/research groups, i.e. 3GPP RAN4 MIMO OTA ad-hoc (39), CTIA MIMO OTA Sub-Group (MOSG, 21), COST 2100 (3) and COST IC1004 Topic Working Group OTA (TWGO, 17). The full content of these documents are not included in this thesis, as they are complementary to the main focus of this work.

Over the course of this research the following paper [11] and patent disclosures [7' and 8'] were also submitted. These paper and patent disclosures were submitted in IEEE APS 2014 and United States Patent and Trademark Office (www.uspto.gov) respectively.

[11] Szini, I.; Tatomirescu, A.; Pedersen, G., "On small terminal MIMO Antenna Correlation Optimization Adopting Characteristic Mode Theory," *Antennas and Propagation Society International Symposium (APSURSI), 2014 IEEE*, accepted March 2014.

[7'] Szini, I.; Krenz, E., "Method and Apparatus for an Adaptive Multi-Antenna System," *United States Patent and Trademark Office (USPTO)*, patent pending, submitted December 2012.

[8'] Szini, I.; Peters, J.; Krenz, E., "Method and Apparatus for Wireless Device Performance Testing," *United States Patent and Trademark Office (USPTO)*, patent pending, submitted November2013.

This thesis has been submitted for assessment in partial fulfillment of the PhD degree. The thesis is based on the submitted or published scientific papers which are listed above. Parts of the papers are used directly or indirectly in the extended summary of the thesis. As part of the assessment, co-author statements have been made available to the assessment committee and are also available at the Faculty. The thesis is not in its present form acceptable for open publication but only in limited and closed circulation as copyright may not be ensured.

CHAPTER 1

INTRODUCTION

Mobiles devices; more specifically smartphones and tablets; became a multi-function household device capable of consolidate several functions in a single device. More than a trend, in a society which relies everyday more in cloud computing and virtual financial transactions, personal computing is a necessity. Nowadays smartphones equipped with with multi-core processors have far more processing power than laptops, notebooks or even desktops of few years ago. For an user that need personal computing for basic functions the computing power of some high tier smartphones surpasses their more advance requests. The question about the possibility of mobile devices replacing laptops or desktops in most of the households is debatable, while lack of battery life and limitation of graphic user interface accessibility might refrain the sole use of hand held devices as unique personal computing. Advances in High Definition wireless audio-visual interfaces, voice and body/gesture recognition are filling this gap, allowing small handsets to be seamless part of larger audio-visual systems, integrating all personal computing and entertainment needs in a single device.

Understandably the utilization of personal mobile devices had grown exponentially in all social classes around the world. In addition to popular demand, equipments and machines traditionally connected in network by wire, had been migrating to wireless connections due the reliability and security offered by wireless networks. In this scenario where wireless connectivity is ever expanding, spectral and bandwidth optimization have high priority addressing the high demand of the new generation of emerging wireless technologies, independently of the modulation or carrier aggregation scheme, the common characteristic of the new generation of wireless technologies is the adoption of MIMO antenna systems. MIMO antenna systems isn't a new topic, however in this thesis is investigated with a perspective of state of the art test methodology and dedicated reference antenna systems uniquely designed for this purpose. Part of the research present in this thesis was instrumental to MIMO OTA research and standard groups in CTIA [1], 3GPP [2]and COST IC1004 [3], towards the better understanding of MIMO antenna systems and its iterations with next generation of mobile devices.

1.1 Structure of the Thesis

This thesis is structured in three main parts. Section 2 introduces the theoretical background and nomenclature adopted in this work, section 3 defines the motivation for this work and how the collection of papers are related and part of a long term plan to support technical correctness in the MIMO OTA industry. Lastly section 4 is formed by a collection of papers and patents generated during this research.

Most of this work is based on state of the art MIMO OTA measurements and handset antenna topologies. Test methodologies are still under investigation as well as its respective limitations and trade-offs. Section 5 brings a preliminary conclusion based on the work done so far, and indicated the research direction following up this work.

CHAPTER 2

THEORETICAL BACKGROUND

In this chapter the most relevant MIMO OTA figure of merit (FoM) are defined in details as well as its interdependence towards the optimization of the MIMO 2x2 capacity Eq. (2.2), in this context several aspects of the antenna system design need to be considered, as summarized below:

- Both antennas, Main Antenna and Secondary Antenna, need to have minimum branch power ratio, ideally BPR = 0 dB, i.e. perfect channel state information (CSI);
- In a rich scattered environment the maximum capacity will occur when both receiver antennas are uncorrelated, i.e. perfect CSI;
- The absolute phase responses of the reference antennas are irrelevant, but not the phase per direction or the relative phase relationship between the antennas, both of which define the antenna system correlation coefficient;
- Considering the special case of the isotropic environment and perfect CSI, the ideal MIMO 2x2 antenna system, with ideal isolation between antennas S_{21} <-20 dB, high efficiency $\eta > 90\ \%$, low gain imbalance (BPR$\approx$ 0 dB), and correlation coefficient ($\rho \approx 0$), should provide double the capacity of a SISO Eq. (2.1) system (this statement is based solely on antenna parameters and assumes ideal propagation);
- The antenna's radiation patterns need to have similar directivity. Two directional antennas with the main lobe in opposite directions, will not enable acceptable MIMO performance in an environment with few signal propagating reflections. There is no isotropy in the real world, real environments are defined by spatial channel models.

$$C = log\ (1 + \rho \|H|^2), where |H|^2 = 1 \tag{2.1}$$

$$C = 2log\ (1 + \rho) \tag{2.2}$$

2.1 MIMO Antenna Figure Of Merit

Correlation Coefficient

The Magnitude of the complex correlation coefficient between two antennas is shown in [4]. As demonstrated the correlation coefficient is predominantly defined by the difference in the antennas complex radiation patterns, antennas with identical complex radiation patterns will be correlated (ρ=1), while antennas with completely different complex radiation patterns will be uncorrelated (ρ=0). The Eq. (2.3) presented the generic scenario of uniform incoming power is uniformly distributed in both θ and ϕ directions.

$$\rho = \frac{\oint \left[XPR\, \vec{E}_{\theta X}(\Omega)\vec{E}^{*}_{\theta Y}(\Omega)p_{\theta}(\Omega) \; + \vec{E}_{\phi X}(\Omega)\vec{E}^{*}_{\phi Y}(\Omega)p_{\phi}(\Omega) \right] d\Omega}{\sqrt{\oint \left[XPR\, G_{\theta,1}(\Omega)p_{\theta}(\Omega) + G_{\phi,1}(\Omega)p_{\phi}(\Omega) \right] d\Omega \; \oint \left[XPR\, G_{\theta,2}(\Omega)p_{\theta}(\Omega) + G_{\phi,2}(\Omega)p_{\phi}(\Omega) \right] d\Omega}} \tag{2.3}$$

While $\vec{E}_{\theta X}(\Omega)$ is the vertical polarization complex radiation pattern from main antenna, $\vec{E}^{*}_{\theta Y}(\Omega)$ is the vertical polarization complex radiation pattern from secondary antenna. Respectively $\vec{E}_{\phi X}(\Omega)$ is the horizontal polarization complex radiation pattern from main antenna, and $\vec{E}^{*}_{\phi Y}(\Omega)$ is the horizontal polarization complex radiation pattern from the secondary antenna. G θ and G ϕ are the antennas respective vertical and horizontal polarizations gain, while Ω is the solid angle for a spherical coordinate system and XPR is the cross-polarization discrimination of the antennas.

Mean Effective Gain

The typical antenna parameters used here are the MEG from Eq. (2.4) [5], BPR from Eq. (2.6) and correlation coefficient from Eq. (2.3) [6],

$$MEG = \oint \left[\frac{XPR}{1+XPR} G_{\theta}(\Omega)p_{\theta}(\Omega) + \frac{1}{1+XPR} G_{\phi}(\Omega)p_{\phi}(\Omega) \right] d\Omega \tag{2.4}$$

$$BPR = 10\log_{10}\frac{MEG_1}{MEG_2} \tag{2.5}$$

Where Ω indicates variation over both θ and ϕ, $\oint p_{\theta/\phi}(\Omega)d\Omega = 1$ is the normalized power distribution for each polarization, XPR is the cross polarization ratio of the environment and $G_{\theta/\phi}(\Omega)$ and $\vec{E}_{\theta/\phi}(\Omega)$ are the gain and complex electric field patterns for each polarization, respectively. $*$ stands for complex conjugate and the indexes $X_{1/2}$ stands for the two antennas.

Branch Power Ratio

This is also sometimes called Gain Imbalance. The BPR is defined as the time averaged power received at branch number n, relative to the power received at branch number m:

$$BPR = 10\log_{10}\frac{MEG_1}{MEG_2} \tag{2.6}$$

Where n is not equal to m for any two branches. If they are equal the BPR is always 0dB. For a device under test (DUT) with two branches, there is only one combination (i.e. m=1 and n=2) so one single BPR. For four branches there are six combinations and thus six different BPRs.

2.2 Channel Models

The channel model is a spatial stochastic representation of each scattered signal; represented by a sinusoid; therefore to fully describe the channel impulse response, the sum of sinusoids between the departure Tx and arrival Rx are defined by angle of arrival/departure, magnitude, phase and delay. 3GPP [2] ad-hoc group released in September 2003 the initial channel model adopted for MIMO modeling; so called 3GPP Spatial Channel Model; at beginning of 2005 an extension of SCM was proposed by WINNER [7] under SCME name, late in the same year WINNER group proposed WINNER channel model phase I (WIM1), and subsequently phase 2 (WIM2).

As shown in Table 2.1 the channel models used in MIMO OTA are well defined and derived by extensive effort analyzing propagation survey measurements. 3GPP RAN1 had been adopting SCM channel models for link and system level simulations for several years, recently a newly formed 3D Channel Model Sub-Group is evaluating WINNER channel models for the same purpose. Based on fundamental research defining realistic channel models, and the work from 3GPP RAN1, the UE industry had been developing chipsets and LTE algorithms based on spatial channel models. The research presented in this thesis will be solely based on spatial channel models.

Table 2.1: Channel Models Basic Characteristics

Feature	SCM	SCME	WINNER I	WINNER II
Bandwidth > 100MHz	No	Yes	Yes	Yes
Indoor scenarios	No	No	Yes	Yes
Outdoor-to-indoor and indoor-to-outdoor scenarios	No	No	No	Yes
AoA/AoD elevation	No	No	Yes	Yes
Intra-cluster delay spread	No	Yes	No	Yes
TDL model based on the generic model	No	Yes	Yes*	Yes
Cross-correlation between LSPs	No	No	Yes	Yes
Time evolution of model parameters	No	Yes**	No	Yes
Parameter				
Max. bandwidth (MHz)	5	100***	100****	100****
Frequency range (GHz)	2	2~6	2~6	2~6
# of scenarios	3	3	7	12
# of clusters	6	6	4~24	4~20
# of mid-paths per cluster	1	3~4	1	1~3
# of sub-paths per cluster	20	20	10	20
# of taps	6	18~24	4~24	4~24
Base Station angle spread (°)	5~19	4.7~18.2	3~38	2.5~53.7
Mobile Station angle apread (°)	68	62.2~67.8	9.5~53	11.7~52.5
Delay spread (ns)	170~650	231~841	1.6~313	16~630
Shadow fading standard deviation (dB)	4~10	4~10	1.4~8	2~8

* TDL model is based on the same measurements as generic model, but analyzed separately
** Continuous time evolution
*** Artificial extension from 5MHz bandwidth
**** Based on 100MHz measurements

2.3 MIMO OTA test Methodologies

For most of the last four years MIMO OTA standards groups were still considering seven MIMO OTA test methodologies as shown in [8] clause 6:

- Anechoic Chamber Multi-Cluster;
- Anechoic Chamber Single-Cluster;
- Reverberation Chamber
- Reverberation Chamber plus Temporal Channel Emulation;
- Decomposition Method;
- Two Stage Method Conducted;
- Two Stage Method Radiated.

During the conclusion of the 3GPP RAN4 work item [8], a criterion to validate MIMO OTA test methodologies was created and four methodologies were considered valid and qualify to further investigation in the next working item, where those methods will attempt to be harmonized against a single data throughput threshold for a defined device type and test condition. The ultimate goal of the harmonization process will be to validate at least one test method for a given device type and test condition.

The summary of the validation criterion and mutual agreement regarding the capabilities of each accepted as valid MIMO OTA test methodology, were capture in the tables Table 2.2 and Table 2.3

The test methodology adopted in this work is based on Anechoic Chamber Multi-Cluster boundary array shown in Fig. 2.1. The implementation of the anechoic chamber boundary array adopted in this work, consists of eight active dual polarized (DP) antennas driven by two 8 output channel emulators (CE) for a total of 16 total output channels. These 16 antennas are used to generate the desired fields within the test volume, by applying power weighting and Rayleigh fading in the CEs. Two 8-channel power amplifiers were used to amplify the outputs of the CEs to produce the required signal levels within the test volume. The reported measurements are captured using a base-station emulator/communication tester. The two outputs of the tester were each split and fed into the two CEs. The antenna for uplink transmissions from the UE to the base-station emulators was a separate monopole. The uplink path was then fed through a pre-amplifier to provide additional downlink isolation prior to feeding the signal to the base-station emulator input.

2.4 Characteristic Mode Theory

The theory of characteristic modes or eigenfunctions of conducting bodies, introduced by Garbacz in 1968 [9] and improved by Harrington and Mautz [10], provides a set of orthogonal spherical field distributions in the far-field. These field modes, also known as characteristic fields, have the useful property that they are radiated from an orthogonal set of current distributions running along the surface of the conducting body of arbitrary shapes. These current distributions, the modal or characteristic currents, are real or equiphasal currents that diagonalize the generalized impedance matrix for the surface for which they were defined [11]. The generalized impedance matrix is defined as the operator $L(J)$ that maps a surface current distribution J to the tangential component of the incident electric field E^i using Eq. (2.7) .

$$[L(J) - E^i]_{tan} = 0 \tag{2.7}$$

Because $L(J)$ relates the electric field to the current distributions, it has the dimensions of impedance and can expressed as in Eq. (2.8) and Eq. (2.9) using a real and imaginary decomposition, as derived in [11].

$$Z(J) = [L(J)]_{tan} \tag{2.8}$$

$$Z(J) = R(J) + jX(J) \tag{2.9}$$

As defined in [10], the characteristic currents $\overrightarrow{J_n}$ are the eigenfunctions of the following eigenvalue problem applied to the impedance operator $Z(J)$:

$$X(\overrightarrow{J_n}) = \lambda_n R(\overrightarrow{J_n}) \tag{2.10}$$

A very useful aspect of the characteristic mode analysis for antenna design is the variation of the eigenvalue(λ_n) of a certain eigenfunction or vector (J_n) over frequency. By evaluating it, one can determine the resonance frequency and bandwidth of a mode using the modal significance (MS_n) [12], as defined in Eq. (2.11). It measures the quantity of the normalized amplitude of a mode that contributes to the radiation. A maximum value of 1 represents a 100% contribution to radiation by the current distribution of current mode.

$$MS_n = \left| \frac{1}{1 + \lambda_n} \right| \tag{2.11}$$

The electric fields E_n generated by the eigen current distributions $\overrightarrow{J_n}$ as defined in Eq. (2.12), generically named characteristic fields [11], are described in the following equation.

$$E_n(\overrightarrow{J_n}) = Z(\overrightarrow{J_n}) = R(\overrightarrow{J_n})(1 + j\lambda_n) \tag{2.12}$$

The fields radiated by eigen currents have the important property that they are orthogonal over the sphere at infinite. In other words, different modes will have orthogonal far-field radiation patterns which will lead to a zero correlation according to Eq. (2.3), ideal for the design of MIMO antennas. However when it comes to compact phones, in the low bands, the ground plane is the main radiator which has only one efficient mode.

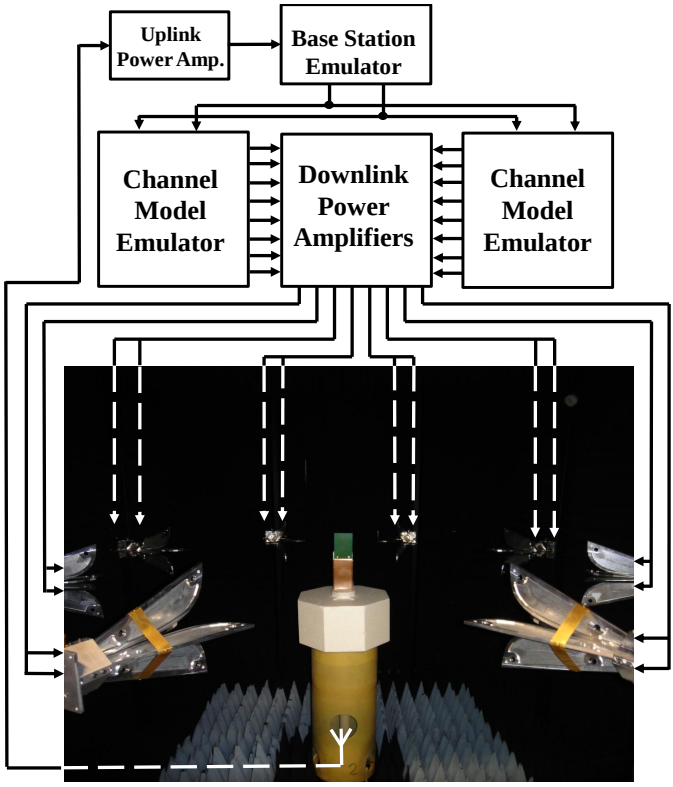

Figure 2.1: Anechoic Chamber Multi-Cluster boundary array at Motorola Mobility.

Table 2.2: Simplified methodology comparison, channel modeling aspects

Attribute	**Reverberation Chamber**		**Anechoic Chamber**	**Multi-stage methods**
	RC	**RC + CE**	**Multi probe**	**2 stage method rad.**
Channel Modelling aspects				
2D/3D dimension over which the signals simultaneously arrive at the DUT location	3D[1]	3D[1]	2D	2D[11]
Directional distribution of angles of arrival	Random	Random	Selected as defined by SCME channel model in Clause 8	Selected as defined by SCME channel model in Clause 8
Channel model with controllable spatial characteristics	no	no	Yes[2]	Yes[2]
Angular spread	Statistically isotropic	Statistically isotropic	Selected as defined by SCME channel model in Clause 8	Selected as defined by SCME channel model in Clause 8
Ability to control angular spread	no	no	Yes[2]	Yes[2]
Power delay profile	Exponential decay	Selected as defined by channel model in Annex C	Selected as defined by SCME channel model in Clause 8	Selected as defined by SCME channel model in Clause 8
Ability to control power delay profile	Partly controllable[2,3]	Yes[2]	Yes[2]	Yes[2]
UE speed	Approximately 1Km/h	30Km/h	30Km/h	30Km/h
Ability to control UE speed	No	Yes[2]	Yes[2]	Yes[2]
UE direction of travel	N/A	N/A	120º as specified in Clause 8	120º as specified in Clause 8
Ability to control direction of travel	N/A	N/A	Yes[2]	Yes[2]
Supported channel models	NIST	Short Delay Spread Long Deay Spread	SCME Uma SCME Umi	SCME Uma SCME Umi
BS antenna configuration	Uncorrelated	Selected as defined in Clause 8.5	Selected as defined in Clause 8.5	Selected as defined Clause 8.5
Ability to control BS antenna configuration	No	Yes[2]	Yes[2]	Yes[2]
XPR (defined in Clause 8.2)	N/A	N/A	9dB	9dB
V/H ratio	0dB on average	0dB on average	0.83 dB for SCME UMi 8.13 dB for SCME UMa	0.83 dB for SCME UMi 8.13 dB for SCME UMa
Ability to control XPR and V/H	No	No	Yes[2]	Yes[2]
MIMO OTA attributes not yet tested				
Ability to control noise and interference direction	Limited[4]	Limited[4]	Yes[2]	Yes[2]
DUT size constraints	Depends on chamber size[5] and stirrer size	Depends on chamber size[5] and stirrer size	Depends on chamber size[5], and number of active antenna probes and channel emulator ports to fit required active antenna probes	Depends on chamber size[5] (SISO chamber quiet zone)

Table 2.3: Simplified methodology comparison, other considerations

Attribute	Reverberation Chamber		Anechoic Chamber	Multi-stage methods
	RC	**RC + CE**	**Multi probe**	**2 stage method rad.**
Other Considerations				
Non-intrusive test mode for DUT antenna pattern measurement	Not required	Not required	Not required	Required
Ability to distinguish performance based on device orientation relative to the field	No	No	Yes	Yes
Major equipment elements for MIMO OTA test setup (all need MIMO BS emulator)	MIMO capable reverberation chamber	MIMO capable reverberation chamber and channel emulator	MIMO capable anechoic chamber to fit antenna probes and channel emulator	SISO anechoic chamber with additional antenna and channel emulator
Number of channel emulator ports[7]	N/A	4	16[6]	2
DUT antenna polarization discrimination[8]	No	No	Yes	Yes
DUT Antenna radiation pattern adaptation, performance discrimination	Feasibility study not yet performed	Feasibility study not yet performed	Yes[9]	Feasibility study not yet performed[10]
Number of independent measurements	1 after sufficient number of stirrers states to ensure isotropy[12]	1 after sufficient number of stirrers states to ensure isotropy[12]	12 device rotations for 2D evaluation	Measurement of radiation pattern in 1st stage and measurement in radiated stage for 12 rotations for 2D evaluation

Note 1: Random distribution of angles of arrival. Isotropy is achieved after sufficient amount of test time as per Annex C [12];
Note 2: Requires validation;
Note 3: PDP modification will require new loading of chamber;
Note 4: Feasibility study under progress;
Note 5: Chamber size depends on the size of the UE and the frequency of the test;
Note 6: Minimum setup configuration as per table 6.3.1.1-1 [12];
Note 7: Configuration reflects what has been tested. Optimization may be possible;
Note 8: Assuming that correlation, gain imbalance, total efficiency are equivalent among DUT, purely isolating antennas polarization;
Note 9: Based on preliminary feasibility study;
Note 10: It will require DUT feedback mechanism;
Note 11: 3D is possible without new test setup if 3D channel models are specified. It requires validation;
Note 12: Isotropy is achieved after sufficient amount of isotropic states as per Annex C [12]. The guideline for TRS, number of independent samples should be larger than 100, preferable 200 or 400 (3GPP TS 34.114).

CHAPTER 3

WORK MOTIVATION

The physical layer of MIMO communication systems is a subject with numerous ramifications, from the research on channel models that emulate somewhat diverse realistic conditions, mobile devices antennas systems which attempt to optimize radiated performance based on technical characteristic of those channel conditions, and test methodologies that accurately emulate the defined channel models and mobile devices radiated performance in controlled environment. This thesis is formed by a collection of work from a perspective of mobile devices antenna designers, whom from the beginning realize the opportunity for innovation on this field, and the possibility to contribute for the the MIMO over the air problem definition and clarification analyzing the whole problem from a broader perspective. From the contact with MIMO OTA community it was clear that any attempt for measurement campaign was destined to fail, besides the unknown discrepancies between adopted test methodologies, the methods measurement uncertainty was (and still is) undetermined, as long as the stability of the preliminary devices under test. Facing this scenario we propose a creation of the MIMO reference antennas (as shown in 4.1) which it was fully accepted by most active MIMO OTA standard and research groups (3GPP RAN4, CTIA and COST IC1004), the objective was to partially eliminate the unknowns surrounding the device under test antenna radiation characteristics, and fully emulate the iteration of the mobile device antenna systems channel model and base station antenna system.
As the MIMO OTA community progressed adopting the reference antennas in diverse labs and new measurement campaigns, it was evident that besides the channel model validation methods put in place, it was necessary a framework to verify or ”sanity check” that the all MIMO OTA test methodologies had well defined channel models, and if those channel models can be emulated in the OTA test environment, this was the motivation behind the creation of the ”Absolute Data Throughput Framework” as shown in 4.2.
With these mechanisms in place the MIMO OTA test method start to be more controllable and reliable, truly enabling the innovation in MIMO antenna design systems as demonstrated in 4.3. Today the challenges on MIMO OTA test methodologies are related to the harmonization of fundamentally different test methodologies towards the same certification threshold, in other words a deterministic value that indicates the OTA performance of mobile devices, a value that can be used by the industry to determine if an specific mobile device is acceptable or not to be place in the field. Contributing to this ongoing effort we produced the work shown in 4.5, showcasing fundamental differences among test methodologies, indicating realistic test conditions that where those test methodologies will generate different results, therefore posing a real problem to the acceptance of certain MIMO OTA test methodologies.

The work on this thesis was guided by the research for technical correctness in MIMO OTA, enabling antenna innovation under realistic emulation of the test environment. Some novel and relevant work towards this goal was generated and adopted by peers, paving a solid ground for continue research in this field.

3.1 The "Big Picture"

MIMO Over the Air test methodologies had been intensively discussed in several standard organizations such as CTIA [1] and 3GPP RAN4 [2] for the last four years. Since no agreement regarding the optimal test methodology was reached, the discussion in these organizations is still ongoing. In mid 2010 3GPP RAN4 through the MIMO OTA ad-hoc group initiated a measurement campaign adopting several HSPA devices and test methodologies, the devices under test at that time were USB dongles and data cards. An extensive round robin measurement campaign was initiated, including test labs in Europe, Asia and USA. The results of this measurement campaign wasn't encouraging, same devices measured in different labs with different test methodologies presented results far apart beyond and reasonable test methodology measurement uncertainty.
Several aspects of this initial measurement campaign contribute for its failure:

- The behavior of the LTE 2x2 Base Station emulators was inconsistent, since different equipment from different vendors had different conducted and radiated performance despite identical settings;
- The devices under test (DUT) were immature presenting non-linear performance over temperature;
- Since in this initial campaign only data-cards (dongles) were utilized, a laptop was part of the setup, generating additional noise into the measurement, and altering the LTE dongle antenna system performance [13];
- The channel model emulator settings across different vendors were not completely defined [14];
- Lack of definition of the BS antenna assumptions, and lack of procedures to validate the channel model emulation in the test environment [15];
- Finally, an important root cause for the unsuccessful 3GPP RAN WG4 measurement campaign is the fact that none of the evaluated devices under test (DUT) had the MIMO antenna system characterized, meaning the measurement results could not be compared against expected performance.

3.2 Defining the MIMO Reference Antenna system

Understanding that the industry was overlooking fundamental aspects of good academic and engineering practices the work presented in this thesis was planned. Initially solving the issue surrounding the unknown antenna radiated performance in all devices under test, the MIMO reference antennas described in the attached papers 1, 2, 3 and 5 was proposed as a solution to this problem, therefore eliminating this variable from the list of unknowns that affect the initial 3GPP measurement campaign outcome. Those antennas were proposed in mid 2011 during the first face-to-face meeting of the recently formed CTIA MIMO OTA Sub-Group (MOSG), and it was widely accepted by the industry as important element for research and development of MIMO OTA test methodologies. The MIMO reference antennas were adopted during two additional measurement campaigns organized by CTIA and supported by 3GPP RAN4 MIMO OTA ad-hoc as shown in [8] clause 9.

Despite the efforts to define a valid MIMO OTA test method, nowadays the industry still adopts MIMO antenna system figure of merit (FoM) based on farfield measurements taken in anechoic chambers with uniform incoming power (SISO), thus defining total efficiency branch power ratio and envelope correlation coefficient. The paper 5 was a follow up work on the concept of MIMO reference antennas, demonstrating that the MIMO antenna FoM defined in the isotropic environment will not necessarily agree with similar figure of merit measured in channel environment with directive spatial characteristics, in this paper it was demonstrated that mean effective gain, branch power ratio and envelope correlation coefficient are defined by the iteration of the device under test antennas radiation pattern, applied channel model and base station antennas antennas characteristics, and will differ from the FoM results of same antennas measured in uniform incoming power test environments.

The reference antennas previously described were created to emulate the handset industry most commonly adopted MIMO antenna system design technique; the radiation pattern diversity. The work on paper 6 brought a different perspective on this problem, where a MIMO antenna system based on pure polarization diversity was presented. The objective of this paper was to bring the attention of the industry that conclusions based on limited sample of reference antennas, can't be extrapolated to a wide variety of MIMO antenna systems. In this paper we demonstrated that test methodologies with fundamental differences regarding channel model and cross-polarization definitions, will provide different results while evaluating the same devices. This paper demonstrated that due the lack of cross-polarization control, the reverberation chambers base methods can't discriminate MIMO antenna systems based on pure polarization diversity. While pure polarization diversity is a great challenge to be achieved in low frequency and small form factors such as a handset, is common in larger mobile devices such as tablets, laptops, M2M, etc. This important finding was capture in [8] clause 12.4. This paper was invited and accepted to IEEE AWPL Special Cluster on "Terminal Antenna Systems for 4G and Beyond", as well as showcased in the COST IC1004 6th MC newsletter.

3.3 Validating the Radiated Test Environment

With the MIMO antenna performance issue addressed, the next issue to be faced was the validation of Base Station settings and channel model emulation in the test environment. These technical problems were the motivation for the follow up work presented in the paper 4. The Absolute Data Throughput Framework was a method coined to establish a deterministic MIMO OTA figure of merit and stimulate the industry to proper defined the channel model pertinent to each proposed MIMO OTA test methodology. Adopting the MIMO reference antennas already accepted by the industry, the Absolute Data Throughput Framework compared the conducted data throughput measurement through the channel emulator including the spatial and temporal characteristics of the defined channel model and complex radiation pattern of the MIMO reference antennas, with an over the air measurement using the same channel model, same device under test and same reference antenna which the complex radiation pattern was measured. Therefore validating the expectation of radiated channel model emulation. This methodology was extensively used during the conclusion of the 3GPP RAN4 MIMO OTA work item, and was considered one of the fundamental criteria to validate MIMO OTA test methodology, as shown in [8] clauses 9.3.1 and 10. Nowadays the Absolute Data Throughput Framework is being considered to be adopted as "sanity check" for all CTIA certified labs, and an instrument to assess test methodology measurement uncertainty.

3.4 The MIMO Antenna Challenge

The work done on antenna polarization discrimination in paper 6, implicitly propose a challenge to design a MIMO antenna system with pure polarization diversity in small form factor, however following realistic packaging found in current smartphones. Based on this motivation the work described in the paper 7 was done. To further validate the antenna design technique, the antenna system was designed based on feature cell phone dimensions; 100x50x10mm; adopting a printed circuit board shape and antennas placement commonly found in real designs.
Over the past years, small antenna array design has been the subject of numerous research articles [6, 16–35]. Receiver diversity and MIMO have improved the reliability and data rate of wireless links enabling 4G communications standards see e.g. [6, 16, 17]. Ideally, by taking advantage of the multi-path properties of the wireless channel.

In classical array design, the distance between the elements has been kept to $\lambda/2$ to minimize the unwanted coupling between the elements of an array and to minimize the spatial correlation [36]. The MIMO antenna system introduced in this paper, defines realistic antenna placements, independent excitation modes and feeding mechanisms, manipulation of ground plane geometry to control ground surface current and application of characteristic mode theory. The synergy of these techniques enables the design of pure polarization diversity, highly isolated and uncorrelated antennas at low frequency bands, with adequate gain imbalance and total efficiency, within the constrains of realistic implementation in small terminals.
This fundamental feasibility research motivate further envisioning in how to implement in real devices. Several of possible embodiments were capture in the submission of the patent "Method and Apparatus for an Adaptive Multi-Antenna System". The work described in paper 10 brings yest another ramification of the MIMO antenna system design, focused on adaptive antenna systems.

3.5 Novel MIMO OTA 3D flexible setup

The work on paper 5 indicated the difference in performance of the same antenna system between 2D and 3D channel models. Its agreed in all MIMO OTA standard groups that the ultimate goal is to define a test methodology capable to emulate 3D spatial channel models, such as WINNER [7]. Based on the current implementation of the 2D multi-cluster boundary array where the probes ate fixed in equidistant positions, the channel model emulator generate the desired spatial channel model mapping the available antennas defining different weights accordingly. Expanding this concept to 3D channel models, more probes and consequently more channel model emulator ports are required. The concept demonstrated in paper 8 propose a paradigm shift, where the probes are positioned based on the mapping optimization. This multi-cluster boundary array was found to be novel and a patent was submitted to United States Patent and Trademark Office.

3.6 Investigating MIMO OTA Measurement Uncertainty

One of the relevant open issues in the MIMO OTA industry and standards nowadays is the definition of the test measurement uncertainty (MU), different test methodologies have different hardware and software requirements and unique system implementations. While some test methodologies require multiple channel emulator ports, power amplifiers, probe antennas, cables, connectors etc. Other MIMO OTA methods are based on antenna system complex radiation pattern gather in SISO anechoic chambers and conducted measurements, clearly a single MU value can't capture both methods uncertainty properly. The investigation on the root cause for measurement uncertainty on anechoic chamber multi-cluster boundary array was a motivation behind paper 9. In this work three independent implementations of the same test methodology where investigated and compared, while two

of these implementations wee based on research laboratories setups built from ground-up ;Aalborg University and Motorola Mobility; the third setup was based on commercially available installation. This work sponsored by COST IC1004 STSM, was instrumental to define root causes of MU due reflections and instabilities in the test environment, as well as was novel demonstrating for the first time the accuracy of plane wave emulation in horizontal polarization. This paper was nominated for the best paper award on EuCAP 2014 conference.

CHAPTER 4

SUMMARY OF PAPERS

4.1 MIMO Reference Antenna

Paper 1

"MIMO 2X2 Reference Antennas Concept"
6th European Conference on Antennas and Propagation (EUCAP), March 2012.

Motivation

The MIMO 2x2 Reference Antenna concept was created based on the need of eliminate the unknown antenna performance of the few LTE MIMO 2x2 devices available for radiated data throughput measurements. The initial concept was created to aid researchers working in both anechoic and other test environments. The adoption of reference antennas eliminate part of the measurement uncertainty, and increase repeatability among different MIMO OTA test methodologies

Paper

The MIMO 2x2 antenna system was initially simulated on CST Microwave Studio [37]. Following basic guidelines the MIMO antenna system was design intentionally to isolate the MIMO centric FoM, total efficiency, gain imbalance and magnitude of complex correlation coefficient.

Main results

Tne MIMO reference antennas design is based on radiation pattern diversity technique, where a simple but effective set of MIMO reference antennas concept was created. By design all antennas have BPR near 0 dB, however BPR can be controlled by utilization of passive RF attenuators in the antennas RF ports. The MIMO reference antenna set has magnitude of complex correlation coefficient with values 0.1, 0.5 and 0.9. Enabling research on MIMO OTA test methodologies where the DUT antenna system is known and controllable.

Paper 2

"Design and Verification of MIMO 2x2 Reference Antennas"
IEEE Antennas and Propagation Society International Symposium (APSURSI), July 2012.

Motivation

The purpose of the MIMO 2x2 reference antennas is to eliminate an unknown variable from the test methodology, the MIMO antenna system performance, thus guaranteeing that any MIMO OTA test methodology can be analyzed based on reliable and well defined DUT radiated performance. The MIMO reference antenna is an external antenna. This allows separation of the DUT RF/base-band/LTE performance from the antenna performance. Thus the external MIMO reference antenna concept enables the comparison of different test methodologies with the purpose of discriminating between so called good and bad MIMO antennas.

Paper

To optimize MIMO capacity several aspects of the antenna system design need to be considered, as summarized below:

- Both antennas, Main Antenna and Secondary Antenna, need to have minimum branch power ratio, ideally BPR = 0 dB;
- In a rich scattered environment the maximum capacity will occur when both receiver antennas are uncorrelated. There are exceptional cases where co-polarized antennas can still be uncorrelated, however this is hard to accomplish in hand-held form factors due to the limited spacing between antennas;
- The absolute phase responses of the reference antennas are irrelevant, but not the phase per direction or the relative phase relationship between the antennas, both of which define the antenna system correlation coefficient;
- Considering the special case of the isotropic environment, the ideal MIMO 2x2 antenna system, with ideal isolation between antennas S_{21} <-20 dB, high efficiency $\eta > 90$ %, low gain imbalance (BPR$\approx$ 0 dB), and correlation coefficient ($\rho \approx 0$), should provide double the capacity of a SISO system (this statement is based solely on antenna parameters and assumes ideal propagation conditions);
- The antenna's radiation patterns need to have similar directivity. Two directional antennas with the main lobe in opposite directions, will not enable acceptable MIMO performance in an environment with few signal propagating reflections, such signal reflections are generated by non-uniformities in the radiated environment also known as scattering.

Main results

In this paper the MIMO reference antenna prototype was built and measurement results on uniform incoming power test environment was gathered. The farfield measurements and respective post-processing data, fully agreed with previously published simulated results.

Paper 3

"LTE Radiated Data Throughput Measurements Adopting, MIMO 2x2 Reference Antennas"
IEEE Vehicular Technology Conference (VTC Fall), September 2012

Motivation

In this paper the first attempt to realize a MIMO OTA measurement with Reference antenna is presented. The antenna was measured in a MIMO OTA Multi-Cluster boundary array test methodology, emulating an Spatial Channel Model Extended (SCME) Urban Micro (Umi) and 16 QAM.

Paper

This paper conclude the trilogy of conference papers on MIMO OTA Reference Antennas, comparing preliminary simulation and measured antenna FoM data results, with expected discrimination in OTA environment, therefore certifying the antenna to be used as a valid resource on MIMO OTA test methodology research.

Main results

The MIMO OTA measurement data agree with expected simulated results, indicating a discrimination between so called ”Good” and ”Bad” MIMO Reference Antennas of approximately 8 dB. Such range prove to be sufficient to move forward with the MIMO Reference Antenna design, and initiate mass production.

Paper 5

”MIMO Reference Antennas Performance in Anisotropic Channel Environments”
IEEE Transaction on Antenna and Propagation, May 2013.

Motivation

The objective of this paper is to evaluate the radiated performance of the MIMO reference antennas using anisotropic (non-uniform power angular spread) channel environments. The performance of the reference antennas in anisotropic environments is different to that in an isotropic environment, due to the antenna orientation in the three dimensional space relative to the channel.

Paper

This paper focus on the characterization of a reference MIMO antenna system, discussing isotropic and anisotropic antenna figures of merit, and offering a solution to minimize the uncertainty in MIMO OTA measurements.

Main results

The magnitude of the reference antenna complex correlation coefficient was somewhat unchanged between the isotropic and anisotropic environments for the most DUT rotations. However the MEG and BPR demonstrated significant variation, mainly when the reference antenna radiation pattern null aligned with the main power beam defined in the anisotropic propagation environment. The significant variation in MEG and BPR must be recognized and mitigated while designing MIMO antenna systems.

4.2 Absolute Data Throughput Framework

Paper 4

”MIMO 22 absolute data throughput concept”
7th European Conference on Antennas and Propagation (EuCAP), April 2013.

Motivation

The motivation of this concept is to recommend a framework of utilizing absolute radiated data throughput as a method for comparing the radiated throughput results measured in any MIMO OTA testing methodology with conducted reference performance under the ideal channel model implementation. It is not implied that the conducted reference is ”ideal” or ”perfect.” For instance, the way that the pattern data is interpolated and quantized may contribute variations in the conducted reference that are not present in the radiated test. The methodology will be used to understand each MIMO OTA testing method’s ability to emulate the specified network and channel propagation characteristics based on an absolute throughput metric.

Paper

The basic concept in this measurement is to determine a baseline data throughput over downlink conducted sensitivity, while the measurement encapsulates the following characteristics:

- Network characteristics inherent in the base station emulator settings (the reference measurement channel, MCS, etc.); these settings are documented in Section 7.1 of [8];
- Emulated base station antenna characteristics; these settings have been defined in Section 7.2 of [8];
- Propagation channel characteristics (channel model, multipath profile, defined drop characterizing spatial and temporal parameters, etc.); these settings have been defined in Section 8.2 of [8];
- DL signal power level;
- Complex antenna radiation pattern of the DUT (radiation patterns of CTIA MIMO 2x2 reference antennas shall be applied to the emulated propagation channel characteristics);
- Chipset characteristics (such as the receiver algorithm implementation).

Main results

The Absolute Data Throughput Framework had been successfully adopted in CTIA MOSG and 3GPP RAN4 MIMO OTA ad-hoc group, as one of the MIMO OTA test methodology validation criterion. Several independent labs were able to perform this measurement with high accuracy validating the OTA emulated channel model. This framework might be used as ”sanity check” in test labs as well.

4.3 MIMO Antenna System design

Paper 7

”On Small Terminal MIMO Antennas, harmonizing Characteristic Modes with Ground Plane Geometry”
IEEE Transaction on Antenna and Propagation, December 2013.

Motivation

This work was motivated by the need to have a MIMO antenna system for mobile terminals, based on a realistic form factor and packaging implementation, with a very low magnitude of the complex correlation coefficient and an impressive isolation, using a platform with a very small form factor (100x50x10mm).

Paper

The MIMO antenna system introduced in this paper, defines realistic antenna placements, independent excitation modes and feeding mechanisms, manipulation of ground plane geometry to control ground surface current and application of characteristic mode theory. The synergy of these techniques enables the design of highly isolated and uncorrelated antennas at low frequency bands, with adequate gain imbalance and total efficiency, within the constrains of realistic implementation in small terminals.

Main results

This investigation demonstrates that commonly adopted antennas following an application of characteristic mode theory, and manipulation of the GND and optimal placement, can achieve strong uncorrelation between low band antennas in electrically small devices. A significant reduction of the magnitude of complex correlation coefficient was achieved while maintaining the total antenna efficiency and BPR in realistic antenna volume and device form factors. Simulation and measured results confirmed that an antenna system with commonly used PIFA antennas can be configured to excite the handset chassis in orthogonal modes, maintaining high isolation between antennas and orthogonal radiation patterns, therefore enabling radiation pattern uncorrelation.

4.4 MIMO Over The Air Test Methodology

Paper 6

”On antenna polarization discrimination, validating MIMO OTA test methodologies”
IEEE Antennas and Wireless Propagation Letters, February 2014

Motivation

This paper was motivated by the need to further understand the performance and behavior of MIMO antenna systems, under test methodologies based on random channel models with uniform (isotropic) power distributions, which fully randomize the signal’s polarizations at the DUT receiver antennas.

Paper

The work described in this paper includes the design and creation of several sets of MIMO antennas, where uncorrelated signals at the antenna outputs are obtained either by pure polarization diversity, or by spatial diversity where both co-polarized antennas were placed half a wavelength (λ) apart.

Main results

The antennas were demonstrated to have different MIMO OTA radiated performance when evaluated under the assumption of the spatial channel models defined in [38], and with a channel cross polarization power difference other than 0 dB. However, the relative performance differences of the same antennas could not be reproduced in the statistically uniform MIMO OTA test environment due its intrinsic inability to generate cross-polarization power differences other than 0 dB. While is known that the RC based OTA test methodology can discriminate antenna systems with different correlation coefficients based on polarization diversity, it does not demonstrate that an antenna system with the same correlation coefficient but different antenna polarizations can be discriminated.

Paper 8

"Channel Spatial Correlation Reconstruction in Flexible Multi-Probe Setups"
IEEE Antennas and Wireless Propagation Letters, January 2014

Motivation

While conventional Multi-Cluster anechoic based MIMO OTA test methods, define the probes weights based on fixed position and mapping algorithm. This paper proposes a paradigm shift, where the probes are relocated based on mapping optimization genetic and multi-shot algorithms.

Paper

In one possible installation for the flexible setup, a large number probes are installed with fixed locations, and a switch box drives a subset of probes based on the target channel models. To reduce mutual coupling and reflection between probes, a minimum separation between probes is required. Thus, fixing the probe locations in the chamber will often result in suboptimal probe locations for a given channel model. In this paper, we propose a flexible system arrangement, where the number of probes (consequently the channel emulator output ports) are optimized to the minimum necessary to generate the desirable spatial channel model.

Main results

This paper introduce the novel concept of probes with flexible weights and angular locations, as an alternative method to emulate spatial channel models with reduced number of probes and consequently channel model emulators ports. Simulation results indicated the feasibility of this concept in both single cluster and multi cluster boundary array systems.

Paper 10

"Beam-Steered Adaptive Antenna System for MIMO OTA test Methodology Validation"
IEEE Transaction on Antenna and Propagation, to be submitted in March 2013

Motivation

This work was motivated by the need to better understand how fundamentally different test methodologies evaluate MIMO Adaptive Antenna Systems.

Paper

This paper is based on an elaborate test setup adopting the same concept of reference antennas (papers 1, 2, 3 and 5). Where a mobile device is inserted in an RF enclosure and connected to fully characterized external antennas. In this paper it was developed a simplified but realistic MIMO adaptive antenna system with four tuning positions. The antenna was fully characterized in SISO chamber and the whole system was evaluated in MIMO OTA test methodologies based on anechoic chamber boundary array (SCME UMi and SCME Uma), as well as reverberation chamber (NIST).

Main results

The concept of AAS antenna was proven and demonstrated in anechoic chamber test methodology, indicating relevant MIMO performance improvement.

4.5 MIMO Over The Air Measurement Uncertainty

Paper 9

"Measurement Uncertainty Investigation in the Multi-probe OTA Setups"
8th European Conference on Antennas and Propagation (EuCAP), April 2014

Motivation

This paper attempts to compare and understand measurement uncertainty levels with different labs, i.e. at Aalborg University (AAU), Denmark, Motorola Mobility (MM), USA and ETS-Lindgren (ETS), USA., thus to show key aspects related to the multi-probe system setup design. Fundamental aspects of measurement uncertainty were investigated, benchmarking measurement results and hardware implementation of the same test methodology in different labs. This effort was sponsored by COST IC1004 STSM grant.

Paper

Three independent but similar implementations of the multi-cluster boundary array test methodology were compared in this paper. One built by Aalborg University in Denmark, other built in Motorola Mobility design center in Illinois-USA, and the setup built in ETS-Lindgren plant in Texas - USA. Only the ETS-Lindgren can be considered a commercial setup, while Aalborg University and Motorola Mobility were built locally from ground up. In this paper we investigate important aspects of this MIMO OTA test methodology, such as radiation pattern measurements, turntable stability, channel emulator stability, system frequency flatness, power coupling between probes, chamber reflection and plane wave syntheses.

Main results

During this investigation we identified several sources of uncertainty among labs, while the Base Station and Channel emulators and power amplifiers didn't contribute much to increase measurement uncertainty, some aspects of the test setup construction were identified as large contributors, untreated coaxial cables, and certain dielectric materials connecting and supporting the device under test, proven to be considerable sources of reflections and distortions in the measurements.

CHAPTER 5

CONCLUSIONS

The discussion surrounding MIMO Over the Air valid test methodologies is far from over. The limited progress in defining proper test methodologies for certification is related rather to economical interests than technical limitations. In spite of the great effort on realizing measurement campaigns, post-processing large amount of data and defining spatial channel models that somewhat reproduce realistic environments, standard groups are forced to discuss MIMO OTA test methodologies based on statistically isotropic channel models, despite to the fact that there are no evidence that such model can be found outside reverberation chambers. The seek for technical correctness and unbiased evaluation of the MIMO OTA problem, was the motivation behind this work. The collection of papers here presented, are a small but relevant contribution to this effort, isolating the antenna from OTA test, validating the emulated channel model over the air, defining new techniques to emulate 3D spatial channel models and discussing measurement uncertainty.

Additional product related research; not disclosed in this thesis; increase the confidence level of the relevance of this work. Field measurements with MIMO reference antennas in live networks, confirm the theoretical predictions, and are providing important insights into de development of the new generation of MIMO devices equipped with Adaptive Antenna System, uplink MIMO and Carrier Aggregation.

The future of MIMO antenna system design and measurements is exciting and full of opportunities for research and innovation.

REFERENCES

[1] C.-T. W. Association. (2011) Ctia official website @ONLINE. [Online]. Available: http://www.ctia.org/

[2] 3GPP, 3GPP, Tech. Rep., October 2010. [Online]. Available: http://www.3gpp.org/LTE

[3] I. A. C. R. C. for Green Smart Environments. (2011) European cooperation in the field of scientific and technical research @ONLINE. [Online]. Available: http://www.ic1004.org/

[4] W. C. Jakes and D. C. Cox, Eds., *Microwave Mobile Communications*. Wiley-IEEE Press, 1994.

[5] T. Taga, "Analysis for mean effective gain of mobile antennas in land mobile radio environments," *Vehicular Technology, IEEE Transactions on*, vol. 39, no. 2, pp. 117 –131, May 1990.

[6] R. Vaughan and J. Andersen, "Antenna diversity in mobile communications," *Vehicular Technology, IEEE Transactions on*, vol. 36, no. 4, pp. 149 – 172, nov. 1987.

[7] WINNER, "Winner2 channel models," September 2007. [Online]. Available: http://www.ist-winner.org/WINNER2-Deliverables/D1.1.2v1.1.pdf

[8] 3GPP, "3rd generation partnership project; technical specification group radio access networks; universal terrestrial radio access (UTRA) and evolved universal terrestrial radio access (E-UTRA); verification of radiated multi-antenna reception performance of user equipment (UE) (release 11)," May 2012, 3GPP TR 37.977 V0.2.0 (2012-05). [Online]. Available: http://www.3gpp.org/ftp/Specs/archive/37_series/37.977/37977-020.zip

[9] R. J. Garbacz, "Data-Driven Batch Scheduling," Ph.D. dissertation, Ohio State University, Columbus, 1968.

[10] R. F. Harrington and J. Mautz, "Computation of characteristic modes for conducting bodies," *Antennas and Propagation, IEEE Transactions on*, vol. 19, no. 5, pp. 629–639, 1971.

[11] ——, "Theory of characteristic modes for conducting bodies," *Antennas and Propagation, IEEE Transactions on*, vol. 19, no. 5, pp. 622–628, 1971.

[12] B. Austin and K. Murray, "The application of characteristic-mode techniques to vehicle-mounted nvis antennas," *Antennas and Propagation Magazine, IEEE*, vol. 40, no. 1, pp. 7–21, 30, 1998.

[13] Motorola, "LTE antenna system figure of merit. techniques and trade-offs probing antennas on LTE devices." October 2010, 3GPP TSG-RAN WG4 AH4-2010 . [Online]. Available: http://www.3gpp.org/ftp/tsg_ran/WG4_Radio/TSGR4_AHs/R4_AH04_Xian_Oct_2010/Docs/R4-103869.zip

[14] SATIMO Industries, Elektrobit, SPIRENT Communications, "Anechoic chamber based MIMO OTA: Channel emulators, and channel models implementation comparison," February 2012, 3GPP TSG-RAN WG4 Meeting No.62. [Online]. Available: http://www.3gpp.org/ftp/tsg_ran/WG4_Radio/TSGR4_62/Docs/R4-120675.zip

[15] Spirent Communications, Elektrobit, Satimo, "MIMO OTA channel model alignment," February 2012, 3GPP TSG-RAN WG4 62 MIMO OTA Ad-hoc Meeting. [Online]. Available: http://www.3gpp.org/ftp/tsg_ran/WG4_Radio/TSGR4_62/Docs/R4-120739.zip

[16] G. J. Foschini and M. J. Gans, "On limits of wireless communications in a fading environment when using multiple antennas," *Wireless Personal Communications*, vol. 6, pp. 311–335, 1998.

[17] H. Holma, A. Toskala, K. Ranta-aho, and J. Pirskanen, "High-speed packet access evolution in 3gpp release 7 [topics in radio communications]," *Communications Magazine, IEEE*, vol. 45, no. 12, pp. 29–35, 2007.

[18] A. Tulino, A. Lozano, and S. Verdu, "Impact of antenna correlation on the capacity of multi-antenna channels," *Information Theory, IEEE Transactions on*, vol. 51, no. 7, pp. 2491–2509, 2005.

[19] A. Molisch, M. Steinbauer, M. Toeltsch, E. Bonek, and R. Thoma, "Capacity of mimo systems based on measured wireless channels," *Selected Areas in Communications, IEEE Journal on*, vol. 20, no. 3, pp. 561–569, 2002.

[20] J. Wallace and M. Jensen, "Mutual coupling in mimo wireless systems: a rigorous network theory analysis," *Wireless Communications, IEEE Transactions on*, vol. 3, no. 4, pp. 1317–1325, 2004.

[21] B. Guo, K. Karlsson, and O. Sotoudeh, "Study of diversity gain obtained with two pifa antennas on a small ground plane for a umts terminal," in *Antennas and Propagation Society International Symposium, 2008. AP-S 2008. IEEE*, 2008, pp. 1–4.

[22] R. Kuonanoja, "Low correlation handset antenna configuration for lte mimo applications," in *Antennas and Propagation Society International Symposium (APSURSI), 2010 IEEE*, 2010, pp. 1–4.

[23] H. Li, B. K. Lau, and Z. Ying, "Optimal multiple antenna design for compact mimo terminals with ground plane excitation," in *Antenna Technology (iWAT), 2011 International Workshop on*, 2011, pp. 218–221.

[24] B. K. Lau and J. Andersen, "Simple and efficient decoupling of compact arrays with parasitic scatterers," *Antennas and Propagation, IEEE Transactions on*, vol. 60, no. 2, pp. 464–472, 2012.

[25] J. Andersen and H. Rasmussen, "Decoupling and descattering networks for antennas," *Antennas and Propagation, IEEE Transactions on*, vol. 24, no. 6, pp. 841–846, 1976.

[26] A. Chebihi, C. Luxey, A. Diallo, P. Le Thuc, and R. Staraj, "A novel isolation technique for closely spaced pifas for umts mobile phones," *Antennas and Wireless Propagation Letters, IEEE*, vol. 7, pp. 665–668, 2008.

[27] M. Han and J. Choi, "Dual-band mimo antenna using a symmetric slotted structure for 4g usb dongle application," in *Antennas and Propagation (APSURSI), 2011 IEEE International Symposium on*, 2011, pp. 2223–2226.

[28] I. Dioum, A. Diallo, C. Luxey, and S. Farsi, "Compact dual-band monopole antenna for lte mobile phones," in *Antennas and Propagation Conference (LAPC), 2010 Loughborough*, 2010, pp. 593–596.

[29] S.-W. Su, C.-T. Lee, and F.-S. Chang, "Printed mimo-antenna system using neutralization-line technique for wireless usb-dongle applications," *Antennas and Propagation, IEEE Transactions on*, vol. 60, no. 2, pp. 456–463, 2012.

[30] A. Diallo, C. Luxey, P. Le Thuc, R. Staraj, and G. Kossiavas, "Enhanced two-antenna structures for universal mobile telecommunications system diversity terminals," *Microwaves, Antennas Propagation, IET*, vol. 2, no. 1, pp. 93–101, 2008.

[31] A. Tatomirescu, M. Pelosi, M. Knudsen, O. Franek, and G. Pedersen, "Port isolation method for mimo antenna in small terminals for next generation mobile networks," in *Vehicular Technology Conference (VTC Fall), 2011 IEEE*, 2011, pp. 1–5.

[32] R.-A. Bhatti, S. Yi, and S.-O. Park, "Compact antenna array with port decoupling for lte-standardized mobile phones," *Antennas and Wireless Propagation Letters, IEEE*, vol. 8, pp. 1430–1433, 2009.

[33] S.-C. Chen, Y.-S. Wang, and S.-J. Chung, "A decoupling technique for increasing the port isolation between two strongly coupled antennas," *Antennas and Propagation, IEEE Transactions on*, vol. 56, no. 12, pp. 3650–3658, 2008.

[34] C. Volmer, J. Weber, R. Stephan, K. Blau, and M. Hein, "An eigen-analysis of compact antenna arrays and its application to port decoupling," *Antennas and Propagation, IEEE Transactions on*, vol. 56, no. 2, pp. 360–370, 2008.

[35] K. Sato and T. Amano, "Improvements of impedance and radiation performances with a parasitic element for mobile phone," in *Antennas and Propagation Society International Symposium, 2008. AP-S 2008. IEEE*, 2008, pp. 1–4.

[36] W. Y. C. Lee, *Wireless and Cellular Communications*. McGraw-Hil, 2006.

[37] CST. (2013) Computer simulation technology. [Online]. Available: http://www.cst.com/

[38] 3GPP, "Verification of radiated multi-antenna reception performance of user equipment (UE)," 3GPP, Tech. Rep. 3GPP TR 37.977 v1.0.0, 2013.

Contributions

Paper 1

MIMO 2x2 Reference Antennas Concept

Istvan Szini, Gert Pedersen, Alessandro Scannavini and Lars Foged

Published as:
Szini, I.; Pedersen, G.F.; Scannavini, A.; Foged, L.J.,
"MIMO 2x2 reference antennas concept"
Antennas and Propagation (EUCAP), 2012 6th European Conference on ,
vol., no., pp.1540,1543, 26-30 March 2012
doi: 10.1109/EuCAP.2012.6206567

MIMO 2X2 Reference Antennas Concept

I. Szini[1,2], G. F. Pedersen[1], A. Scannavini[3] , L.J. Foged[3]

[1] Antennas, Propagation and Radio Networking, Department of Electronic Systems,Faculty of Engineering and Science, Aalborg University, Denmark
Email: gfp@es.aau.dk

[2] Motorola Mobility Inc., Libertyville, USA.
Email: Istvan.Szini@motorola.com

[3] SATIMO, Pomezia, Italy
Email: ascannavini@satimo.com,lfoged@satimo.com

Abstract— **Long Term Evolution (LTE) adopt multi-antenna mechanisms to increase coverage and physical layer capacity, therefore Multiple Impute Multiple Output (MIMO) antenna systems are required on LTE systems. Besides the antenna system figure of merit (FoM), i.e. absolute system gain, gain imbalance, correlation coefficient the MIMO system performance is defined by radiated data throughput. Different standard bodies are working towards test methodologies to proper emulate the radio propagation environment therefore determining MIMO performance. This task had become very complex based on several implementation details pertinent of each test methodology. This paper will introduce the concept of MIMO 2x2 reference antenna for the special case of uniform incoming power distribution. Hereby part of measurement uncertainty is eliminated through the adoption of a set of MIMO 2x2 antennas with known FoM, and controllable performance.**

Keywords-component; LTE, MIMO, OTA, antennas.

I. INTRODUCTION

Recent comparison campaigns, based on measurement of radiated MIMO data throughput on available LTE MIMO 2x2 reference devices have shown to be ineffective as a correlation instrument since they have been based on different test devices and different test methodologies[1]. Since the MIMO over the air (OTA) standard test procedure is still under development, all currently available reference devices, have been designed as optimum performance devices and not with the specific scope as a measurement verification devices [2].

In order to properly test and verify, the correlation and accuracy of different MIMO data throughput measurement systems, the reference antennas must represent the full range of "good", "nominal" and "bad" MIMO 2x2 antenna performance. The MIMO 2x2 reference antenna concept has been created specifically to emulate these three performances ranges.

II. REFERENCE ANTENNA CONCEPT

The MIMO 2x2 Reference Antenna concept was created based on the need of eliminate the unknown antenna performance of the few LTE MIMO 2x2 devices available for radiated data throughput measurements. The initial concept was created to aid researchers working in both anechoic and other test environments. The adoption of reference antennas eliminate part of the measurement uncertainty, and increase repeatability among different MIMO OTA test methodologies and test facilities, The final antenna design is simple and low cost to enable widespread use.

These antennas were conceived during the first CTIA (Cellular Telecommunications and Internet Association) MIMO OTA Sub-Group meeting, and initially were designed to cover three LTE bands (2, 7 and 13). Conceptually for each band three antennas were designed to emulate a "good" MIMO antenna system FoM, i.e. low correlation coefficient ($\rho<0.1$), high total antenna efficiency ($>90\%$) and low gain imbalance ($\Delta G \cong 0dB$). Respectively the "nominal" MIMO antenna system has moderate correlation coefficient ($\rho\leq0.5$), moderate total antenna efficiency ($\geq 50\%$) and low gain imbalance ($\Delta G\cong0dB$). And finally the "bad" MIMO antenna system, having poor correlation coefficient ($\rho\geq0.9$), moderate-to-poor total antenna efficiency ($\leq 50\%$) and low gain imbalance ($\Delta G\cong0dB$).

Other than the electrical performance constrains, the reference antenna also needs to solve the potential problem with connecting any external antenna into a portable device. The connection between the portable device RF port and the external antenna, normally a coaxial cable, can potentially carry current in the outer conductor. The associated radiation perturbs the antenna system radiation and influence system parameters like correlation coefficient, absolute gain and gain imbalance [3]. For this reason the antenna was conceived attaching MIMO 2x2 external antennas to a RF enclosure, where the DUT and its RF connections are located. The initial prototype is shown in Fig. 1.

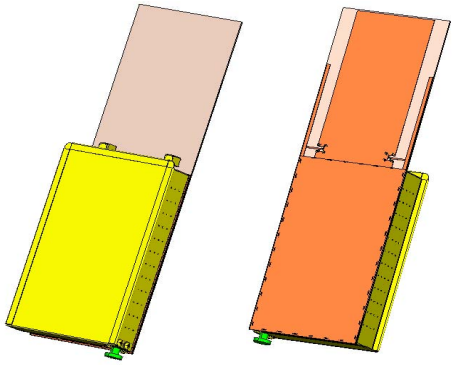

Figure 1a. MIMO 2x2 Reference Antenna concept. Front (left) and back (right) view of the closed antenna.

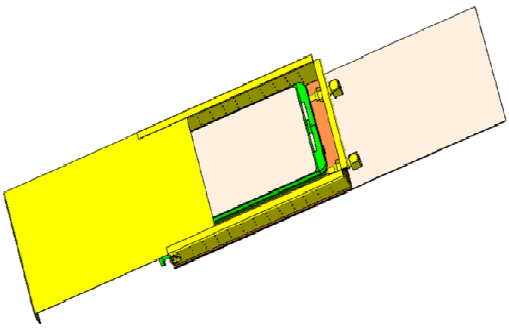

Figure 1b. MIMO 2x2 Reference Antenna concept. Open antenna with inserted active device.

III. Analysis of Magnitude of Correlation Coefficient Impact on MIMO 2x2 System Capacity

The magnitude of the complex correlation coefficient between two antennas is shown in [4]. It can be seen, that the coefficient is predominantly defined by the complex radiation patterns of the antennas, in this case a generic scenario is presented where the incoming power is uniformly distributed in both theta and phi directions, it's understood that in the real environment this condition is unlikely to happen, however true in the reverberation and controlled anechoic test environment.

$$\rho_{12} = \frac{\left| \oint \{ (XPR \cdot E_{\theta MA}(\Omega) \cdot E^{*}_{\theta SA}(\Omega) + E_{\phi MA}(\Omega) \cdot E^{*}_{\phi SA}(\Omega) \} d\Omega \right|^{2}}{\oint \{ XPR \cdot G_{\theta MA}(\Omega) + G_{\phi MA}(\Omega) \} d\Omega \cdot \oint \{ XPR \cdot G_{\theta SA}(\Omega) + G_{\phi SA}(\Omega) \} d\Omega} \quad (1)$$

$E_{\theta MA}$ (Ω) is the vertical polarization complex radiation pattern from Main Antenna, $E_{\theta SA}$ (Ω) is the vertical polarization complex radiation pattern from Secondary Antenna, E_{MA} (Ω) is the horizontal polarization complex radiation pattern from Main Antenna, E_{SA} (Ω) is the horizontal polarization complex radiation pattern from Secondary Antenna. Ω is the solid angle for a spherical coordinate system and *XPR* is cross-polar discrimination of the antennas.

The primary objective of implementing a MIMO system is to improve the system capacity. Considering the MIMO 2x2 system as focus in this study, the basic graphical representation of the antenna arrangement is shown in Fig 2.

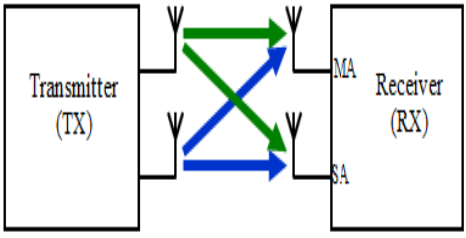

Fig 2. MIMO 2x2 system, graphical representation

Considering (1) from an analytic perspective only, the correlation coefficient can be controlled by varying both arguments and it appears that the cross correlation can be minimized simply by increasing the gain imbalance between the two antennas. However, from a system performance perspective, a high gain imbalance will not lead to improved MIMO performance since this condition in its extreme form is equivalent to the pure MISO system with just one antenna [5].

A successful MIMO antenna design requires that each pair of antennas have approximately the same power loss, same gain and closely uncorrelated. To optimize MIMO capacity several basic properties needs to be observed as summarized below:

1. Both antennas; Main Antenna and Secondary Antenna; needs to have appropriate radiated performance with minimum gain imbalance, ideally 0dB;
2. In the rich scattered environment the maximum capacity will occur when both receiver antennas where cross-polarized, consequently the antennas need to be uncorrelated;
3. The absolute phase response of the reference antennas are irrelevant, but not the phase per direction neither the relative phase relationship between the antennas and the gain imbalance, which defines the MIMO antenna system correlation coefficient;
4. The ideal MIMO 2x2 antenna system, considering ideal isolation between antennas (>20dB), gain imbalance 0dB, and correlation coefficient 0, will provide the double of capacity of counterpart SISO system (this statement is based solely on antenna parameters).
5. The antennas radiation patterns need to have similar directivity, two directional antennas with main lobe in opposite directions, will not enable acceptable MIMO performance in poor scattered environment.

IV. Simulation Results

The MIMO 2x2 antenna system was initially simulated on CST Microwave Studio [6]. The antennas are self-resonant and based on the Inverted "F" antenna topology, as shown in Fig. 3 to 9. The figures illustrate the 3D radiation patterns of each of the two antennas in the nominal, good and bad configurations including return loss and impedance characteristics.

The control of the magnitude of complex correlation coefficient is achieved through the reference ground plane placement between antennas radiators. Since the antennas are absolutely symmetric, the gain imbalance between the antennas is always near to 0dB, considering an environment which the fields arrives from all directions. With this feature, the gain imbalance between antennas can be artificially controlled through discrete RF attenuators placed between the DUT and reference antenna RF port, inside the RF enclosure. The tables 1 and 2 summarize the simulation results taken with MIMO 2x2 references antennas simulation models.

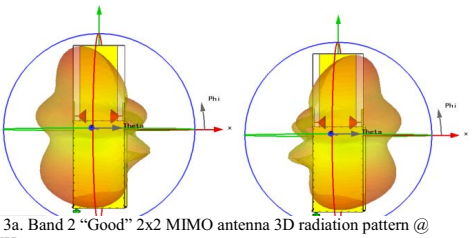

Figure 3a. Band 2 “Good” 2x2 MIMO antenna 3D radiation pattern @ 1960MHz.

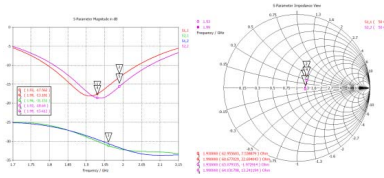

Figure 3b. Band 2 “Good” 2x2 MIMO antenna Return Loss and Impedance characteristic.

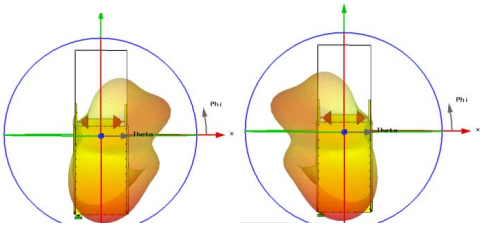

Figure 4a. Band 2 “Nominal” 2x2 MIMO antenna 3D radiation pattern @ 1960MHz.

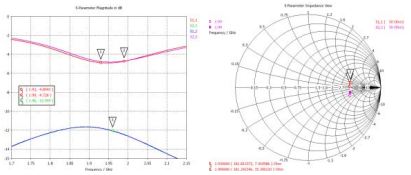

Figure 4b. Band 2 “Nominal” 2x2 MIMO antenna Return Loss and Impedance characteristic

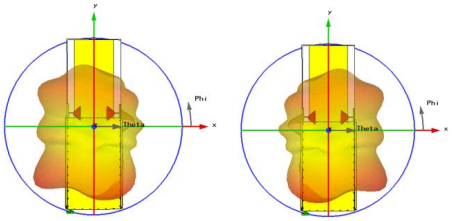

Figure 5a. Band 7 “Good” 2x2 MIMO antenna 3D radiation pattern @ 2.655GHz.

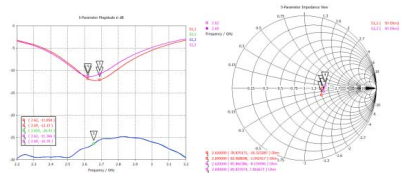

Figure 5b. .Band 7 “Good” 2x2 MIMO antenna Return Loss and Impedance characteristic

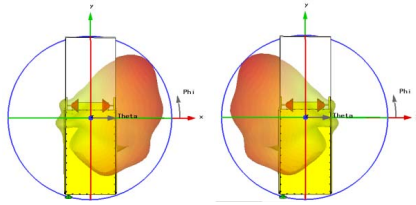

Figure 6a.Band 7 “Nominal” 2x2 MIMO antenna 3D radiation pattern @ 2.655GHz.

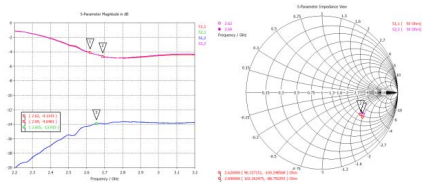

Figure 6b. .Band 7 “Nominal” 2x2 MIMO antenna Return Loss and Impedance characteristic

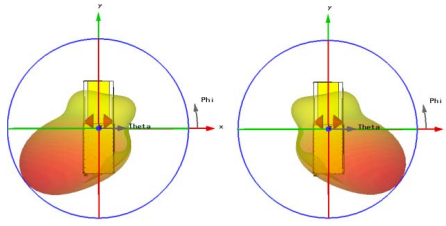

Figure 7a. Band 13 “Good” 2x2 MIMO antenna 3D radiation pattern @ 751MHz.

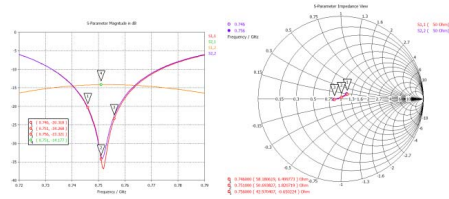

Figure 7b. Band 13 “Good” 2x2 MIMO antenna Return Loss and Impedance characteristic

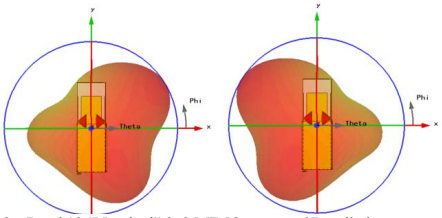

Figure 8a. Band 13 “Nominal” 2x2 MIMO antenna 3D radiation pattern @ 751MHz.

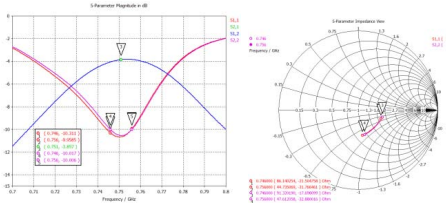

Figure 8b. Band 13 “Nominal” 2x2 MIMO antenna Return Loss and Impedance characteristic

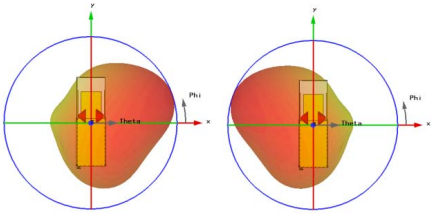

Figure 9a. Band 13 “Bad” 2x2 MIMO antenna 3D radiation pattern @ 751MHz.

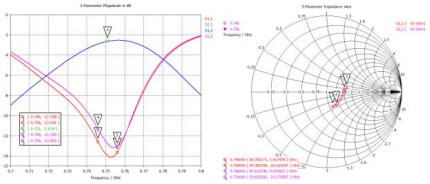

Figure 9b. Band 13 “Bad” 2x2 MIMO antenna Return Loss and Impedance characteristic

TABLE I, Total Antenna Efficiency

		Antenna 1			Antenna 2		
		1930MHz	1960MHz	1990MHz	1930MHz	1960MHz	1990MHz
Band	Antenna Configuration	SE (%)	SE (%)	SE (%)	SE (%)	SE (%)	SE (%)
2	"Good" 2x2 MIMO	96.7	95.6	93.5	97.3	97.1	95.9
	"Nominal" 2x2 MIMO	59.9	60.4	59.7	58.7	59.7	59.3
Band	Antenna Configuration	2.62GHz	2.655GHz	2.69GHz	2.62GHz	2.655GHz	2.69GHz
7	"Good" 2x2 MIMO	91.4	91.2	91.1	90.1	90.1	88.9
	"Nominal" 2x2 MIMO	55.5	58.0	59.5	55.8	58.0	59.1
Band	Antenna Configuration	746MHz	751MHz	756MHz	746MHz	751MHz	756MHz
13	"Good" 2x2 MIMO	93.6	94.6	94.5	93.6	94.6	94.4
	"Nominal" 2x2 MIMO	53.7	58.5	54.9	52.5	57.3	54.1
	"Bad" 2x2 MIMO	40.6	41.6	37.9	40.4	41.8	38.4

TABLE II, Gain Imbalance and Magnitude of Complex Correlation Coefficient

		Gain Imbalance (dB)			Mag Complex Cor. Coef.		
Band	Antenna Configuration	1930MHz	1960MHz	1990MHz	1930MHz	1960MHz	1990MHz
2	"Good" 2x2 MIMO	0.027	0.068	0.110	0.009	0.004	0.001
	"Nominal" 2x2 MIMO	0.088	0.051	0.027	0.45	0.46	0.46
Band	Antenna Configuration	2.62GHz	2.655GHz	2.69GHz	2.62GHz	2.655GHz	2.69GHz
7	"Good" 2x2 MIMO	0.062	0.053	0.106	0.019	0.024	0.029
	"Nominal" 2x2 MIMO	0.023	0.001	0.031	0.37	0.39	0.40
Band	Antenna Configuration	746MHz	751MHz	756MHz	746MHz	751MHz	756MHz
13	"Good" 2x2 MIMO	0.000	0.001	0.005	0.02	0.05	0.08
	"Nominal" 2x2 MIMO	0.101	0.087	0.065	0.61	0.58	0.54
	"Bad" 2x2 MIMO	0.025	0.027	0.054	0.92	0.91	0.89

V. CONCLUSIONS

A reference MIMO 2x2 antenna concept has been presented including simulation results. In this work the investigation has been carried out for the special case of uniform incoming power distribution only. These antennas will aid future research on MIMO OTA measurement methodologies, playing an important role minimizing measurement uncertainty, and validating test methodologies. These antennas are currently in production and measurement data will be available shortly.

Acknowledgement

The authors wish to acknowledge the support from CTIA, Aalborg University, Motorola Mobility and Satimo.

REFERENCES

[1] Agilent Technologies, “Analysis of initial measurement campaign results”, 3GPP TSG RAN WG4#59, R4-113097, Barcelona, May 2011

[2] Elektrobit, Nokia, “Comparison of full Anechoic chamber measurement results”, 3GPP TSG RAN WG4#61, R4-115927, San Francisco, November 2011

[3] B. Yanakiev, J. O. Nielsen, G.F. Pedersen, “On small antenna measurements in a realistic MIMO scenario”, EuCAP 2010

[4] W. C. Jakes, “Microwave Mobile Communications”, New York: Wiley, 1974

[5] A. Stjernman, “Antenna Mutual Coupling Effect on Correlation Efficiency and Shannon Capacity”. Antenna and Propagation EuCap 2006

[6] http://www.cst.com

Paper 2

Design and Verification of MIMO 2x2 Reference Antennas

Istvan Szini, Gert Pedersen, John Strada, Alessandro Scannavini and Lars Foged

Published as:
Szini, I.; Pedersen, G. F.; Estrada, J.; Scannavini, A.; Foged, L.J.,
"Design and verification of MIMO 2x2 reference antennas"
Antennas and Propagation Society International Symposium (APSURSI), 2012 IEEE ,
vol., no., pp.1,2, 8-14 July 2012
doi: 10.1109/APS.2012.6348702

Design and Verification of MIMO 2x2 Reference Antennas

I Szini[1, 2], G.F. Pedersen[1], J. Estrada[3], A. Scannavini[4], L. J. Foged[4]

[1]Antennas, Propagation and Radio Networking,
Department of Electronic Systems, Faculty of Engineering
and Science, Aalborg University, Denmark
Email: gfp@ee.aau.edu

[2]Motorola Mobility Inc. Libertyville, Illinois, USA
Email: Istvan.Szini@motorola.com

[3]SATIMO, Kennesaw, Georgia, USA
Email: jestrada@satimo.com

[4]SATIMO, Pomezia, Italy
Email: ascannavini@satimo.com, lfoged@satimo.com

***Abstract*—The development and initial discussion of a reference MIMO 2x2 antenna concept has been presented in [1]. The reference antenna concept has been created to eliminate the uncertainties linked to the unknown antenna performance of the few LTE MIMO 2x2 reference devices or golden standards currently available for evaluating radiated data throughput measurement methodologies and test facilities. The proposed concept is based on simple antennas with a well-known Figure of Merit (FoM) and controllable performance. In this paper we present the recent developments on the antenna concept and report on the first measured performance at uniform incoming power distribution, figures and correlations between different measurement labs.**

I. INTRODUCTION

Long Term Evolution (LTE) adopt multi-antenna mechanisms to increase coverage and physical layer capacity. Therefore, Multiple Input Multiple Output (MIMO) antenna systems are required on LTE systems. Other than the specific antenna system figure of merit (FoM), i.e. total antenna efficiency, gain imbalance, correlation coefficient also the MIMO system performance is defined by radiated data throughput. Different standardization bodies are working towards test methodologies and procedures to proper emulate a realistic scattered environment to determine true MIMO performance. This task had become very complex based on several implementation details pertinent of each test methodology [2].

Recent comparison campaigns, based on measurement of radiated MIMO data throughput on available LTE MIMO 2x2 reference devices have shown to be ineffective as a correlation instrument since they have been based on different test devices and different test methodologies. Since the MIMO OTA standard test procedure is still under development, all currently available reference devices, have been designed as optimum performance devices and not with the specific scope as a measurement verification devices [3].

In order to properly test and verify, the correlation and accuracy of different MIMO data throughput measurement systems, the reference antennas must represent the full range of "good", "nominal" and "bad" MIMO 2x2 antenna performance. The MIMO 2x2 Reference Antenna concept has been created specifically to emulate these three performances ranges. The adoption of simple reference antennas with well-known performance also eliminate part of the measurement uncertainty and increase the correlation among different MIMO OTA test methodologies and test facilities. The final antenna design is simple and low cost to enable widespread use.

II. REFERENCE ANTENNA CONCEPT

The MIMO 2x2 Reference Antenna concept was conceived during the first CTIA (Cellular Telecommunications and Internet Association) MIMO OTA Sub-Group meetings and initially were intended to cover three LTE bands (2, 7 and 13).

For each band, three antennas were designed to emulate a "good" MIMO antenna system, i.e. low correlation coefficient ($\rho<0.1$), high total antenna efficiency (>90%) and low gain imbalance ($\Delta G\cong 0$dB). Respectively the "nominal" MIMO antenna system has moderate correlation coefficient ($\rho\leq 0.5$), moderate total antenna efficiency ($\geq$50%) and low gain imbalance ($\Delta G\cong 0$dB). Finally the "bad" MIMO antenna system, having poor correlation coefficient ($\rho\geq 0.9$), moderate-to-poor total antenna efficiency ($\leq$50%) and low gain imbalance ($\Delta G \cong 0$dB).

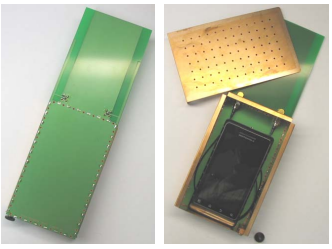

Figure 1. Band 13 "Good" MIMO 2x2 antenna prototype.

Other than the electrical performance constrains, the reference antenna also needs to solve the potential problem with connecting any external antenna into a portable device. The connection between the portable device RF port and the external antenna, normally a coaxial cable, can potentially carry current in the outer conductor [4]. The associated radiation perturbs the antenna system radiation and influence

system parameters like correlation coefficient, absolute gain and gain imbalance. For this reason the antenna was conceived attaching MIMO 2x2 external antennas to a RF enclosure, where the DUT and its RF connections are located. The initial prototype is shown in Fig. 1.

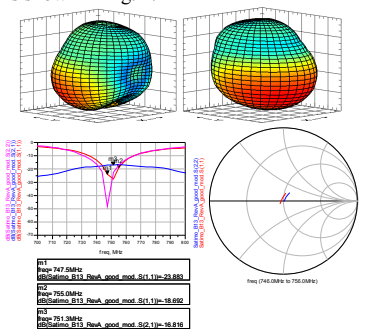

Figure 2. B13 "Good" MIMO 2x2 antennas, measured 3D radiation pattern (751MHz), Return Loss and impedance Characteristic.

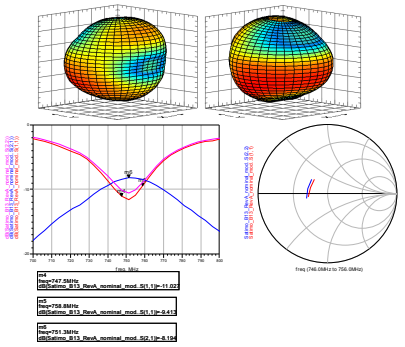

Figure 3. B13 "Nominal" MIMO 2x2 antennas, measured 3D radiation pattern (751MHz), Return Loss and impedance Characteristic.

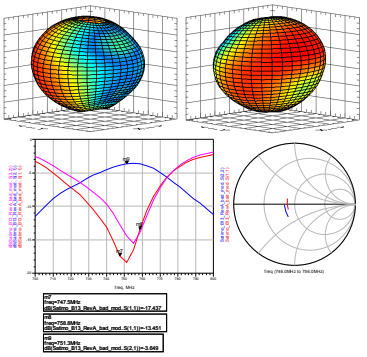

Figure 4. B13 "Bad" MIMO 2x2 antennas, measured 3D radiation pattern (751MHz), Return Loss and impedance Characteristic.

The MIMO 2x2 antenna system was initially simulated on CST Microwave Studio [5]. The antennas are self resonant based on the Inverted "F" antenna topology, as shown in Fig. (1). The control of magnitude of complex correlation coefficient is achieved through the reference ground plane placement between antennas radiators. Since the antennas are absolutely symmetric, the gain imbalance between the antennas is always near to 0dB, considering an environment which the fields arrives from all directions. With this feature, the gain imbalance between antennas can be artificially controlled through discrete RF attenuators placed between the DUT and reference antenna RF port, inside the RF enclosure. The tables 1 and 2 summarize the measurement results taken with MIMO 2x2 references antennas prototypes.

Table 1 B2/7/13 Total Antenna Efficiency

		Antenna 1			Antenna 2		
		1930MHz	1960MHz	1990MHz	1930MHz	1960MHz	1990MHz
Band	Antenna Configuration	SE (%)	SE (%)	SE (%)	SE (%)	SE (%)	SE (%)
2	"Good" 2x2 MIMO	88.5	93.1	95.8	88.6	91.2	94.2
	"Nominal" 2x2 MIMO	62.9	63.1	60.8	65.9	63.8	62.4
Band	Antenna Configuration	2.62GHz	2.655GHz	2.69GHz	2.62GHz	2.655GHz	2.69GHz
7	"Good" 2x2 MIMO	91.9	93.6	87.9	95.3	89.9	82.2
	"Nominal" 2x2 MIMO	70.8	69.9	62.1	74.1	63.8	57.9
Band	Antenna Configuration	746MHz	751MHz	756MHz	746MHz	751MHz	756MHz
13	"Good" 2x2 MIMO	89.2	93.2	88.6	87.5	91.8	87.6
	"Nominal" 2x2 MIMO	60.1	58.8	57.2	60.0	58.8	57.3
	"Bad" 2x2 MIMO	50.9	49.7	45.3	51.7	50.3	45.8

Table 2 Gain Imbalance and Magnitude of Complex Correlation Coefficient

		Gain Imbalance (dB)			Mag Complex Cor. Coef.		
Band	Antenna Configuration	1930MHz	1960MHz	1990MHz	1930MHz	1960MHz	1990MHz
2	"Good" 2x2 MIMO	0.00	0.09	0.07	0.04	0.04	0.04
	"Nominal" 2x2 MIMO	0.20	0.05	0.11	0.40	0.40	0.38
Band	Antenna Configuration	2.62GHz	2.655GHz	2.69GHz	2.62GHz	2.655GHz	2.69GHz
7	"Good" 2x2 MIMO	0.16	0.17	0.29	0.06	0.05	0.05
	"Nominal" 2x2 MIMO	0.20	0.39	0.31	0.35	0.35	0.34
Band	Antenna Configuration	746MHz	751MHz	756MHz	746MHz	751MHz	756MHz
13	"Good" 2x2 MIMO	0.08	0.07	0.05	0.01	0.03	0.06
	"Nominal" 2x2 MIMO	0.00	0.00	0.01	0.60	0.56	0.52
	"Bad" 2x2 MIMO	0.07	0.06	0.05	0.93	0.92	0.90

III. CONCLUSIONS

A reference MIMO 2x2 antenna concept has been presented including measurement results. In this work the investigation has been carried out for the special case of uniform incoming power distribution only. These antennas will aid future research on MIMO OTA measurement methodologies, playing an important role minimizing measurement uncertainty, and validating test methodologies.

Acknowledgement

The authors wish to acknowledge the support from CTIA, Aalborg University, Motorola Mobility and Satimo.

REFERENCES

[1] Motorola Mobility, "Reference Antennas proposal for MIMO OTA", 3GPP TSG RAN WG4#59, R4-113032, Barcelona, Spain, May 2011

[2] Agilent Technologies, "Analysis of initial measurement campaign results", 3GPP TSG RAN WG4#59, R4-113097, Barcelona, May 2011

[3] Elektrobit, Nokia, "Comparison of full Anechoic chamber measurement results", 3GPP TSG RAN WG4#61, R4-115927, San Francisco, November 2011

[4] B. Yanakiev, J. O. Nielsen, G.F. Pedersen, "On small antenna measurements in a realistic MIMO scenario", EuCAP 2010

[5] www.cst.com

Paper 3

LTE Radiated Data Throughput Measurements Adopting, MIMO 2x2 Reference Antennas

Istvan Szini, Gert Pedersen, Samantha Del Barrio and Michael Foegelle

Published as:
Szini, I.; Pedersen, G. F.; Del Barrio, S.C.; Foegelle, M.D.,
”LTE Radiated Data Throughput Measurements, Adopting MIMO 2x2 Reference Antennas”
Vehicular Technology Conference (VTC Fall), 2012 IEEE ,
vol., no., pp.1,5, 3-6 Sept. 2012
doi: 10.1109/VTCFall.2012.6399235

LTE Radiated Data Throughput Measurements, Adopting MIMO 2x2 Reference Antennas

I. Szini[1,2], G. F. Pedersen[1], S. C. Del Barrio[1] , M. D. Foegelle[3]

[1] Antennas, Propagation and Radio Networking, Department of Electronic Systems,Faculty of Engineering and Science, Aalborg University, Denmark
{gfp, scdb}@es.aau.dk

[2] Motorola Mobility Inc., Libertyville, USA.
Istvan.Szini@motorola.com

[3] ETS-Lindgren, L. P., Cedar Park, USA
Michael.Foegelle@ets-lindgren.com

Abstract— **Long Term Evolution (LTE) requires Multiple Input Multiple Output (MIMO) antenna systems. Consequently a new over-the-air (OTA) test methodology need to be created to make proper assessment of LTE devices radiated performance. The antenna specific parameters i.e. total antenna efficiency, gain imbalance and correlation coefficient, are essential for a proper MIMO antenna system design. However it can't be use directly to assess the LTE device system performance, since a multiplicity of other factors are involved, e.g. power amplifier load-pull, low noise amplifier source-pull, self interference noise, baseband algorithm and other factors. Several standard organizations are working towards a consensus over the proper OTA MIMO test method, however so far results of measurement campaigns have ambiguous results not allowing a desirable progress [1]. Initially presented at one of several MIMO OTA standard meetings [2], the reference antenna was conceived considering the special case of uniform distribution of incoming power. This paper shows an antenna system that will aid standard organizations and research labs adopting anechoic or reverberation chambers to proper investigate OTA radiated performance, ruling out the LTE devices unknown MIMO 2x2 antenna performance.**

Keywords-component; LTE; MIMO; OTA; antennas; data; throughput

I. INTRODUCTION

With main objective to benchmark MIMO OTA test methodologies, the MIMO 2x2 reference antennas were created to rule out the unknown LTE device antenna performance, and replace the device antenna by an MIMO 2x2 antenna system with known performance, eliminating this element from the OTA measurement variables. In this context a set of three antennas per each desirable band was created, allowing better repeatability and less measurement uncertainty among labs.

II. REFERENCE ANTENNA CONCEPT

The MIMO 2x2 reference antennas were conceived during the first CTIA (Cellular Telecommunications and Internet Association) MIMO OTA Sub-Group meeting, and initially were designed to cover three LTE bands (2, 7 and 13). Conceptually for each band three antennas were designed to emulate a "good" MIMO antenna system figure of merit (FoM), i.e. low correlation coefficient ($\rho<0.1$), high total antenna efficiency ($\eta>90\%$) and low gain imbalance ($\Delta G \cong 0dB$). Respectively the "nominal" MIMO antenna system has moderate correlation coefficient ($\rho \leq 0.5$), moderate total antenna efficiency ($\eta \geq 50\%$) and low gain imbalance ($\Delta G \cong 0dB$). And finally the "bad" MIMO antenna system, having poor correlation coefficient ($\rho \geq 0.9$), moderate-to-poor total antenna efficiency ($\eta \leq 50\%$) and low gain imbalance ($\Delta G \cong 0dB$).

Other than the electrical performance constrains, the reference antenna also needs to solve the potential problem with connecting any external antenna into a portable device. The connection between the portable device RF port and the external antenna, normally a coaxial cable, can potentially carry current in the outer conductor. The associated radiation perturbs the antenna system radiation and influence system parameters like correlation coefficient, absolute gain and gain imbalance [3]. For this reason the antenna was conceived attaching MIMO 2x2 external antennas to a RF enclosure, where the DUT and its RF connections are located. The initial prototype is shown in Fig. 1.

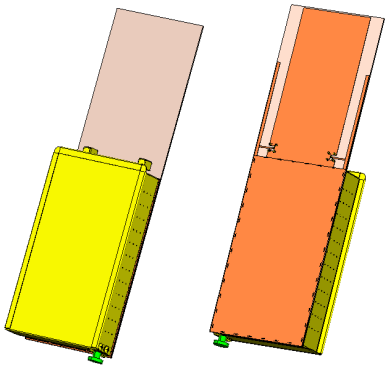

Figure 1a. MIMO 2x2 Reference Antenna concept. Front (left) and back (right) view of the closed antenna.

978-1-4673-1881-5/12/$31.00 ©2012 IEEE

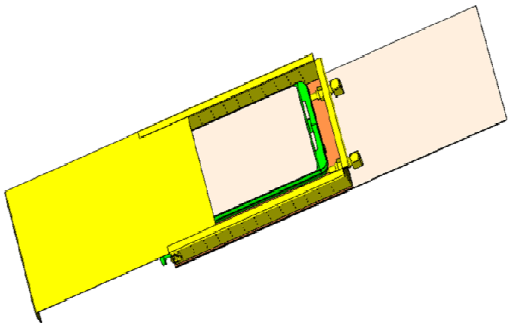

Figure 1b. MIMO 2x2 Reference Antenna concept. Open antenna with inserted active device.

III. Analysis of Magnitude of Correlation Coefficient Impact on MIMO 2x2 System Capacity

The magnitude of the complex correlation coefficient between two antennas is shown in [4]. It can be seen, that the coefficient is predominantly defined by the complex radiation patterns of the antennas, in this case a generic scenario is presented where the incoming power is uniformly distributed in both theta and phi directions, it's understood that in the real environment this condition is unlikely to happen, however true in the reverberation and controlled anechoic test environment.

$$\rho_{12} = \frac{\left| \oint \{ (XPR \cdot E_{\theta MA}(\Omega) \cdot E^*_{\theta SA}(\Omega) + E_{\phi MA}(\Omega) \cdot E^*_{\phi SA}(\Omega) \} d\Omega \right|^2}{\oint \{ XPR \cdot G_{\theta MA}(\Omega) + G_{\phi MA}(\Omega) \} d\Omega \cdot \oint \{ XPR \cdot G_{\theta SA}(\Omega) + G_{\phi SA}(\Omega) \} d\Omega} \quad (1)$$

$E_{\theta MA}$ (Ω) is the vertical polarization complex radiation pattern from Main Antenna, $E_{\theta SA}$ (Ω) is the vertical polarization complex radiation pattern from Secondary Antenna, $E_{\phi MA}$ (Ω) is the horizontal polarization complex radiation pattern from Main Antenna, $E_{\phi SA}$ (Ω) is the horizontal polarization complex radiation pattern from Secondary Antenna. Ω is the solid angle for a spherical coordinate system and *XPR* is cross-polar discrimination of the antennas.

The primary objective of implementing a MIMO system is to improve the system capacity. Considering the MIMO 2x2 system as focus in this study, the basic graphical representation of the antenna arrangement is shown in Fig 2.

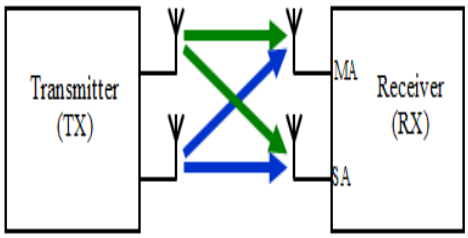

Fig 2. MIMO 2x2 system, graphical representation

Considering (1) from an analytic perspective only, the correlation coefficient can be controlled by varying both arguments and it appears that the cross correlation can be minimized simply by increasing the gain imbalance between the two antennas. However, from a system performance perspective, a high gain imbalance will not lead to improved MIMO performance since this condition in its extreme form is equivalent to the pure MISO system with just one antenna [5].

A successful MIMO antenna design requires that each pair of antennas have approximately the same power loss, same gain and closely uncorrelated. To optimize MIMO capacity several basic properties needs to be observed as summarized below:

1. Both antennas; Main Antenna and Secondary Antenna; needs to have appropriate radiated performance with minimum gain imbalance, ideally 0dB;
2. In the rich scattered environment the maximum capacity will occur when both receiver antennas where cross-polarized, consequently the antennas need to be uncorrelated;
3. The absolute phase response of the reference antennas are irrelevant, but not the phase per direction neither the relative phase relationship between the antennas and the gain imbalance, which defines the MIMO antenna system correlation coefficient;
4. The ideal MIMO 2x2 antenna system, considering ideal isolation between antennas (>20dB), gain imbalance 0dB, and correlation coefficient 0, will provide the double of capacity of counterpart SISO system (this statement is based solely on antenna parameters).
5. The antennas radiation patterns need to have similar directivity, two directional antennas with main lobe in opposite directions, will not enable acceptable MIMO performance in poor scattered environment.

IV. Simulation Results

The MIMO 2x2 antenna system was initially simulated on CST Microwave Studio [6]. The antennas are self-resonant and based on the Inverted "F" antenna topology, as shown in Fig. 3 to 5. The figures illustrate the band 13 3D radiation patterns of each of the two antennas in the nominal, good and bad configurations including return loss and impedance characteristics.

The control of the magnitude of complex correlation coefficient is achieved through the reference ground plane placement between antennas radiators. Since the antennas are absolutely symmetric, the gain imbalance between the antennas is always near to 0dB, considering an environment which the fields arrives from all directions. With this feature, the gain imbalance between antennas can be artificially controlled through discrete RF attenuators placed between the DUT and reference antenna RF port, inside the RF enclosure.

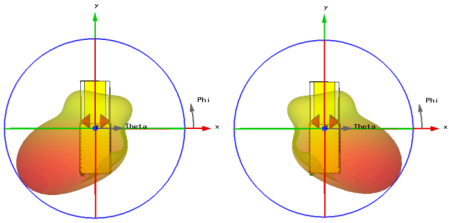

Figure 3a. Band 13 “Good” 2x2 MIMO antenna 3D radiation pattern @ 751MHz.

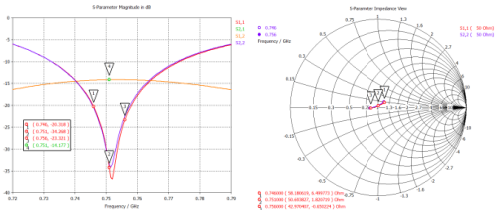

Figure 3b. Band 13 “Good” 2x2 MIMO antenna Return Loss and Impedance characteristic

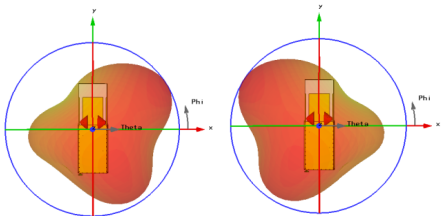

Figure 4a. Band 13 “Nominal” 2x2 MIMO antenna 3D radiation pattern @ 751MHz.

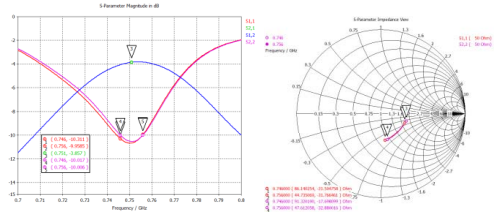

Figure 4b. Band 13 “Nominal” 2x2 MIMO antenna Return Loss and Impedance characteristic

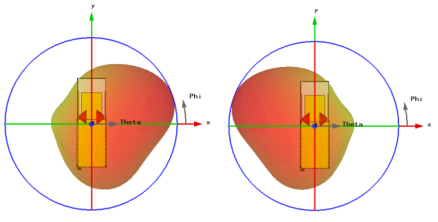

Figure 5a. Band 13 “Bad” 2x2 MIMO antenna 3D radiation pattern @ 751MHz.

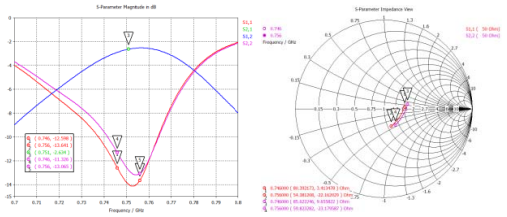

Figure 5b. Band 13 “Bad” 2x2 MIMO antenna Return Loss and Impedance characteristic

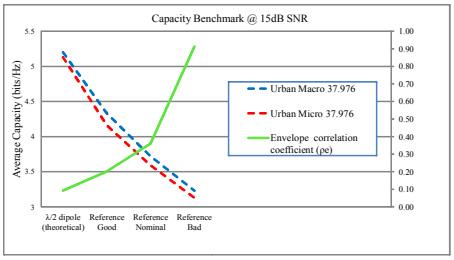

Figure 6. Simulated average capacity adopting B13 MIMO 2X2 reference antennas complex radiation pattern

Adopting the drops defined in 3GPP TR 37.976 [7], the average capacity was predicted based on full link simulation model, adopting SCME channel model and CTIA MIMO 2x2 reference B13 antennas measured radiation patterns (figure 6). These simulations only considered azimuth cut and vertical polarization.

V. MEASUREMENTS RESULTS

The figure 7 demonstrates the realization of this antenna concept, the left picture indicates the bare PCB with the 2 antennas at the top on each side. Right, the RF shield attached and the active device inserted and the RF lit shown.

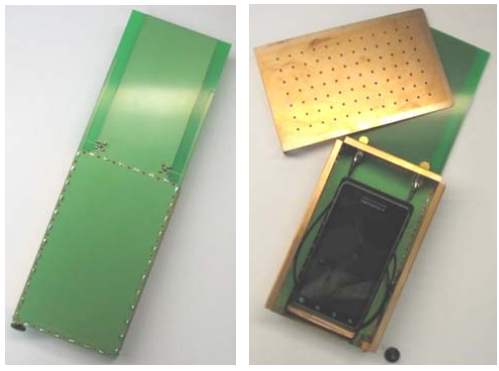

Figure 7. Band 13 “Good” MIMO 2x2 antenna prototype.

Similar to the simulation results, the figures 8 to 10, shows radiation pattern measured at full anechoic chamber, return loss and impedance characteristic of band 13

reference antennas. The overall FoM benchmark between simulation and measurements is done on tables 1 and 2.

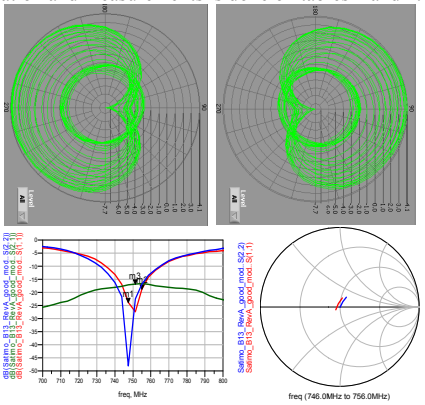

Figure 8. B13 “Good” MIMO 2x2 antennas, measured 2D radiation pattern (751MHz), Return Loss and impedance Characteristic.

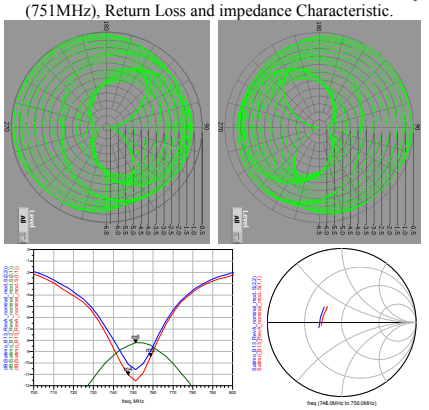

Figure 9. B13 “Nominal” MIMO 2x2 antennas, measured 2D radiation pattern (751MHz), Return Loss and impedance Characteristic.

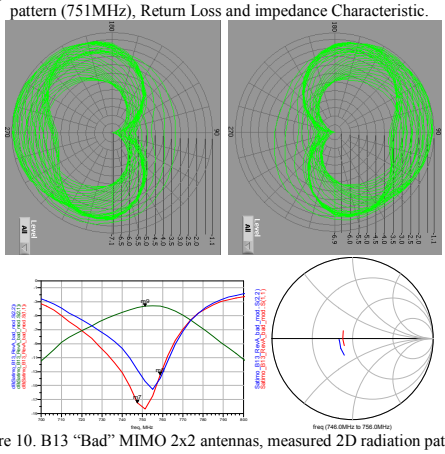

Figure 10. B13 “Bad” MIMO 2x2 antennas, measured 2D radiation pattern (751MHz), Return Loss and impedance Characteristic.

Table 1 B2/7/13 Total Antenna Efficiency

		Antenna 1			Antenna 2		
		1930MHz	1960GHz	1990MHz	1930MHz	1960MHz	1990MHz
Band	Antenna Configuration	η (%)	η (%)	η (%)	η (%)	η (%)	η (%)
2	Simulated "Good" 2x2 MIMO	96.7	95.6	93.5	97.3	97.1	95.9
	Measured "Good" 2x2 MIMO	88.5	93.1	95.8	88.6	91.2	94.2
	Simulated "Nominal" 2x2 MIMO	59.9	60.4	59.7	58.7	59.7	59.3
	Measured "Nominal" 2x2 MIMO	62.9	63.1	60.8	65.9	63.8	62.4
Band	Antenna Configuration	2.62GHz	2.655GHz	2.69GHz	2.62GHz	2.655GHz	2.69GHz
7	Simulated "Good" 2x2 MIMO	91.4	91.2	91.1	90.1	90.1	88.9
	Measured "Good" 2x2 MIMO	91.9	93.6	87.9	95.3	89.9	82.2
	Simulated "Nominal" 2x2 MIMO	55.5	58.0	59.5	55.8	58.0	59.1
	Measured "Nominal" 2x2 MIMO	70.8	69.9	62.1	74.1	63.8	57.9
Band	Antenna Configuration	746MHz	751MHz	756MHz	746MHz	751MHz	756MHz
13	Simulated "Good" 2x2 MIMO	93.6	94.62	94.46	93.61	94.59	94.35
	Measured "Good" 2x2 MIMO	89.2	93.2	88.6	87.5	91.8	87.6
	Simulated "Nominal" 2x2 MIMO	53.7	58.5	54.9	52.5	57.3	54.1
	Measured "Nominal" 2x2 MIMO	60.1	58.8	57.2	60.0	58.8	57.3
	Simulated "Bad" 2x2 MIMO	40.6	41.6	37.9	40.4	41.8	38.4
	Measured "Bad" 2x2 MIMO	50.9	49.7	45.3	51.7	50.3	45.8

Table 2 B2/7/13 Gain Imbalance and Magnitude of Complex Correlation Coefficient

		Gain Imbalance (dB)			Mag Complex Cor. Coef.		
Band	Antenna Configuration	1930MHz	1960MHz	1990MHz	1930MHz	1960MHz	1990MHz
2	Simulated "Good" 2x2 MIMO	0.027	0.068	0.110	0.009	0.004	0.001
	Measured "Good" 2x2 MIMO	0.005	0.089	0.070	0.039	0.040	0.044
	Simulated "Nominal" 2x2 MIMO	0.088	0.051	0.027	0.450	0.460	0.460
	Measured "Nominal" 2x2 MIMO	0.202	0.048	0.113	0.403	0.395	0.377
Band	Antenna Configuration	2.62GHz	2.655GHz	2.69GHz	2.62GHz	2.655GHz	2.69GHz
7	Simulated "Good" 2x2 MIMO	0.062	0.053	0.106	0.019	0.024	0.029
	Measured "Good" 2x2 MIMO	0.155	0.174	0.288	0.056	0.054	0.049
	Simulated "Nominal" 2x2 MIMO	0.023	0.001	0.031	0.370	0.390	0.400
	Measured "Nominal" 2x2 MIMO	0.196	0.393	0.307	0.348	0.353	0.343
Band	Antenna Configuration	746MHz	751MHz	756MHz	746MHz	751MHz	756MHz
13	Simulated "Good" 2x2 MIMO	0.000	0.001	0.005	0.018	0.052	0.083
	Measured "Good" 2x2 MIMO	0.084	0.066	0.046	0.007	0.026	0.063
	Simulated "Nominal" 2x2 MIMO	0.101	0.087	0.065	0.614	0.576	0.539
	Measured "Nominal" 2x2 MIMO	0.004	0.000	0.009	0.603	0.556	0.519
	Simulated "Bad" 2x2 MIMO	0.025	0.027	0.054	0.921	0.906	0.888
	Measured "Bad" 2x2 MIMO	0.074	0.057	0.053	0.933	0.918	0.899

The antennas were tested in an MIMO OTA test system (figure 10), consisting of a circular array of dual polarized antennas in an anechoic chamber, fed by an 8 channel emulator through a set of low noise amplifiers, properly correlating, fade, scale, delay, and distribute the signal to each test probe in the chamber.

For the purpose of this test, the DUT was oriented vertically polarized, so only eight evenly spaced vertically polarized elements located every 45 degrees were used to generate the test environment. This configuration has been shown to produce an environment equivalent to the ideal free space condition for devices of the target size [8], and is thus considered sufficient for the purposes of this evaluation. The test procedure followed that outlined in 3GPP TR 37.976, for a 16 QAM downlink. The device under test (DUT) was rotated in 45 degree steps to capture throughput vs. power curves at each position and then determine the average throughput vs. power across all orientations. In addition to the OTA tests, a series of conducted tests were performed using both a constant tap (through connection) model and conducted models based on each of the OTA models where ideal dipoles were used as the modeled receiving antennas. The constant tap result was also compared to direct connection tests between the base station emulator and the DUT to confirm that the calibrated path through the channel emulator produced the same result as a direct connection.

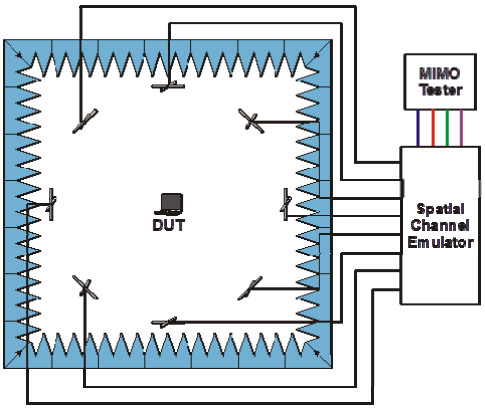

Figure 10. OTA data throughput measurement setup

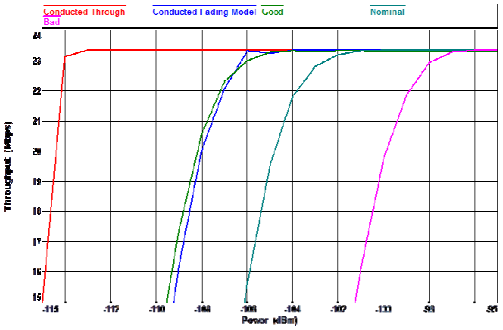

Figure 11. Data throughput measured with LTE device and B13 MIMO 2x2 Reference antenna

As indicated on figure 11, the band 13 reference antenna was evaluated in a MIMO anechoic chamber, where an arbitrarily spatial channel model was applied. The data throughput measured with "good" reference MIMO antenna (green curve), agrees well with LTE device conducted data throughout measured under same channel model (dark blue curve). While the "nominal" (light blue curve) and "bad" (pink curve), indicates that the reference antenna system can be used to discriminate over 8dB range, the "good" from "bad" MIMO antennas.

VI. CONCLUSIONS

A reference MIMO 2x2 antenna concept has been presented including simulated and measurement benchmarked results. In this work the antenna related investigation has been carried out for the special case of uniform incoming power distribution only, however the system data throughput is demonstrated in a non-uniform spatial channel environment. These antennas demonstrate good discrimination between "good", "nominal" and "bad" designs, either on uniform or non-uniform environments, and will aid future research on MIMO OTA measurement methodologies, playing an important role minimizing measurement uncertainty, and validating test methodologies.

Acknowledgement

The authors wish to acknowledge the support from CTIA and Motorola Mobility.

REFERENCES

[1] Agilent Technologies, "Analysis of initial measurement campaign results", *3GPP TSG RAN WG4#59*, R4-113097, Barcelona, May 2011

[2] Motorola Mobility, "Reference Antennas proposal for MIMO OTA", *3GPP TSG RAN WG4#59*, R4-113032, Barcelona, Spain, May 2011

[3] Yanakiev, Boyan; Nielsen, Jesper O.; Pedersen, Gert F.; , "On small antenna measurements in a realistic MIMO scenario," *Antennas and Propagation (EuCAP), 2010 Proceedings of the Fourth European Conference on* , vol., no., pp.1-5, 12-16 April 2010

[4] W. C. Jakes, *Microwave Mobile Communications*, New York: Wiley, 1974

[5] Stjernman, Anders; , "Antenna mutual coupling effects on correlation, efficiency and Shannon capacity," *Antennas and Propagation, 2006. EuCAP 2006. First European Conference on* , vol., no., pp.1-6, 6-10 Nov. 2006

[6] http://www.cst.com

[7] http://www.3gpp.org/ftp/Specs/html-info/37976.htm

[8] M.D. Foegelle, "Creating a Complex Multipath Environment in an Anechoic Chamber", *Microwave Journal*, Vol. 53, No. 8, August, 2008, p. 56-64

Paper 4

MIMO 2x2 absolute data throughput concept

Istvan Szini, Gert Pedersen,Alexandru Tatomirescu and Anatoliy Ioffe

Published as:
Szini, I.; Pedersen, G.; Tatomirescu, A.; Ioffe, A.,
"MIMO 2x2 absolute data throughput concept"
Antennas and Propagation (EuCAP), 2013 7th European Conference on ,
vol., no., pp.299,302, 8-12 April 2013

MIMO 2x2 Absolute Data Throughput Concept

Charaterizing UE Performance in a Geometrically Defined Spatial Fading Scenario

I. Szini[1,2], G. Pedersen [2], A. Tatomirescu[2], A. Ioffe[3]

[1] Motorola Mobility Inc, Antenna Innovation Research Lab, Libertyville/IL, USA, Istvan.Szini@morotorola.com

[2] Antennas, Propagation and Radio Networking section at the Department of Electronic Systems, Faculty of Engineering and Science, Aalborg University, Niels Jernes Vej 12, 9220, Aalborg, Denmark,{ ijs, gfp, ata }@es.aau.dk

[3] Intel Corporation, Hillsboro/OR, USA, anatoliy.ioffe@intel.com

Abstract— **MIMO over the air (OTA) test methodologies had been investigated in diverse standard bodies around the world, despite the concentrated efforts towards the determination of a valid test method which emulates realistic environment, up to this date there are no consensus towards a single MIMO OTA test methodology.**

The definition of a test methodology which emulates real scattered environment is a complex task, a sum of several factors contribute for the variability of measurement results. Observing recent measurement campaign sponsored by the Third Generation Partnership Project through its Technical Specification Group defined as Radio Access Network 4 (3GPP TSG RAN4), several sources of uncertainty were observed. Starting from the unknown radiated performance of devices under test (DUT), an effort to create a set of reference antennas was identified, generating the MIMO 2x2 reference antennas [1], thus partially reducing the uncertainty over the candidate test methodologies.

While the reference antennas defines a known radiated performance of the DUT, other sources of measurement uncertainty still invalidate the search for an accurate MIMO OTA test methodology, as learnt in the previous measurement campaign from 3GPP RAN4, any measurement campaign of this complexity must start from well defined baseline measurements among participant labs. Initially a simulation campaign was proposed to define such baseline. Soon this approach was refused due intellectual property (IP) embedded in each DUT manufacturer mobile device ship set, therefore disabling any attempt to share realistic DUT dependent LTE MIMO full-link simulation models.

Investigating other technical sound options to establish a baseline measurement, and protect IP from every DUT manufacturer, as specialized conducted measurement was elaborated. This work will introduce the concept behind this measurement, also known as MIMO 2x2 Absolute Data Throughput.

Index Terms—antennas, antennas radiation pattern, mobile antennas, anisotropic, MIMO, 4G mobile communication.

I. INTRODUCTION

In an effort to compare different MIMO OTA methodologies' results to conducted results under the implementations of channel models defined in [2], the absolute data throughput comparison framework has been defined by utilizing the reference antennas [1] and reference mobile devices (LTE capable handsets).

The goal of this concept is to recommend a framework of utilizing absolute radiated data throughput as a method for comparing the radiated throughput results measured in any MIMO OTA testing methodology with conducted reference performance under the ideal channel model implementation. The conducted reference will be used to compare data against. It is not implied that the conducted reference is "ideal" or "perfect." For instance, the way that the pattern data is interpolated and quantized may contribute variations in the conducted reference that are not present in the radiated test.

The methodology will be used to understand each MIMO OTA testing method's ability to emulate the specified network and channel propagation characteristics based on an absolute throughput metric. This comparison framework will be used to understand the ability of different testing methodologies to provide comparable results.

II. CONDUCTED MEASUREMENT

The conducted portion of the absolute data throughput baseline, evaluates the conducted performance of the DUT under special circumstances. As illustrated on figure 1, the conducted measurement is evaluated with DUT connected to the base station emulator through a dual port channel emulator. The channel emulator is programmed to generate a channel model characteristics (temporal and spatial), identical of the channel emulated in the radiated test environment.

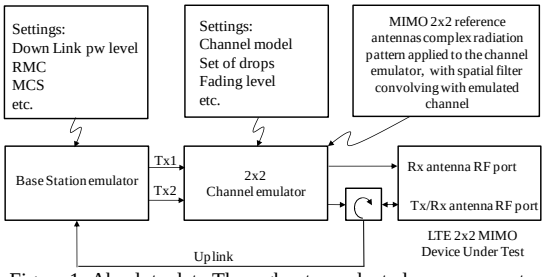

Figure 1: Absolute data Throughput, conducted measurement block diagram

The basic concept in this measurement is to determine a baseline data throughput over downlink conducted sensitivity, while the measurement encapsulates the following characteristics:

1. Network characteristics inherent in the base station emulator settings (the reference measurement channel, MCS, etc.); these settings are documented in Section 7.1 of 3GPP TR 37.977 [2];
2. Emulated base station antenna characteristics; these settings have been defined in Section 7.2 of 3GPP TR 37.977 [2];
3. Propagation channel characteristics (channel model, multipath profile, defined drop characterizing spatial and temporal parameters, etc.); these settings have been defined in Section 8.2 of 3GPP TR 37.977 [2];
4. DL signal power level;
5. Complex antenna radiation pattern of the DUT (radiation patterns of CTIA MIMO 2x2 reference antennas [1] shall be applied to the emulated propagation channel characteristics);
6. Chipset characteristics (such as the receiver algorithm implementation).

The conducted reference measurement does not encapsulate the following characteristics:

1. Interference/coupling between antenna elements integrated into the UE;
2. Sources of self-interference coupling to the receiver chains via antenna elements integrated into the UE.

A. Emulation of Antenna Pattern Rotation

To proper benchmark absolute data throughout measurements taken in different labs, besides the format used to present the antennas complex radiation pattern, the resolution of the antenna measurement also need to be defined. Based on experiments taken with low (<1GHz) and high (>1.8GHz) frequency band antennas, the post processed complex of magnitude of correlation coefficient remain unchanged from higher resolution antenna pattern measurements up to 15° resolution in theta and phi orientations. To align with current COST IC1004 MIMO OTA topic group proposed resolution for 3D MIMO OTA complex radiation pattern measurements, the antenna pattern measurement resolution is defined as $\theta = 5^\circ$ and $\phi = 5^\circ$. In the specific case of 2D measurements $\theta=90^\circ$.

For the conducted portion of the absolute data throughput framework, it is necessary to generate the spatially filtered channel impulse response per polarization and then combine to generate the emulated channel impulse response coefficients. The measured antenna pattern shall be interpolated to match the spatial resolution of the angles of arrival of the SCME channel emulator (this value is typically 1°). Figure 4 below illustrates an example of this procedure using a simplified antenna pattern and channel PAS.

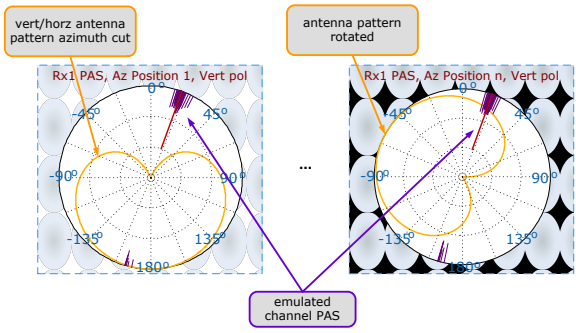

Figure 4: Rotation of antenna pattern over azimuth positions

Antenna pattern rotation shall be performed over 360° in 5° steps (72 total positions). This process may be automated with channel emulator control software or performed manually. The output data format described in Section 5 below captures the throughput vs. SNR sweep results for each rotation position.

B. Antenna Pattern Data Format

The antenna pattern data format used in the conducted portion of the measurements shall be in the 3D AAU format as defined by COST IC1004 [3]. Table 1 below illustrates the header structure with a sample data set.

Table 1: Auxiliary informational header

Line(s)	Pos.	Description	Values - *examples* or **defaults**
1	1	Pattern frequency	free (*750*)
	2	Frequency units	{Hz,KHz,**MHz**,GHz}
	3	Port index (to resolve antennas automatically)	free (*1*)
	4	Pattern type (Directivity, Gain, Realized Gain, E-field)	{D,G,**Gr**,E} - possible more
	5	Units format (as in touchstone plus the E-field format)	{DB,MA,**RI**,V/m}
	NOTE: There is no freedom in the column arrangement but the labels can vary. Done for ease of use.		
2	1	θ scan stepping - must be constant	Theta [deg]
	2	ϕ scan stepping - must be constant	Phi [deg]
	3	Absolute of the field X(1-4) in [units(1-5)]	Abs X [units]
	4	θ polarized field X(1-4) in [units(1-5)]	XTh [units]
	5	phase of the θ polarized field - always in degrees	phase Th [deg]
	6	ϕ polarized field X(1-4) in [units(1-5)]	XPh [units]
	7	phase of the ϕ polarized field - always in degrees	phase Ph [deg]
3,4 ...	NOTE: Any number additional lines can be added, always beginning with Matlab comment sign %		
N/A		Some custom comment, ID etc.	% File version 1.0

In this table we further define the following parameters:

1. Position 1 on Line 1 shall indicate the measurement frequency.
2. Position 2 on Line 1 shall indicate the frequency units to be MHz.
3. Position 3 on Line 1 shall indicate the antenna index 1 or 2.Antenna index is defined as: antenna index 1 defined as left antenna (portrait front view, from RF enclosure side), antenna index 2 defined as right antenna (portrait front view, from RF enclosure side)
4. Position 4 on Line 1 shall be G.
5. Position 5 on Line 1 shall be dBi
6. Positions 3, 4, and 6 on Line 2 shall describe the measured gain in dBi.

III. RADIATED MEASUREMENT

Analogous to the conducted portion of the measurement, the radiated portion of the absolute data throughput, applies the same channel model, the physical representation of the MIMO 2x2 reference antenna complex radiation pattern, and the same (physically) DUT measured in the conducted portion of the measurement.

As indicated in the figure 2, the DUT is connected to the MIMO 2x2 reference antennas, representing the embodiment measured conductively, where the complex radiation patterns are applied to the DUT.

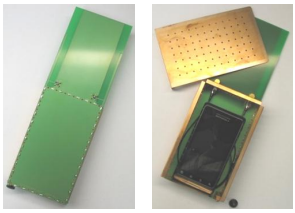

Figure 2: MIMO 2x2 reference antennas connected to DUT

The figure 3, represents the implementation of one of the proposed MIMO OTA valid test methodologies, consisting of a circular array of eight dual polarized antennas in an anechoic chamber, fed by an two 8 port channel emulator through a set of low noise amplifiers, properly correlating, fade, scale, delay, and distribute the signal to each test probe in the chamber.

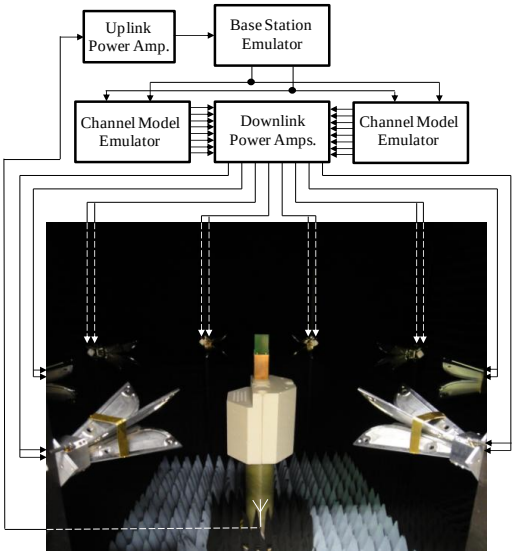

Figure 3: Anechoic base MIMO OTA test methodology

The radiated portion of the absolute data throughput measurement encapsulates the following characteristics:

1. Network characteristics inherent in the base station emulator settings (the reference measurement channel, MCS, etc.); these settings have been documented in Section 7.1 of 3GPP TR 37.977 [2];
2. Emulated base station antenna characteristics; these settings have been documented in Section 7.2 of 3GPP TR 37.977 [2];
3. Propagation channel characteristics (channel model, multipath profile, defined drop characterizing spatial and temporal parameters, etc.); these settings have been defined in Section 8.2 of 3GPP TR 37.977 [2]. As shown in the Figure 3 above, the fading emulator shall be configured to emulate the agreed channel model over the air: this configuration, while correlating with theoretical characteristics of the channel model, must be determined based on theoretical analysis of the test setup configuration, i.e. number of test probes, location and orientation;
4. DL signal power level;
5. Complex antenna radiation pattern of the DUT (the UE shall be placed inside the RF enclosure of the CTIA MIMO 2x2 reference antennas [8] and cabled to its antenna ports);
6. Chipset characteristics (such as the receiver algorithm implementation).

Since we place the DUT inside the RF enclosure and connect its transceiver ports to the antenna feeds of the MIMO 2x2 reference antenna fixture, the radiated measurement does not encapsulate the following characteristics:

1. Interference/coupling between antenna elements integrated into the DUT;
2. Sources of self-interference coupling to the receiver chains via antenna elements integrated into the DUT.

IV. CONCLUSION

The absolute radiated data throughput calibration method can be used to assess how accurately each test method is able to emulate the network and channel characteristics defined in the MIMO OTA testing methodology, and eventually would provide a direction towards acceptance of test method(s). This decision will be based on an absolute throughput metric defined in this paper.

REFERENCES

[1] I. Szini, G. Pedersen, A. Scannavini, and L. Foged, "MIMO 2x2 reference antennas concept," in Antennas and Propagation (EUCAP), 2012 6th European Conference on, march 2012, pp. 1540 –1543.

[2] "Verification of radiated multi-antenna reception performance of User Equipment (UE)", 3GPP TR 37.977 v2

[3] B. Yanakiev, J. O. Nielsen, M. Christensen, G. F. Pedersen, "The AAU 3D antenna pattern format- proposal for IC1004"

Paper 5

MIMO Reference Antennas Performance in Anisotropic Channel Environments

Istvan Szini, Boyan Yanakiev and Gert Pedersen

Accepted for publication (final) in:
IEEE Transaction on Antenna and Propagation, March 2014

MIMO Reference Antennas Performance in Anisotropic Channel Environments

Istvan Szini, Boyan Yanakiev, and Gert Frølund Pedersen

***Abstract*—The new generation of cellular wireless communications, Long Term Evolution (LTE), requires multiple antennas at both the transmit and receive ends of the radio link to improve system performance. This use of the radio link is termed Multiple Input - Multiple Output (MIMO) and in this work the focus is on the downlink (base station transmit, mobile receive). Efforts to define Over The Air (OTA) downlink MIMO measurement methodologies are still being carried out within several standards bodies and are based on the evaluation of so-called good, nominal and bad MIMO reference antennas. The reference antennas were necessarily defined independently of the channel environment which is still under discussion. The reference antenna figures of merit, for an isotropic channel environment, were chosen as efficiency, branch power ratio (BPR) and correlation. The objective of this work is to evaluate the radiated performance of the MIMO reference antennas using anisotropic (non-uniform power angular spread) channel environments. The performance of the reference antennas in anisotropic environments is different to that in an isotropic environment, due to the antenna orientation in the three dimensional space relative to the channel. This leads to a statistical description of the Branch Power Ratio (BPR), correlation and efficiency, which is expressed in terms of Mean Effective Gain (MEG). The outcome of this new anisotropic evaluation is that the reference antennas are seen to vary significantly for BPR and Mean Effective Gain (MEG) and somewhat less for correlation, relative to the isotropic environment.**

***Index Terms*—antennas, antenna radiation patterns, mobile antennas, anisotropic, MIMO, 4G mobile communication.**

I. Introduction

SEVERAL groups and standards bodies around the world are currently investigating MIMO OTA measurement techniques. The definition of a valid test methodology, which represents the real world conditions is complex; unlike conventional Single Input Single Output (SISO) measurements, the MIMO OTA test methodology must consider anisotropic channel environments, where the temporal and spatial characteristics of the channel model must be reproduced. Most recently the Third Generation Partnership Project (3GPP) through its Technical Specification Group (TSG) defined as Radio Access Network (RAN) Working Group 4, conducted in the second half of 2010 a large measurement campaign, in which several labs in Europe, Asia and North America participated [1]. The goal of this first large-scale measurement campaign was to define a valid MIMO OTA test methodology, which can discriminate "good" MIMO devices from "bad" MIMO devices under anisotropic channel conditions.

I. Szini is with Motorola Mobility LLC, Libertyville, USA; email: Istvan.Szini@motorola.com.

B. Yanakiev is with Molex Antenna Business Unit in Aalborg, Denmark; email: boyany@gmail.com.

I. Szini, B. Yanakiev and G. F. Pedersen are with the Antennas, Propagation and Radio Networking section at the Department of Electronic Systems, Faculty of Engineering and Science, Aalborg University, Denmark; email: {ijs; by; gfp}@es.aau.dk

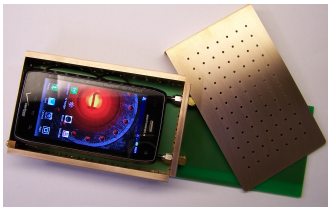

(a) front open

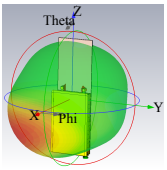

(b) Coordinate system definition.

Fig. 1. MIMO reference antenna concept RF enclosure with inserted active DUT

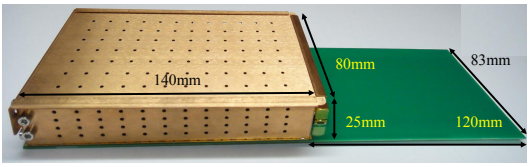

Band	Dimension	Good	Nominal	Bad
2	a (mm)	29.5	34.65	
	b (mm)	119	13.8	NA
7	a (mm)	22.5	23.1	
	b (mm)	119	12.1	
13	a (mm)	76.7	78.5	79.3
	b (mm)	119	85.7	77.2

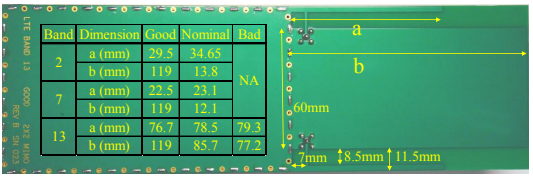

Fig. 2. Reference antenna dimensions - side view (top), bottom view (bottom)

The measurement campaign organized by 3GPP RAN WG4 MIMO OTA ad hoc group did not achieve its goals during this first campaign. Several technical and logistics issues were identified during the campaign:

- The behavior of the LTE 2x2 Base Station (BS) emulators was inconsistent, since different equipment from different vendors had different conducted and radiated performance despite identical settings;
- The DUT was immature presenting non-linear performance over temperature;
- Since in this initial campaign only data-cards (dongles) were utilized, a laptop was part of the setup, generating additional noise into the measurement, and altering the LTE dongle antenna system performance [2];

- The channel model emulator settings across different vendors were not completely defined [3];
- Lack of definition of the BS antenna assumptions, and lack of procedures to validate the channel model emulation in the test environment [4];
- Finally, an important root cause for the unsuccessful 3GPP RAN WG4 measurement campaign is the fact that none of the evaluated DUTs had the MIMO antenna system characterized, meaning the measurement results could not be compared against expected performance.

This study will focus on the characterization of a reference MIMO antenna system, discussing isotropic and anisotropic antenna figures of merit, and offering a solution to minimize the uncertainty in MIMO OTA measurements.

The 3GPP RAN WG4 MIMO OTA measurement campaign was closely observed by USA-based Cellular Telecommunications Industry Association (CTIA), with several CTIA members also being 3GPP RAN WG4 MIMO OTA participating members. In March 2011 CTIA created a dedicated group to define the MIMO OTA standard for North America: the MIMO OTA Sub Group (MOSG). Learning from 3GPP RAN WG4 issues, CTIA started the definition of their own MIMO OTA specifications based on 3GPP RAN WG4 prior work, but with refinements to improve the usefulness of the measurement campaign results.

One significant evolution in the MIMO OTA test procedure was the proposal of the creation of MIMO OTA reference antennas [5], enabling the adoption of fully characterized MIMO antenna systems in the future measurement campaigns.

The purpose of the MIMO 2x2 reference antennas is to eliminate an unknown variable from the test methodology, the MIMO antenna system performance, thus guaranteeing that any MIMO OTA test methodology can be analyzed based on reliable and well defined DUT radiated performance. As shown in Fig. 1(a), the MIMO reference antenna is an external antenna. This allows separation of the DUT RF/baseband/LTE performance from the antenna performance. Thus the external MIMO reference antenna concept enables the comparison of different test methodologies with the purpose of discriminating between so-called good and bad MIMO antennas. To optimize MIMO capacity several aspects of the antenna system design need to be considered, as summarized below:

- Both antennas, Main Antenna and Secondary Antenna, need to have minimum branch power ratio, ideally BPR = 0 dB;
- In a rich scattered environment the maximum capacity will occur when both receiver antennas are uncorrelated. There are exceptional cases where co-polarized antennas can still be uncorrelated, however this is hard to accomplish in hand-held form factors due to the limited spacing between antennas;
- The absolute phase responses of the reference antennas are irrelevant, but not the phase per direction or the relative phase relationship between the antennas, both of which define the antenna system correlation coefficient;
- Considering the special case of the isotropic environment, the ideal MIMO 2x2 antenna system, with ideal isolation between antennas S_{21} <-20 dB, high efficiency $\eta > 90$ %, low gain imbalance (BPR≈ 0 dB), and correlation coefficient ($\rho \approx 0$), should provide double the capacity of a SISO system (this statement is based solely on antenna parameters and assumes ideal propagation conditions);
- The antenna's radiation patterns need to have similar directivity. Two directional antennas with the main lobe in opposite directions will not enable acceptable MIMO performance in an environment with few signal propagating reflections. Such signal reflections are generated by non-uniformities in the radiated environment also known as scattering.

The CTIA MIMO OTA Sub Group (MOSG) agreed to the following proposal guidelines for the reference antenna development [5]:

- Initially focusing on LTE frequency bands: band 2 (1.9 GHz), band 7 (2.6 GHz) and band 13 (750 MHz);
- The reference antennas should be able to clearly emulate "good", "nominal" and "bad" MIMO 2x2 antenna system designs;
- The design should be simple to enable production in large quantity;
- Low cost.

The "good", "nominal" and "bad" MIMO reference antenna were defined as:

- "Good" MIMO antenna system - low envelope correlation coefficient ($\rho_e \leq 0.1$), high total antenna efficiency ($\eta \geq 90$ %), and low gain imbalance (BPR ≈ 0 dB);
- "Nominal" MIMO antenna system - moderate envelope correlation coefficient ($\rho_e \approx 0.5$), moderate total antenna efficiency ($\eta \geq 50$ %), and low gain imbalance (BPR ≈ 0 dB);
- "Bad" MIMO antenna system - poor envelope correlation coefficient ($\rho_e \approx 0.8$), moderate to poor total antenna efficiency ($\eta \leq 50$ %), and low gain imbalance (BPR ≈ 0 dB).

The low BPR approaching 0 dB was intentionally defined to enable the gain imbalance to be controlled by adding attenuators in series with the antenna ports. The use of attenuators on both branches can also equalize the gain of all three antennas. Thus it is possible to control independently all three Figures of Merit (FoM) in radiated measurements. The independent control of total antenna efficiency, BPR and correlation coefficient allows in-depth analysis of the influence of each MIMO antenna FoM on the radiated data throughput, e.g. in different LTE channel coding scenarios or SNR conditions.

Other than the electrical performance constraints, the reference antennas also mitigate a potential radiation leakage issue, common when connecting an external antenna to a DUT RF port. The connection between the DUT RF port and the reference antennas are coaxial cables which can potentially carry current in the outer conductor. The associated radiation perturbs the antenna system radiation and influences system parameters like correlation coefficient, absolute gain and BPR [6]. For this reason, the reference antennas were conceived with an integrated RF enclosure as shown in Fig. 1(a), in which the DUT and its RF port connections are located, therefore

eliminating the potential for undesired coaxial cable radiation.

This paper describes in detail the performance and the fundamental characteristics of the reference antennas in anisotropic channel environments as well as the consequences for the overall system performance.

II. Antenna Figures of Merit and Computational Definitions

A. Figures of merit definitions

To address the issue of unknown antenna system parameters encountered during the development of [1], the work done in [5] and [7] is extended here to the non-uniform (anisotropic) propagation environment. The goal is to evaluate the reference antenna performance in the anisotropic channels and assess the implications on the overall system performance.

The typical antenna parameters used here are the MEG from Eq. (2) [8], BPR from Eq. (3) and correlation coefficient from Eq. (1) [9],

$$MEG = \oint \Big[\frac{XPR}{1+XPR}\, G_\theta(\Omega) p_\theta(\Omega) + \frac{1}{1+XPR}\, G_\phi(\Omega) p_\phi(\Omega) \Big] d\Omega \tag{2}$$

$$BPR = 10 \log_{10} \frac{MEG_1}{MEG_2} \tag{3}$$

where Ω indicates variation over both θ and ϕ, $\oint p_{\theta/\phi}(\Omega) d\Omega = 1$ is the normalized power distribution for each polarization, XPR is the cross polarization ratio of the environment and $G_{\theta/\phi}(\Omega)$ and $\vec{E}_{\theta/\phi}(\Omega)$ are the gain and complex electric field patterns for each polarization, respectively. $*$ stands for complex conjugate and the indexes $X_{1/2}$ stand for the two antennas. With the above definitions and assuming isotropic power distribution $p_{\theta/\phi}(\Omega) = const = 1/(4\pi)$ the values presented initially in [5] can be computed. The focus of this paper however is the non-uniform influence of the propagation environment on such parameters and ultimately on the system performance.

Since non-uniform incoming power implies rotational dependence of the antenna parameters, the procedure shown in [10] is used to post-process the antenna system's simulated and measured data. Each of the above parameters is computed with the patterns defined in Section II-B and the power distribution defined in Section II-C, for a number of antenna orientations. Since the exact extreme values for a particular orientation are not necessarily important, the results in the following section are presented as statistical distributions showing the spreads of the parameters. Using the three Euler angles with 30 degree stepping, an arbitrary three-dimensional orientation can be represented and is here referred to as the 3D case, in which a rich variety of possible orientations is included. Another relevant case is the azimuth (AZ) only rotation, which is also included here with 5 degrees stepping. With this definition, the statistical sample sizes are 864 and 72 for the 3D and AZ cases, respectively.

B. Radiation pattern definitions

The radiation patterns from simulations used in Eq. (2) and Eq. (1) were generated using Computer Simulation Technology (CST) Microwave Studio, with models and pattern files available freely at [11]. The CST models were then manufactured and measured in an anechoic chamber to verify the simulated results (also available at [11]). Table I and Table II (to be discussed in sec. III) compare the simulated and measured patterns in an isotropic environment. Ideally these results would be identical to the values shown in [5], but slight differences exist. Differences for the simulated patterns are due to differences in model meshing and CST versions. Differences for the measured values come from the finer 5 degree stepping of the measured patterns used for Tables I and II and full θ span from 0 to 180 degrees vs. 0 to 165 degrees in the case of [5], and extra prototype losses due to antenna feeding through decoupling sleeves not reproduced in the simulations. However, the differences are very small and within acceptable measurement uncertainties.

For the computations in Eq. (2) and Eq. (1) the coordinate system shown in Fig. 1(b) was used, where the largest device length is along the z axis as in a typical dipole [12]. Assuming the RF enclosure as the front view of the antenna system, the antenna at the right side is referred to as Antenna 1 and the antenna at the left side as antenna 2. The simulated radiation patterns were exported with 40 dB dynamic range and 5^0 resolution in elevation (theta) and azimuth (phi). The same angular resolution was used for the measured patterns.

C. Spherical power distributions

For the purposes of this paper, two spherical power distribution models are used: the isotropic, providing a baseline reference case and corresponding to the existing SISO case, and a directional model derived in [13] (here referred to as the AAU model). The AAU model is based on outdoor-to-indoor measurements for a typical urban environment and has similar directional properties to some of the channel models considered today for MIMO OTA such as HUT [14], Spatial Channel Model Extended (SCME) and Wireless World Initiative New Radio (WINNER) II. While the AAU model is not considered in [1] it is simple to implement and process numerically, and preserves the essential antenna properties such as incoming power direction and limited angular spread. Relative to the WINNER II model for example, the AAU model lacks fading and delay spread but since this part of the analysis is for the passive antennas and does not include

$$\rho = \frac{\oint \Big[XPR\ \vec{E}_{\theta X}(\Omega) \vec{E}^*_{\theta Y}(\Omega) p_\theta(\Omega)\ + \vec{E}_{\phi X}(\Omega) \vec{E}^*_{\phi Y}(\Omega) p_\phi(\Omega) \Big] d\Omega}{\sqrt{\oint \left[XPR\ G_{\theta,1}(\Omega) p_\theta(\Omega) + G_{\phi,1}(\Omega) p_\phi(\Omega) \right] d\Omega \ \oint \left[XPR\ G_{\theta,2}(\Omega) p_\theta(\Omega) + G_{\phi,2}(\Omega) p_\phi(\Omega) \right] d\Omega}} \tag{1}$$

TABLE I
BANDS 2/7/13 TOTAL ANTENNA EFFICIENCIES.

Band	Antenna Configuration	Antenna 1			Antenna 2		
		$\eta(\%)$	$\eta(\%)$	$\eta(\%)$	$\eta(\%)$	$\eta(\%)$	$\eta(\%)$
2		1930 MHz	1960 MHz	1990 MHz	1930 MHz	1960 MHz	1990 MHz
	Simulated "Good"	96.9	95.8	93.9	97.2	97.0	95.9
	Measured "Good"	90.2	84.7	83.9	88.1	83.4	83.4
	Simulated "Nominal"	60.1	60.5	59.7	58.9	59.7	59.4
	Measured "Nominal"	65.7	61.6	61.2	63.9	57.8	57.3
7		2620 MHz	2655 MHz	2690 MHz	2620 MHz	2655 MHz	2690 MHz
	Simulated "Good"	91.3	91.9	90.7	90.6	90.5	88.1
	Measured "Good"	89.1	81.4	75.1	82.6	86.3	78.5
	Simulated "Nominal"	55.7	57.8	59.4	56.0	57.8	58.7
	Measured "Nominal"	69.8	69.6	56.3	75.9	65.4	52.1
13		746 MHz	751 MHz	756 MHz	746 MHz	751 MHz	756 MHz
	Simulated "Good"	93.8	94.8	94.6	93.8	94.8	94.5
	Measured "Good"	77.0	80.8	74.4	80.9	84.9	80.7
	Simulated "Nominal"	48.7	46.7	44.4	48.0	46.4	44.5
	Measured "Nominal"	55.2	55.0	54.7	56.1	54.9	53.7
	Simulated "Bad"	41.2	38.7	36.2	39.3	37.4	35.5
	Measured "Bad"	45.8	44.6	40.4	46.5	44.4	39.7

TABLE II
BANDS 2/7/13 GAIN IMBALANCE AND CORRELATION COEFFICIENT.

Band	Antenna Configuration	Gain Imbalance [dB]			Correlation Coefficient		
		BPR [dB]	BPR [dB]	BPR [dB]			
2		1930 MHz	1960 MHz	1990 MHz	1930 MHz	1960 MHz	1990 MHz
	Simulated "Good"	0.01	0.05	0.09	0.01	0.05	0.09
	Measured "Good"	0.10	0.07	0.03	0.02	0.01	0.01
	Simulated "Nominal"	0.09	0.06	0.02	0.45	0.46	0.46
	Measured "Nominal"	0.12	0.28	0.29	0.35	0.37	0.38
7		2620 MHz	2655 MHz	2690 MHz	2620 MHz	2655 MHz	2690 MHz
	Simulated "Good"	0.03	0.07	0.13	0.02	0.02	0.04
	Measured "Good"	0.33	0.25	0.19	0.01	0.03	0.04
	Simulated "Nominal"	0.02	0.00	0.05	0.37	0.39	0.40
	Measured "Nominal"	0.37	0.27	0.34	0.36	0.35	0.33
13		746 MHz	751 MHz	756 MHz	746 MHz	751 MHz	756 MHz
	Simulated "Good"	0.00	0.00	0.01	0.05	0.02	0.01
	Measured "Good"	0.22	0.21	0.35	0.01	0.04	0.09
	Simulated "Nominal"	0.06	0.03	0.01	0.67	0.62	0.58
	Measured "Nominal"	0.07	0.01	0.08	0.44	0.38	0.32
	Simulated "Bad"	0.21	0.15	0.09	0.81	0.77	0.73
	Measured "Bad"	0.07	0.02	0.08	0.88	0.85	0.80

the receiver, this simplification is considered acceptable. In terms of angular properties, the AAU model is similar to the single cluster SCME model defined in [15].

III. ANTENNA FOM RESULTS

The antenna computations based on measured and simulated patterns and using an isotropic environment for the uniform incoming power distribution, are presented in Table I and Table II. It is under these channel conditions that the reference antennas are defined as "good", "nominal" and "bad" MIMO antennas. As can be seen from the tables, the measured values are close to the simulated ones, so for the remainder of this paper the measured patterns are used unless stated otherwise.

A primary question to be answered is to what extent the known reference antennas actually provide stable performance in a non-uniform environment. Previous studies have shown that typical mobile phone antenna performance varies widely in directive environments [16], and those SISO cases have been extended in [10] for reference dipoles and some MIMO cases. Similar differences using MIMO reference antennas are shown in Figs. 3, 5 and 6.

From the MEG Figs. 3(a), 3(b), 5(a), 5(b), 6(a) and 6(b), it can be seen that the simulated and measured patterns result in very similar statistical behavior except for the horizontal offset due to the slight differences in antenna efficiency between simulated and measured results. This is true for both the 3D and AZ cases as expected, but AZ case represents a statistical subset of the 3D case with smaller variance. However, as can be seen from the median values, this subset is not necessarily symmetric around the median, but favors the particular AZ orientation, offsetting the curve. The figures show that the AZ median is always higher than the 3D median, however it is also the case that the top-performing orientations are not included in the AZ subset. For the AZ case, the variation of the MEG is around $1-1.5\,$dB. For the 2D MIMO OTA such variation might be acceptable but if the industry moves towards full 3D evaluation, variations of up to $6-7\,$dB can be expected. At first sight the distinction between "bad", "nominal" and "good" is preserved and that is also somewhat true for the AZ case, but

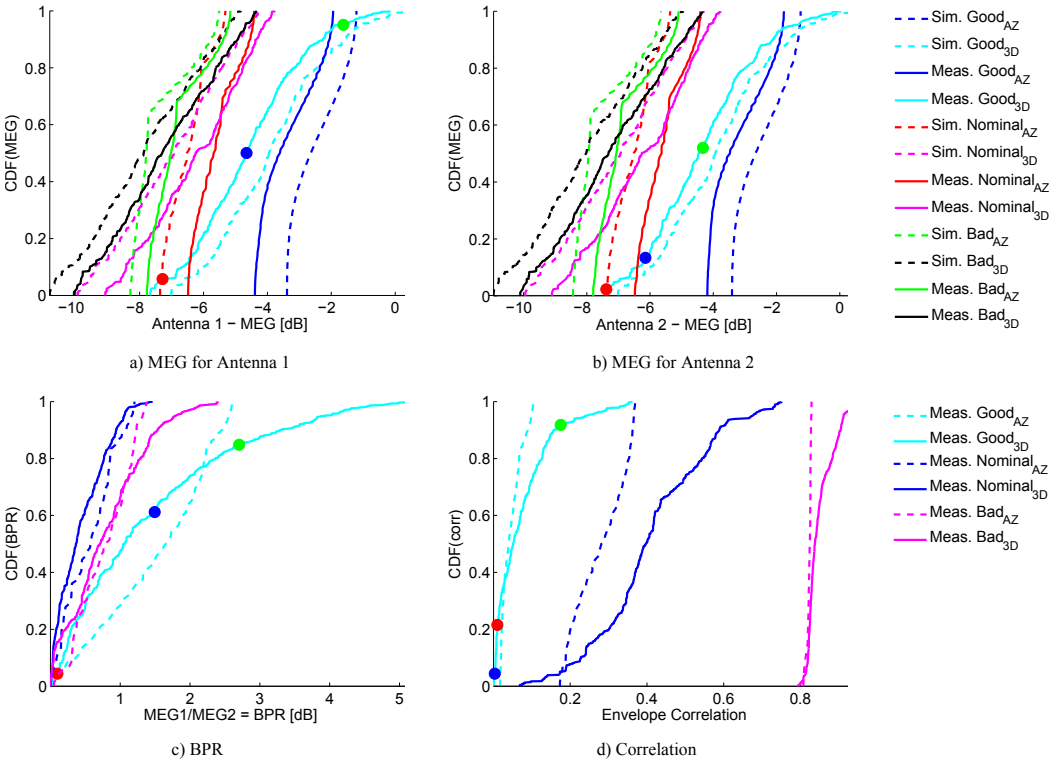

a) MEG for Antenna 1

b) MEG for Antenna 2

c) BPR

d) Correlation

Fig. 3. B13 statistics at 751 MHz in the AAU environment. The 3D subscript indicates the 3D rotations and AZ indicates the azimuth spin only.

when arbitrary orientations are allowed for the 3D case, it is obvious, although less likely, that a good antenna can have worse performance than the bad one (for ex. Fig. 3(a)).

The reference antennas were designed to have low BPR in an isotropic environment. However, in the directive AAU environment, it can be seen from Figs. 3(c), 5(c) and 6(c) that the probability of BPR $= 0$ dB is almost zero. For both 3D and AZ cases, and for all bands, the median BPR is between $0.5 - 2$ dB (Fig. 6(c)).

In spite of the fact that high, medium and low correlation reference antenna design goals are clearly distinguishable in Fig. 3(d), within correlation below 0.5 which is considered adequate for proper MIMO system performance, the performance of the B13 ”nominal” and ”good” antennas might be difficult to discriminate in system measurements, e.g. radiated data throughput. The data shown in Fig. 3 and respective analysis confirms the conclusions in [10] regarding the stability of the correlation coefficient with rotation, however it should be noted that the stability depends on the directivity of the channel.

Finally it should be noted that any one of the curves presented in Fig. 3 does not fully describe the antenna system and they should be taken together in a statistical manner. For example, taking the 3D case for the measured ”good” B13 antenna from Fig. 3 (solid cyan curve), the MEG percentiles for antenna 1 of 5 % (red), 50 % (purple) and 95 % (green) can be used to determine the orientations at which these MEG values occur. The same color coded dots are shown in Figs. 3(b), 3(c) and 3(d), indicating the corresponding variable for the same rotation vectors. The corresponding rotation vectors and pattern measurement results presented here, and power distribution superpositions shown in Fig. 4, are presented in one elevation for better readability. In all subplots of Fig. 4 the blue curve is the gain of antenna 1, the red curve is the gain of antenna 2 and the cyan curve is the incoming power. The color coded values for MEG relate to the same gain patterns. As can be expected in the low range of MEG for antenna 1, the high gain area of the antenna (at about 250 degrees in the left polar plot) is well away from peak incoming power (at about 90 degrees in the left polar plot). Alternatively the right side plot in Fig. 4 has the peak incoming power aligning with a high gain region resulting in high MEG values. Of course, orientations similar to those produce similar results contributing samples to the high, middle and low ranges of the MEG curve. Note however that the values at any given region of the CDF curves are not necessarily computed from similar orientations. This is best understood with the simple ideal dipole example, where the nulls at theta 0 and 180 degrees

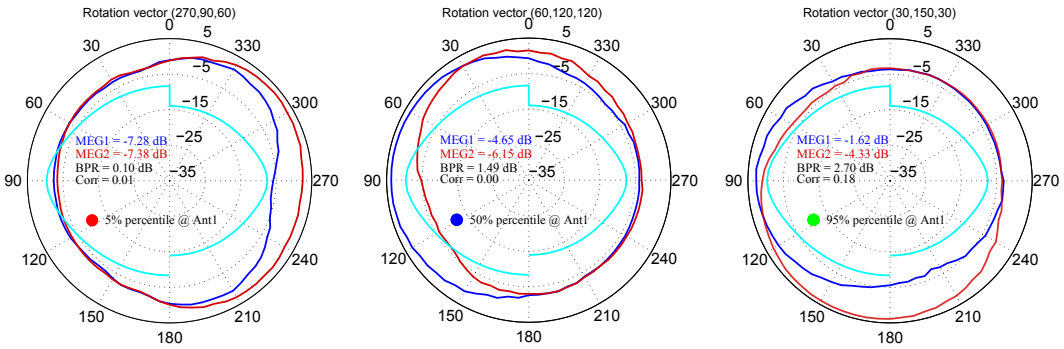

Fig. 4. Realized gain and incoming power (cyan curve) superposition in the XZ Plane - 5% (left), 50% (middle) and 95% (right) percentile values for MEG1 (blue marked number and gain pattern curve) and the corresponding influence on MEG2 (red marked number and gain pattern curve), BPR and Correlation.

would produce equally low MEG value but at completely different orientations. However what is obvious from the figure is that high MEG for antenna 1 in one orientation does not necessarily mean BPR near 0 dB. Looking at the right hand side plot in Fig. 4 shows that while antenna 1 MEG is high the BPR is actually further away from 0 dB with these antennas. Therefore a balance has to be sought between MEG and BPR to optimize performance.

IV. Throughput Measurements

The radiated LTE throughput measurements were performed using a MIMO OTA test system as shown in the setup (Fig. 7). It consists of a circular array of dual polarized antennas in an anechoic chamber, fed by two eight-port channel emulators through a set of low-noise amplifiers, properly correlating, fading, scaling, delaying, and distributing the signal to each test probe in the chamber to emulate the desired channel environment.

This configuration has been shown to produce an environment equivalent to free space condition for devices with dimensions not exceeding the limitations of the test volume. Some procedures to validate the signal conditions in the test volume are described in section 8.3.2 of [17]. The conclusion that the environment is sufficient is restricted for the reference antennas, not for an arbitrary type of MIMO antenna system. Therefore, the configuration is considered sufficient for the purpose of evaluating the MIMO antenna system in active data throughput measurements.

The test procedure used followed that outlined in [17], for the R.11 16 Quadrature Amplitude Modulation (QAM) reference channel defined in Table A.3.3.2.1-1 of [18]. An LTE band 13 off-the-shelf commercial LTE handset was measured with the reference antennas at 751 MHz, as well as with a cable for conducted performance. The chosen low band is considered the most critical in terms of antenna design. The first goal was to verify if the reference antennas provided the needed distinction between good, nominal and bad antenna system performance in the real anisotropic environment, and the second goal was to characterize the directional variability of the throughput and potentially correlate it to the variability of the antenna system parameters from Section III. Since the same LTE receiver was used, all throughput variations should be explainable by the changing performance of the reference antennas. Note that additional variation may be introduced by time-variant uncertainties in the measurement system, such as temperature variation. Since much of the test system is still under development this can be a problem.

For the throughput measurements, the DUT was placed in an upright position as shown in Fig. 7, and then rotated in 45 degree azimuth steps to capture throughput vs. power curves at each position. This corresponds to the AZ rotation of the antenna system but with only 8 orientations instead of 72 in order to constrain the test time. For each orientation, measurements are made from -80 dBm to -116 dBm in 1 dB steps. The result is an $8\ x\ 37$ matrix of throughput values. The validation of the downlink power within the test volume was part of the MIMO chamber calibration process, using a Vector Network Analyzer and standard reference antennas. In addition to the OTA data throughput measurements with spatial channel models, a series of conducted tests were performed using both constant tap (no fading) model, and emulation of the spatial channel models based on the SCME Urban Micro (UMi)/ Urban Macro (UMa) models from [17] (see Figs. 9 and 10) and modified outdoor-to-indoor WINNER II [1] as shown in Fig. 11. In these measurements ideal dipoles were used as the modeled receiving antennas. The constant tap result was also compared to direct connection tests between the base station emulator and the DUT, to confirm that the calibrated path through the channel emulator produced the same result as a direct connection. The Figs. 9 and 10 are generated from the table data in [17]. The polar plots (Figs. 9(a), 10(a) and 11(a)) have color coded all tap delays with their angle of arrival and power on the radial scale, while the bar plots (Figs. 9(b), 10(b) and 11(b)) have the same color-coded delays on the right Y axis and powers on the left Y axis. The groups in Figs. 9(b) and 10(b) show the intra-cluster split, and in Fig. 11(b) this is presented with tightly grouped bars for the first and seventh taps.

The results of the throughput measurements are shown in Figs. 8(a) to 8(c). Since the DUT drops the call at different

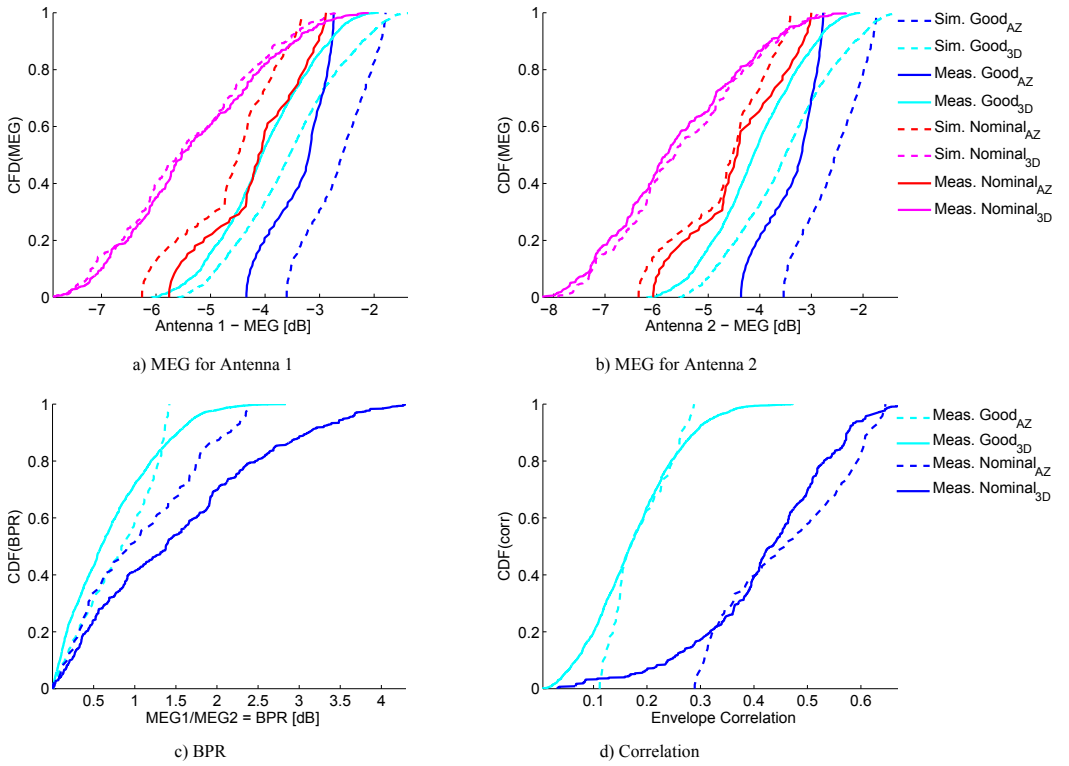

a) MEG for Antenna 1

b) MEG for Antenna 2

c) BPR

d) Correlation

Fig. 5. B2 statistics at 1960 MHz in the AAU environment. The 3D subscript indicates the 3D rotations and AZ indicates the azimuth spin only.

power levels, depending on the measurement type described above, zeros were added for the throughput at the low powers to match the statistical sample sizes of the conducted measurements. The selected R.11 Modulation and Coding Scheme (MCS) defines the maximum throughput as 2 * 11.664 = 23.3280 Mbps, and all results were normalized to that value. Treating all orientations equally the Complementary Cumulative Distribution Function (CCDF) was computed, resulting in a vertical offset based on the amount of padded zeros. In this way the reference conducted case has a probability of almost one representing maximum performance. The introduction of delays in the conducted measurements reduces the performance from the reference conducted case, and further reductions are seen in the radiated measurements due to the good, nominal and bad reference antennas. The right hand side of the plots shows the power level in dBm at which the performance drops below 99 % (the knee in the graph). Those numbers are also color coded to match the line colors. Wherever the 3 km/h and 30 km/h plots have the same knee position only one number is shown. Since the selected R.11 reference channel has a robust coding rate, the maximum throughput is almost always achieved at sufficiently high power, despite the ”bad” antenna system having a correlation coefficient of nearly 0.8. For the SCME UMa case at 30 km/h, the ”bad” antenna system does not reach maximum throughput. This phenomenon is related to the specific Angle of Departure (AoD) adopted in the SCME UMa channel model, which produces a composite correlation at the base station of about 95 %. The issue is exacerbated by the higher emulated DUT speed. Finally, the reason for why in a few cases the good antenna system provides higher throughput than the conducted case is due to the favorable antenna gain in some orientations resulting in higher MEG than the 0 dBi assumption for the conducted case.

V. Conclusions

A 2x2 MIMO reference antenna was created to establish a mechanism whereby a DUT can be fitted with external antennas having pre-determined characteristics and hence radiated performance. The use of known antennas enables MIMO device performance prediction through numerical analysis of the antenna system performance characteristics. In this work the 2x2 MIMO reference antennas have been presented, showing good agreement between simulated and measured results. The performance of the reference antenna has been measured for the special case of isotropic (uniform) incoming power distribution as well as for anisotropic channel environments (AAU power distribution channel, SCME and

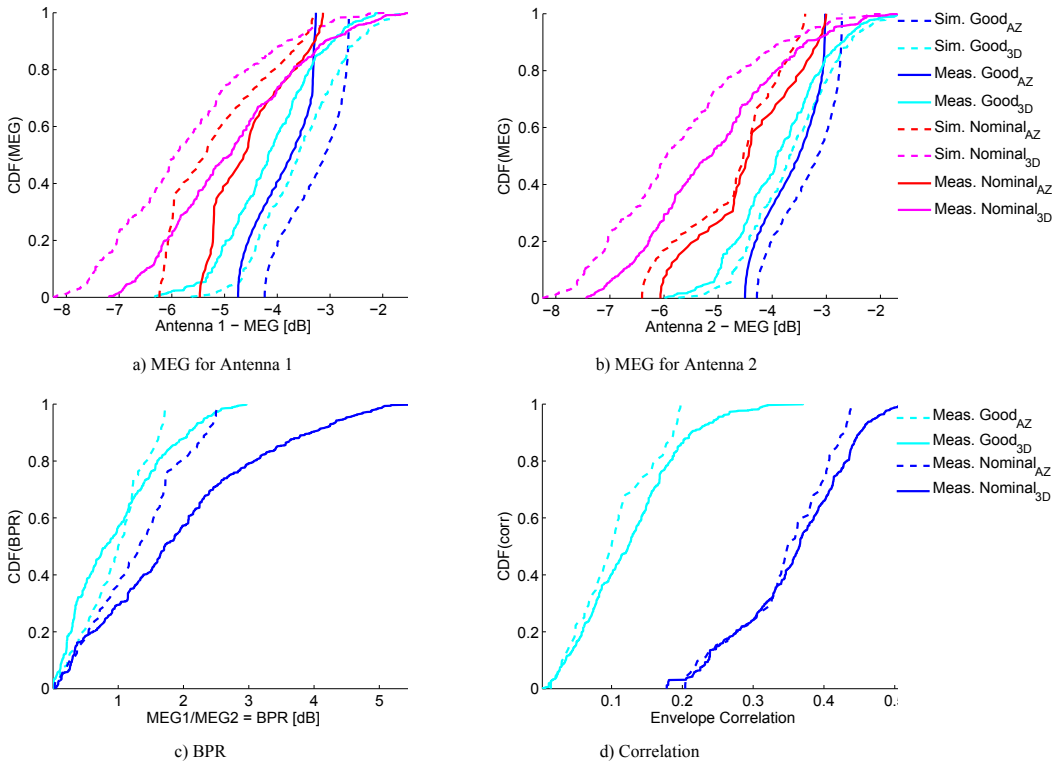

Fig. 6. B7 statistics at 2655 MHz in the AAU environment. The 3D subscript indicates the 3D rotations and AZ indicates the azimuth spin only.

WINNER II). The measurement uncertainty for the used MIMO OTA test system is still under investigation, nevertheless, adopting the known TIS measurement uncertainty defined in [19], the MIMO reference antennas throughput measurements in anisotropic channel environments, indicated a sufficient discrimination between "good" and "bad" antennas of approximately 8 dB. Therefore confirming the simulated radiated performance using exclusively the antennas complex radiation patterns. The magnitude of the reference antenna complex correlation coefficient was largely unchanged between the isotropic and anisotropic environments. However the MEG and BPR demonstrated significant variation, mainly when the reference antenna radiation pattern null aligned with the main power beam defined in the anisotropic propagation environment. The significant variation in MEG and BPR must be recognized and mitigated while designing MIMO antenna systems, mainly when the primary environment has low SNR, e.g. in indoor, fringe or rural areas [20]. However for MIMO radiated performance with high Signal to Noise Ratio (SNR) > 24 dB, the antenna MEG is secondary while the correlation between antennas is more relevant to discriminate "good" from "bad" MIMO antennas. The topology adopted for the 2x2 MIMO reference antennas will continue to be developed, in order to aid future research on MIMO OTA measurement methodologies, providing a known reference to help evaluate and minimize measurement uncertainty, and for validating test methodologies.

ACKNOWLEDGMENT

The authors wish to acknowledge the technical support from ETS-Lindgren, in providing system measurements results Fig. 8.

REFERENCES

[1] 3GPP, "3rd generation partnership project; technical specification group radio access networks; measurement of radiated performance for MIMO and multi-antenna reception for HSPA and LTE terminals(release 10)," May 2010. [Online]. Available: http://www.3gpp.org/ftp/Specs/archive/37_series/37.976/37976-110.zip

[2] Motorola, "LTE antenna system figure of merit. techniques and trade-offs probing antennas on LTE devices." October 2010, 3GPP TSG-RAN WG4 AH4-2010 . [Online]. Available: http://www.3gpp.org/ftp/tsg_ran/WG4_Radio/TSGR4_AHs/R4_AH04_Xian_Oct_2010/Docs/R4-103869.zip

[3] SATIMO Industries, Elektrobit, SPIRENT Communications, "Anechoic chamber based MIMO OTA: Channel emulators, and channel models implementation comparison," February 2012, 3GPP TSG-RAN WG4 Meeting No.62. [Online]. Available: http://www.3gpp.org/ftp/tsg_ran/WG4_Radio/TSGR4_62/Docs/R4-120675.zip

[4] Spirent Communications, Elektrobit, Satimo, "MIMO OTA channel model alignment," February 2012, 3GPP TSG-RAN WG4 62 MIMO OTA Ad-hoc Meeting. [Online]. Available: http://www.3gpp.org/ftp/tsg_ran/WG4_Radio/TSGR4_62/Docs/R4-120739.zip

[5] I. Szini, G. Pedersen, A. Scannavini, and L. Foged, "MIMO 2x2 reference antennas concept," in *Antennas and Propagation (EUCAP), 2012 6th European Conference on*, march 2012, pp. 1540 –1543.
[6] W. Kotterman, G. Pedersen, K. Olesen, and P. Eggers, "Cable-less measurement set-up for wireless handheld terminals," in *Personal, Indoor and Mobile Radio Communications, 2001 12th IEEE International Symposium on*, vol. 1, 2001, pp. B–112–B–116 vol.1.
[7] Stone, W., "Review of radio science 1996-1999 - handset antennas for mobile communications: Integration, diversity, and performance," in *Review of Radio Science 1996-1999*. Wiley-IEEE Press, 1999, pp. 119–137.
[8] T. Taga, "Analysis for mean effective gain of mobile antennas in land mobile radio environments," *Vehicular Technology, IEEE Transactions on*, vol. 39, no. 2, pp. 117 –131, May 1990.
[9] R. Vaughan and J. Andersen, "Antenna diversity in mobile communications," *Vehicular Technology, IEEE Transactions on*, vol. 36, no. 4, pp. 149 – 172, nov. 1987.
[10] B. Yanakiev, J. Nielsen, M. Christensen, and G. Pedersen, "Antennas in real environments," in *Antennas and Propagation (EUCAP), Proceedings of the 5th European Conference on*, 2011, pp. 2766–2770.
[11] B. Yanakiev. (2011, August) Antennas, propagation and radio networking group unofficial website @ONLINE. [Online]. Available: https://www.apnet.es.aau.dk/tiki/tiki-index.php
[12] C. A. Balanis, *Antenna Theory: Analysis and Design*, 2nd ed. John Wiley & Sons Inc., 1997.
[13] M. Knudsen and G. Pedersen, "Spherical outdoor to indoor power spectrum model at the mobile terminal," *Selected Areas in Communications, IEEE Journal on*, vol. 20, no. 6, pp. 1156 – 1169, Aug. 2002.
[14] K. Kalliola, K. Sulonen, H. Laitinen, O. Kivekas, J. Krogerus, and P. Vainikainen, "Angular power distribution and mean effective gain of mobile antenna in different propagation environments," *Vehicular Technology, IEEE Transactions on*, vol. 51, no. 5, pp. 823 – 838, sep 2002.
[15] D. Baum, J. Hansen, and J. Salo, "An interim channel model for beyond-3g systems: extending the 3gpp spatial channel model (scm)," in *Vehicular Technology Conference, 2005. VTC 2005-Spring. 2005 IEEE 61st*, vol. 5, may-1 june 2005, pp. 3132 – 3136 Vol. 5.
[16] J. Ø. Nielsen and G. Pedersen, "Mobile handset performance evaluation using radiation pattern measurements," *Antennas and Propagation, IEEE Transactions on*, vol. 54, no. 7, pp. 2154 – 2165, july 2006.
[17] 3GPP, "3rd generation partnership project; technical specification group radio access networks; universal terrestrial radio access (UTRA) and evolved universal terrestrial radio access (E-UTRA); verification of radiated multi-antenna reception performance of user equipment (UE) (release 11)," May 2012, 3GPP TR 37.977 V0.2.0 (2012-05). [Online]. Available: http://www.3gpp.org/ftp/Specs/archive/37_series/37.977/37977-020.zip
[18] ——, "3rd generation partnership project; technical specification group radio access network; evolved universal terrestrial radio access (E-UTRA); user equipment (UE) conformance specification radio transmission and reception part 1: Conformance testing; (release 10)," May 2012, 3GPP TS 36.521-1 V10.2.0 (2012-06). [Online]. Available: http://www.3gpp.org/ftp/Specs/archive/36_series/36.521-1/36521-1-a20.zip
[19] CTIA, "Test plan for wireless device over-the-air performance; method of measurement for radiated RF power and receiver performance," November 2012, CTIA Certification Test Plan for Mobile Station Over The Air Performance. rev. 3.2. [Online]. Available: http://http://www.ctia.org/
[20] S. S. M. Schwartz, W.R Bennett, *Communication Systems and Techniques*. McGraw-Hill, 1966.

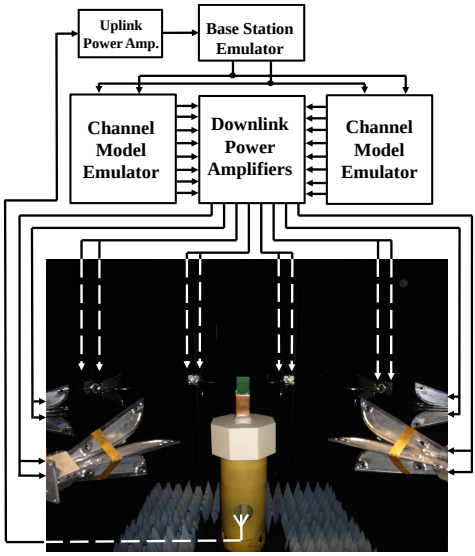

Fig. 7. Data throughput measurement setup LTE device and B13 MIMO 2x2 reference antenna.

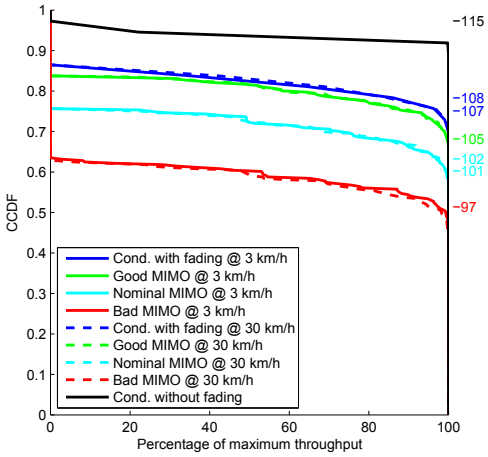

(a) SCME UMi

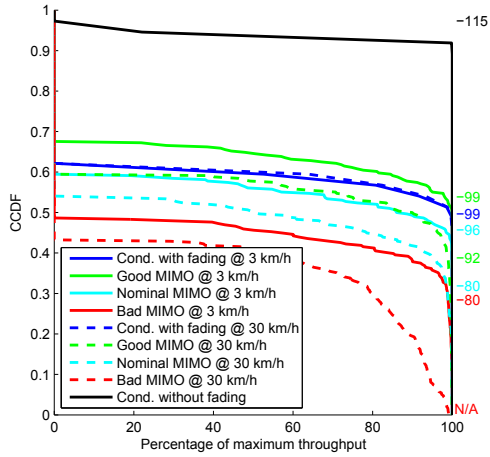

(b) SCME UMa

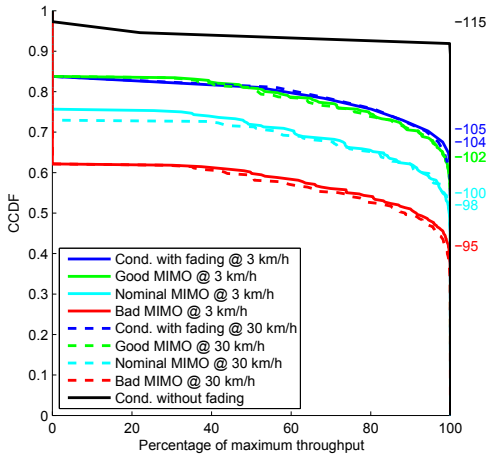

(c) Modified WINNER

Fig. 8. Data throughput measured with LTE device and B13 MIMO 2x2 reference antenna in different environments.

Istvan Szini received bachelors degree in Electrical Engineering from Mogi das Cruzes University, Brazil in 1990. Currently he is employed by Motorola Mobility L.L.C. as Distinguished Member of Technical Staff at Antenna Innovation Research Lab, in Libertyville design center in USA, and PhD candidate at Aalborg University. His primary interests are related to research, innovation and design on electrically small antennas for mobile devices, antenna adaptive tuning systems , RF Front-end design and MIMO antenna systems. Prior to his research role, he was the antenna lead designer for dozens handsets antenna systems including the iconic StarTAC Tri-mode Dual-band (1998), he lead the design of the first Motorola 3G handset with internal autonomous GPS antenna (A920/925, 2000), the first Motorola 3G Smartphone with four internal antennas (A/M1000, 2004), and the first handset with aluminum extruded housing (Devour/2009). Currently he had been involved with LTE MIMO antenna system design, Over The Air MIMO measurements and LTE Carrier Aggregation antenna systems enablers, he is Motorola delegate to MIMO OTA groups in CTIA, 3GPP RAN4, and COST IC1004 with liaison to CTIA. He holds 15 granted and pending patents.

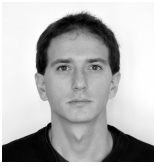

Boyan Yanakiev received a bachelors degree in physics from Sofia University, Bulgaria in 2006 and a master's degree in Wireless Communication and a PhD degree from Aalborg University, Denmark in 2008 and 2011 respectively. His current position is as an antenna design engineer at Molex Antenna Business Unit and an industrial postdoctoral fellow at Aalborg University. His primary interests are in the area of small integrated mobile antennas, optical antenna measurement techniques and radio channel measurements. He has been involved in the design and development of multiple RF-to-optical converters, for on board handset measurements.

Gert Frølund Pedersen was born in 1965 and married to Henriette and have 7 children. He received the B.Sc. E. E. degree, with honor, in electrical engineering from College of Technology in Dublin, Ireland, and the M.Sc. E. E. degree and Ph. D. from Aalborg University in 1993 and 2003. He has been employed by Aalborg University since 1993 where he is now full Professor heading the Antenna, Propagation and Networking group and is also the head of the doctoral school on wireless which some 100 PhD students enrolled. His research has focused on radio communication for mobile terminals especially small Antennas, Diversity systems, Propagation and Biological effects and he has published more than 75 peer reviewed papers and holds 20 patents. He has also worked as consultant for developments of more than 100 antennas for mobile terminals including the first internal antenna for mobile phones in 1994 with lowest SAR, first internal triple-band antenna in 1998 with low SAR and high TRP and TIS, and lately various multi antenna systems rated as the most efficient on the market. He has been one of the pioneers in establishing over-the-air measurement systems. The measurement technique is now well established for mobile terminals with single antennas and he was chairing the COST2100 SWG2.2 group with liaison to 3GPP for over-the-air test of MIMO terminals.

APPENDIX

Below are some details of the channel models specified in [1] and [17] used for the data in Section IV.

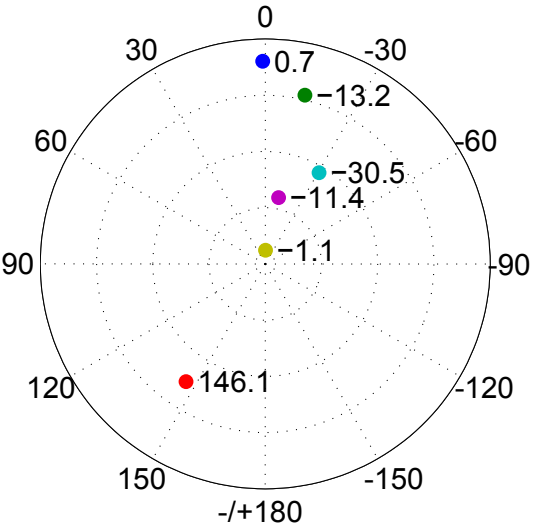

(a) Angle of Arrival

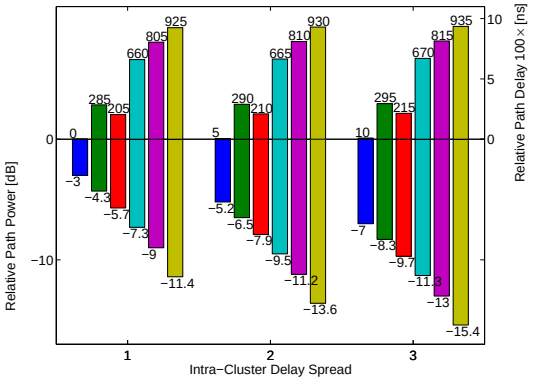

(b) Power and Delay Spreads

Fig. 9. SCME UMi channel properties.

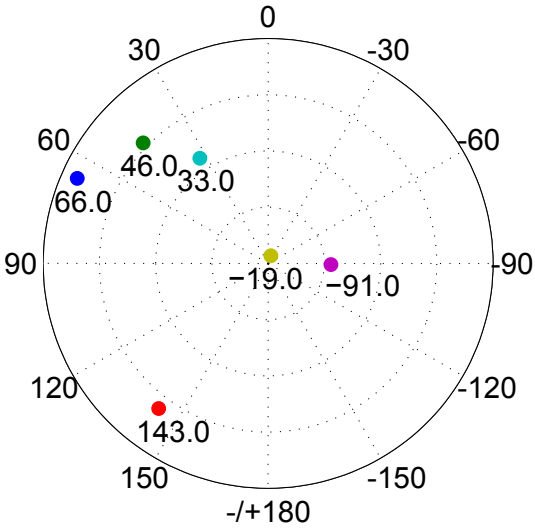

(a) Angle of Arrival

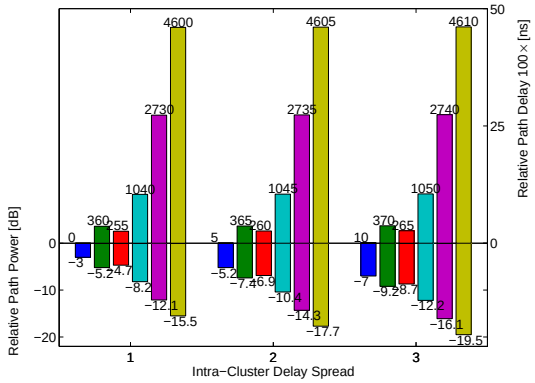

(b) Power and Delay Spreads

Fig. 10. SCME UMa channel properties.

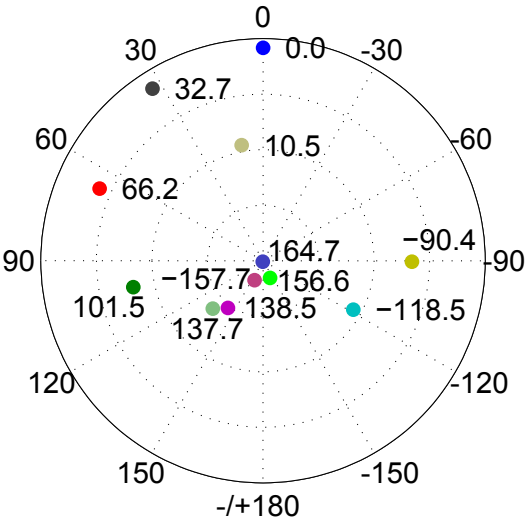

(a) Angle of Arrival

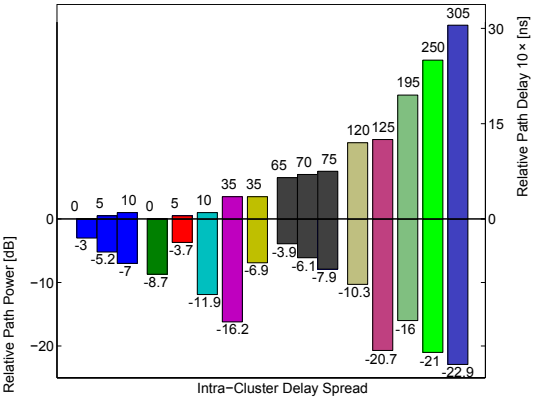

(b) Power and Delay Spreads

Fig. 11. Modified WINNER II channel properties.

Paper 6

On antenna polarization discrimination, validating MIMO OTA test methodologies

Istvan Szini, Michael Foegelle, Doug Reed, Tyler Brown and Gert Pedersen

Published as:
Szini, I.; Pedersen, G.; Reed, D.; Brown, T; Foegelle, M.,
IEEE Antennas and Wireless Propagation Letters, February 2014
vol., no., pp.265,268, 4 February 2014

On Antenna Polarization Discrimination, Validating MIMO OTA Test Methodologies

Istvan Szini, Michael Foegelle, Doug Reed, Tyler Brown, and Gert Frølund Pedersen

***Abstract*—The radiated performance of a multiple-input–multiple-output (MIMO) antenna system is commonly evaluated based on a set of antenna-centric figures of merit (FoM). These generally include the antenna's total efficiency, branch imbalance, and magnitude of the complex (or envelope) correlation coefficient. On the other hand, to validate the over-the-air (OTA) performance of the MIMO system, including both antennas and other parts of the real transceivers, test methodologies were created based on a single FoM: the absolute data throughput. While an antenna-centric FoM provides a preliminary overall insights into the radiated performance of the MIMO antenna system, these FoMs are limited in their overall applicability. Each of these FoMs is based on far-field antenna measurements and assuming a uniform distribution of the incoming power, meaning that passive antenna measurements are made in single-input–single-output (SISO) anechoic chambers. Furthermore, without the implementation of channel models with controllable spatial characteristics, it is impossible to isolate the effect of polarization changes on MIMO performance. In this letter, the radiated performance of MIMO antenna systems will be compared in terms of data throughput using different channel models both with and without controllable cross-polarization ratio and other spatial characteristics.**

***Index Terms*—Antenna, correlation coefficient, handset, low-band, multiple-input–multiple-output (MIMO), polarization.**

I. Introduction

THE FAST and expansive progress of fourth-generation (4G) wireless technology has mobilized different standards groups in the US, Europe, and Asia, i.e., CTIA The Wireless Association (CTIA [1], US) and Third Generation Partnership Project Radio Access Network 4 (3GPP RAN4 [2], Europe and Asia), as well as the European Cooperation in Science and Technology (COST IC1004 [3], topical working group OTA). All are searching for a definition of valid multiple-input–multiple-output (MIMO) over-the-air (OTA) test methodologies that can effectively and realistically evaluate the radiated performance of user equipment (UE). In the beginning of this search, 3GPP RAN4 and CTIA recognized candidate test methodologies in three categories [4]: anechoic chamber (AC)-based methodologies with arbitrary anisotropic spatial channel models obtained through channel emulators (CEs), methodologies using a reverberation chamber (RC) emulating isotropic channel models with or without control of the channel's temporal characteristics, and finally so-called multistage test methodologies. The latter methodologies rely on the nonintrusive gathering of the complex radiation patterns of the UE in a single-input–single-output (SISO) AC, which is then used in a conducted data throughput measurement where a CE emulates the combined channel/antenna responses.

The objective of this letter is first to verify whether the antenna-centric MIMO figure of merit (FoM) is sufficient to predict UE radiated performance, and second to determine if the current MIMO OTA test methodologies can adequately discriminate between MIMO device performance [5]. Thus, this letter is organized into four parts. Section I describes the experiment and the devices under test (DUTs), Section II describes the MIMO OTA test methodologies adopted in this study, whereas Section III analyzes the measured and simulated results. Finally, the conclusions are given in Section IV.

A. Description of the Experiment

The work described in this letter was motivated by the need to further understand the performance and behavior of MIMO antenna systems, under test methodologies based on random channel models with uniform (isotropic) power distributions, which fully randomize the signal's polarizations at the DUT receiver antennas. The results can then be compared to similar results obtained with the AC-based test methodologies that can emulate spatial channel models and polarization control [6]. The experiment includes the design and creation of several sets of MIMO antennas, where uncorrelated signals at the antenna outputs are obtained either by pure polarization diversity or by spatial diversity where both copolarized antennas were placed half a wavelength (λ) apart. Since the multistage method described in Section I relies on the UE antenna complex radiation patterns and emulation of the spatial channel model, proper discrimination of antenna polarization should be feasible. Results with the multistage method will be presented in future work.

B. Description of the Device Under Test

In this first preliminary study, five two-antenna systems were investigated as shown in Figs. 1 and 2. All antennas' configurations were based on commercially available downlink LTE Band 13 (746–756 MHz), single-band reference antennas used

Manuscript received October 18, 2013; revised December 19, 2013 and January 16, 2014; accepted February 01, 2014. Date of publication February 04, 2014; date of current version February 12, 2014.

I. Szini is with Motorola Mobility LLC, Libertyville, IL 60048 USA, and also with the Antennas, Propagation and Radio Networking Section, Department of Electronic Systems, Faculty of Engineering and Science, Aalborg University, Aalborg 9220, Denmark (e-mail: Istvan.Szini@motorola.com; ijs@es.aau.dk).

M. Foegelle is with ETS-Lindgren, Inc., Cedar Park, TX 78613 USA (e-mail: Michael.Foegelle@ets-lindgren.com).

D. Reed is with Spirent Communications, Fort Worth, TX 76107 USA (e-mail: Doug.Reed@spirent.com).

T. Brown is with Motorola Mobility LLC, Libertyville, IL 60048 USA (e-mail: Tyler.Brown@motorola.com).

G. F. Pedersen is with the Antennas, Propagation and Radio Networking Section, Department of Electronic Systems, Faculty of Engineering and Science, Aalborg University, Aalborg 9220, Denmark (e-mail: gfp@es.aau.dk).

Color versions of one or more of the figures in this letter are available online at http://ieeexplore.ieee.org.

Digital Object Identifier 10.1109/LAWP.2014.2304534

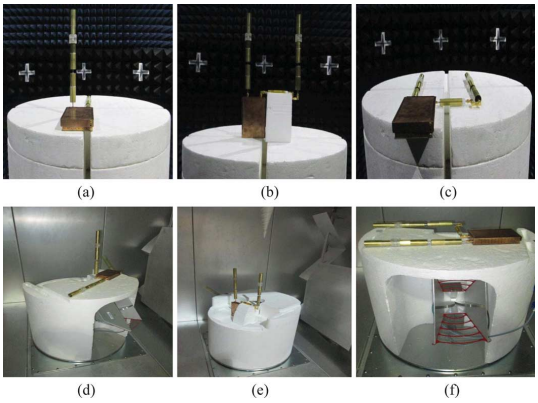

Fig. 1. MIMO antenna system based on $\lambda/2$ dipoles: (a) cross-polarized in AC; (b) vertical (V) copolarized in AC; (c) horizontal (H) copolarized in AC; (d) cross-polarized in RC; (e) vertical (V) copolarized in RC; (f) horizontal (H) copolarized in RC .

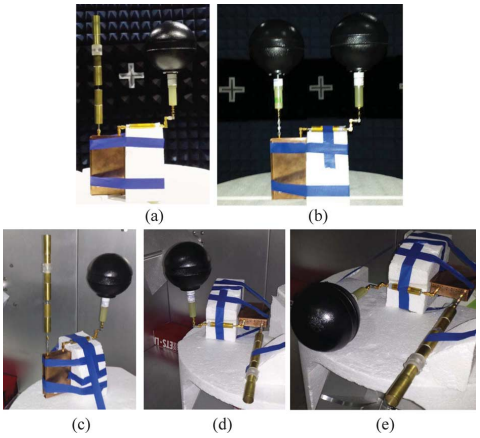

Fig. 2. MIMO antenna system based on $\lambda/2$ dipoles and loop antennas: (a) cross-polarized in AC; (b) H copolarized in AC; (c) cross-polarized in RC; (d) H copolarized in RC; (e) cross-axis cross-pol.

for chamber calibration[7], and a radio frequency (RF) enclosure (see [8]). During the measurements for the passive FoMs, each branch of all antenna systems was measured in the SISO chamber, one at the time, while the other antenna was terminated at 50 Ω.

The setup shown in Fig. 1 is based on two Band-13 $\lambda/2$ dipoles. While adopting two dipoles to represent horizontal copolarized antennas [Fig. 1(c)], there is a known shift in the absolute level, which is due to the pattern shape of a horizontally oriented $\lambda/2$ dipole. The total average power of a horizontally oriented dipole receiving a horizontally polarized signal is -3.5 dB compared to a vertically oriented dipole receiving a vertically polarized signal. This effect is demonstrated in Fig. 3. To compare results to a similar setup, i.e., antennas with purely vertical or horizontal polarization, the setup shown in Fig. 2 was created based on a Band-13 $\lambda/2$ dipole as the

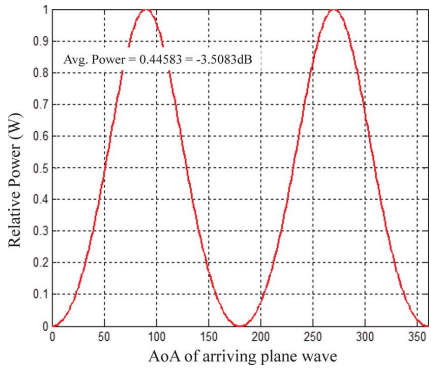

Fig. 3. Horizontal dipole average power versus angle of arrival for horizontally oriented dipole.

pure vertically polarized antenna, and a resonant loop antenna as the pure horizontal polarized antenna.

II. Description of the MIMO OTA Test Methodologies

A. Anechoic Chamber Boundary Array

The anechoic chamber boundary array consists of eight active dual-polarized (DP) antennas at a radius of 1.95 m driven by two eight-output channel emulators for a total of 16 total output channels. These 16 antennas are used to generate the desired fields within the test volume by applying power weighting and Rayleigh fading in the CEs [9]. Two eight-channel power amplifiers were used to amplify the outputs of the CEs to produce the required signal levels within the test volume. The reported measurements were captured using a base-station emulator/communication tester. The two outputs of the tester were each split and fed into the two CEs. The antenna for uplink transmissions from the UE to the base-station emulators was a separate circularly polarized conical log. The uplink path was then fed through a preamplifier to provide additional downlink isolation prior to feeding the signal to the base-station emulator input.

B. Reverberation Chamber

The RC-based test system illustrated in Fig. 5 was used to create the statistically isotropic channel, where the angles of arrivals of the rays are uniformly distributed over the sphere. The system consists of a compact RC ($2.00 \times 1.20 \times 1.50$ m^3) with two independent stirring paddles and a UE turntable. It has a lowest operating frequency of 700 MHz and is connected to a base-station emulator/communication tester. The RC was selectively loaded to produce an RMS delay spread of 80 ns for the statistically isotropic channel model. Tests were performed using continuous stirring for an integral number of rotations of all positioners at a fixed ratio and time, in such a way that one long throughput measurement was performed per revolution of the slowest positioner, thus producing one average throughput measurement per 1 dB of downlink power-level step.

III. Measurement Results

A. Antennas Passive FoM

Table I shows the antenna-centric FoMs obtained by post-processing the far-field complex radiation pattern of each antenna pair. The table compares all five antenna systems for

TABLE I
MIMO ANTENNA-CENTRIC FOM, BASED ON 3-D ISOTROPIC MEASUREMENTS AT 751 MHZ

MIMO B13 antennas		ant. position	Total Efficiency (%)	Polarization Ratio V/H (dB)	Branch imbalance (dB)	ecc
Fig1 a,d	Cross-polarized (two dipoles)	Antenna 1 (V)	90.68	21.9	0.4	0.0059
		Antenna 2 (H)	81.76	-4.9		
Fig1 b,e	Vertical co-polarized (two dipoles)	Antenna 1 (V)	86.10	22.8	0.0	0.0001
		Antenna 2 (V)	86.15	22.5		
Fig1 c,f	Horizontal co-polarized (two dipoles)	Antenna 1 (H)	87.76	-5.0	0.2	0.0017
		Antenna 2 (H)	83.58	-4.8		
Fig2 a,c	Cross-polarized (V dipole, H loop)	Antenna 1 (V)	98.65	23.0	4.3	0.0001
		Antenna 2 (H)	36.29	-18.6		
Fig2 b	Horizontal co-polarized (two loops)	Antenna 1 (H)	26.43	-16.6	1.4	0.0065
		Antenna 2 (H)	36.85	-18.6		

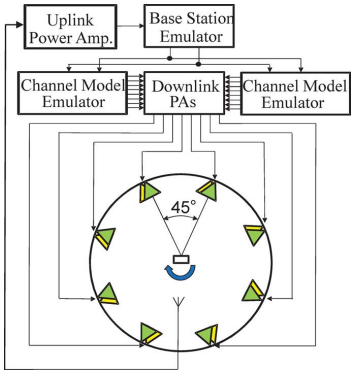

Fig. 4. Anechoic chamber boundary array, test setup simplified diagram.

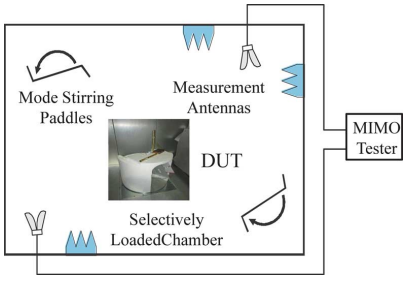

Fig. 5. Reverberation chamber, test setup simplified diagram.

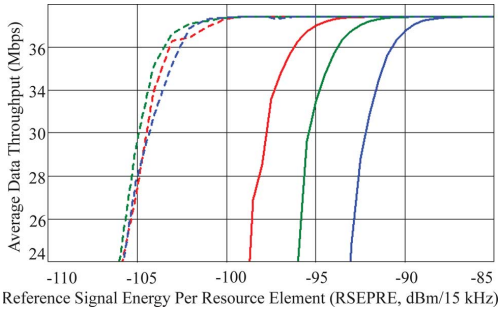

Fig. 6. Anechoic chamber boundary array with eight DP antennas, SCME Umi, 30 kph, XPR = 9 dB, 12 UE azimuth positions throughput average benchmark, solid red [Fig. 1(a)] cross-pol, solid green [Fig. 1(b)] V-pol, solid blue [Fig. 1(c)] H-pol. Reverberation chamber, antennas benchmark, (80 ns RMS delay spread) statistically isotropic channel model, same antenna configuration as shown in Fig. 1(d)–(f) in respective colored dashed lines.

total efficiency, polarization ratio, branch imbalance, and envelope correlation coefficient (ecc). These data were measured in the SISO chamber one element at a time, i.e., while main antenna (1) was being measured, the secondary antenna (2) was terminated in 50 Ω, and vice versa. The antenna setup based on dipoles as shown in Fig. 1 has a high total efficiency near 90%, low branch imbalance around 0.5 dB, and envelope correlation coefficient lower than 0.1. However, the placement of dipoles horizontally did not provide the pure horizontal polarization. To achieve pure horizontal polarization, a new set of antennas was designed as shown in Fig. 2. Note that for this work, loop antennas tuned to LTE Band 13 (751 MHz) were not available. Instead, loop antennas tuned near 700 MHz were used, thereby compromising the total efficiency at 751 MHz. However, since the objective was to analyze the impact of polarization discrimination among different test methodologies, the lower efficiency, or higher branch imbalance, in the setup with loop antennas has no relevance to the conclusion since the envelope correlation remains lower than 0.01 and the polarization ratio is higher than 16 dB.

B. Data Throughput

For the cross-polarized experiment in the AC shown in Fig. 1(a), the antennas consist of one vertical and one horizontal dipole element in the test zone. The Spatial Channel Model Extended Urban Micro (SCME UMi) was emulated using channel emulators with the proper mapping algorithm. However, there is a slight advantage to the vertical polarization by about 0.88 dB for the SCME Umi model with channel emulator cross-polarization settings equal to 9 dB. In this case, low correlation is achieved when the UE receives signals on orthogonal branches since the BS correlation observed on the vertical polarization is about $+82\%$, and the BS correlation observed on the horizontal is about -70%, thus resulting in low correlation due to near cancellation when observed between branches as shown in Fig. 6. In this case, the vertical polarization has slightly more power that the horizontal by 0.88 dB as defined by the channel model. Since the horizontal dipole attenuates the average signal by 3.5 dB, there is a slight power

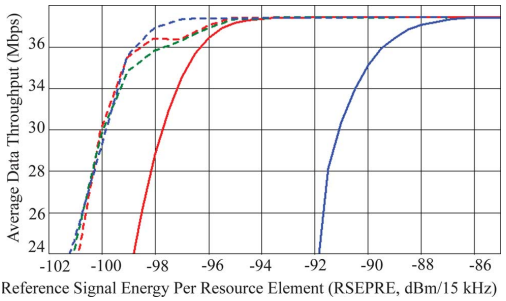

Fig. 7. Anechoic chamber boundary array with eight DP antennas, SCME Umi, 30 kph, XPR = 9 dB, 12 UE azimuth positions throughput average benchmark. Solid red [Fig. 2(a)] cross-pol V dipole H loop, solid blue [Fig. 2(b)] H copol two loops. Reverberation chamber, antennas benchmark, (80 ns RMS delay spread) statistically isotropic channel model, same antenna configuration as shown in Fig. 2(c) (dashed red), Fig. 2(d) (dashed green), and Fig. 2(e) (dashed blue).

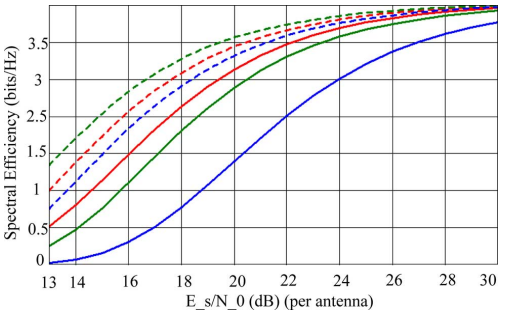

Fig. 8. Simulated results, SCME Umi, 30 kph, XPR = 9 dB. Solid red [Fig. 1(a)] cross-pol, solid green [Fig. 1(b)] V-pol, solid blue [Fig. 1(c)] H-pol. Statistically isotropic channel model (80 ns RMS delay spread), same antenna configuration as shown in Fig. 1(d)–(f) in respective colored dashed lines.

advantage to the curve with the channel emulator cross-polarization ratio (XPR) setting equal to 9 dB, which is the default cross-polarization value defined in [4].

The same three antennas described in Fig. 1(d)–(f) were measured with the MIMO OTA test method based on an RC. While the performance of the same antennas could be discriminated in an anechoic chamber by their unique polarization characteristics by ≈ 6 dB, in the reverberation chamber, such discrimination could not be verified due to its intrinsic polarization randomization, as also shown in Fig. 6.

Yet another set of antennas was evaluated, shown in Fig. 2. In this case, both antennas have high polarization purity since the vertically polarized antenna is a dipole and the horizontally polarized antenna is a loop, as expected further discrimination in data throughput (≈ 8 dB) is observed when comparing both antenna setups; see Fig. 7.

The preliminary link-level simulation results in Fig. 8 agreed with measurements in Fig. 6. The discrimination of the horizontally polarized dipole over the cross-polarized dipole in the simulation results is 5 dB versus 6 dB for the experimental results. The curves offset and slope differences between the curves for the simulated and measured cases may be due to differences in calibration of absolute power between the two methodologies and to the fact that the RC simulations were run in stirrer step mode (20 000 subframes per isotropic state), while the RC measurements were done in continuous stirring mode.

IV. Conclusion

A set of MIMO antennas was considered for verification of MIMO OTA test methodologies. The antennas have similar 3-D fundamental FoMs, but different polarization characteristics. The antennas were demonstrated to have different MIMO OTA radiated performance when evaluated under the assumption of the spatial channel models defined in [4], and with a channel cross-polarization power difference other than 0 dB. However, the relative performance differences of the same antennas could not be reproduced in the statistically uniform MIMO OTA test environment due its intrinsic inability to generate cross-polarization power differences other than 0 dB. While [10]–[12] report that the RC-based OTA test methodology can discriminate antenna systems with different correlation coefficients based on polarization diversity, they do not demonstrate that an antenna system with the same correlation coefficient but different antenna polarizations can be discriminated. The measured and simulated performances of the antennas presented in this letter effectively challenge the validity of relative "MIMO devices ranking" as pass/fail criteria for OTA performance. As demonstrated, the same MIMO antenna systems can have different relative performance in different test methodologies due to fundamental limitations in a test methodology, i.e., lack of antenna polarization discrimination.

References

[1] CTIA, Washington, DC, USA, "CTIA official Website," 2011 [Online]. Available: http://www.ctia.org/

[2] 3GPP, "LTE," Tech. Rep., Oct. 2010 [Online]. Available: http://www.3gpp.org/LTE

[3] COST IC1004, "European cooperation in the field of scientific and technical research," 2011 [Online]. Available: http://www.ic1004.org/

[4] 3GPP, "Verification of radiated multi-antenna reception performance of user equipment (UE)," Tech. Rep. 3GPP TR 37.977 v1.0.0, 2013.

[5] K. Ogawa, H. Iwai, A. Yamamoto, and J.-i. Takada, "Channel capacity of a handset MIMO antenna influenced by the effects of 3D angular spectrum, polarization, and operator," in *Proc. IEEE Antennas Propag. Soc. Int. Symp.*, 2006, pp. 153–156.

[6] D. Baum, J. Hansen, and J. Salo, "An interim channel model for beyond-3G systems: Extending the 3GPP spatial channel model (SCM)," in *Proc. 61st IEEE VTC-Spring*, Jun. 1, 2005, vol. 5, pp. 3132–3136.

[7] ETS-Lindgren, Cedar Park, TX, USA, "ETS-Lindgren," 2013 [Online]. Available: http://www.ets-lindgren.com/

[8] I. Szini, G. Pedersen, A. Scannavini, and L. Foged, "MIMO 2×2 reference antennas concept," in *Proc. 6th EuCAP*, Mar. 2012, pp. 1540–1543.

[9] P. Kyosti, J.-P. Nuutinen, and T. Jamsa, "MIMO OTA test concept with experimental and simulated verification," in *Proc. 4th EuCAP*, Apr. 2010, pp. 1–5.

[10] M. Andersson, C. Orlenius, and M. Franzen, "Very fast measurements of effective polarization diversity gain in a reverberation chamber," in *Proc. 2nd EuCAP*, 2007, pp. 1–4.

[11] J. Valenzuela-Valdes, M. Garcia-Fernandez, A. Martinez-Gonzalez, and D. Sanchez-Hernandez, "The role of polarization diversity for MIMO systems under Rayleigh-fading environments," *IEEE Antennas Wireless Propag. Lett.*, vol. 5, pp. 534–536, 2006.

[12] J. Valenzuela-Valdes, M. Garcia-Fernandez, A. Martinez-Gonzalez, and D. Sanchez-Hernandez, "Evaluation of true polarization diversity for MIMO systems," *IEEE Trans. Antennas Propag.*, vol. 57, no. 9, pp. 2746–2755, Sep. 2009.

Paper 7

On Small Terminal MIMO Antennas, harmonizing Characteristic Modes with Ground Plane Geometry

Istvan Szini, Alexandru Tatomirescu and Gert Pedersen

Accepted for publication in:
IEEE Transaction on Antenna and Propagation, December 2013

On Small Terminal MIMO Antennas, Harmonizing Characteristic Modes with Ground Plane Geometry

Istvan Szini, Alexandru Tatomirescu,
and Gert Frølund Pedersen

***Abstract*—MIMO antenna systems are defined by fundamental figure of merits (FoM), such as branch imbalance, total efficiency, Mean Effective Gain (MEG) and the correlation coefficient.Those FoM requirements are challenging, specially when applied to electrically small mobile devices i.e. smartphones, due to the form factor reduced dimensions and multiplicity of adjacent frequency bands of operation. Uncorrelated antennas are especially important for Multiple Input - Multiple Output (MIMO) antenna systems, other than few exceptional cases, the reduction of magnitude of complex correlation coefficient will increase system capacity and data throughput. This work proposes a MIMO antenna system for mobile terminals, based on a realistic form factor and packaging implementation, with a very low magnitude of the complex correlation coefficient and an impressive isolation. An isolation better than 20 dB has been achieved using a folded monopole and a commonly adopted PIFA (planar inverted F antenna) on a platform with a very small form factor (100x50x10 mm). The proposed implementation is based in the synergy of two known techniques where the first technique consists in the reference ground plane geometry manipulation and the other technique consists in the application of the characteristic mode theory to obtain orthogonal radiation modes. Since MIMO antenna systems at frequencies higher than 1.7 GHz are naturally proper isolated and decorreleated, this work demonstrates the proposed antenna topology enabling higher isolation and uncorrelated antenna system at 750 MHz which it is more difficult to achieve in form factors smaller than 1λ , while maintaining high total efficiency and adequate gain imbalance. In this paper a simulation model as well as prototype ($1/4\lambda$ long) measurement results are presented, demonstrating the implementation feasibility of such antenna system in realistic mobile device embodiment.**

***Index Terms*—MIMO, correlation coefficient, low-band, antenna, handset.**

I. Introduction

THE widespread use of MIMO in current and future wireless communications systems has spurred considerable attention in the research community. Over the past years, small antenna array design has been the subject of numerous research articles [1]–[21]. Receiver diversity and MIMO have improved the reliability and data rate of wireless links enabling 4G communications standards see e.g. [1]–[3]. Ideally, by taking advantage of the multi-path properties of the wireless channel, MIMO uses parallel data streams to linearly increase capacity with the number of array elements [2]. In practice, the increase in system capacity is strongly depended on the channel proprieties governed by the various wireless channel propagation characteristics such as the power imbalance between the multiple links or their correlation [4], [5].

In classical array design, the distance between the elements has been kept to $\lambda/2$ to minimize the unwanted coupling between the elements of an array and to minimize the spatial correlation [22]. However, the size of even the modern smart phones does not allow for this criterion to be satisfied if we consider the low bands standardized and implemented by some mobile operators for Long Tern Evolution (LTE), the total array size is much smaller that the requirement of $\lambda/2$ and at these lower frequencies the antennas rely on the shared electrically small Printed Circuit Board (PCB) ground plane for efficient radiation. Consequently, the antennas will have a very strong electromagnetic coupling and high far-field pattern correlation thus a limited capacity [6]. Therefore, MIMO antenna systems adopted in handsets size devices need to rely on radiation pattern diversity and isolation enhanced techniques to enable somewhat adequate MIMO performance.

The MIMO antenna system introduced in this paper, defines realistic antenna placements, independent excitation modes and feeding mechanisms, manipulation of ground plane geometry to control ground surface current and application of characteristic mode theory. The synergy of these techniques enables the design of highly isolated and uncorrelated antennas at low frequency bands, with adequate gain imbalance and total efficiency, within the constrains of realistic implementation in small terminals. This work is presented starting with an investigation of the most adopted techniques to reach similar results, then a discriminative characterization of the concept proposed in this paper, the proof of this concept through simulation and measurement results, and finally the conclusion.

There is vast amount of literature demonstrating MIMO antenna system design techniques to improve antennas isolation and decorrelation [8]–[21], [23]–[25]. Guo et al [7] demonstrated that at higher frequencies (above 1.7GHz), a PIFA antenna system design can achieve envelope correlation coefficient < 0.5. Using PIFA antennas placed on a uniform ground plane, and small distance between antennas, the overall envelope correlation coefficient between them remains suitable for MIMO applications. Kuonanoja [8], presents a solution which addressed partially the correlation coefficient and isolation in lower bands, i.e. bellow 960MHz. His work is based on ground clearance underneath both antennas, and dynamic

I. Szini is with Motorola Mobility LLC., Libertyville, USA; email: Istvan.Szini@motorola.com.

I. Szini, A. Tatomirescu and G. F. Pedersen are with the Antennas, Propagation and Radio Networking section at the Department of Electronic Systems, Faculty of Engineering and Science, Aalborg University, Denmark; email: {ijs; ata; gfp}@es.aau.dk

matching network. Li et al [9] demonstrates that adequate isolation between antennas at low frequencies can be achieved in a relatively small ground plane, even if both antennas rely on ground plane excitation. The isolation between antennas can be optimized based on antenna excitation technique and antenna placement over the ground plane. However decoupling is achieved with reduced bandwidth because of the ground plane electrical length reduction. Furthermore, the magnitude of complex correlation coefficient is larger than 0.7. Based on his findings the optimal uncorrelated MIMO antennas are placed at the center of the ground plane which limits the number of practical use cases. In fact several other techniques had been individually presented to mitigate the lack of isolation between antennas in electrically small mobile devices, including:

- Parasitic Scatterers have the main drawback of the limited operating frequency bandwidth, lowered radiation efficiency, bulky antennas and rely on on static near-fields [10], [11].
- Neutralization lines require a connecting structure between the array elements to introduce a coupling cancellation path [12]–[16]. This in turn introduces extra losses, high complexity in dual/multi-band implementations, limits the antenna design by the symmetry requirement and is very susceptible to near-field interactions.
- Decoupling structures require complex and often lossy feeding networks for canceling the over the air antenna coupling at the feeding point [17]–[20]. Similar to the previous methods, it limits the system bandwidth and its performance is significant degraded if the antenna impedance changes.
- Ground plane current flow requires a significant antenna volume [21].

One characteristic which is common to most of the related literature, is that the antenna system solution isn't suitable to real application in small mobile terminals, due to antenna placement interference with required hardware such as display bezels, batteries, large dimension of the ground plane or spacing between antennas. In this work a antenna system is presented within the constrains of realistic smart-phone dimensions and parts placement.

II. Proposed Antenna Design Technique

A. Correlation impact on a MIMO 2x2 system capacity

From Eq. (1), the magnitude of the complex correlation coefficient is defined by the magnitude and phase of the complex radiation pattern of both antennas as well as the propagation environment [26]. While $\vec{E}_{\theta X}(\Omega)$ is the vertical polarization complex radiation pattern from main antenna, $\vec{E}^{*}_{\theta Y}(\Omega)$ is the vertical polarization complex radiation pattern from secondary antenna. Respectively $\vec{E}_{\phi X}(\Omega)$ is the horizontal polarization complex radiation pattern from main antenna, and $\vec{E}^{*}_{\phi Y}(\Omega)$ is the horizontal polarization complex radiation pattern from the secondary antenna. $\mathrm{G}\,\theta$ and $\mathrm{G}\,\phi$ are the antennas respective vertical and horizontal polarizations gain, while Ω is the solid angle for a spherical coordinate system and XPR is the cross-polarization discrimination of the antennas.
From this analytic perspective the correlation coefficient can be mitigated by the manipulation of both antennas complex radiation pattern, however from a system perspective the problem of improving the correlation coefficient between antennas is more complex.

Considering the MIMO 2x2 downlink systems; the focus of this study; the basic system diagram of the antenna array is represented in Fig. 1.

The ultimate objective in implementing a MIMO system is improving system capacity. As demonstrated previously; depending on the SNR value; the MIMO system with severe gain imbalance between antennas, despite uncorrelated antennas, will not realize significant MIMO capacity gain [27].

To optimize MIMO capacity several general properties need to be observed as summarized below:

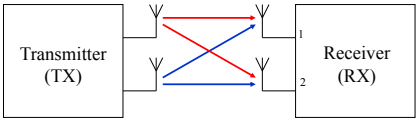

Fig. 1. MIMO 2x2 system, graphical representation.

- Both antennas; Main Antenna (Tx/Rx) and Secondary Antenna (Rx only); need to have appropriate radiated performance with minimum gain imbalance, ideally $0\ dB$;
- Considering that the rich scattered environment will increase the rank of the channel gain matrix [28], the maximum capacity will occur in most cases when both receiver antennas are uncorrelated. There are exceptional cases where co-polarized antennas can still be uncorrelated, however hard to accomplish in hand-held form factors due the limited spacing between antennas;
- The absolute phase of both the Main (Tx/Rx) and Secondary (Rx) antennas are irrelevant, but the phase per direction or the relative phase relationship between the antennas define the antenna system correlation coefficient.
- Considering the special case of a hypothetical isotropic environment, a good design for a MIMO antenna system is one with good isolation between antennas $S_{21} < -20\ dB$, high total efficiency per antenna $\eta > 90\ \%$, low Branch Power Ratio ($BPR \approx 0\ dB$), and low correlation coefficient ($\rho \approx 0$). It will provide double the capacity of the counterpart Single Input Single Output (SISO) system (this statement is based solely on antenna parameters and assumes ideal uniform angular power spectrum).

$$\rho = \frac{\oint \left[XPR\ \vec{E}_{\theta X}(\Omega)\vec{E}^{*}_{\theta Y}(\Omega)p_{\theta}(\Omega)\ + \vec{E}_{\phi X}(\Omega)\vec{E}^{*}_{\phi Y}(\Omega)p_{\phi}(\Omega) \right] d\Omega}{\sqrt{\oint \left[XPR\ G_{\theta,1}(\Omega)p_{\theta}(\Omega) + G_{\phi,1}(\Omega)p_{\phi}(\Omega) \right] d\Omega\ \oint \left[XPR\ G_{\theta,2}(\Omega)p_{\theta}(\Omega) + G_{\phi,2}(\Omega)p_{\phi}(\Omega) \right] d\Omega}} \tag{1}$$

B. Manipulation of the ground plane geometry

The antenna system described in this work can be extended to MIMO channel matrices with $nTransmitters(nTx)$ x $nReceivers(nRx)$ where $nRx = 2$, for simplification the considered MIMO 2x2 antenna topology comprises of two antennas, i.e. Antenna 1 also referred as the Main Antenna that is used as a Tx/Rx antenna, and Antenna 2 also referred as Secondary Antenna only used as Rx. The antenna system has a ground plane measuring 100x50x1 mm. Both antennas have similar topology and are oriented towards what would be the rear housing in a real implementation. The Main antenna is positioned at the lower part of rear the housing and the Secondary Antenna is placed on the right side of the rear housing. In this study, the width of the antennas elements are fixed to 1mm, and the thickness of the conductors are fixed to 0.2 mm.

The individual antenna elements described in this work has its origins based on the Windom antenna [29]. The Windom antenna concept had been adapted to electrically small planar antennas and reduced reference ground plane. Electrically small devices equipped with low-band antenna system; e.g. 746 - 960 MHz; relies on the chassis ground plane to generate a dipole mode excitation [30]. In the preliminary embodiment adopted in his study a shown in Fig. 2, the ground plane measures approximately $\lambda/4$ at lower bands ($<$1 GHz). Sharing the same excitation mode and being driven against the same reference ground plane, antennas following conventional topologies and placement will be naturally correlated, thus arbitrarily designed 2x2 MIMO antenna systems will present strong coupling due to lack of isolation between elements and identical excitation modes [11], [18]–[20], [31].

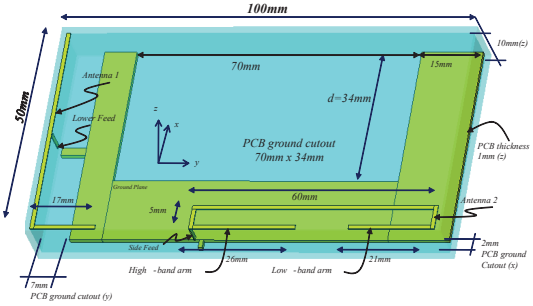

Fig. 2. MIMO 2x2 multi-band antenna system geometry.

The antenna topology proposed in this work, combines the placement of high and low impedance regions of the individual antennas associated with the change in ground plane geometry to improve isolation between antennas, therefore improvement in absolute total efficiency is achieved [16], [32], [33]. The asymmetry of the ground plane also enables a degree of freedom in controlling the antennas radiation pattern, tilt and directivity [23]–[25]. While the Main Antenna excites the chassis in dipole mode, the Secondary Antenna excites the chassis in the orthogonal mode. Therefore, creating a highly uncorrelated (envelope correlation coefficient= 0.08) low-band antenna system with adequate free space isolation between antennas ($>$12 dB), as indicated on measurement results shown in Fig. 3 measured in anechoic chamber.

Notwithstanding satisfactory isolation and correlation coefficient, the borderline acceptable isolation between antennas obtained in free space as shown in Fig. 3, does not meet different user cases e.g. head plus hand, portrait with single hand or landscape with two hands grips. These design shortcomings which afflict most of the MIMO antenna system designs, motivates the evolution of this antenna design topology towards further improvement on the antenna isolation. Such improvement can be achieved through the application of the characteristic mode theory described as follows.

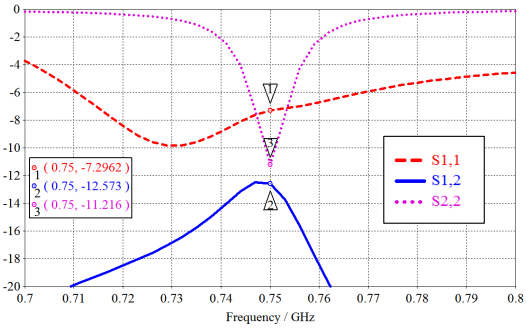

Fig. 3. Antenna system return loss and isolation in dB for d=34mm.

C. Characteristic Mode Theory

With the recent increase of complexity in the shape of mobile phone antennas, the use of numerical electromagnetic solvers has become an imperative step in the antenna design process. Although this approach can accelerate considerably the design process, it does not provide a deep physical insight into the radiation mechanism of the antenna and in some cases the real working principle of the antenna can be obscured. Numerous publications on the topic of mobile antennas, especially the ones targeting hand-held wireless devices, focus their effort on describing the geometry of the antenna rather than explaining the design procedure and its physical aspects e.g. [34]–[36]. In order to obtain a deeper understanding of the fundamental working principle of the antenna, alternative methods should be used.

Any conducting object has natural resonant frequencies at which its entire structure oscillates sinusoidally. From an antenna perspective, maximum radiation is achieved when the structures is exited at these frequencies. They can be linked to the physical shape of the object by describing the radiant mechanism with a set of oscillating modes. Modal analysis has been used extensively in the past and is well established in the electromagnetic analysis of closed, bounded structures such as waveguides and cavities, for which it is straight forward to arrive at close form solutions [37]. However, open radiating structures, such as antennas and scattering problems, pose a different challenge which is more computationally demanding. Nevertheless, the increase in processing power in

current computers make this method very attractive compared to decades ago when it was first introduced.

The theory of characteristic modes or eigen functions of conducting bodies, introduced by Garbacz in 1968 [38] and improved by Harrington and Mautz [39], provides a set of orthogonal spherical field distributions in the far-field. These field modes, also known as characteristic fields, have the useful property that they are radiated from an orthogonal set of current distributions running along the surface of the conducting body of arbitrary shapes. These current distributions, the modal or characteristic currents, are real or equiphasal currents that diagonalize the generalized impedance matrix for the surface for which they were defined [40]. The generalized impedance matrix is defined as the operator $L(J)$ that maps a surface current distribution J to the tangential component of the incident electric field E^i using Eq. (2) .

$$[L(J) - E^i]_{tan} = 0 \tag{2}$$

Because $L(J)$ relates the electric field to the current distributions, it has the dimensions of impedance and can expressed as in Eq. (3) and Eq. (4) using a real and imaginary decomposition, as derived in [40].

$$Z(J) = [L(J)]_{tan} \tag{3}$$

$$Z(J) = R(J) + jX(J) \tag{4}$$

As defined in [39], the characteristic currents $\overrightarrow{J_n}$ are the eigen functions of the following eigen value problem applied to the impedance operator $Z(J)$:

$$X(\overrightarrow{J_n}) = \lambda_n R(\overrightarrow{J_n}) \tag{5}$$

A very useful aspect of the characteristic mode analysis for antenna design is the variation of the eigen value(λ_n) of a certain eigen function or vector (J_n) over frequency. By evaluating it, one can determine the resonance frequency and bandwidth of a mode using the modal significance (MS_n) [41], as defined in Eq. (6). It measures the quantity of the normalized amplitude of a mode that contributes to the radiation. A maximum value of 1 represents a 100% contribution to radiation by the current distribution of current mode.

$$MS_n = \left| \frac{1}{1 + \lambda_n} \right| \tag{6}$$

The electric fields E_n generated by the eigen current distributions $\overrightarrow{J_n}$ as defined in Eq. (8), generically named characteristic fields [40], are described in the following equation.

$$E_n(\overrightarrow{J_n}) = Z(\overrightarrow{J_n}) = R(\overrightarrow{J_n})(1 + j\lambda_n) \tag{7}$$

The fields radiated by eigen currents have the important property that they are orthogonal over the sphere at infinite. In other words, different modes will have orthogonal far-field radiation patterns which will lead to a zero correlation according to Eq. (1), ideal for the design of MIMO antennas. However when it comes to compact phones, in the low bands, the ground plane is the main radiator which has only one efficient mode. The dipole mode [30], which will be exemplified further.

$$E_n(\overrightarrow{J_n}) = Z(\overrightarrow{J_n}) = R(\overrightarrow{J_n})(1 + j\lambda_n) \tag{8}$$

The form factor 100x50 mm, is a typical lower bound for a modern phone size that supports MIMO. In the low band used for communications, the phone is considerably smaller than the wavelength of operation and thus designing two decoupled and efficient radiators is not straightforward. For a compact phone the ground plane of the Printed Circuit Board (PCB) is the main radiator and hence, the characteristic modes of the ground plane offer insight into the required design of the exciting elements in order to obtain decoupled radiation modes. The current distribution of the first two characteristic modes of two types of ground planes, a realistic C shaped with space for the battery and a classical rectangular shape, have been plotted in Fig. 4 and Fig. 5, respectively. Only the fist two modes have been shown because the modal significance of the higher modes at low frequency is very small resulting in a negligible contribution to total radiation, as it can be seen in Fig. 6. The modes have been computed by eigen mode decomposition of the impedance matrix, obtained using the code from [42].

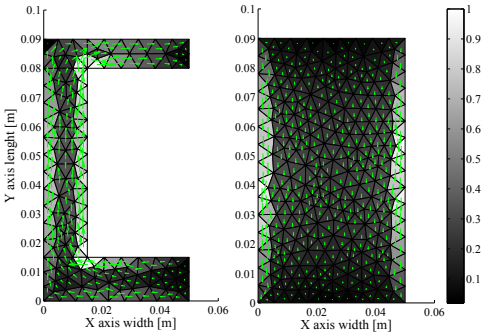

Fig. 4. The normalized current distribution of the first mode for the two types of ground planes considered in linear scale. The arrows represent the direction of the current.

The current distributions shown in Fig. 4 and Fig. 5 suggest that for both ground plane types the first mode, the dipole mode, the radiated structure can be easily exited by an element that capacitive couples to the GND with an element at the top or bottom second mode, the cross polar dipole mode, can be excited be placing a similar element in the middle of the sides. Nevertheless, the analysis of the modal significance of the two

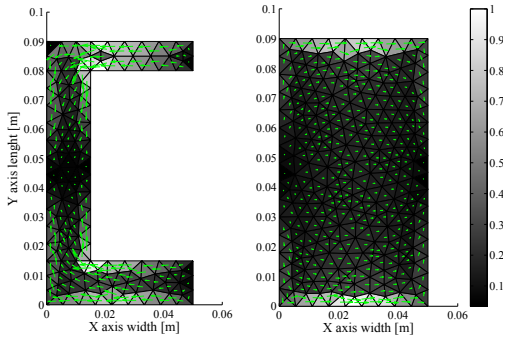

Fig. 5. The normalized current distribution of the second mode for the two types of ground planes considered in linear scale. The arrows represent the direction of the current.

modes from Fig. 6 indicates that the second mode is going to have poor radiation characteristics and a low bandwidth in both cases. In addition, the PCB resembling a "C" shape, with a centered ground cutout for the battery placement, improves significantly the bandwidth of the dipole mode by shifting the resonance from 1.4 GHz to 0.9 GHz while only degrading slightly the other modes.

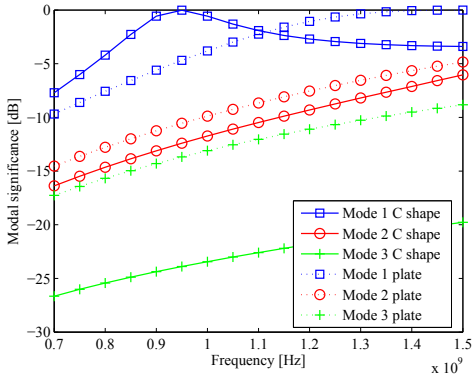

Fig. 6. The modal significance of the tree most important modes. The other modes

In literature, there are examples of different ways of exiting these modes, by using a loop antenna combined with a Planar Inverted F Antenna (PIFA) [43], with the help of hybrid couplers for the higher frequencies [44] or by using symmetry of an electrically large exciting element [45]. In this paper, consideration is given to practical design of a compact MIMO antenna for phones, where the antenna design is constrained by its integration with large components as well as the limited volume allocated for the antenna.

III. SIMULATION RESULTS

The simulation model of the antenna system topology defined in section II, was built combining the preliminary concept defined on Fig. 2, the manipulation of the GND plane geometry, and further optimizing the current distribution on the radiated structure applying modal analysis as shown in Fig. 7.

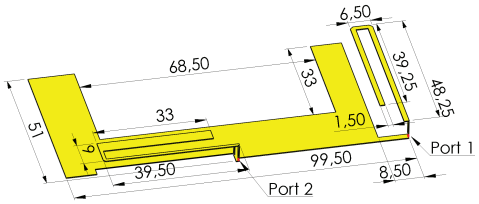

Fig. 7. Simulation model of the antenna system comprising the optimization of manipulation of ground plane and characteristic mode theory.

The final simulation was conducted using the commercial software Computer Simulation Technology (CST) Microwave Studio [46]. As predicted, the return loss in Fig. 8 and impedance characteristics Fig. 9 remains basically unchanged from previous antenna design on Fig. 3, however the isolation between antennas demonstrates substantial improvement from the preliminary concept shown in Fig. 2. The envelope correlation coefficient post-processed from isotropic incoming power farfield simulation was 0.0096, confirming the proper uncorrelation between antennas, also indicated in the 3D farfield radiation pattern of both antennas shown in Fig. 10.

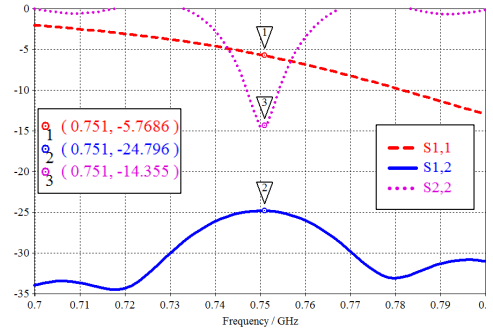

Fig. 8. Simulated Return Loss and Isolation between antennas

IV. MEASUREMENT RESULTS

A. PROTOTYPE MEASUREMENT RESULTS

The prototype shown in Fig. 11 was built following the optimized simulation model dimensions. The self resonant antenna system was built over a high density Styrofoam support to mimic free pace conditions, and the semi-rigid coaxial cables from the antennas were routed to a low e-field region to avoid coupling with radiated elements. All measurements including the S parameters in Fig. 14 and radiated performance in Fig. 12 and Fig. 13, were taken with both antennas being probed through a $\lambda/4$ sleeve cylindrical RF choke. The 3D radiation pattern presented on Fig. 12 and

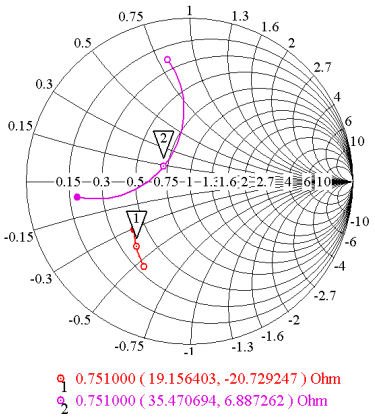

Fig. 9. Simulated antenna S parameters.

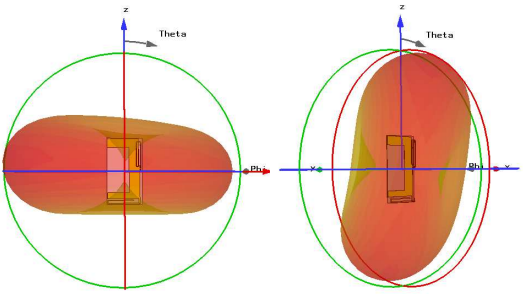

Fig. 10. Simulated 3D farfield radiation patterns, main antenna (left) and secondary antenna (right).

Fig. 13 are based on free space measurements in full anechoic chamber at 751MHz.

The measured prototype presented adequate radiated performance at the desired frequency of interest (751MHz), while the main antenna (1) had total efficiency (82.5%), the secondary antenna (2) presented total efficiency (47.9%), therefore with the BPR between antennas ($2.4dB$). The 3D isotropic envelope correlation coefficient post-processed from the measured farfield complex radiation pattern of the prototype antenna system is 0.08, in spite of the difference between simulated and measured results due measurement uncertainties, the measured envelope correlation coefficient smaller than 0.1, confirms the optimal uncorrelation between antennas.

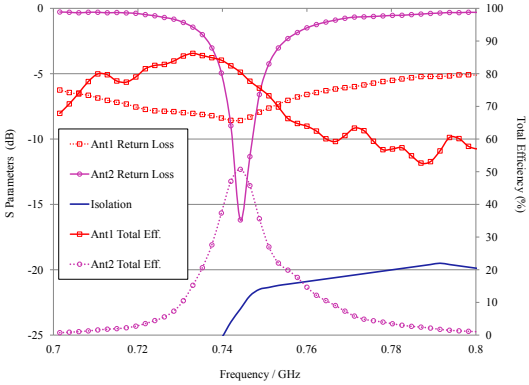

Fig. 14. MIMO 2x2 antenna system, Return Loss and Total Efficiency

B. DATA THROUGHPUT

Figure Fig. 15 shows a simplified version of the multi-probe MIMO OTA setup assembled at Aalborg University [47], [48], for the evaluation of the prototype antenna described in this work connected to a stand alone LTE modem (handset). The device under test was placed on a pedestal in an anechoic chamber surrounded by 16 probes [47] mounted in a boundary array ring with 4 meters of diameter. The number of probes makes the setup suitable to test any of the currently available LTE phones and most of the LTE tablets at the standardized LTE bands [49].

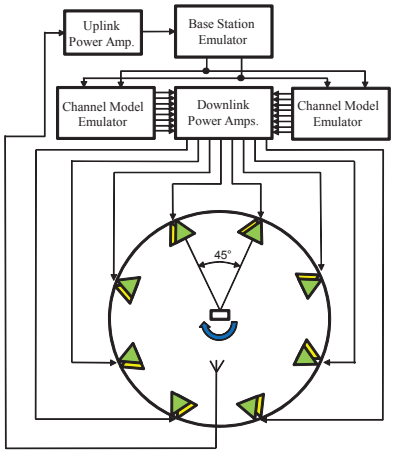

Fig. 15. Block diagram of the MIMO OTA test setup

The probes are connected to a base station emulator through channel emulator. The Power Amplifiers (PAs) are inserted in the system so that the dynamic range is suitable for terminal testing. The pedestal, made of polystyrene, is provided with a rotation axis at the center and a linear motion system, therefore allowing to rotate and move the DUTs in the azimuth plane.

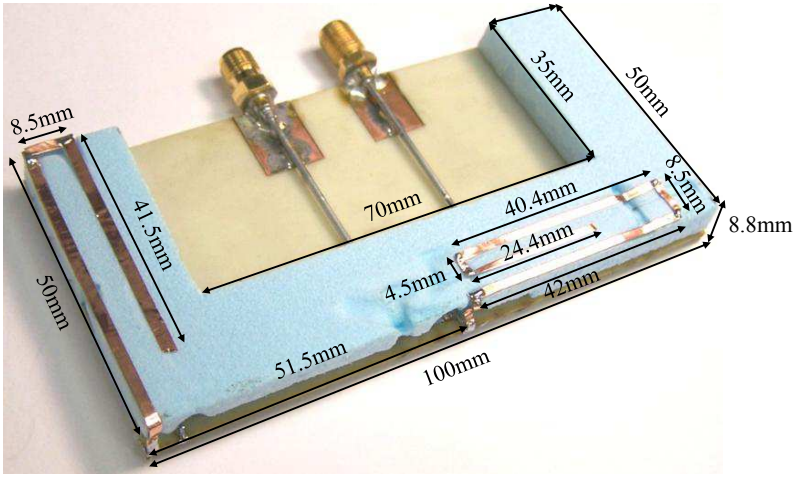

Fig. 11. MIMO 2x2 antenna system prototype

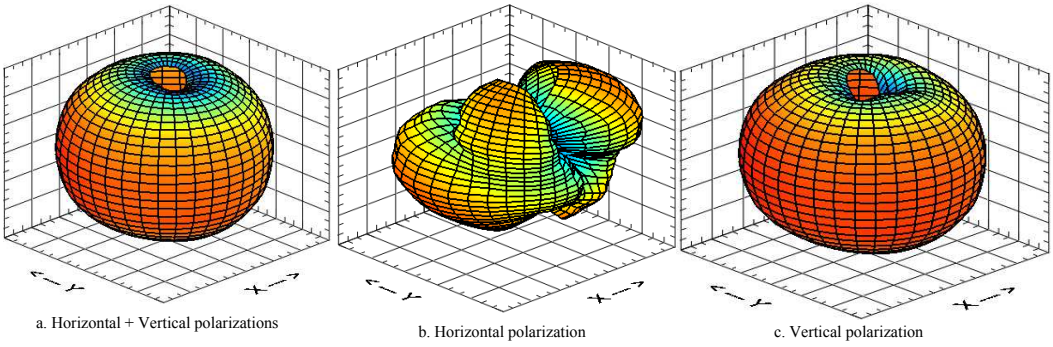

a. Horizontal + Vertical polarizations b. Horizontal polarization c. Vertical polarization

Fig. 12. Measured antenna 1, 3D radiation pattern at 751MHz

The test procedure followed the one outlined in [49], for the R.11 reference channel with 64 Quadrature Amplitude Modulation (QAM) defined in Table A.3.3.2.1-1 of [50]. For the measurements the antenna prototype was placed in an upright position, as shown in Fig. 17, and then rotated in 30 degree steps around azimuth to capture throughput vs. power curves at each position. This corresponds to the AZ rotation of the antenna system with 12 orientations. The power level is set to 36 values for each orientation, corresponding to a power sweep from -80 dBm to -116 dBm. As specified in the standard, the test scenario includes two realizations of different channels types that models the characteristics of the mobile channel in a micro-cellular environment rich in multi-path (SCME-Umi) and a more spatially selective environment with larger delay spread (SCME-Uma).

The prototype antenna proposed in this work was compared with MIMO reference antennas [51] and [52] shown in Fig. 16.

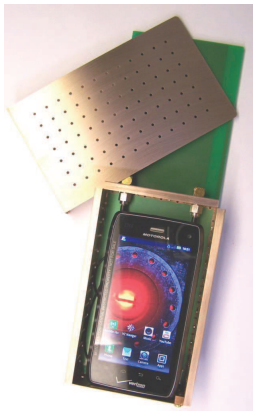

Fig. 16. MIMO reference antenna connected to the LTE B13 reference handset

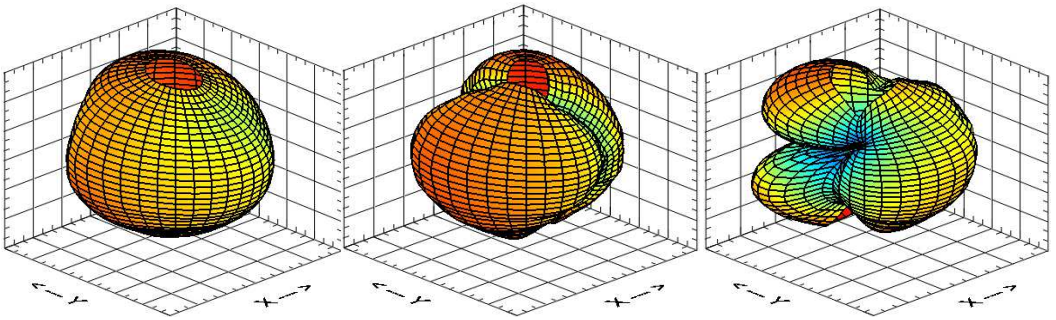

a. Horizontal + Vertical polarizations b. Horizontal polarization c. Vertical polarization

Fig. 13. Measured antenna 2, 3D radiation pattern at 751MHz

Throughput measurements were done in the MIMO OTA setup, using the reference LTE Band 13 handset with a modem as illustrated in Fig. 17.

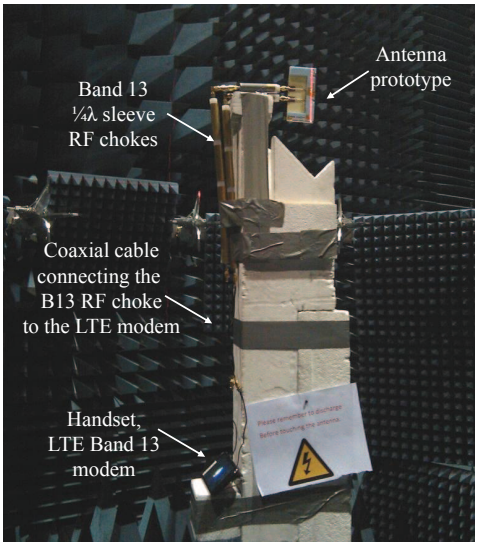

Fig. 17. MIMO OTA test setup with the mockup

The three reference antennas pairs were designed for LTE Band 13 to have different levels of correlation and efficiency, exemplifying the performance of "good" MIMO antenna system (efficiency grater than 80% and low correlation coef. of 0.1), moderate values of efficiency and correlation or a "nominal" (efficiency equal to 50% and low correlation coef. of 0.5), and a "bad" one with lower efficiency and high correlation (efficiency equal to 45% and low correlation coef. of 0.9). The Signal-to-Noise (SNR) and Reference Signal - Energy per Resource Element (RS EPRE) vs. data throughput measurements presented in Fig. 18 and Fig. 19 respectively, supports the performance discrimination among the three MIMO reference antennas. In both realizations of the two channel scenarios, the prototype of the antenna presented here demonstrates comparable performance with good reference antenna despite the reduced size, indicating that the design is a strong candidate for a MIMO electrically small form-factor device antenna system. While the prototype antenna outperform the reference antenna in the SNR controlled setup, which evaluates the MIMO system in higher signal level therefore isolating the effect of the antenna correlation as shown in Fig. 18, the performance in the scenario which isolates the receiver sensitivity and antenna total efficiency Fig. 19, the prototype radiated performance is also equivalent to the good reference antenna. The comparable but slightly under-performance in higher sensitivity SCME Uma is owed to the fact that the proposed design, despite having very efficient and uncorrelated antennas, it also has higher polarization discrimination for the antenna 2. Intrinsically the SCME Uma delivers more vertical polarized power in the setup test volume, thus an antenna with less cross-polarization ratio have advantage in this scenario, e.g. CTIA reference antennas. Due to its default high base-station correlation, the SCME Uma channel model as defined in [49] is very demanding, there's a balancing act between received power and correlation, and each of the prototypes complex antenna radiation pattern will perceive different branch imbalance and correlation coefficient.

V. CONCLUSIONS

This investigation demonstrates that commonly adopted antennas following an application of characteristic mode theory, and manipulation of the GND and optimal placement, can achieve strong uncorrelation between low band antennas in electrically small devices. A significant reduction of the magnitude of complex correlation coefficient was achieved while maintaining the total antenna efficiency and BPR in realistic antenna volume and device form factors. Simulation and measured results confirmed that an antenna system with commonly used PIFA antennas can be configured to excite the handset chassis in orthogonal modes, maintaining high isolation between antennas and orthogonal radiation patterns,

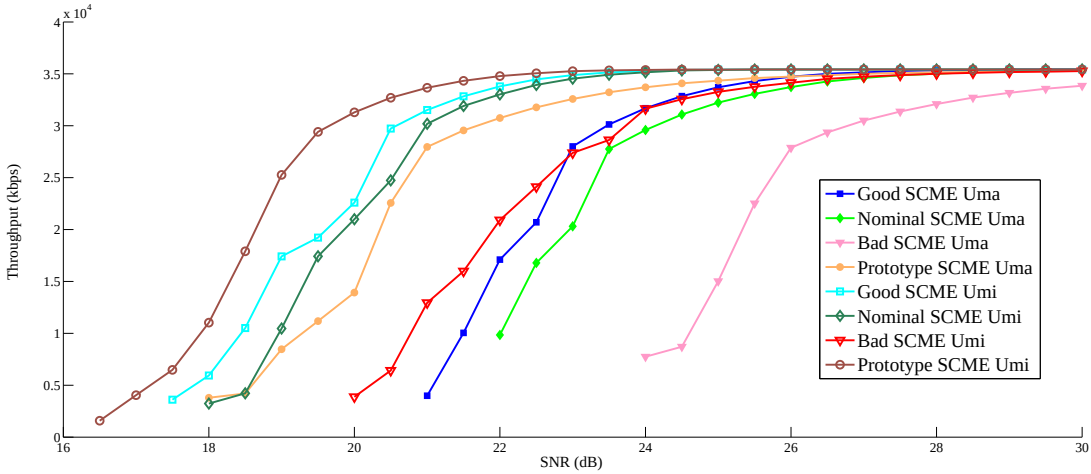

Fig. 18. MIMO OTA throughput SNR sweep measurements benchmark, 64 QAM adopting the same handset (modem).

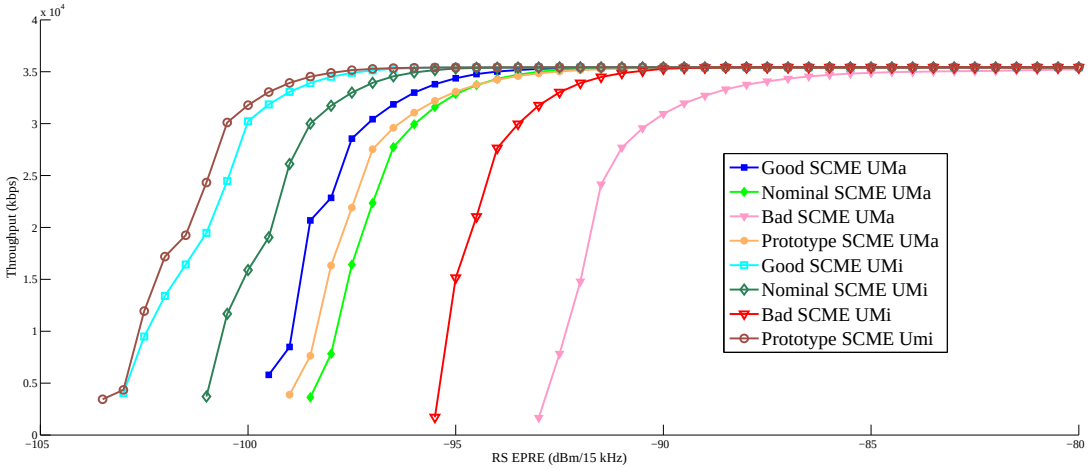

Fig. 19. MIMO OTA throughput sensitivity sweep measurements benchmark, 64 QAM adopting the same handset (modem).

therefore enabling radiation pattern uncorrelation. Uncorrelated antennas will result in lower magnitude of complex correlation coefficient, therefore higher system capacity fulfilling the Long Term Evolution (LTE) requirements towards handsets with fourth generation capabilities and beyond.

Preliminary MIMO OTA performance measurement results of the prototype confirm the expected high performance of this design principle. The dual polarization characteristic of the antenna will provide a low correlation even in directive environments as long as the channel does not have a high cross-polar correlation.

REFERENCES

[1] R. Vaughan and J. Andersen, "Antenna diversity in mobile communications," *Vehicular Technology, IEEE Transactions on*, vol. 36, no. 4, pp. 149 – 172, nov. 1987.

[2] G. J. Foschini and M. J. Gans, "On limits of wireless communications in a fading environment when using multiple antennas," *Wireless Personal Communications*, vol. 6, pp. 311–335, 1998.

[3] H. Holma, A. Toskala, K. Ranta-aho, and J. Pirskanen, "High-speed packet access evolution in 3gpp release 7 [topics in radio communications]," *Communications Magazine, IEEE*, vol. 45, no. 12, pp. 29–35, 2007.

[4] A. Tulino, A. Lozano, and S. Verdu, "Impact of antenna correlation on the capacity of multiantenna channels," *Information Theory, IEEE Transactions on*, vol. 51, no. 7, pp. 2491–2509, 2005.

[5] A. Molisch, M. Steinbauer, M. Toeltsch, E. Bonek, and R. Thoma, "Capacity of MIMO systems based on measured wireless channels," *Selected Areas in Communications, IEEE Journal on*, vol. 20, no. 3, pp. 561–569, 2002.

[6] J. Wallace and M. Jensen, "Mutual coupling in MIMO wireless systems: a rigorous network theory analysis," *Wireless Communications, IEEE Transactions on*, vol. 3, no. 4, pp. 1317–1325, 2004.

[7] B. Guo, K. Karlsson, and O. Sotoudeh, "Study of diversity gain obtained with two PIFA antennas on a small ground plane for a umts terminal," in *Antennas and Propagation Society International Symposium, 2008. AP-S 2008. IEEE*, 2008, pp. 1–4.

[8] R. Kuonanoja, "Low correlation handset antenna configuration for LTE MIMO applications," in *Antennas and Propagation Society International Symposium (APSURSI), 2010 IEEE*, 2010, pp. 1–4.

[9] H. Li, B. K. Lau, and Z. Ying, "Optimal multiple antenna design for compact MIMO terminals with ground plane excitation," in *Antenna Technology (iWAT), 2011 International Workshop on*, 2011, pp. 218–221.

[10] B. K. Lau and J. Andersen, "Simple and efficient decoupling of compact arrays with parasitic scatterers," *Antennas and Propagation, IEEE Transactions on*, vol. 60, no. 2, pp. 464–472, 2012.

[11] J. Andersen and H. Rasmussen, "Decoupling and descattering networks for antennas," *Antennas and Propagation, IEEE Transactions on*, vol. 24, no. 6, pp. 841–846, 1976.

[12] A. Chebihi, C. Luxey, A. Diallo, P. Le Thuc, and R. Staraj, "A novel isolation technique for closely spaced pifas for umts mobile phones," *Antennas and Wireless Propagation Letters, IEEE*, vol. 7, pp. 665–668, 2008.

[13] M. Han and J. Choi, "Dual-band MIMO antenna using a symmetric slotted structure for 4g usb dongle application," in *Antennas and Propagation (APSURSI), 2011 IEEE International Symposium on*, 2011, pp. 2223–2226.

[14] I. Dioum, A. Diallo, C. Luxey, and S. Farsi, "Compact dual-band monopole antenna for lte mobile phones," in *Antennas and Propagation Conference (LAPC), 2010 Loughborough*, 2010, pp. 593–596.

[15] S.-W. Su, C.-T. Lee, and F.-S. Chang, "Printed MIMO-antenna system using neutralization-line technique for wireless usb-dongle applications," *Antennas and Propagation, IEEE Transactions on*, vol. 60, no. 2, pp. 456–463, 2012.

[16] A. Diallo, C. Luxey, P. Le Thuc, R. Staraj, and G. Kossiavas, "Enhanced two-antenna structures for universal mobile telecommunications system diversity terminals," *Microwaves, Antennas Propagation, IET*, vol. 2, no. 1, pp. 93–101, 2008.

[17] A. Tatomirescu, M. Pelosi, M. Knudsen, O. Franek, and G. Pedersen, "Port isolation method for MIMO antenna in small terminals for next generation mobile networks," in *Vehicular Technology Conference (VTC Fall), 2011 IEEE*, 2011, pp. 1–5.

[18] R.-A. Bhatti, S. Yi, and S.-O. Park, "Compact antenna array with port decoupling for lte-standardized mobile phones," *Antennas and Wireless Propagation Letters, IEEE*, vol. 8, pp. 1430–1433, 2009.

[19] S.-C. Chen, Y.-S. Wang, and S.-J. Chung, "A decoupling technique for increasing the port isolation between two strongly coupled antennas," *Antennas and Propagation, IEEE Transactions on*, vol. 56, no. 12, pp. 3650–3658, 2008.

[20] C. Volmer, J. Weber, R. Stephan, K. Blau, and M. Hein, "An eigen-analysis of compact antenna arrays and its application to port decoupling," *Antennas and Propagation, IEEE Transactions on*, vol. 56, no. 2, pp. 360–370, 2008.

[21] K. Sato and T. Amano, "Improvements of impedance and radiation performances with a parasitic element for mobile phone," in *Antennas and Propagation Society International Symposium, 2008. AP-S 2008. IEEE*, 2008, pp. 1–4.

[22] W. Y. C. Lee, *Wireless and Cellular Communications*. McGraw-Hil, 2006.

[23] C.-Y. Chiu, C.-H. Cheng, R. Murch, and C. Rowell, "Reduction of mutual coupling between closely-packed antenna elements," *Antennas and Propagation, IEEE Transactions on*, vol. 55, no. 6, pp. 1732–1738, 2007.

[24] A. Arya, A. Patnaik, and M. Kartikeyan, "A compact array with low mutual coupling using defected ground structures," in *Applied Electromagnetics Conference (AEMC), 2011 IEEE*, 2011, pp. 1–4.

[25] Y. Chung, S.-S. Jeon, D. Ahn, J.-I. Choi, and T. Itoh, "High isolation dual-polarized patch antenna using integrated defected ground structure," *Microwave and Wireless Components Letters, IEEE*, vol. 14, no. 1, pp. 4–6, 2004.

[26] G. F. Pedersen and J. B. Andersen, "Handset antennas for mobile communications: Integration diversity, and performance," *Review of Radio Science 1996-1999*, pp. 119 – 137, 1999, Oxford Univ. Press.

[27] L. Yeung and Y. Wang, "A decoupling technique for compact antenna arrays in handheld terminals," in *Radio and Wireless Symposium (RWS), 2010 IEEE*, 2010, pp. 80–83.

[28] O. Souihli and T. Ohtsuki, "Benefits of rich scattering in MIMO channels: A graph-theoretical perspective," *Communications Letters, IEEE*, vol. 17, no. 1, pp. 23–26, 2013.

[29] W. Everitt and J. F. Byrne, "Single-wire transmission lines for short-wave antennas," *Radio Engineers, Proceedings of the Institute of*, vol. 17, no. 10, pp. 1840–1867, 1929.

[30] P. Vainikainen, J. Ollikainen, O. Kivekas, and I. Kelander, "Resonator-based analysis of the combination of mobile handset antenna and chassis," *Antennas and Propagation, IEEE Transactions on*, vol. 50, no. 10, pp. 1433–1444, 2002.

[31] B. K. Lau, J. Andersen, G. Kristensson, and A. Molisch, "Impact of matching network on bandwidth of compact antenna arrays," *Antennas and Propagation, IEEE Transactions on*, vol. 54, no. 11, pp. 3225 –3238, nov. 2006.

[32] P. Vainikainen, J. Holopainen, C. Icheln, O. Kivekas, M. Kyro, M. Mustonen, S. Ranvier, R. Valkonen, and J. Villanen, "More than 20 antenna elements in future mobile phones, threat or opportunity?" in *Antennas and Propagation, 2009. EuCAP 2009. 3rd European Conference on*, 2009, pp. 2940–2943.

[33] A. Diallo, C. Luxey, P. Le-Thuc, R. Staraj, and G. Kossiavas, "Reduction of the mutual coupling between two planar inverted-f antennas working in close radiocommunication standards," in *Applied Electromagnetics and Communications, 2005. ICECom 2005. 18th International Conference on*, 2005, pp. 1–4.

[34] F.-H. Chu and K.-L. Wong, "Simple folded monopole slot antenna for penta-band clamshell mobile phone application," *Antennas and Propagation, IEEE Transactions on*, vol. 57, no. 11, pp. 3680–3684, 2009.

[35] M. Tzortzakakis and R. Langley, "Quad-band internal mobile phone antenna," *Antennas and Propagation, IEEE Transactions on*, vol. 55, no. 7, pp. 2097–2103, 2007.

[36] C. Rowell and E. Lam, "Mobile-phone antenna design," *Antennas and Propagation Magazine, IEEE*, vol. 54, no. 4, pp. 14–34, 2012.

[37] R. Mittra and S. W. Lee, *Analytical Techniques in the Theory of Guided Waves*. Macmillan Company, 1971.

[38] R. J. Garbacz, "Data-Driven Batch Scheduling," Ph.D. dissertation, Ohio State University, Columbus, 1968.

[39] R. F. Harrington and J. Mautz, "Computation of characteristic modes for conducting bodies," *Antennas and Propagation, IEEE Transactions on*, vol. 19, no. 5, pp. 629–639, 1971.

[40] ——, "Theory of characteristic modes for conducting bodies," *Antennas and Propagation, IEEE Transactions on*, vol. 19, no. 5, pp. 622–628, 1971.

[41] B. Austin and K. Murray, "The application of characteristic-mode techniques to vehicle-mounted nvis antennas," *Antennas and Propagation Magazine, IEEE*, vol. 40, no. 1, pp. 7–21, 30, 1998.

[42] S. Makarov, *Antenna and EM Modeling with Matlab, 1 edition*. Wiley-Interscience, July 4, 2002.

[43] H. Li, Y. Tan, B. K. Lau, Z. Ying, and S. He, "Characteristic mode based tradeoff analysis of antenna-chassis interactions for multiple antenna terminals," *Antennas and Propagation, IEEE Transactions on*, vol. 60, no. 2, pp. 490–502, 2012.

[44] S. Chaudhury, W. Schroeder, and H. Chaloupka, "MIMO antenna system based on orthogonality of the characteristic modes of a mobile device," in *Antennas, 2007. INICA '07. 2nd International ITG Conference on*, 2007, pp. 58–62.

[45] M. Cabedo Fabres, "Systematic Design of Antennas Using the Theory of Characteristic Modes," Ph.D. dissertation, Politechnic University of Valencia, 2007.

[46] CST. (2013) Computer simulation technology. [Online]. Available: http://www.cst.com/

[47] O. Franek and G. Pedersen, "Spherical horn array for wideband propagation measurements," *Antennas and Propagation, IEEE Transactions on*, vol. 59, no. 7, pp. 2654–2660, 2011.

[48] X. Carreno, W. Fan, J. Nielsen, J. Singh Ashta, G. Pedersen, and M. Knudsen, "Test setup for anechoic room based MIMO OTA testing of lte terminals," in *Antennas and Propagation (EuCAP), 2013 7th European Conference on*, 2013, pp. 1417–1420.

[49] 3GPP, "Verification of radiated multi-antenna reception performance of user equipment (UE)," 3GPP, Tech. Rep. 3GPP TR 37.977 v2, 2012.

[50] ——, "LTE; evolved universal terrestrial radio access (E-UTRA); user equipment (UE) conformance specification; radio transmission and reception; part 1: Conformance testing," 3GPP, Tech. Rep. 3GPP TS 36.521-1 version 10.2.0 Release 10, 2012.

[51] I. Szini, G. Pedersen, A. Scannavini, and L. Foged, "MIMO 2x2 reference antennas concept," in *Antennas and Propagation (EUCAP), 2012 6th European Conference on*, march 2012, pp. 1540 –1543.

[52] I. Szini, B. Yanakiev, and G. Pedersen, "Mimo reference antennas performance in anisotropic channel enviroments," *IEEE Transactions Antennas and Propagation*, accepted.

Istvan Szini received bachelors degree in Electrical Engineering from Mogi das Cruzes University, Brazil in 1990. Currently he's Distinguished Member of Technical Staff at Motorola Mobility Antenna Innovation Research Lab, at Libertyville design center in USA, and PhD candidate at Aalborg University. He's primary interests are related to research, innovation and design on electrically small antennas for mobile devices, antenna adaptive tuning systems , RF Front-end design and MIMO antenna systems. Prior to his research role, he was the antenna lead designer for dozens handsets antenna systems including the iconics StarTAC Tri-mode Dual-band (1998), he lead the design of the first Motorola 3G handset with internal autonomous GPS antenna (A920/925, 2000), the first Motorola 3G Smartphone with four internal antennas (A/M1000, 2004), and the first handset with alluminum extruded housing (Devour/2009). Currently he's involved with smartphones LTE MIMO antenna system design, Over The Air MIMO measurements and LTE Carrier Agregation antenna systems enablers, he's Motorola delegate to MIMO OTA groups in CTIA, 3GPP RAN4, and COST IC1004 with liaison to CTIA. He holds 15 granted and pending patents.

Alexandru Tamomirescu , born in January 1987, has received a bachelors degree in Electronics and Telecommunication from the Polytechnic University Bucharest(2009)and a Master degree in Mobile Communications from Aalborg University(2011). Currently, he is working towards obtaining a PhD degree from Aalborg University on mobile antenna design. His main topics of research include mobile phone antenna design, reconfigurable antennas, antenna decoupling and the practical limits of electrically small antennas. He is an active IEEE member and he is participating in the COST IC1004 action.

Gert Frølund Pedersen was born in 1965 and married to Henriette and have 7 children. He received the B.Sc. E. E. degree, with honour, in electrical engineering from College of Technology in Dublin, Ireland in 1991, and the M.Sc. E. E. degree and Ph. D. from Aalborg University in 1993 and 2003. He has been with Aalborg University since 1993 where he is a full Professor heading the Antenna, Propagation and Networking LAB with 36 researcher. Further he is also the head of the doctoral school on wireless communication with some 100 phd students enrolled. His research has focused on radio communication for mobile terminals especially small Antennas, Diversity systems, Propagation and Biological effects and he has published more than 175 peer reviewed papers and holds 28 patents. He has also worked as consultant for developments of more than 100 antennas for mobile terminals including the first internal antenna for mobile phones in 1994 with lowest SAR, first internal triple-band antenna in 1998 with low SAR and high TRP and TIS, and lately various multi antenna systems rated as the most efficient on the market.He has worked most of the time with joint university and industry projects and have received more than 12 M Euros in direct research funding. Latest he is the project leader of the SAFE project with a total budget of 8 M Euros investigating tunable front end including tunable antennas for the future multiband mobile phones. He has been one of the pioneers in establishing Over-The-Air (OTA) measurement systems. The measurement technique is now well established for mobile terminals with single antennas and he was chairing the various COST groups (swg2.2 of COST 259, 273, 2100 and now ICT1004) with liaison to 3GPP for over-the-air test of MIMO terminals. Presently he is deeply involved in MIMO OTA measurement.

Patent disclosure related to Paper 7

Method and Aparatus for an Adaptive Multi-Antenna System

Istvan Szini and Eric Krenz

Patent pending, submitted to:
United States Patent and Trademark Office , December 2012

METHOD AND APPARATUS FOR AN ADAPTIVE MULTI-ANTENNA SYSTEM

FIELD OF THE DISCLOSURE

[0001] The present disclosure relates generally to multi-antenna systems and more particularly to adaptively reconfiguring multi-antenna systems.

BACKGROUND

[0002] Next generation wireless systems make use of multiple transmitters and receivers (i.e., multiple or multi- antenna systems) in a mobile device and in a base station. Multi-antenna systems are also known as Multiple Input-Multiple Output (MIMO) systems. The availability of MIMO enables communicating data over multiple paths or streams in the uplink and downlink directions

[0003] In a MIMO system, spatial multiplexing can be used to increase bandwidth for data transmissions by, for example, dividing a high rate data stream into multiple low rate data streams and sending each low rate data stream over the same channel using different antennas. In other words, different data streams are transmitted over the same channel using different antennas. Carrier aggregation (CA) is another technique that uses multiple antennas to increase effective bandwidth of wireless communications, wherein multiple (e.g., different) data streams are sent over multiple channels in the same or different bands using different antennas. .

[0004] In addition, in a MIMO system spatial diversity can be used to make data transmissions more robust or reliable. More specifically, using spatial diversity, robustness or reliability is increased by creating multiple data streams of the same data and transmitting the same data redundantly over the same channel using multiple antennas. In other words, the same data stream is transmitted redundantly over the same channel using multiple antennas.

[0005]

[0006] With the increasing implementation of multi-antenna systems and techniques that utilize the multi-antenna systems, there is a need for an adaptive multi-antenna system.

BRIEF DESCRIPTION OF THE FIGURES

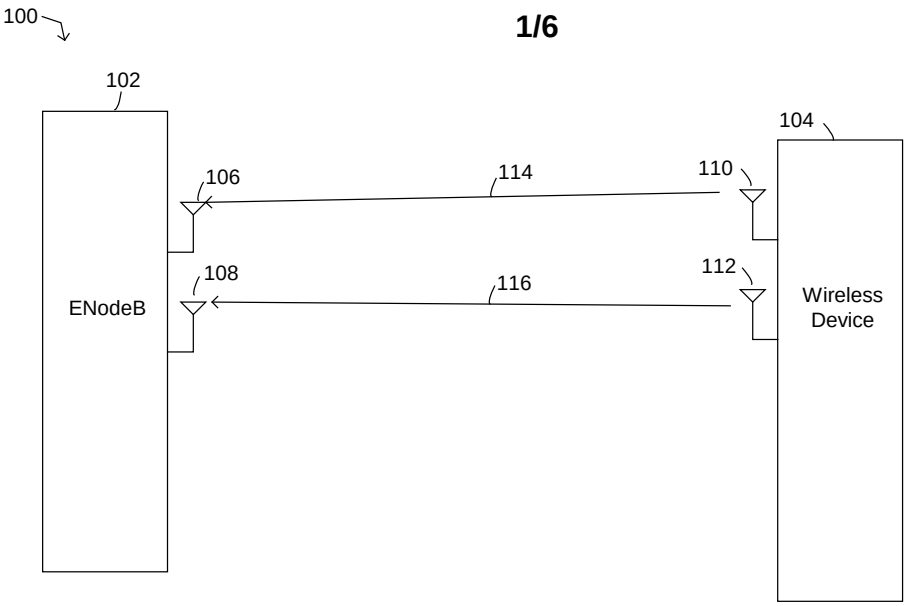

FIG. 1
CS40267

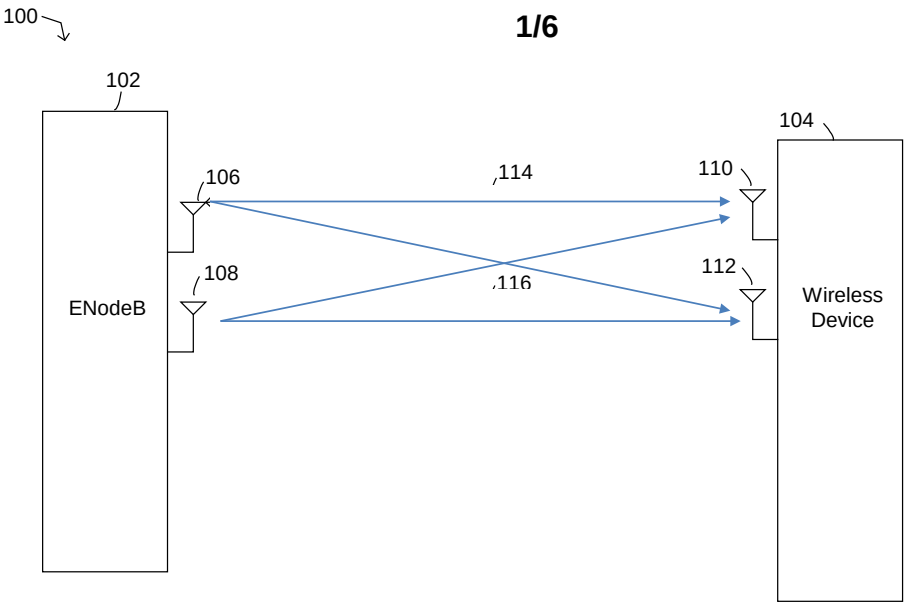

FIG. 1

ISv1

CS40267

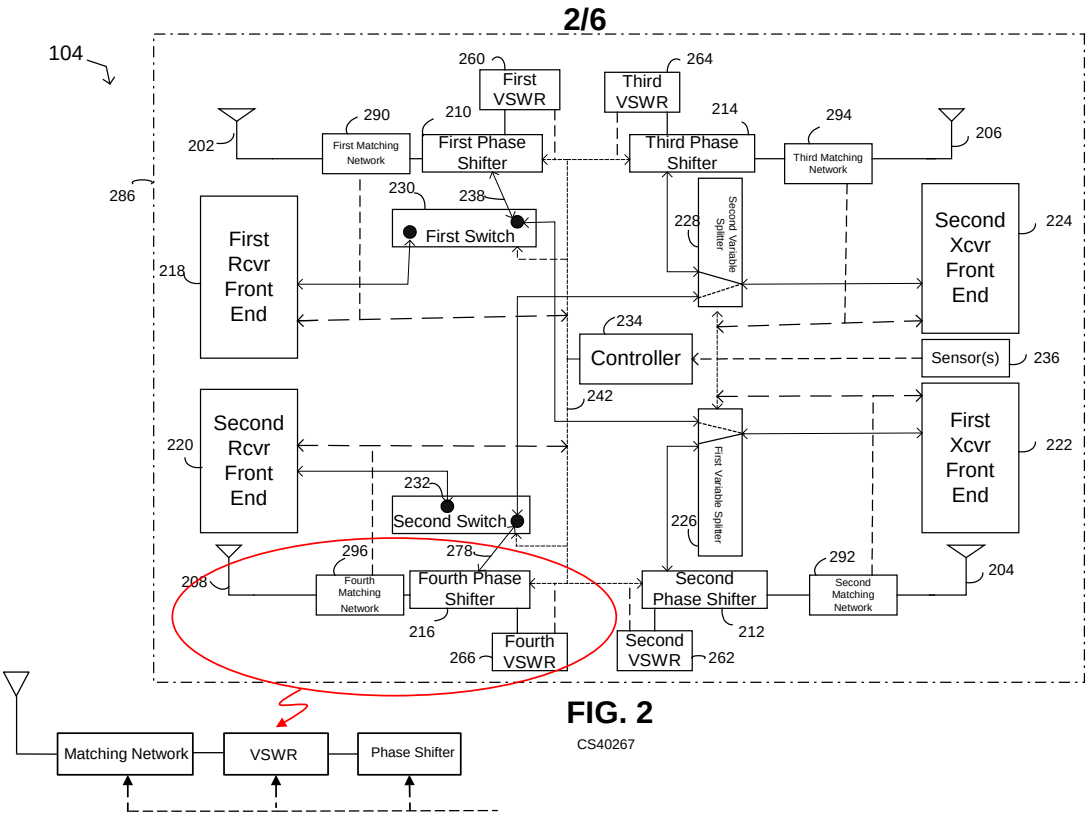

FIG. 2

CS40267

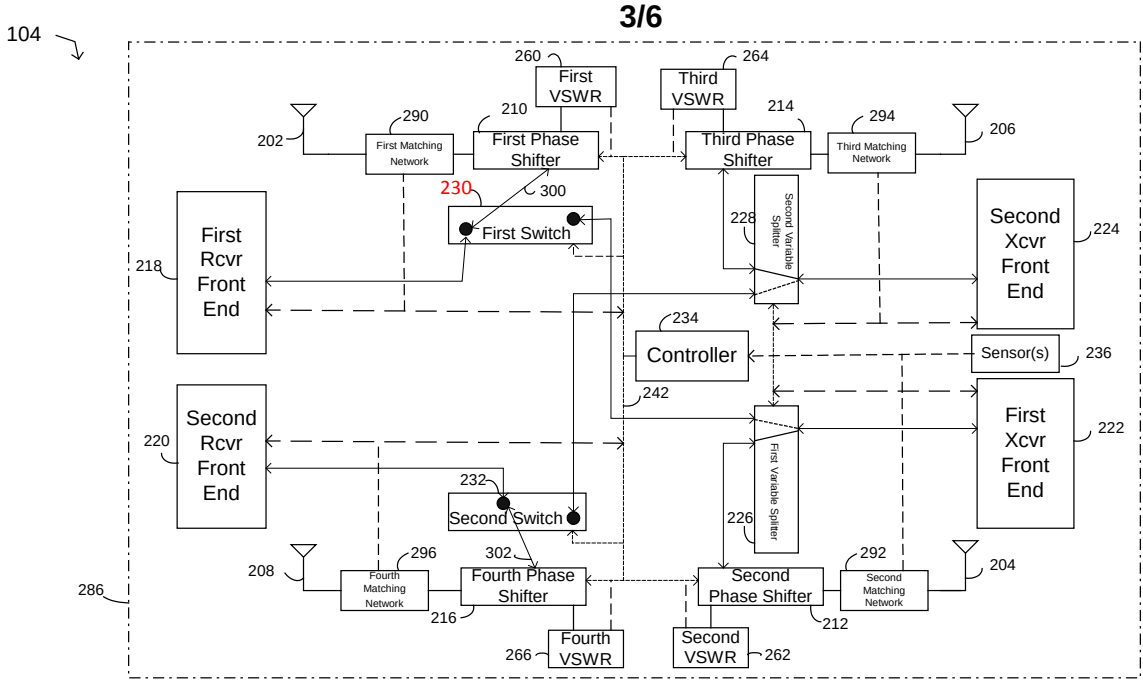

FIG. 3

CS40267

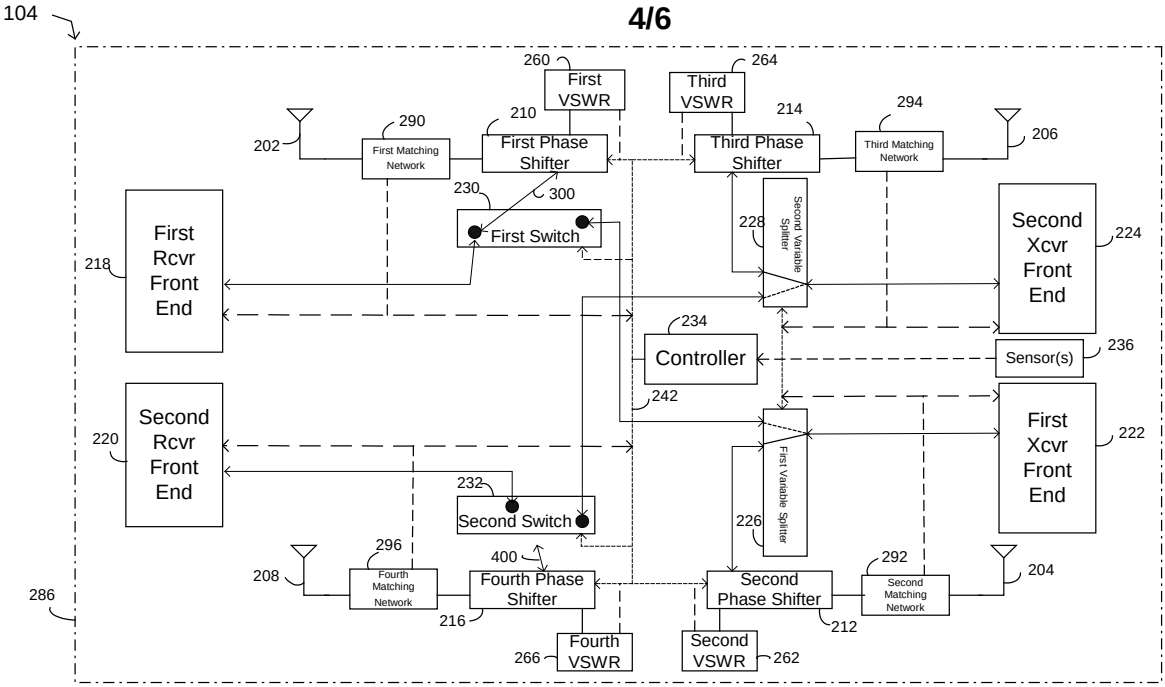

FIG. 4

CS40267

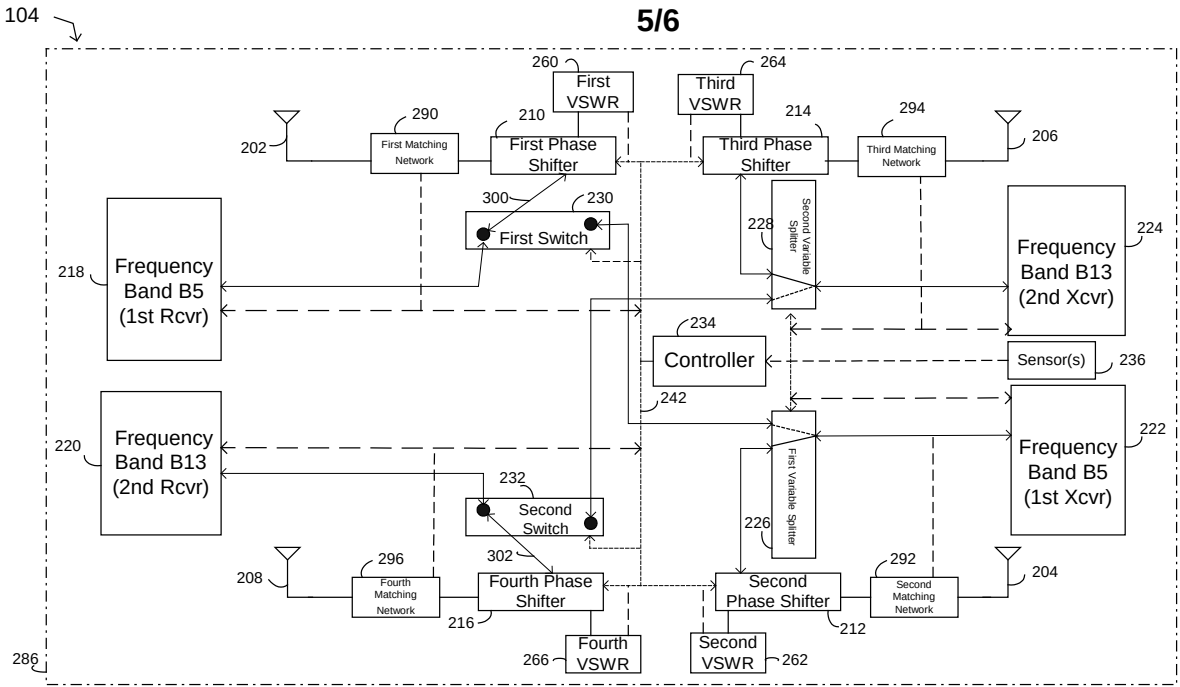

FIG. 5

CS40267

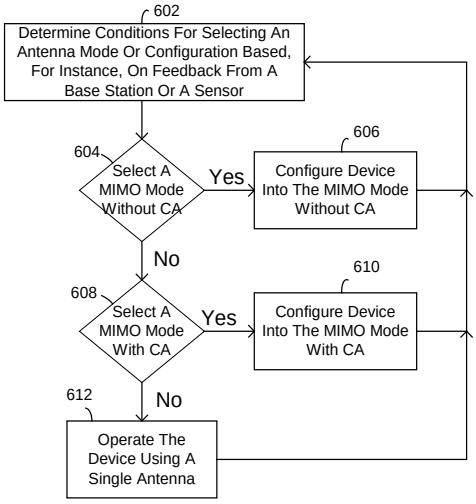

FIG. 6

CS40267

[0007] The accompanying figures, where like reference numerals refer to identical or functionally similar elements throughout the separate views, together with the detailed description below, are incorporated in and form part of the specification, and serve to further illustrate embodiments of concepts that include the claimed invention, and explain various principles and advantages of those embodiments.

[0008] FIG. 1 is a block diagram illustrating one example of a next generation wireless network in which embodiments of the present teaching operate.

[0009] FIG. 2 is a block diagram illustrating one example of a MIMO 2x2 antenna topology in accordance with the present teachings.

[0010] FIG. 3 is a block diagram illustrating one example of a MIMO 4x4 antenna topology in accordance with the present teachings.

[0011] FIG. 4 is a block diagram illustrating one example of a MIMO 3x3 antenna topology in accordance with the present teachings.

[0012] FIG. 5 is a block diagram illustrating one example of an antenna topology that supports MIMO 2x2 carrier aggregation in accordance with the present teachings.

[0013] FIG. 6 is a flow chart illustrating one example of a method for configuring a wireless device in accordance with the present teachings.

[0014] Skilled artisans will appreciate that elements in the figures are illustrated for simplicity and clarity and have not necessarily been drawn to scale. For example, the dimensions of some of the elements in the figures may be exaggerated relative to other elements to help to improve understanding of embodiments of the present invention. In addition, the description and drawings do not necessarily require the order illustrated. It will be further appreciated that certain actions and/or steps may be described or depicted in a particular order of occurrence while those skilled in the art will understand that such specificity with respect to sequence is not actually required.

[0015] The apparatus and method components have been represented where appropriate by conventional symbols in the drawings, showing only those specific details that are pertinent to

understanding the embodiments of the present invention so as not to obscure the disclosure with details that will be readily apparent to those of ordinary skill in the art having the benefit of the description herein.

DETAILED DESCRIPTION

[0016] Generally speaking, pursuant to the various embodiments, the present disclosure provides a method and apparatus for adaptively reconfiguring an antenna system into one of a MIMO mode or a carrier aggregation mode. In one example, the antenna system is reconfigured into one of a MIMO 2x2, 3x3, 4x4, NxN or NxM mode, or a 2x2 carrier aggregation mode. When configured into one antenna mode, at least two antenna elements are coupled together to operate as a single antenna, such as in a MIMO 2x2 mode. When configured into at least one other antenna mode, multiple antenna elements are operated or driven individually as separate antennas, such as in a MIMO 3x3 or 4x4 mode or in a MIMO 2x2 carrier aggregation mode.

[0017] For example, in accordance with an embodiment of the teachings herein is a method for reconfiguring an electronic device, having at least three antenna elements, between different antenna modes. The method comprises: configuring, by a controller, the electronic device into a first antenna mode, wherein at least two of the antenna elements are coupled together to operate as a single antenna; and reconfiguring, by the controller, the electronic device from the first antenna mode into a second antenna mode, wherein each antenna configured for use during the second antenna mode includes only a single antenna element.

[0018] In accordance with another embodiment of the teaching herein is an electronic device that includes at least three antenna elements and a controller. The controller is operative to: configure the antenna elements into a first antenna configuration comprising at least two of the antenna elements coupled together to operate as a single antenna; and reconfigure the antenna elements into a second antenna configuration, wherein each antenna in the second antenna configuration includes only a single antenna element, which is configured to individually operate as a separate antenna.

[0019] Referring now to the drawings and in particular to FIG. 1, a next generation multiple antenna network or system 100 is shown. The network 100 is adapted in accordance with the

present teachings as described herein. In an embodiment, network 100 is a 3rd Generation Partnership Project (3GPP) network, such as a Long Term Evolution (LTE) network 100, meaning that network infrastructure equipment, e.g., 102, and wireless devices, e.g., 104 (both referred to herein generally as electronic devices or devices), operating within the system 100 operate in conformance with at least portions of one or more standards documents developed by 3GPP, such as one or more LTE standards documents developed by 3GPP. In general, as used herein, devices such as 102 and 104, being "configured," "operative" or "adapted" means that such devices are implemented using one or more hardware devices such as memory devices, network interfaces such as transceivers, and/or processors that are operatively coupled, for example, as is shown in FIGs. 2-5. The memory devices, network interfaces, and/or processors, when programmed (e.g., using software or firmware), form the means for these system elements to implement their desired functionality, for example, as illustrated by reference to the methods shown in FIG. 6. Although the system 100 is described as a 3GPP LTE system, the present teachings can be incorporated into other types of multiple antenna systems such as WiMax systems, Evolved High Speed Packet Access (HSPA+) systems, Wireless Local Area Network (WLAN) 802.11n systems, etc.

[0020] The system 100 network infrastructure equipment includes an Evolved Packet Core (EPC), which functions as the network core. The EPC is coupled to an Evolved Universal Terrestrial Radio Access Network (E-UTRAN), which serves as the access network for the one or more wireless devices 104 that communicate using the system 100. The E-UTRAN includes one or more eNodeBs (eNBs) 102, which are the LTE equivalent of base stations. At least one eNB 102 includes multiple antenna elements, e.g., 106 and 108, operatively coupled to multiple transmitters and/or multiple receivers. As used herein, an antenna element is a radiating component within an electronic device, such as electronic device 102 or 104, which is used to send or receive, over the air, a radio wave containing a data stream. In accordance with the present teachings, multiple (e.g., two) radiating elements can operate collectively as a single antenna that is coupled to a single transmitter and/or receiver for enabling data communications; or any one or more of the radiating elements can operate individually as an antenna that is

coupled to a single transmitter and/or receiver for enabling data communications. Accordingly, an antenna is defined as comprising one or more antenna elements coupled to a single transmitter, a single receiver, or a single transceiver during the communication by the antenna of a data stream.

[0021] In example implementations, the wireless device 104 comprises a User Equipment (UE) such as a radio telephone, a tablet computer, a personal digital assistant, a gaming console, a remote controller, an electronic book reader, or any other type of electronic device capable of interconnecting with a telecommunications network via the eNB 102. The wireless device 104 is used to establish connections with the eNB 102 to communicate data. Data, as used herein, means any type of information that can be transferred or communicated between two or more devices operating in a communication system, such as the system 100. Accordingly, data includes information such as, by way of example, voice data, control data, video data, etc. In this illustrated embodiment, the wireless device 104 includes multiple antenna elements, e.g., 110 and 112, dynamically coupled to multiple transmitters and/or multiple receivers.

[0022] An expectation of next generation systems having multiple antenna elements is providing higher data rates and more reliable and robust data transmissions than predecessor networks. To this end and in accordance with the present teachings, multiple antenna elements (e.g., 106, 108, 110, 112) are adaptively configured or, in other words, configured "on the fly" between multiple antenna modes to communicate (i.e., transmit and/or receive) multiple data streams over one or more channels within signals 114, 116 in a way that maximizes transmission and reception capability while, for instance, minimizing the area on a device needed to support the antenna architecture. A signal is defined as a waveform (such as a radio wave) that carries a data stream. A data stream (also referred to herein as a stream or a stream of data) is defined as a sequence of digitally encoded data units (such as data packets containing data), which is used to transmit or receive information. A channel (also referred to herein as a carrier and a component carrier) is defined as the logical representation of radio frequency (RF) resources carrying data streams; and the channel is characterized by a transmit or receive frequency (within a given frequency band) and a capacity, such as bandwidth in Hz or data rate in bits per second. A frequency band

is defined as a range of frequencies (e.g., 700-800 MHz) from which channels are selected and allocated to electronic devices for data communications.

[0023] In the uplink direction (i.e., from a wireless device to the network infrastructure), for example, antenna element 110 transmits data comprising a stream carried by the signal 114, which is intended for at least one of the antenna elements such as antenna element 106; and antenna element 112 transmits data comprising a stream carried by the signal 116, which is intended for at least one of the antenna elements such as antenna element 108. In this example, the wireless device 104 transmits data streams to the eNB 102, but in actual systems, the eNB 102 also transmits data streams in the downlink direction to the wireless device 104. In that alternative example, the antenna element 106 transmits a data stream intended for antenna element 110, and the antenna element 108 transmits a data stream intended for antenna element 112. Moreover, the streams transported by the signals 114, 116 are shown as being transmitted directly from antenna elements 110, 112 to antenna elements 106, 108. However, in at least some scenarios, when transmissions occur in the uplink or downlink direction, the receiving antennas also receive indirect components of the transmitted streams due, for instance, to reflections, interference, and/or varying propagation paths. Thus, in this particular example, in the uplink direction, each of the antenna elements 106, 108 might receive signals emanating from both antenna elements 110, 112. The eNB 102 would then be configured to reconstruct the transmitted data from the multiple received direct and indirect stream components.

[0024] FIGs. 2-5 illustrate various embodiments of the present teachings. More particularly, a multiple antenna structure for an electronic device, such as a wireless device 104, is shown having different antenna configurations (also referred to herein as antenna modes) in the FIGs. 2-5. Although the wireless device 104 is described, the antenna structure shown in FIGs. 2-5 is applicable to an infrastructure device such as the eNB 102. Moreover, the wireless device 104 components are the same throughout the various FIGs. 2-5 and will, therefore, only be described in detail with respect to FIG. 2. However, switch components are reconfigured between the FIGs. 2-5 to illustrate the different antenna modes in which the wireless device 104 (or eNB 102) is configurable in accordance with the present teachings.

[0025] In general, the electronic device illustrated in FIG. 2-5 comprises: at least three antenna elements (in this case four antenna elements, but there could be additional antenna elements in other embodiment); and a controller operative to: configure the antenna elements into a first antenna configuration comprising at least two of the antenna elements coupled together to operate as a single antenna; and reconfigure the antenna elements into a second antenna configuration, wherein each antenna in the second antenna configuration includes only a single antenna element, which is configured to individually operate as a separate antenna. In one embodiment, the first antenna configuration supports communication of a first plurality of data streams using a same first carrier within a first carrier frequency band, and the second antenna configuration supports communication of a second plurality of data streams using a same second carrier within a second carrier frequency band. The first carrier can be the same or different than the second carrier. For example, the first antenna configuration supports multiple-input multiple-output (MIMO) 2x2 communications (as illustrated by reference to FIG. 2), and the second antenna configuration supports MIMO 4x4 communications (as illustrated by reference to FIG. 3) or MIMO 3x3 communications (as illustrated by reference to FIG. 4).

[0026] In another embodiment, the second antenna configuration supports communication of a plurality of data streams using a plurality of component carriers from the same or from multiple frequency bands. This embodiment supports carrier aggregation, wherein a plurality of component carriers comprise the plurality of channels used to send or receive different data streams using multiple antennas. In yet another embodiment, the wireless device 104 further comprises a set of switches coupled to the controller and to the at least three antenna elements to configure the antenna elements into the first antenna configuration and to reconfigure the antenna elements into the second antenna configuration, or in other words to configure the antenna elements between a plurality of different antenna modes, such as a plurality of different MIMO modes to support MIMO communications.

[0027] As used herein, MIMO communications are wireless transmissions or receptions over the same channel using multiple antennas. For example, MIMO 2x2 communications use two transmitting antennas (that transmit two data streams) and two receiving antennas (that receive

the two transmitted data streams); and MIMO 3x3 communications use three transmitting antennas (that transmit three data streams) and three receiving antennas (that receive the three transmitted data streams), etc. MIMO NxN communications use N transmitting antennas (that transmit N data streams) and N receiving antennas (that receive the N transmitted data streams). Also, MIMO NxM communications, where N is not equal to M, use N transmitting antennas (that transmit M or fewer data streams) and M receiving antennas (that receive the M or fewer transmitted data streams). Moreover, an antenna mode or configuration is defined as a current configuration from multiple possible configurations of antenna elements of a device to enable data communications. A MIMO mode is defined as an antenna mode or configuration that supports the transmission or reception of multiple data streams over one or more channels using multiple antennas. A carrier aggregation mode is a MIMO mode that supports the transmission or reception of multiple data streams over multiple channels and or frequency bands using multiple antennas.

[0028] Although the embodiments depicted in FIG. 2-5 show a topology using four antenna elements configured to operate in a MIMO 2x2, 3x3, 4x4 mode, and a MIMO 2x2 carrier aggregation mode, in other embodiments, an electronic device, such as wireless device 104 is configured with more than four antennas. For example, the wireless device 104 may comprise a smart phone, laptop, tablet, or some other type of wireless device large enough to accommodate more than four antennas and more than four transceiver/receiver front ends. When more than four antenna elements are disposed on or in the wireless device 104, the antenna topology of the wireless device 104 is able to support higher orders of MIMO communications.

[0029] Turning now to FIG. 2, which shows a block diagram illustrating an embodiment of a wireless device 104 having an antenna topology configured into a first antenna mode in accordance with the teachings herein. The antenna mode shown in FIG. 2 comprises a MIMO mode and more particularly a MIMO 2x2 mode. However, the “first” antenna mode can be any one of a plurality of possible antenna modes for the wireless device 104, including one or more of the antenna modes shown in FIGs 3-5.

[0030] The illustrated antenna topology of FIG. 2 includes a first antenna element 202, a second antenna element 204, a third antenna element 206, a fourth antenna element 208, a first phase shifter 210, a second phase shifter 212, a third phase shifter 214, a fourth phase shifter 216, a first receiver front end 218, a second receiver front end 220, a first transceiver front end 222, a second transceiver front end 224, a first variable splitter 226, a second variable splitter 228,specifically in the topology illustrated in the FIG. 2, MIMO 2x2 can be achieved by combining the excitation of all four antennas 202, 204, 206 and 208, where the both variable splitters 226 and 228 in fact split the Front-End 222 and 224 signals respectively, where the first Front-End 222 drives both antennas 202 and 204 with variable magnitude and phase, correspondently the second Front-End 224 drives the antennas 206 and 208 with arbitrarily magnitude and phase as well. First switch 230 and second switch 232 (which comprise a set of switches), a first voltage standing wave ratio (VSWR) detector 260, a second VSWR detector 262, a third VSWR detector 264, a fourth VSWR detector 266, a first matching network 290, a second matching network 292, a third matching network 294, a fourth matching network 296, a controller 234 and at least one sensor 236. Following is a brief description of the components of wireless device 104, their connectivity and their functionality.

[0031] In an embodiment, the at least three (in this case four) antenna elements comprises a first antenna element 202 disposed near a first corner of a planar rectangular ground plane 286 of the electronic device 104, a second antenna element 204 disposed near a second corner of the planar rectangular ground plane 286 and diagonal to the first antenna element 202, a third antenna element 206 disposed near a third corner of the planar rectangular ground plane 286 adjacent to the first and second corners, and a fourth antenna element 208 disposed near a fourth corner of the planar rectangular ground plane 286 adjacent to the first and second corners and diagonal to the third antenna element 206. The first antenna element 202, the second antenna element 204, the third antenna element 206, and the fourth antenna element 108 can be the same type of antenna element or a combination of different types of antenna elements. In one example implementation, the types of antenna elements are one or more of the following: L-shaped, inverted F-shaped antenna (IFA), planar inverted F-shaped antenna (PIFA), monopole, folded

inverted conformal antenna (FICA), or patch, for example. The type of antenna elements used can depend on a number of factors including, but not limited to, the operational frequencies of the electronic device, its size and shape, and the various antenna system performance targets. Moreover, antenna elements may be positioned differently within the wireless device 104 depending, for instance, on the size and shape of the device. Also, in some implementations, one or more antenna elements may partially or fully overlap with the ground plane 286.

[0032] As shown, the first adjustable phase shifter 210 is coupled to the first antenna element 202 and is coupled to the controller 234 and to the first VSWR 260. The second adjustable phase shifter 212 is coupled to the second antenna element 204 and is coupled to the controller 234 and to the second VSWR 262. The third adjustable phase shifter 214 is coupled to the third antenna element 206 and is coupled to the controller 234 and to the third VSWR 264; and the fourth adjustable phase shifter 216 is coupled to the fourth antenna element 208 and is coupled to the controller 234 and to the fourth VSWR 266. As shown, the controller 234 is coupled to the phase shifters 210-216, the matching networks 290-296, and the VSWRs 260-266. The controller is configured to provide control signals to the phase shifters 210-216 and the matching networks 290-296 to, in one embodiment, adjust the parameters of these components to effectively operate in different frequency bands. Furthermore, the controller is configured to receive input or readings from the VSWRs 260-266 to control one or more other components in the wireless device 104 such as the matching networks 290-296, by way of example.

[0033] In one embodiment, the controller 234 is a baseband processor. In another embodiment, the functionality of the controller 234 is implemented on an integrated circuit separate from a baseband processor. For example, as a baseband processor, the controller 234 is comprised one or more integrated circuit chips having data processing hardware, a memory (e.g., random access memory (RAM)) and firmware or software used to configure, e.g., program, the baseband processor to perform a number of radio control functions that require an antenna element for data communications. The functions include, but are not limited to: encoding and decoding digital data; generating or parsing out certain control, controlling matching network and phase shift components, sensor reading, VSWR measurement analysis; etc.

[0034] Accordingly, in one embodiment, matching networks 290-296 are adjustable matching networks (and tuners) configured to provide an input impedance to the antenna elements 202-208, respectively, in response to control signals communicated from the controller 234. More particularly, each matching network matches the load impedance of the antenna element, to which it is connected, to the impedance of a transmitter and/or receiver. This is done to maximize power transfer and minimize reflections from the antenna element over a broad range of frequencies including, in one example implementation, multiple frequency bands. In another embodiment, each adjustable matching network is operable in response to feedback from the set of (i.e., one or more) sensors 236 on the wireless device 104, which are used to determine a manner of use of the electronic device. For example, but not by way of limitation, the manner of operating an electronic device includes: in proximity to the head (i.e., head), from the head to the hand and vice versa (i.e., head+hand), with two hands, with a car kit, with a lapdoc, etc. Example sensor implementations are described below in additional detail.

[0035] Each first phase shifter 210-216, in one example implementation, provides a controllable phase shift of a radio frequency (RF) signal (modulated with a bit stream) that is to be radiated by an antenna coupled to the phase shifter. In one embodiment, the phase shift provided by each phase shifter 210-216 is controlled by control signals from the controller 234 and depends, at least partially, on the particular antenna mode or configuration and the frequency band of operation. For example, in an implementation where two diagonally-positioned antenna elements are coupled together to form a single antenna, the phase shifters coupled to the two antenna elements may be controlled to drive the RF signals to the two antenna elements out-of-phase during low-band transmissions. During high band transmissions, the phase shifters coupled to the two diagonally-positioned and coupled antenna elements may be controlled to drive the RF signals to the two antenna elements either out-of-phase or in-phase.

[0036] The VSWR detectors 260-266, in one example implementation, are each configured to monitor forward and reflected RF power of first antenna element 202 transmissions on a transmission line between a transmitter and/or receiver and an antenna in order to calculate VSWR measurements. The VSWR measurements indicate the degree of mismatch between the

transmitter and/or receiver and the antenna. The VSWR detectors 260-266 communicate the VSWR measurements to the controller 234 for use, in one embodiment, as tuning parameters to correct the mismatch, for example, using the phase shifters 210-216.

[0037] Continuing the description of the components of the electronic device 104, the first receiver front end 218 is coupled to the controller 234 and to the first switch 230, wherein the first switch 230 is also coupled to the first variable splitter 226 and the controller 234. The first transceiver front end 222 is coupled to the controller 234 and the first variable splitter 226, wherein the first variable splitter 226 is also coupled to the second adjustable phase shifter 212 and the controller 234. The second receiver front end 220 is coupled to the controller 234 and to the second switch 232, wherein the second switch 232 is also coupled to the second variable splitter 228 and the controller 234. The second transceiver front end 224 is coupled to the controller 234 and the second variable splitter 228, wherein the second variable splitter 228 is also coupled to the third adjustable phase shifter 214 and the controller 234.

[0038] In one example implementation, the first and second transceiver front ends 222, 224 and the first and second receiver front ends 218, 220 each include a high/low diplexer, high and low band selectors, and a plurality of duplexers each operative over a different frequency band. By way of an illustrative LTE implementation, the plurality of duplexers comprises six duplexers operative over frequency bands B1, B2, B3 (high bands over which the high band selector is also operative) and bands B5, B8, B13 (low bands over which the low band selector is also operative). However, any suitable combination of frequency bands can be used depending, for instance, on the wireless access technology used. Moreover, the first and second transceiver front ends 222, 224 each further include a plurality of transmitters and receivers each operative over different frequency bands. Whereas, the first and second receiver front ends 218, 220 each further include only the plurality receivers each operative over different frequency bands. Alternatively, all of the front ends could be transceiver front ends to provide further flexibility in the antenna configurations and antenna modes of operation available to the electronic device.

[0039] During a transmit operation, where the controller 234 is a baseband processor, the controller 234 receives data, for instance, audio (e.g., voice) data from a microphone, video data

from a recording device, or other data from an application in the electronic device 104. The controller 234 supplies a digital information signal containing the data (also referred herein as a data stream) to one or more of the transmitters within transceivers 222, 222. Accordingly, the processing device selects the one or more transmitters, duplexers, and high or low band selectors based on the frequency band within which the channel(s) fall, which is used to transmit the data stream). Each transmitter modulates the data stream onto a carrier signal, and the antenna radiates the modulated data stream.

[0040] The one or more sensors 236 may be disposed within or on a housing of the wireless device 104. In one example implementation, at least some of sensors 236 are adapted, during operation, to detect the proximity of the wireless device 104 to external objects, such as parts of a user's body or other objects. Sensors 236 include, for example but not by way of limitation, one or more capacitive sensors, infrared (IR) proximity sensors, pressure sensors, or other types of sensors. A capacitive sensor may be activated when a nominally conductive material (e.g., a user's hand or cheek) contacts or is sufficiently close to the sensor. An IR proximity sensor may be activated when it is in proximity with any material that scatters IR energy. The one or more sensors 236 may be positioned, for example, on the front, back, and/or sides of the phone housing. According to another embodiment, sensors 236 include one or more accelerometers, which enable a determination of whether the wireless device 104 is being used in a portrait or landscape mode, for example. In one embodiment, the sensors 236 provide sense signals to the controller 234 that indicate whether an antenna is impaired, which in one example indicates a user's hand is covering the antenna. The controller 234, in one embodiment, as explained below by reference to FIG. 6, reconfigures the wireless device 104 in response to the sense signals.

[0041] As mentioned above, the controller 234 controls the position of the first switch 230 and the second switch 232 to configure the antenna mode for the wireless device 104. In the particular implementation scenario illustrated in FIG. 2, the first switch 230 is configured (to a position 238) to connect the first adjustable phase shifter (210) to the first variable splitter (226) in order to couple the first and second antenna elements 202, 204 together to operate as a first antenna; and the second switch (232) is configured (to a position 278) to connect the fourth

adjustable phase shifter 216 to the second variable splitter 228 in order to couple the third and fourth antenna elements 206, 208 together to operate as a second antenna.

[0042] With the first switch 230 in the position 238, the first antenna element 202 is coupled to the first transceiver front end 222, which is also coupled to the second antenna element 204. Moreover, the controller configures the first variable splitter 226 so that signals from both the first antenna element 202 and the second antenna element 204 are propagated to and/or from the first transceiver front end 222. When configured in this manner, the first antenna element 202 and the second antenna element 204 operate pair-wise as a single antenna. This single antenna, in one embodiment, operates as the first antenna in the MIMO 2x2 mode.

[0043] Similarly, with the second switch 232 in the position 278, the fourth antenna element 208 is coupled to the second transceiver front end 224, which is also coupled to the third antenna element 206. Moreover, the controller configures the second variable splitter 228 so that signals from both the third antenna element 206 and the fourth antenna element 208 are propagated to and/or from the second transceiver front end 224. When configured in this manner, the third antenna element 206 and the fourth antenna element 208 operate pair-wise as a single antenna. This single antenna, in one embodiment, operates as the second antenna in the MIMO 2x2 mode. The resulting antenna configuration shown in FIG. 2 is, accordingly, a MIMO 2x2 mode that supports MIMO 2x2 communications. In one embodiment, the MIMO 2x2 mode supports spatial diversity. This includes transmit diversity where both antennas are used to redundantly transmit the same data stream over the same channel and receive diversity where both antennas are used to receive a data stream redundantly transmitted over the same channel. In another embodiment, the MIMO 2x2 mode supports spatial multiplexing where two different streams and transmitted or received over the same channel using the two pair-wise antennas.

[0044] As stated above, as shown in FIG. 2, the wireless device 104 is configured, by the controller 234, into a first antenna mode, wherein at least two of the antenna elements are coupled together to operate as a single antenna. More particularly, the controller 234 configures first switch 230 to couple the first and second antenna elements 202, 204 together to operate pair-wise as a single antenna; and the controller 234 configures second switch 232 to couple the

third and fourth antenna elements 206, 208 together to operate pair-wise as a single antenna. FIGs. 3-5, in contrast, illustrate embodiments, of where the controller 234 configures or reconfigures the wireless device into a second antenna mode, wherein each antenna configured for use during the second antenna mode includes only a single antenna element. More particularly, in the second antenna configuration shown in FIGs 3-5, the first switch 230 is configured to disconnect the first adjustable phase shifter from the first variable splitter in order to decouple the first and second antenna elements, and the second switch is configured to disconnect the fourth adjustable phase shifter from the second variable splitter in order to decouple the third and fourth antenna elements.

[0045] Turing first to FIG. 3, an antenna topology configured to support MIMO 4x4 communications is shown, in accordance with the present teachings. In the embodiment depicted in FIG. 3, the first switch 230 is configured (to a position 300) to couple the first antenna element 202 to the first receiver front end 218 using first matching network 290, the first phase shifter 210, and the first switch 230. In this configuration, the antenna element 202 operates individually (i.e., on its own) as a first antenna. The second antenna element 204 is coupled to the first transceiver front end 222 using the first variable splitter 226, such that the antenna element 204 operates individually as a second antenna. In this case, the first variable splitter 226 is configured such that all of the signal communicated from the first transceiver front end 222 is routed to the second antenna204. The third antenna element 206 is coupled to the second transceiver front end 224 using the second variable splitter 228, such that the antenna element 206 operates individually as a third antenna. In this case, the second variable splitter 228 is configured such that all of the signal communicated from the second transceiver front end 224 is routed to the second antenna 206. The second switch 232 is configured (to a position 302) to couple the fourth antenna element 208 to the second receiver front end 220 using the fourth matching network 296, the fourth phase shifter 216, and the second switch 232. In this configuration, the antenna element 208 operates individually as a fourth antenna. This MIMO 4x4 mode can be used to support spatial diversity and/or spatial multiplexing for one to four data streams using, in one embodiment, the same channel.

[0046] FIG. 4 shows an antenna topology configured to support MIMO 3x3 communications, in accordance with an embodiment. The configuration shown in FIG. 4 is similar to the configuration depicted in FIG. 3 except that the second switch 232 is configured such that the fourth antenna element 208 is not connected to the receiver front end 220. Thus, the fourth antenna element 208 does not operate as an antenna in this configuration. This MIMO 3x3 mode can be used to support spatial diversity and/or spatial multiplexing for one to three data streams using, in one embodiment, the same channel.

[0047] FIG. 5 shows an antenna topology configured to support carrier aggregation, in accordance with an embodiment. The configuration of FIG. 5 supports communication of a plurality of data streams using component carriers from the same or from multiple frequency bands. The switch configuration shown in FIG. 5 is the same as the switch configuration depicted in FIG. 3. However, the transceivers 224 and 222 are shown as operating in different frequency bands (e.g., bands B13 and B5), thereby indicating that the transmission and/or reception channels were allocated from different frequency bands. Similarly, the receivers 218 and 220 are shown as operating in different frequency bands (e.g., bands B13 and B5), thereby indicating that the reception channels were allocated from different frequency bands. This carrier aggregation mode can be used to support spatial diversity and/or spatial multiplexing for two to four data streams using different channels that may be in the same or different frequency bands.

[0048] In an alternate carrier aggregation configuration (not shown), the switch configuration is the same as the switch configuration depicted in FIG. 2. Thus, when configured in this manner, the third antenna element 206 and the fourth antenna element 208 operate pair-wise as a single antenna; and the first antenna element 202 and the second antenna element 204 operate pair-wise as a single antenna. This antenna topology enables 2x2 carrier aggregation in the same or different frequency bands.

[0049] Turning now to FIG. 6, a logical flow chart is shown illustrating a method 600 for determining an antenna mode in which to configure an electronic device for communicating data, in accordance with an embodiment. In an embodiment, the controller 234 performs the method

600 to reconfigure an electronic device such as the wireless device 104 (as described) or the eNB 102 into the different antenna modes or configurations.

[0050] Turning now to the details of method 600. At 602, the controller 234 determines conditions for selecting an antenna mode for wireless communications. In one embodiment, the antenna mode is determined based on at least one of (i.e., one or both of): feedback from a base station (such as the eNB 102) or feedback from a sensor on the wireless device 104. This enables the controller 234 to adaptively configure the antenna elements in response to, for instance, the environment around the electronic device or network conditions within which the device communicates.

[0051] For example, the controller 234 configures or reconfigures the antenna topology of the wireless device 104 in accordance with measurements or signals (the feedback) communicated from the sensors 236 and/or one or more of the VSWR detectors 260, 262, 264, 266. In the process of monitoring sensor 236 measurements, the controller 234, in one example, determines the position of the wireless device 104 with respect to a user, or in other words determines a manner or use or a use case for the wireless device 104, and responsively determines a suitable antenna configuration. For example, the use case scenario may be head, head-to-hand, two hands, car kit, lapdoc, etc. In one illustrative implementation, the controller 234 determines that the wireless device is near the user's head (i.e., head position) and responsively selects the ____ antenna configuration because…. antenna configuration which enables better system efficiency, e.g depending on user case, head, head+hand, different hand grips etc. the low frequency band antennas can be allocated in the bottom of the handset, and the high band antennas at the top, or vice-versa depending on the user case.

[0052] In another example implementation, the eNB 102 communicates messages (the feedback) to the controller 234 of the wireless device 104, which includes network information about ongoing communications between the wireless device 104 and the eNB 102. During these communications, in one example, the eNB 102 and the wireless device 104 exchange network messages concerning the MIMO and carrier aggregation capabilities of the wireless device 104 and the eNB 102. In accordance with this network messaging, the eNB 102 instructs the wireless

device 104 to reconfigure itself based on, for example, network configuration parameters, signal strength measurements, or channel requirements.

[0053] Using the information determined at 602, the controller determines, at 604 and 608, respectively, whether to select a MIMO mode without carrier aggregation or with carrier aggregation. If the MIMO mode without carrier aggregation is selected, the controller 234 configures or reconfigures the electronic device into this mode at 606. If the MIMO mode with carrier aggregation is selected, the controller 234 configures or reconfigures the electronic device into this mode at 610. If neither MIMO mode is selected at 608 or 608, the wireless device 104 operates using a single antenna at 612.

[0054] For example, at one point in time at 606, the controller 234 configures the wireless device 104 into a first antenna mode, wherein at least two of the antenna elements (such as, antenna element 202, 204, 206 and 208) are coupled together to operate as a single antenna. At another point in time, at 608 the controller 234 reconfigures the wireless device 104 from the first antenna mode into a second antenna mode, wherein each antenna configured for use during the second mode comprises a single antenna element. In one example, the first antenna mode comprises a first MIMO mode, and the second antenna mode comprises a second MIMO mode. Where the first MIMO mode comprises a MIMO NxN mode and the second MIMO mode comprises an MIMO MxM mode , where N=2 and M=3 or 4. In this example implementation, the first antenna mode is used for communicating a first plurality data streams using a same first channel, and the second antenna mode is used for communicating a second plurality data streams using a same second channel. The first and second channels can be the same or different channels.

[0055] In another embodiment, the first antenna mode comprises a MIMO mode and the second antenna mode comprises a carrier aggregation mode. In this example implementation, the first antenna mode is used for communicating a first plurality data streams using a same first channel, and the second antenna mode is used for communicating a second plurality data streams using a plurality of different channels. In one embodiment, at least two channels of the plurality of

different channels are from different frequency bands. Alternatively, all of the channels of the plurality of different channels are from the same frequency band.

[0056] In the foregoing specification, specific embodiments have been described. However, one of ordinary skill in the art appreciates that various modifications and changes can be made without departing from the scope of the invention as set forth in the claims below. Accordingly, the specification and figures are to be regarded in an illustrative rather than a restrictive sense, and all such modifications are intended to be included within the scope of present teachings.

[0057] The benefits, advantages, solutions to problems, and any element(s) that may cause any benefit, advantage, or solution to occur or become more pronounced are not to be construed as a critical, required, or essential features or elements of any or all the claims. The invention is defined solely by the appended claims including any amendments made during the pendency of this application and all equivalents of those claims as issued.

[0058] Moreover in this document, relational terms such as first and second, top and bottom, and the like may be used solely to distinguish one entity or action from another entity or action without necessarily requiring or implying any actual such relationship or order between such entities or actions. The terms "comprises," "comprising," "has," "having," "includes," "including," "contains," "containing" or any other variation thereof, are intended to cover a non-exclusive inclusion, such that a process, method, article, or apparatus that comprises, has, includes, contains a list of elements does not include only those elements but may include other elements not expressly listed or inherent to such process, method, article, or apparatus. An element proceeded by "comprises … a," "has … a," "includes … a," or "contains … a" does not, without more constraints, preclude the existence of additional identical elements in the process, method, article, or apparatus that comprises, has, includes, contains the element. The terms "a" and "an" are defined as one or more unless explicitly stated otherwise herein. The terms "substantially," "essentially," "approximately," "about" or any other version thereof, are defined as being close to as understood by one of ordinary skill in the art, and in one non-limiting embodiment the term is defined to be within 10%, in another embodiment within 5%, in another embodiment within 1% and in another embodiment within 0.5%. The term "coupled" as used

herein is defined as connected, although not necessarily directly and not necessarily mechanically. A device or structure that is "configured" in a certain way is configured in at least that way, but may also be configured in ways that are not listed.

[0059] It will be appreciated that some embodiments may be comprised of one or more generic or specialized processors (or "processing devices") such as microprocessors, digital signal processors, customized processors and field programmable gate arrays (FPGAs) and unique stored program instructions (including both software and firmware) that control the one or more processors to implement, in conjunction with certain non-processor circuits, some, most, or all of the functions of the method and/or apparatus described herein. Alternatively, some or all functions could be implemented by a state machine that has no stored program instructions, or in one or more application specific integrated circuits (ASICs), in which each function or some combinations of certain of the functions are implemented as custom logic. Of course, a combination of the two approaches could be used.

[0060] Moreover, an embodiment can be implemented as a computer-readable storage medium having computer readable code stored thereon for programming a computer (e.g., comprising a processor) to perform a method as described and claimed herein. Examples of such computer-readable storage mediums include, but are not limited to, a hard disk, a CD-ROM, an optical storage device, a magnetic storage device, a ROM (Read Only Memory), a PROM (Programmable Read Only Memory), an EPROM (Erasable Programmable Read Only Memory), an EEPROM (Electrically Erasable Programmable Read Only Memory) and a Flash memory. Further, it is expected that one of ordinary skill, notwithstanding possibly significant effort and many design choices motivated by, for example, available time, current technology, and economic considerations, when guided by the concepts and principles disclosed herein will be readily capable of generating such software instructions and programs and ICs with minimal experimentation.

[0061] The Abstract of the Disclosure is provided to allow the reader to quickly ascertain the nature of the technical disclosure. It is submitted with the understanding that it will not be used to interpret or limit the scope or meaning of the claims. In addition, in the foregoing Detailed

Description, it can be seen that various features are grouped together in various embodiments for the purpose of streamlining the disclosure. This method of disclosure is not to be interpreted as reflecting an intention that the claimed embodiments require more features than are expressly recited in each claim. Rather, as the following claims reflect, inventive subject matter lies in less than all features of a single disclosed embodiment. Thus the following claims are hereby incorporated into the Detailed Description, with each claim standing on its own as a separately claimed subject matter.

CLAIMS

We claim:

1. A method for reconfiguring an electronic device, having at least three antenna elements, between different antenna modes, the method comprising:

configuring, by a controller, the electronic device into a first antenna mode, wherein at least two of the antenna elements are coupled together to operate as a single antenna; and

reconfiguring, by the controller, the electronic device from the first antenna mode into a second antenna mode, wherein each antenna configured for use during the second antenna mode includes only a single antenna element.

2. The method of claim 1, wherein the first antenna mode comprises a first multiple-input and multiple-output (MIMO) mode, and the second antenna mode comprises a second MIMO mode.

3. The method of claim 2, wherein the first MIMO mode comprises a MIMO NxN mode and the second MIMO mode comprises an MIMO MxM mode.

4. The method of claim 3, wherein N=2 and M=3 or 4.

5. The method of claim 1, wherein the first antenna mode comprises a multiple-input and multiple-output (MIMO) mode, and the second antenna mode comprises a MIMO mode plus carrier aggregation mode.

6. The method of claim 1, wherein the second antenna mode is determined based on at least one of: feedback from a base station or feedback from a sensor on the electronic device.

7. The method of claim 1, wherein the first antenna mode is used for communicating a first plurality data streams using a same first channel, and the second antenna mode is used for communicating a second plurality data streams using a same second channel.

8. The method of claim 1, wherein the first antenna mode is used for communicating a first plurality data streams using a same first channel in the first frequency band, and the second antenna mode is used for communicating a second plurality data streams using a plurality of different channels and frequency bands.

9. The method of claim 8, wherein at least two channels of the plurality of different channels are from different frequency bands.

10. The method of claim 8, wherein all of the channels of the plurality of different channels are from the same frequency band.

11. An electronic device comprising:
at least three antenna elements; and
a controller operative to:
configure the antenna elements into a first antenna configuration comprising at least two of the antenna elements coupled together to operate as a single antenna; and
reconfigure the antenna elements into a second antenna configuration, wherein each antenna in the second antenna configuration includes only a single antenna element, which is configured to individually operate as a separate antenna.

12. The electronic device of claim 11, wherein the second antenna configuration supports communication of a plurality of data streams using a plurality of component carriers from the same or from multiple frequency bands.

13. The electronic device of claim 11, wherein the first antenna configuration supports communication of a first plurality of data streams using a same first carrier within a first

carrier frequency band, and the second antenna configuration supports communication of a second plurality of data streams using a same second carrier within a second carrier frequency band.

14. The electronic device of claim 13, wherein the first antenna configuration supports multiple-input multiple-output (MIMO) 2x2 communications, and the second antenna configuration supports MIMO 4x4 communications or MIMO 3x3 communications.

15. The electronic device of claim 11 further comprising an adjustable matching network coupled to each antenna element and to the controller, wherein each adjustable matching network is operable in response to feedback from a set of sensors on the electronic device, which are used to determine a manner of use of the electronic device.

16. The electronic device of claim 11 further comprising a set of switches coupled to the controller and to the at least three antenna elements to configure the antenna elements into the first antenna configuration and to reconfigure the antenna elements into the second antenna configuration.

17. The electronic device of claim 16, wherein:

the at least three antenna elements comprises a first antenna element disposed near a first corner of a planar rectangular ground plane of the electronic device, a second antenna element disposed near a second corner of the planar rectangular ground plane and diagonal to the first antenna element, a third antenna element disposed near a third corner of the planar rectangular ground plane adjacent to the first and second corners, and a fourth antenna element disposed near a fourth corner of the planar rectangular ground plane adjacent to the first and second corners and diagonal to the third antenna element; and

the first antenna element, the second antenna element, the third antenna element, and the fourth antenna element are the same type of antenna element or a combination of different types of antenna elements.

18. The electronic device of claim 17 further comprising:

a first adjustable phase shifter coupled to the first antenna element and to the controller;

a second adjustable phase shifter coupled to the second antenna element and to the controller;

a third adjustable phase shifter coupled to the third antenna element and to the controller; and

a fourth adjustable phase shifter coupled to the fourth antenna element and to the controller.

19. The electronic device of claim 18 further comprising:

first and second variable splitters;

first and second switches of the set of switches;

a first receiver front end coupled to the controller and to the first switch, which is also coupled to the first variable splitter and the controller;

a first transceiver front end coupled to the controller and the first variable splitter, which is also coupled to the second adjustable phase shifter and the controller;

a second receiver front end coupled to the controller and to the second switch, which is also coupled to the second variable splitter and the controller;

a second transceiver front end coupled to the controller and the second variable splitter, which is also coupled to the third adjustable phase shifter and the controller.

20. The electronic device of claim 19, wherein:

in the first antenna configuration, the first switch is configured to connect the first adjustable phase shifter to the first variable splitter in order to couple the first and second antenna elements together to operate as a first antenna, and the second switch is configured to connect the fourth adjustable phase shifter to the second variable splitter in order to couple the third and fourth antenna elements together to operate as a second antenna;

in the second antenna configuration, the first switch is configured to disconnect the first adjustable phase shifter from the first variable splitter in order to decouple the first and second antenna elements, and the second switch is configured to disconnect the fourth adjustable phase shifter from the second variable splitter in order to decouple the third and fourth antenna elements.

ABSTRACT OF THE DISCLOSURE

A method is used for reconfiguring an electronic device, having at least three antenna elements, between different antenna modes. The method includes configuring, by a controller, the electronic device into a first antenna mode, wherein at least two of the antenna elements are coupled together to operate as a single antenna. The method further includes, reconfiguring, by the controller, the electronic device from the first antenna mode into a second antenna mode, wherein each antenna configured for use during the second antenna mode includes only a single antenna element.

Paper 8

Channel Spatial Correlation Reconstruction in Flexible Multi-Probe Setups

Wei Fan, Istvan Szini, Jesper Nielsen and Gert Pedersen

Published as:
Fan, W.; Szini, I.; Nielsen, J.; Pedersen, G.,
"Channel Spatial Correlation Reconstruction in Flexible Multi-Probe Setups"
Antennas and Wireless Propagation Letters, IEEE ,
vol.PP, no.99, pp.1,1
doi: 10.1109/LAWP.2014.2300096

Channel spatial correlation reconstruction in flexible multi-probe setups

Wei Fan[1], Istvan Szini[1,2], Jesper Ø. Nielsen[1], and Gert F. Pedersen[1]
[1]Department of Electronic Systems, Faculty of Engineering and Science, Aalborg University, Aalborg, Denmark
[wfa, ijs, jni, gfp]@es.aau.dk
[2]Motorola Mobility LLC., Libertyville, USA

***Abstract*—This paper discusses one aspect of over the air (OTA) testing for multiple input multiple output (MIMO) capable terminals in flexible multi-probe setups. Two techniques to obtain weights as well as angular locations for the OTA probes are proposed for accurate reconstruction of the channel spatial correlation at receiver side. Examples show that with a small number of probes in a flexible setup, accurate spatial correlation can still be achieved within the test zone.**

***Index Terms*—OTA testing, flexible multi-probe setup, anechoic chamber, multi-antenna terminal**

I. Introduction

Over the air (OTA) testing of multiple input multiple output (MIMO) capable terminals has attracted huge attention in recent years due to the urgent need for testing the radio performance of mobile terminals with multiple antennas [1]. The multi-probe anechoic chamber method is a promising candidate due to its ability to reproduce desired radio channels.

One major challenge with the multi-probe method is the cost of the system and the setup complexity. Each probe is typically connected to an expensive channel emulator. The cost will likely increase dramatically for 3D probe configurations [2]. The fixed multi-probe setup may not be cost effective, as often many probes are not actually used in synthesizing the radio channels. If the probes can be placed according to the channel spatial characteristics in a flexible manner, a larger test area can be created compared with the fixed probe setups with the same number of probes. Hence, a flexible setup mechanism has the potential to save cost of the system, via reducing the number of required active probes and respective hardware.

In one possible installation for the flexible setup, a large number probes are installed with fixed locations, and a switch box drives a subset of probes based on the target channel models [3]. To reduce mutual coupling and reflection between probes, a minimum separation between probes is required. Thus, fixing the probe locations in the chamber will often result in suboptimal probe locations for a given channel model. In this paper, we propose a flexible system arrangement, where the number of probes (consequently the channel emulator output ports) are optimized to the minimum necessary to generate the desirable spatial channel model. An illustration of the setup is shown in Figure 1, where probes are assembled in a movable semi-arc rail. The probe placement is flexible in both the elevation and azimuth angles, enabling the placement on optimal location defined by the proposed algorithm.

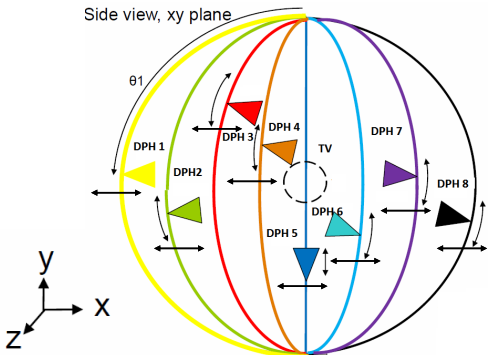

Figure 1. An illustration of the flexible multi-probe setup. DPH denotes dual polarized horn antenna; TV denotes test volume. The elevation and azimuth angle of each probe is to be optimized.

Contributions on the channel emulation techniques have been mainly focused on the fixed multi-probe configurations so far, where the objective is to find the optimum probe weights [2], [4], [5]. Channel emulation for the flexible setup with a small number of probes is more challenging as both the probe weights and the probe angular locations are to be optimized. In this paper, two algorithms, namely the genetic algorithm and the so-called multi-shot algorithm, are proposed to emulate channel spatial correlation in flexible setups. Note that modeling of other channel parameters, e.g. Doppler power spectrum, power delay profile, etc. in the flexible setups are not addressed in the paper.

II. Problem formulation

Channel emulation for fixed multi-probe setups have been detailed in [4], [5], where the focus is on recreating the channel spatial characteristics where the device in located. Spatial correlation is used as a figure of merit to model the channel spatial characteristics. A location pair is used to represent the locations of two spatial samples where two isotropic antennas u and v are placed [5]. The spatial correlation for the mth location pair, for a single polarization, is:

$$\rho(m) = \oint \exp(j\beta(\overline{r}_{u,m} - \overline{r}_{v,m}) \cdot \overline{\Omega}) p(\Omega) d\Omega, \qquad (1)$$

where $\overline{r}_{u,m}$ and $\overline{r}_{v,m}$ are vectors containing the position information of antenna u and v at the mth location pair, respectively. $\overline{\Omega}$ is an unit vector corresponding to the solid angle Ω. β is the wave number. $p(\Omega)$ is spherical power spectrum (SPS) satisfying $\oint p(\Omega)d\Omega = 1$. $(\cdot)$ is the dot product operator. Similar to (1), the emulated spatial correlation for the mth location pair can be calculated as [4], [5]:

$$\hat{\rho}(m, \overline{\mathbf{\Phi}}) = \sum_{n=1}^{N} w_n \exp(j\beta(\overline{r}_{u,m} - \overline{r}_{v,m}) \cdot \overline{\Phi}_n), \qquad (2)$$

where $\boldsymbol{w} = [w_1, ..., w_N]^T$ is a power weighting vector to be optimized. $\overline{\Phi}_n$ is a unit position vector of the nth probe. $\overline{\mathbf{\Phi}} = [\overline{\Phi}_1, ..., \overline{\Phi}_N]^T$ is a matrix that contains the positions of all probes. N is the total number of probes.

To minimize the emulation error over M location pairs, the following objective function is used:

$$\begin{aligned} &\min \ \left\| \hat{\boldsymbol{\rho}}(\boldsymbol{w}, \overline{\mathbf{\Phi}}) - \boldsymbol{\rho} \right\|_2^2, \\ &\text{s.t. } 0 \le w_n \le 1, \ \forall n \in [1, N] \end{aligned} \qquad (3)$$

where $\hat{\boldsymbol{\rho}}$ and $\boldsymbol{\rho}$ are the emulated spatial correlation and the target spatial correlation vectors of size M, respectively, with the mth element described in (2) and (1), respectively. $\hat{\boldsymbol{\rho}} = \mathbf{F_N} \boldsymbol{w}$ with $\mathbf{F_N} \in \mathbb{C}^{M \times N}$ being the transfer matrix for N probes, whose elements are given by:

$$(\mathbf{F_N})_{m,n} = \exp(j\beta(\overline{r}_{u,m} - \overline{r}_{v,m}) \cdot \overline{\Phi}_n), \quad 1 \le m \le M \ \ (4)$$

For fixed multi-probe setups (i.e. $\overline{\mathbf{\Phi}}$ fixed), the objective function (3) is a convex optimization problem, which is easily solved in [2], [5]. For flexible multi-probe setups, the objective function (3) is a non-convex optimization problem as both the probe weights and the probe angular locations are to be optimized.

Probes are limited to a possibly large set of discrete locations for practical reasons. Let us define $\overline{\mathbf{\Psi}} = [\overline{\Phi}_1, ..., \overline{\Phi}_K]^T$ $(K > N)$ as a matrix that contains the K possible discrete locations for the probes. The channel spatial correlation emulation for flexible setups can be treated in two steps as:

1) Select N locations out of K possible discrete locations for the N probes. The problem formulation for the probe selection is as follows:

$$\begin{aligned} &\min_{\mathbf{c}} \ \left\| \mathbf{F_K c} - \boldsymbol{\rho} \right\|_2^2 \\ &\text{s.t. } \left\| \mathbf{c} \right\|_0 = N \end{aligned} \qquad (5)$$

where the norm-0 operation $\|\cdot\|_0$ is defined to be the number of nonzero entries in the vector. $\mathbf{F_K}$ is the transfer matrix for the K possible locations with its element defined in (4). $\boldsymbol{c} = [c_1, ..., c_K]$ is the weighting vector to be optimized.
The problem in (5) is non-convex and NP-hard due to the norm-0 constraint. A brute force method where the optimization is performed for each possible combination of the N locations out of K potential locations can be used, and a total number of combinations is $\binom{K}{N}$. The number of combinations to be tested becomes huge when K is large. Two algorithms are proposed to address the non-convex optimization problem later.
2) After knowing the locations of the N probes, the optimization is simplified to be a convex problem:

$$\min_{\mathbf{c}_{sel}} \left\| \mathbf{F c}_{sel} - \boldsymbol{\rho} \right\|_2^2$$

where $\mathbf{F}$ is the $M \times N$ matrix with N selected columns from $\mathbf{F_K}$, and $\mathbf{c}_{sel}$ is the $N \times 1$ vector with the N selected probe locations.

III. Spatial correlation emulation with flexible setups

A. Genetic algorithm

The genetic algorithm (GA) has been widely used in electromagnetics [6]. The GA is basically a search technique inspired by the principles of genetics and natural selection. A very useful aspect of GA is that it can deal with a large number of variables and it can optimize variables with extremely complex cost surfaces [6]. A limitation is that it can stop in a local optimum, and often, it is not possible to know whether the solution is local or global. We can think of the target channel as the environment and the selected probe locations as the biological species that need to fit in the environment (the channel). The fitness of the probe locations to the environment can be measured by the channel emulation accuracy. In this section, a GA applied to the problem of selecting the optimum probe locations is described. The concept is straightforward: The GA seeks for a set of probe locations that would minimize the channel emulation error. The number of selected probes (N) designates the search space.

A population is the array of chromosomes under examination for the GA. A chromosome contains N variables which represent the N probe locations. Each chromosome will have a cost evaluated by the cost function f, as:

$$f = \min_{\boldsymbol{w}_{GA}} \left\| \mathbf{F}_{GA} \boldsymbol{w}_{GA} - \boldsymbol{\rho} \right\|_2^2, \qquad (6)$$

where $\mathbf{F}_{GA}$ and $\boldsymbol{w}_{GA} = [w_1, ..., w_N]^T$ are the transfer matrix and probe weight vector of the chromosome under evaluation. The cost function actually contains a convex optimization process. A flowchart of the GA shown is shown in Figure 2. The description of the employed GA algorithm is given in [6] and is not detailed here. This complexity of GA is:

$$\underbrace{N_{pop}}_{\text{initial population}} + \underbrace{(N_{pop} - 1)}_{\text{cost evaluations per generation}} \times \underbrace{N_g}_{\text{generations}}$$

cost function evaluations.

B. Multi-shot

One alternative to select the optimum set of probe locations is to use the so-called multi-shot algorithm. The basic idea is that probes with negligible contribution in synthesizing the channels should be removed. Probe locations can be removed in a sequential manner. We denote by k_n the number of

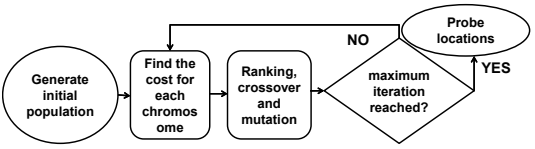

Figure 2. Brief flowchart of the employed GA.

Table I
GA PARAMETER SETUPS

Parameter	maximum number of iterations N_g	population size N_{pop}	selection rate
Value	50	8	50%

potential locations we remove in the nth iteration and we have $K - \sum_{m=0}^{n-1} k_m$ selected locations in the nth iteration. In the multi-shot algorithm, we first perform the optimization for K potential locations. In the nth iteration, based on the individual probe power values $|c_{n,index}|$ $(1 \leq index \leq K)$ in $\mathbf{c}_n$, we remove k_n locations with the least power values. We repeat the location removal process until only $K - \sum_{m=0}^{n-1} k_m = N$ locations are left. In the end, we return both the final probe weights and the corresponding probe locations. The complexity of the multi-shot algorithm is $\frac{K-N}{k} + 1$ convex optimizations if the number of removed locations per iteration is always k.

IV. Optimization Results

A. Optimization setups

To illustrate the algorithms, 2D multi-probe setups are considered for simplicity. $K = 360$ uniformly placed locations are defined as possible locations. The parameters for the GA have been chosen through repeated trials, following the guideline in [6]. The number of generations is a tradeoff between the convergence rate and the computational complexity. The parameters used in the GA are summarized in Table I. In the following computations, the number of removed locations per iteration $k_n = 1$ is defined for the multi-shot algorithm.

We examine a set of representative channel models that are used in standardization for the MIMO OTA testing [1]. The models are: a) Single Laplacian shaped spatial cluster with angle of arrival (AoA) 22.5° and azimuth spread (AS) 35°, b) SCME Urban micro (Umi) TDL model (six Laplacian shaped clusters) and c) SCME Urban macro (Uma) TDL model from [7]. Note that a critical single cluster model for eight probe uniform setup, i.e. the spatial cluster impinging from an angle exactly between two adjacent OTA probes, is selected to show the robustness of the algorithms.

An uniform probe configuration is used for comparison for each of the considered flexible setup, as detailed in Table II. The idea is to show that with a small number of probes in a flexible setup, accurate spatial correlation can still be achieved.

B. Results

The spatial correlation $|\rho|$ for the single spatial cluster model and correlation error $|\hat{\rho} - \rho|$ are shown in Figure 3. The radius d and polar angle ϕ of each point on the plots correspond to the value at antenna separation d and antenna orientation ϕ [5]. Test area size shown in the optimization results denotes the distance between the two antennas and corresponds to the maximum d in the polar plots. A maximum deviation of 0.15 and 0.3 is achieved over the test area size of 1λ for the flexible setup with 3 probes for the GA and multi-shot algorithm, respectively. In contrast, the correlation error is much larger for the uniform setup with 8 probe. The optimized angle locations for the 3 probes with the two proposed algorithms are shown in Figure 4 (left), where the angular locations are in good agreement with the target single spatial cluster. Figure 5 (left) shows the GA algorithm convergence curve in terms of the minimum and mean cost for each generation for the single cluster model.

Table II
NUMBER OF PROBES AND TEST AREA SIZE FOR THE CONSIDERED SETUPS.

Channel models	Flexible setup	Reference setup	Test area size
Single cluster	$N = 3$	Uniform setup with 8 probe	1λ
SCME Umi TDL	$N = 8$	Uniform setup with 16 probe	1.5λ

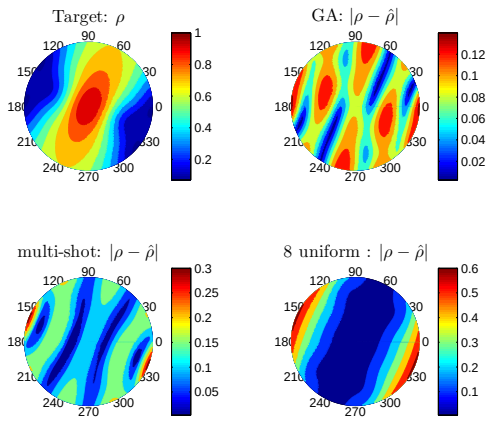

Figure 3. The target spatial correlation $|\rho|$ for the single cluster channel model and the associated correlation error $|\rho - \hat{\rho}|$ for 3 probes with the GA algorithm, 3 probes with the multi-shot algorithm and the uniform probe configuration with 8 probes. Test area size: 1λ.

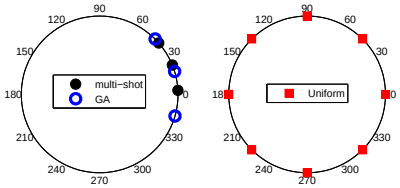

Figure 4. An illustration of the probe configurations detailed in Table II.

The spatial correlation $|\rho|$ for the SCME Umi TDL model and correlation error $|\hat{\rho} - \rho|$ are shown in Figure 6. Narrow-

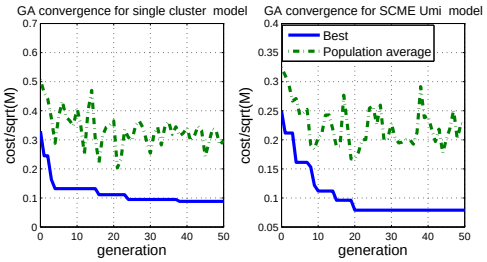

Figure 5. GA convergence curve for the single cluster model (left) and for the SCME Umi TDL model (right).

band multi-cluster models (with delay information removed) are used to obtain the optimal probe locations. Then each cluster is emulated with the selected probe locations, as described in [5]. A maximum deviation of 0.12 is achieved over the test area of 1.5λ for the flexible setup with 8 probes for the multi-shot algorithm. The multi-probe algorithm outperforms the GA for the SCME Umi TDL model. Figure 5 (right) shows the GA convergence curve for each generation for the SCME Umi TDL model. The channel emulation accuracy with the 8-probe flexible setup and the multi-shot algorithm offers slightly worse results than the channel emulation accuracy with the 16 uniform probe setup.

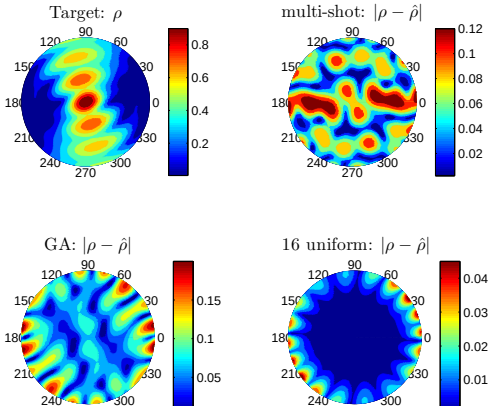

Figure 6. The target spatial correlation $|\rho|$ for the SCME Umi TDL channel model and associated correlation error $|\rho - \hat{\rho}|$ for 8 probes with the multi-shot algorithm, 8 probes with the GA algorithm and uniform probe configuration with 16 probes. Test area size: 1.5λ.

The emulation accuracy for the 6 clusters in the SCME Umi TDL model is shown in Table III. Note that the probe locations are selected based on the SPS of the multi-cluster model, so the emulation accuracy for each of the clusters might be bad. The correlation error $|\rho - \hat{\rho}|$ for the 3rd cluster is up to 0.44 with the multi-shot algorithm due to the fact that the locations selected are favoring the dominant clusters.

The correlation error $|\hat{\rho} - \rho|$ for the SCME Uma TDL model with the multi-shot and the GA are shown in Figure 8. The GA

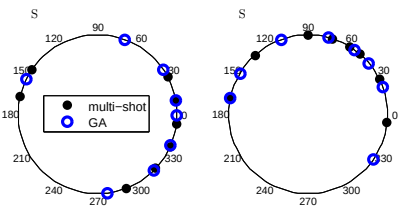

Figure 7. Illustration of optimized locations for SCME Umi TDL (left) and SCME Uma TDL models (right).

Table III
ERROR STATISTICS OF CORRELATION ERROR $|\rho - \hat{\rho}|$ FOR THE 6 CLUSTERS IN THE SCME UMI TDL CHANNEL MODEL FOR DIFFERENT ALGORITHMS.

Algorithm	$\lvert\rho - \hat{\rho}\rvert$	1	2	3	4	5	6
multi-shot	max	0.16	0.09	0.44	0.09	0.10	0.15
	rms	0.07	0.05	0.25	0.05	0.05	0.07
GA	max	0.17	0.20	0.65	0.24	0.21	0.18
	rms	0.05	0.06	0.35	0.07	0.06	0.05

slightly outperforms the multi-shot algorithm, with correlation error up to 0.25 over the test area of 1.5λ.

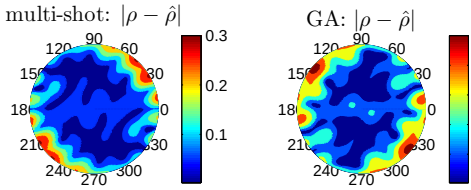

Figure 8. The correlation error $|\rho - \hat{\rho}|$ for 8 probes with the multi-shot algorithm and 8 probes with the GA for the SCME Uma TDL model. Test area size: 1.5λ.

V. CONCLUSIONS

We have introduced two algorithms to determine the weights and angular locations for the probes in flexible setups, i.e. the multi-shot algorithm and the GA. The proposed algorithms offer good spatial correlation accuracy for the flexible setups. The optimization results show that a test area of 1λ can be created for the single cluster channel model with 3 probes, with an emulation error up to 0.14 with the GA. A test area of 1.5λ can be created with 8 probes for the SCME Umi TDL channel model, with an emulation error up to 0.12 with the multi-shot algorithm, and for the SCME Uma TDL channel model, with an emulation error up to 0.25 with the GA.

REFERENCES

[1] "Verification of radiated multi-antenna reception performance of User Equipment," 3GPP, TR 37.977 V1.0.0, Sep. 2013.
[2] W. Fan, F. Sun, P. Kyosti, J. Nielsen, X. Carreno, M. Knudsen, and G. Pedersen, "3D channel emulation in multi-probe setup," *Electronics Letters*, vol. 49, no. 9, pp. 623–625, 2013.
[3] P. Kyösti, J. Nuutinen, and J. Malm, "Over the air test," Patent US 20 130 059 545 A1, Mar. 7, 2013.

[4] P. Kyösti, T. Jämsä, and J. Nuutinen, "Channel modelling for multiprobe over-the-air MIMO testing," *International Journal of Antennas and Propagation*, 2012.
[5] W. Fan, X. Carreño, F. Sun, J. Nielsen, M. Knudsen, and G. Pedersen, "Emulating Spatial Characteristics of MIMO Channels for OTA Testing," *Antennas and Propagation, IEEE Transactions on*, vol. 61, no. 8, pp. 4306–4314, 2013.
[6] R. L. Haupt and D. H. Werner, *Genetic algorithms in electromagnetics*. Wiley. com, 2007.
[7] D. Baum, J. Hansen, and J. Salo, "An interim channel model for beyond-3G systems: extending the 3GPP spatial channel model (SCM)," in *Proc. IEEE VTC-Spring*, May 2005.

Patent disclosure related to Paper 8

Method and Apparatus for Wireless Device Performance Testing

Istvan Szini, John Peters and Eric Krenz

Patent pending, submitted to:
United States Patent and Trademark Office , November 2013

METHOD AND APPARATUS FOR WIRELESS DEVICE PERFORMANCE TESTING

Field of the Invention

[0001] The present invention relates generally to electromagnetic communications, and more specifically to determining wireless device performance using standardized system modeling.

Background

[0002] Standardized radio system modeling has been used extensively for determining the performance of wireless units, such as vehicular phones, cell phones, laptops, and wireless tablets. Standardized radio system testing provides for comparison of different models of wireless devices and can be useful during development of wireless devices when the standardized system model sufficiently models the real world environment. As systems have become more sophisticated, so have the standardized radio system models. Today there are well defined radio system models that use two dimensional modeling, wherein a wireless device under test is placed at a test position within an anechoic chamber that has a plurality of probe antennas placed at regular intervals at 90 degrees elevation and 360 degrees azimuth with reference to a normal position of the wireless device under test. (Note that for this document an elevation angle of zero is along an upper half of an axis that is vertical with reference to the horizontal plane.) With the increasing use of multiple-input-multiple-output antennas within devices, more complex mathematical algorithms are proposed to model the radio systems using radio propagation channels in three dimensional models. This results in greater numbers of antenna probes within anechoic test chambers that have been proposed to improve the modeling of the real world environment. The greater number of antenna probes includes probe antennas that are placed anywhere within the full elevation range of 0 to 180 degrees, that are not used in two dimensional models, and at smaller azimuth angular intervals One result of more antenna probes is the need for a larger anechoic chamber to reduce antenna coupling to limits. The increased size and complexity of the test setups can cost substantially more per unit test to run than earlier test systems.

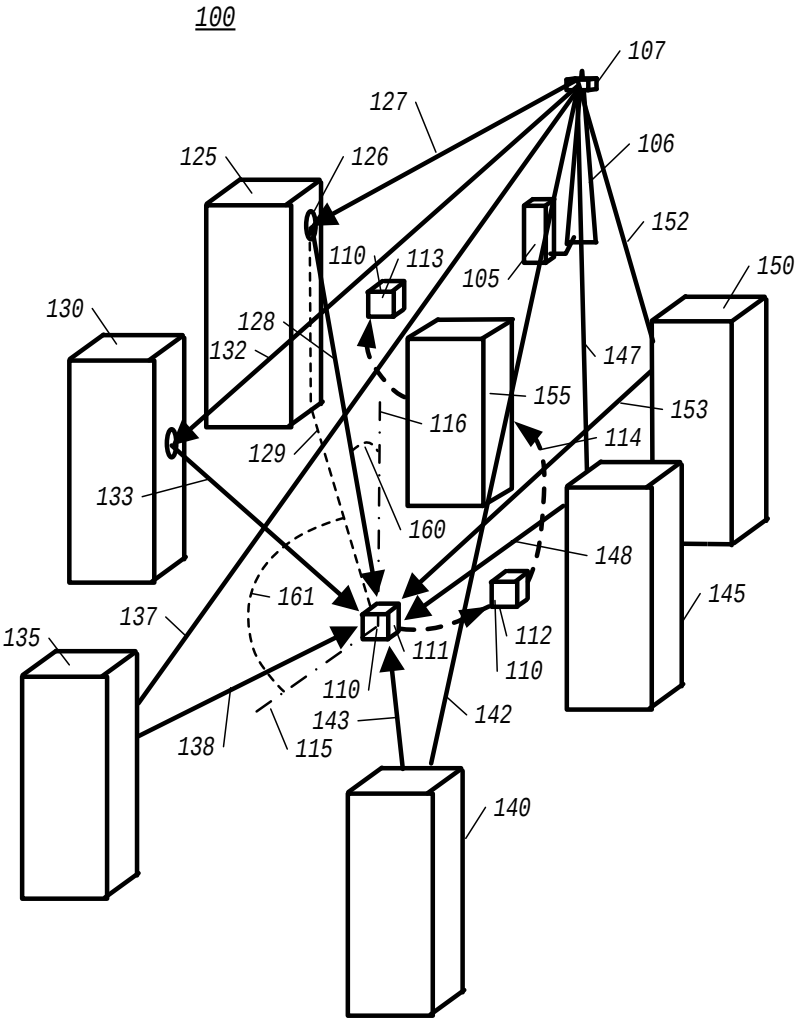
100
107
127
125
126
106
152
110
113
105
150
130
128
132
147
155
153
116
114
129
133
160
148
161
145
137
135
112
111
110
110
143
142
138
115
140

FIG. 1

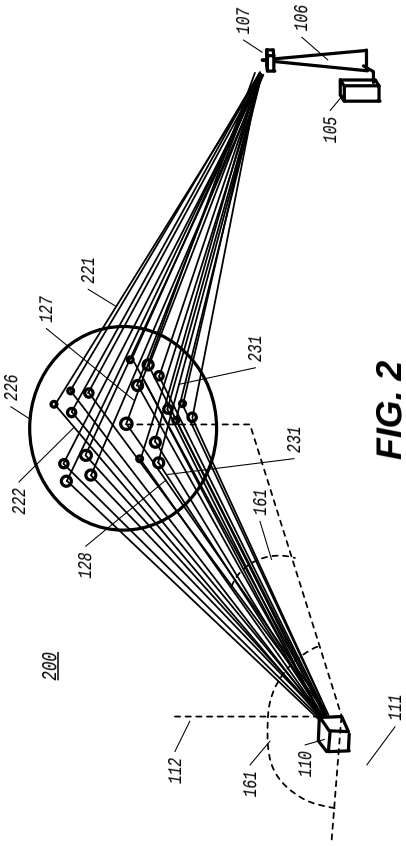

FIG. 2

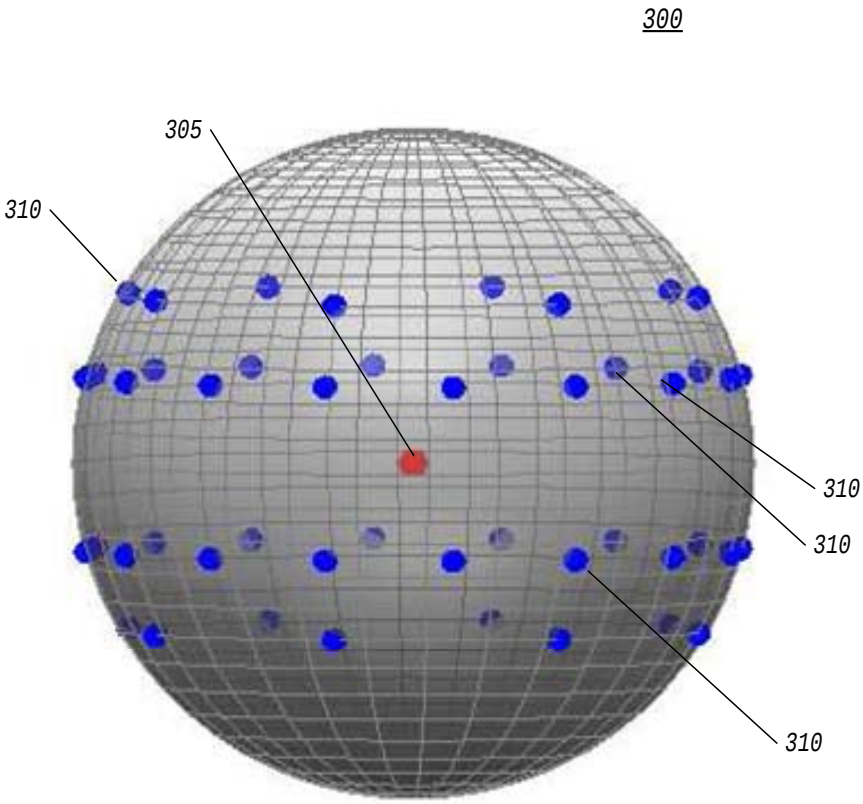

Prior Art

FIG. 3

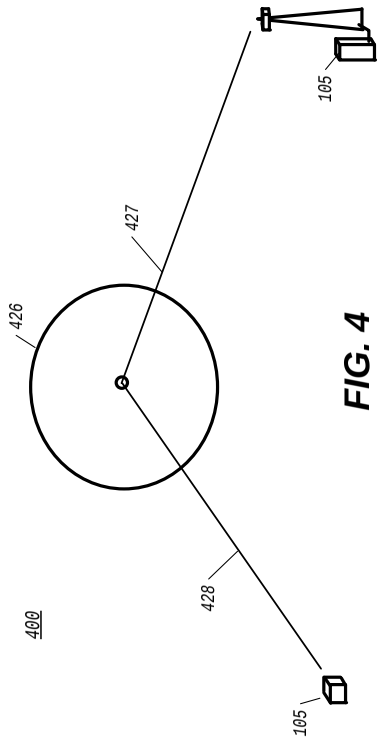

FIG. 4

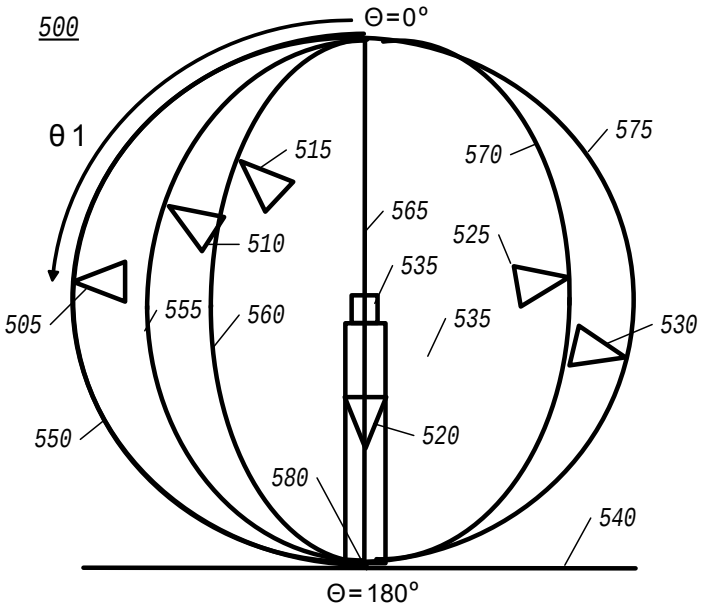
500
Θ=0°
θ 1
515
570
575
565
510
525
535
505
555
560
535
530
550
520
580
540
Θ=180°

FIG. 5

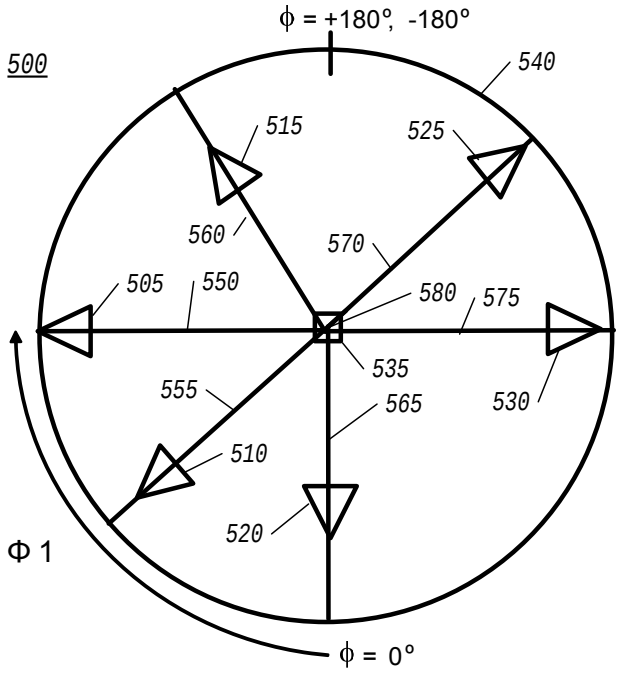
ϕ = +180°, -180°
500
540
515
525
560
570
505
550
580
575
535
555
565
530
510
520
Φ 1
ϕ = 0°

FIG. 6

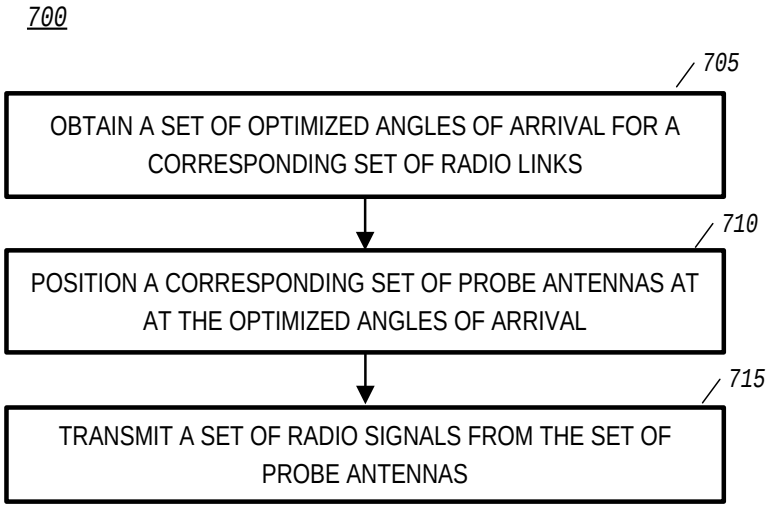
700
705
OBTAIN A SET OF OPTIMIZED ANGLES OF ARRIVAL FOR A CORRESPONDING SET OF RADIO LINKS
710
POSITION A CORRESPONDING SET OF PROBE ANTENNAS AT AT THE OPTIMIZED ANGLES OF ARRIVAL
715
TRANSMIT A SET OF RADIO SIGNALS FROM THE SET OF PROBE ANTENNAS

FIG. 7

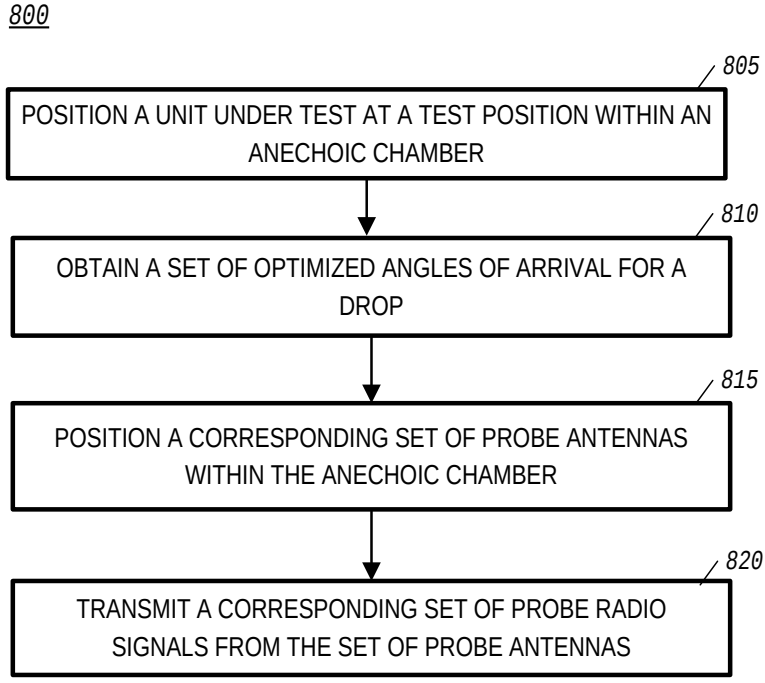
800
805
POSITION A UNIT UNDER TEST AT A TEST POSITION WITHIN AN ANECHOIC CHAMBER
810
OBTAIN A SET OF OPTIMIZED ANGLES OF ARRIVAL FOR A DROP
815
POSITION A CORRESPONDING SET OF PROBE ANTENNAS WITHIN THE ANECHOIC CHAMBER
820
TRANSMIT A CORRESPONDING SET OF PROBE RADIO SIGNALS FROM THE SET OF PROBE ANTENNAS

FIG. 8

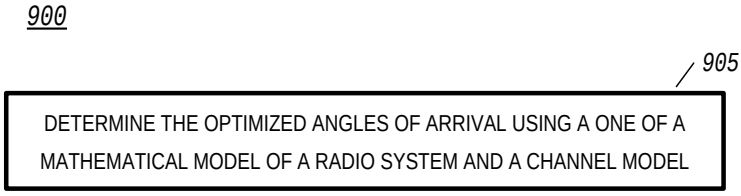

FIG. 9

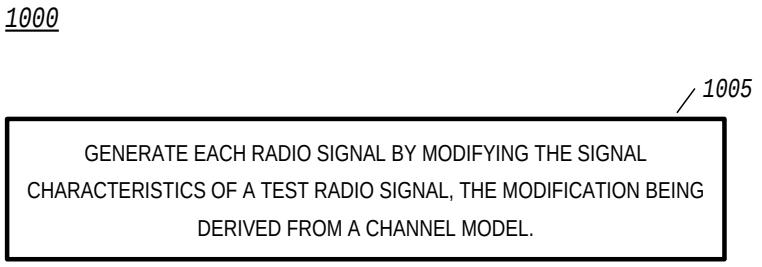

FIG. 10

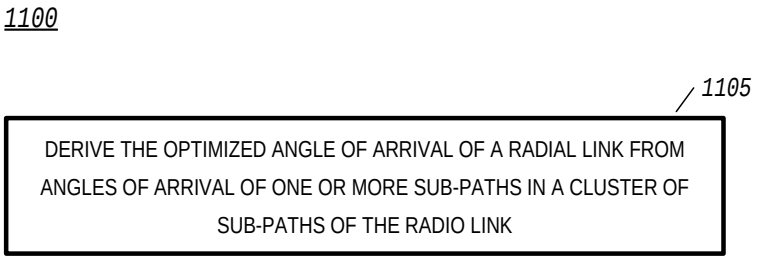

FIG. 11

Brief Description of the Figures

[0003] The accompanying figures, where like reference numerals refer to identical or functionally similar elements throughout the separate views, together with the detailed description below, are incorporated in and form part of the specification, and serve to further illustrate embodiments that include the claimed invention, and explain various principles and advantages of those embodiments.

[0004] FIG. 1 is a geometric block diagram of a wireless system that is used as a basis of modeling radio signal propagation in the wireless system, in accordance with certain embodiments.

[0005] FIG. 2 is a geometric diagram of one cluster of radio rays in the model of the wireless system, in accordance with certain embodiments.

[0006] FIG. 3 is a view of a three dimensional geometric representation of a distribution of antenna probes, in accordance with certain prior art embodiments.

[0007] FIG. 4 is a geometric diagram one cluster of radio rays in the model of the wireless system, in accordance with certain embodiments.

[0008] FIGS. 5-6 are two views of a three dimensional geometric representation of a distribution of antenna probes, in accordance with certain embodiments.

[0009] FIG. 7 is a flow chart of some steps of a method for testing a wireless device, in accordance with certain embodiments.

[0010] FIG. 8 is a flow chart of some steps of a method for testing a wireless device, in accordance with certain embodiments.

[0011] FIGS. 9-11 are each a flow chart of one step of the methods described with reference to **FIGS. 7** and **8**.

[0012] Skilled artisans will appreciate that elements in the figures are illustrated for simplicity and clarity and have not necessarily been drawn to scale. For example, the dimensions of some of the elements in the figures may be exaggerated relative to other elements to help to improve understanding of embodiments of the present invention.

Detailed Description

[0013] Before describing in detail the following embodiments, it should be observed that the embodiments reside primarily in combinations of method steps and apparatus components related to testing of wireless devices in an anechoic chamber, in which a minimum number of antenna probes transmit modified forms of a particular test signal to a device under test. Accordingly, the apparatus components and method steps have been represented where appropriate by conventional symbols in the drawings, showing only those specific details that are pertinent to understanding the embodiments of the present invention so as not to obscure the disclosure with details that will be readily apparent to those of ordinary skill in the art having the benefit of the description herein.

[0014] Referring to **FIG. 1**, a geometric block diagram of a radio system model 100 that is used as a basis of modeling radio signal propagation in actual radio systems is shown, in accordance with certain embodiments. The radio system model 100 may closely represent an actual radio system or may be a channel model of a type of radio system. The characteristics of propagation of the transmitted radio energy in these radio system models are commonly referred to as the channel model. Channel models have been defined for environments such as an urban micro-cell (which FIG. 1 represents), an indoor micro-cell a suburban macro-cell, or a rural macro-cell. The modeling of radio signal propagation in some embodiments is provided for radio energy that propagates from one transceiver 105 to one wireless unit 110. The wireless unit can be any wireless device. The wireless unit may be any client device, of which just a few example are a cellular phone, a vehicular communication device, a PC or a tablet. In some cases the wireless device may not be considered a client device, such as a node of a local area network. Some of these embodiments are described in standardized channel models used in a channel modeling process for wireless unit test procedures, such as channel models and processes described in Chapter 5 of “MIMO Signal Processing”, Sebastian Miron (Ed.), ISBN: 978-953-7619-91-6, InTech. Chapter 5, “MIMO Channel Modelling” was authored by Faisal Darbari, Robert W. Stewart and Ian A. Glover of the University of Strathclyde, Galsgow, United Kingdom. Included in Chapter 5 are descriptions

of newer radio system models such as SCME (extended spatial channel model), WINNER II, as well as some older models. These standardized channel models are included in specifications or documents issued by agencies such as CTIA, 3GPP, and WINNER. CTIA refers to “CTIA – the Wireless Assocation” located at 1400 16th Street, NW, Suite 600 Washington, DC 20036. 3GPP refers to the 3rd Generation Partnership Project, having a location at 3GPP Mobile Competence Centre, c/o ETSI, 650, route des Lucioles, 06921 Sophia-Antipolis Cedex, France. WINNER is a consortium co-ordinated from Nokia Siemens Networks GmbH and Co. KG, SN MN PG NT RA, St. Martinstrasse 76, 81617 Munich, Germany. These channel modeling processes may use random selection techniques to perform many instances of channel propagation emulation in order to determine the performance of a wireless unit in a particular channel model (e.g., an urban micro-cell)

[0015] It will appreciated that these radio system models are not only useful in methods used for testing wireless units to determine their performance according to published standards; these radio system models may alternatively be used for other purposes, such as optimizing the locations of a wireless unit and transceiver relative to each other when both units are going to operated in fixed positions.

[0016] Referring again to **FIG. 1**, in some embodiments the radio signal received at the wireless unit is analyzed for a situation of the wireless unit in which the wireless unit is moving at defined speeds and directions within the radio system, using a particular channel model.In **FIG.1**, a wireless unit 110 is shown as moving along a path 114 that is shown as a dashed line starting at location 111, curving behind a building 155, and ending at location 113. The radio energy received by the wireless unit 110 along the path 114 can be modeled as a set of radio links that include clusters of rays, or sub-paths. Each ray is affected by an environment that is characterized by a variety of propagation parameters. The channel model defines some of these propagation parameters. Some of the propagation parameters are classified as large scale parameters, which are parameters that do not change significantly over distances of a few tens of wavelengths, and therefore for which an average value may be used. Other

propagation parameters may vary within distances of a few tens of wavelengths. In order to provide tractable analysis of the performance of a wireless unit operating in a particular channel model, a concept is used in some embodiments that is called a drop, which reduces the distance and time over which the channel model is analyzed to near zero. Propagation parameters are determined from the channel model for each drop and many drops are simulated to determine the performance of the wireless unit in the system model for the channel model.

[0017] Three drops for the wireless unit 110 are shown in FIG.1 as wireless drops 111, 112, and 113. There may be a plurality of drops at one wireless location, representing changing characteristics of the radio propagation at various times at the one location. The links for the wireless unit when at location 111 are illustrated in FIG. 1. Energy is radiated from the antenna 107 of transceiver 105. (The antenna 107 is mounted on tower or base station 106.) Some of the energy arrives at the wireless unit 110 along each of six multipath routes, each of which involves a reflection. Each reflection is modeled as being at a particular position on buildings 125, 130, 135, 140, 145, 150. There is no multipath to the wireless unit 110 at location 111 for building 155; it is blocking a direct line of sight path to the wireless unit. The positions on the buildings are such that the reflected energy arrives at the wireless unit 110. One of the paths comprises path 127 from the antenna 107 to a position 126 on the building 125, then path 128 from the position 126 to the wireless unit 110 at location 111. The energy arriving that is reflected off of position 126 on building 125 arrives at a specific angle with reference to the wireless unit 110. This is the angle of arrival of the energy.

[0018] The effects of the environment on this energy are modeled in the form of a radio link conveying energy at the angle of arrival of the path 128. The radio link is characterized by propagation parameters of the channel model that modify the energy transmitted by antenna 107, for a particular drop (i.e., for the particular location of the wireless unit, the particular angle of arrival, and the particular time of the drop). The values of the propagation parameters correspond to conditions that would occur along paths 127 and 128 in the type of environment being modeled (e.g., the amplitude may be modified for range and fading effects). The energy received at the wireless unit 110 for this channel

model is reduced to six or fewer radio links having different propagation characteristics and each having an associated angle of arrival at the wireless unit 110.

[0019] The angle of arrival for the radio link 127-128 is the angle of path 128 with reference to the wireless unit 110 at location 111, as shown in **FIG. 1**. This angle of arrival has an azimuth angle 161 and an elevation angle 160. In this example there is a horizontal plane that common to the base of the wireless unit 100 and the buildings 125, 130, 135, 140, 145, 150. An azimuth axis 125 that is within the horizontal plane is defined relative to the wireless unit 110 (at a corner of the base of the wireless unit 110). The azimuth angle 161 is the angle between the projection 129 of path 128 onto the horizontal plane and the azimuth axis 125. The elevation angle 160 is the angle between the path 128 and an axis that is perpendicular to the horizontal plane at the corner of the base of the wireless unit 110. Each of the links 132-133, 137-138, 142-143, 147-148, 152-153 has a (typically different) angle of arrival for the drop of wireless unit 110 at location 111. These angles of arrival are determined using the same wireless unit based coordinate system. Wireless unit 110 will also have additional sets of up to six links, each having an associated angle of arrival, for every drop, including drops 112 and 113. The coordinate system used to define the angles of arrival need not be the same as the one described for this example, where it is a polar coordinate system with a plane of 90 degree elevation (a horizontal plane in this example) that is common to the wireless unit 110 and the base of the buildings 125, 130, 135, 140, 145, 150.

[0020] It will be appreciated that this modelling can be used to provide standardized comparison testing of a wireless unit by radiating the wireless unit with a quantity of radio signals equal to the number of radio links. Such standardized wireless unit testing may be required as a part of a procurement process by radio system operators, such as AT&T, Sprint, Verizon, T-Mobile, and Vodaphone, just to name a few well-known radio system operators. A particular radio system operator may require channel model wireless unit testing performed according to a standard issued by a standards agency, such as CTIA and 3GPP, wherein the standard incorporates channel models such as those described

herein. Alternatively, a radio system operator could require the use of a channel model test method for wireless unit performance testing as described herein, issued by other engineering groups or the operator itself. Each radio signal is generated at its respective angle of arrival with reference to the wireless unit and transmitted by a probe antenna. Each probe radio signal is derived as a modified form of one test signal. The test signal may include information for the wireless unit to decode, allowing the determination of an error rate. The probe radio signals are determined using propagation parameters whose values are determined for each radio set of links for a particular drop. The drops may be determined using a randomized selection process. The angles of arrival and propagation characteristics can then be determined for a large enough number different drops to determine performance of the wireless unit for a particular environment (e.g., urban macro-cell). The angles of arrival and path lengths may be determined by a channel modeling process. The signal characteristics of the modified radio signal transmitted by each probe antenna may be determined from the channel model and specific parameters such as the path lengths of the links. The signal characteristics includes such items as carrier amplitude, carrier phase shift and phase spread, and polarization shift.

[0021] In some embodiments, a mathematical model of the geometry of a particular system may be used to analyze the performance characteristics of a wireless unit, which may be for such purposes as optimizing the position of a fixed wireless unit in a system. In such an instance, a mathematical model of the system geometry (for example, the mathematical model of the system shown in FIG. 1), implementation of which is known, can determine the angles of arrival doe different positions of the wireless unit. Probe antennas can then be placed at those angles and test signals used to optimize the location of the wireless unit.

[0022] Referring to **FIG. 2**, a geometric diagram 200 of one cluster 226 of a radio link in the model of the wireless system is shown, in accordance with certain embodiments. The radio link corresponds to path 128. The reflection of a signal at a position such as position 126 in **FIG. 1** is enhanced in certain embodiments (e.g., SCME and WINNER II) to include a one or more rays at some or all of the reflection positions. The collection of rays is called a cluster.

Each ray is also referred to as a sub-path. This is illustrated in **FIG.2**, where reflection position 126 is cluster 226. As shown in **FIG. 2**, in some embodiments used for standardized testing the clusters may include up to 20 sub-paths (e.g., sub-paths 221-222 and 231-232), each having a small deviation around a parent path. The parent path 127-128 in **FIGS 1** and **2** in some embodiments may be one of the sub paths shown in **FIG. 2**. In some embodiments the parent path may be determined by an average of the angles of the rays in the cluster.

[0023] Referring to **FIG. 3**, a view of a three dimensional geometric representation 300 of a distribution of antenna probes is shown, in accordance with certain prior art embodiments. A few of these are identified in **FIG. 3** with reference number 310. Prior art solutions providing an environment for determining the performance of a wireless unit in a radio system typically involve placing a wireless unit under test in an anechoic chamber. The anechoic chamber is typically equipped with sufficient probe antennas at defined fixed positions to allow testing of any drop expected to be used for a testing a class of wireless units. During a test, a wireless unit 305 is positioned at a test position in the anechoic chamber. The number of probe antennas required and their fixed positions are determined by the angles of arrival in the channel model being emulated. The fixed positions are at regular intervals, so that the test setup can be used for a wide variety of purposes, which may include system models having angles of arrival at many azimuth angles For more sophisticated radio systems employing multiple-input-multiple-output (MIMO) antenna systems, angles of arrival may also include elevation angles other than +90 degrees. For example, elevations within the ranges of +45 to +135 degrees may occur in some embodiments.

[0024] The probe antennas must be located sufficiently apart from each other to achieve an acceptably low level of antenna to antenna coupling. Hence the volume of the sphere upon which the probe antennas are positioned is larger for wireless units requiring a larger volume and is larger when more probe antennas are used. In embodiments that use probe antennas distributed around the test position in patterns, the angle of arrival of the test signal for each radio link in a drop is provided by coupling the test signal to several probe antennas at signal

strengths calculated so that the resultant energy comes for the correct angle of arrival. To accomplish this requires that the probe antennas be sufficiently close to each other so that the combined signal is a plane wave at the test volume, but far enough to avoid coupling. All of these constraints result in a relatively large radius of the sphere at which the probe antennas are mounted. For example, 48 probe antenna locations are described in “3D Channel Model Emulation in a MIMO OTA Setup” authored by Wei Fan, Pekka Kyösti, Fan Sun, Jesper Nielsen, Xavier Carreño, Gert F. Pedersen, and Mikael B. Knudsen, 2013, Department of Electronic Systems, Faculty of Engineering and Science, Aalborg University, Denmark.

[0025] Referring to **FIG. 4**, a geometric diagram 400 of one radio link 427, 428 in the model of the wireless system 100 is shown, in accordance with certain embodiments. The angle of arrival of this radio link is the angle of path 428, which is a consolidated angle of arrival derived from the cluster of rays described with reference to **FIG. 2**. By using one consolidated angle of arrival derived from the angles of arrivals of all of the sub-paths in each cluster, the quantity of angles of arrival is substantially reduced in comparison to models using radio links having multiple angles of arrival for each cluster. The signal characteristics for the consolidated radio link that now represents a cluster are derived by using a combination of the signal characteristics (e.g., amplitude and phase shift) the signals for each sub-path that have been determined by using the propagation parameters for each ray. The combination may be a combination weighted by amplitude. Testing of models using multiple drops for both approaches (that is, with multiple rays for each cluster versus a consolidated radio link for each cluster) show that the difference in wireless performance is less than +-5% when the consolidated angle of arrival is the average of the angles of arrival of each sub-path. Other versions of consolidated angles of arrival may be used, for example, a consolidated angle of arrival that is the parent angle of arrival, or an amplitude weighted average of the angles of arrival of each ray. The use of a consolidated angle of arrival for each radio link allows for a unique probe positioning technique that greatly reduces the amount of equipment needed to perform wireless unit analysis, as described below. This technique may be used as a modification in standard channel modeling processes.

[0026] Referring to **FIGS. 5-6** two views of a three dimensional geometric representation 500 of a distribution of antenna probes are shown, in accordance with certain embodiments. The view in **FIG. 5** is an elevation view of six probe antennas 505, 510, 515, 520, 525, 530. The view in **FIG. 6** is a plan view (top view) of the same six probe antennas 505, 510, 515, 520, 525, 530. The probe antennas 505, 510, 515, 520, 525, 530 are positioned equidistant in space from a wireless unit 535. Each probe antenna is positioned at the angle of a radio link of a model radio system. The performance of a wireless unit in a radio system is therefore modeled by a number of probe antennas that is equivalent to the number of angles of arrival in the radio system model and based on the principle that the consolidated angle of arrival is the average of the angel of arrival for a number of sub-paths. The azimuth and elevation positions of the antennas are changed for different instances of wireless devices, reflectors, and transceiver antenna locations. This approach requires fewer probe antennas, and in some embodiment comparisons, far fewer probe antennas than in prior art radio system models in which the prone antennas are at fixed equidistant positions at regular angular intervals, such as the embodiment described with reference to FIG. 3.

[0027] In some embodiments the probe antennas 505, 510, 515, 520, 525, 530 are movably attached to a rail having the form of an arc of a sphere that is rotatably attached to a base 540 at point 580. The rails in FIGS. 5 and 6 are illustrated as being approximately 180 degree arcs capable of providing an elevation range close to 180 degrees. In other embodiments, if the radio systems being modeled do not require a full range of elevation angles, the arc shaped rails 550, 555, 560, 565, 570, 575 can be shortened at both ends and be designed to move in a circular path on the base 540, in which case the base would be raised closer to the test position). The range of elevation and azimuth angles needed may be determined by tests defined in one or more radio testing standards, or may be determined by a specific set of variations of geometry of a radio system being modeled. When a two dimensional channel model is emulated, the antenna probes 505, 510, 515, 520, 552, 530 are typically placed at the elevation of 90 degrees. In some embodiments the probe antennas and the wireless unit are within an anechoic chamber. In some embodiments, the

probe antennas are dual polarized horn antennas. The use of fewer probe antennas has benefits of reducing cost of emulations because each probe antenna may, for example be driven by a dedicated amplifier. In comparison, when many fixed probe antennas are used, either a larger number of dedicated complex amplifiers are needed and/or high quality radio frequency switches are used, which costs substantially. Also, the distance of the probe antennas from the wireless unit must be larger to prevent antenna coupling, which also increases costs.

[0028] The embodiment described here uses six probe antennas for six consolidated radio links. In embodiments used for some standardized testing, complex environments such as urban microcells are modeled as having six main propagation paths from the transceiver to the wireless unit. This number of propagation paths is deemed sufficiently diverse to provide a realistic model without using more paths. The six probe antenna embodiment described with reference to **FIGS 5** and **6** would be sufficient for these 6 path models. The number of probes used for this unique approach of using a set of probe antennas wherein each probe antenna is positioned at an angle of arrival of a radio link can be increased or decreased as needed for other radio system models. Other means of positioning the probe antennas could be used. For example, rails that are straight vertical rails could be used, as long as the probe antennas are able to be directed at the wireless unit 535. The test signals would have to be compensated for the differing distances of the probe antennas, and for embodiments in which an anechoic chamber is used, the chamber would have to be large enough to accommodate rails that are tall enough to achieve a desired range of elevation angles. The size of the chamber would have to allow for reduction of antennas coupling to acceptable levels. A free space arrangement may avoid the use of an anechoic chamber, as long as the strength of interference signals and reflections off of the nearest ground plane and other reflectors are sufficiently small.

[0029] It will be appreciated that the technique of radio system modeling described above with reference to **FIGS. 1-2**, **4-6** can be used for purposes other than comparative testing of wireless units operating in a radio system. For

example, the technique could be used to optimize the locations of a transmitter and receiver in a fixed environment, by making measurements of performance of the receiver when the angles of arrival are determined for various relative positions of the transmitter and receiver with the fixed environment. An example is the placement of a transmitter and receiver in an environment for which the position and orientation of the reflecting surfaces is known, and the number of such reflecting surfaces (and therefore, the number of probe antennas) is a cost effective approach. Another example is the placement of a transmitter and receiver in an environment to optimize a given location or range of known locations for a wireless unit.

[0030] Referring to **FIG. 7,** a flow chart 700 of some steps of a method for modeling a radio system is shown, in accordance with certain embodiments. At step 705, a set of optimized angles of arrival for a corresponding set of radio links is obtained. The set of radio links model a radio environment of a wireless unit operating at a particular location within in a radio system. In some embodiments, the location is a location of a drop that may be used for performance comparison of wireless units. In some embodiments, the location is a relative location of the wireless unit with reference to the transmitting antenna in a system model used for optimizing relative locations of the wireless unit and the transmitter antenna. In some embodiments the location is a relative location of the wireless unit relative to a system in a system model used to optimize the location of the wireless unit. Other uses may be made of a system model having a wireless unit at a location, such as optimizing the design of the wireless unit. The radio links represent different propagation paths between the wireless unit and another transceiver operating within the radio system. Each optimized angle of arrival represents an angle of arrival of one radio link with reference to the wireless unit. At step 710 a corresponding set of probe antennas is positioned. Each probe antenna is positioned at a corresponding one of the set of optimized angles of arrival. At step 715 a corresponding set of probe radio signals is transmitted from the set of probe antennas. In some embodiments, the optimized angles of arrival may include sub-paths. In those embodiments the optimized angles of arrival are derived from the sub-paths. Otherwise, each angle of arrival is the optimized angle of arrival.

[0031] Referring to **FIG. 8,** a flow chart 800 of some steps of a method for modeling a radio system is shown, in accordance with certain embodiments. At step 805 wireless a wireless unit under test is positioned as a test position within an anechoic chamber. At step 810, a set of optimized angles of arrival for a particular drop is obtained. A channel model of a radio system that includes a wireless unit and a transceiver that transmits radio signals to the wireless unit is used to determine the angles of arrival. At step 815, a corresponding set of probe antennas are positioned within the anechoic chamber. Each probe antenna is positioned at one of the set of optimized angles of arrival. At step 820, a test is performed using a corresponding set of probe radio signals that is transmitted from the set of probe antennas. Each probe radio signal is a modified form of one selected test signal. Each modification is defined by the channel model.

[0032] Referring to **FIG. 9,** a flow chart 900 of one step of a method for modeling a radio system is shown, in accordance with certain embodiments. The method may be one of the methods described with reference to **FIGS. 7** and **8**. At step 905, the optimized angle of arrival of each radio link referred to in step 705 (**FIG. 7**) and step 810 (**FIG. 8**) is derived from one of a mathematical model and a channel model.

[0033] Referring to **FIG. 10,** a flow chart 1000 of one step of a method for modeling a radio system is shown, in accordance with certain embodiments. The method may be one of the methods described with reference to **FIGS. 7** and **8**. At step 1005, each radio signal is generated by modifying the signal characteristics of a test radio signal, wherein the modification is derived from a channel model. The channel model establishes propagation parameters associated with the radio link for a particular location, or drop, of the wireless unit.

[0034] Referring to **FIG. 11** a flow chart 1100 of one step of a method for modeling a radio system is shown, in accordance with certain embodiments. The method may be one of the methods described with reference to **FIGS. 7** and **8**. At step 1105, the optimized angle of arrival of a radio link is derived from angles of arrival of one or more sub-paths in a cluster of sub-paths of the radio link, wherein each sub-path has an angle of arrival with reference to the wireless device.

[0035] In this document, relational terms such as first and second, top and bottom, and the like may be used solely to distinguish one entity or action from another entity or action without necessarily requiring or implying any actual such relationship or order between such entities or actions. The terms "comprises," "comprising," or any other variation thereof, are intended to cover a non-exclusive inclusion, such that a process, method, article, or apparatus that comprises a list of elements does not include only those elements but may include other elements not expressly listed or inherent to such process, method, article, or apparatus. An element proceeded by “comprises …a” does not, without more constraints, preclude the existence of additional identical elements in the process, method, article, or apparatus that comprises the element.

[0036] In the foregoing specification, specific embodiments of the present invention have been described. However, one of ordinary skill in the art appreciates that various modifications and changes can be made without departing from the scope of the present invention as set forth in the claims below. Accordingly, the specification and figures are to be regarded in an illustrative rather than a restrictive sense, and all such modifications are intended to be included within the scope of present invention. The benefits, advantages, solutions to problems, and any element(s) that may cause any benefit, advantage, or solution to occur or become more pronounced are not to be construed as a critical, required, or essential features or elements of any or all the claims. The invention is defined solely by the appended claims including any amendments made during the pendency of this application and all equivalents of those claims as issued.

[0037] The Abstract of the Disclosure is provided to allow the reader to quickly ascertain the nature of the technical disclosure. It is submitted with the understanding that it will not be used to interpret or limit the scope or meaning of the claims. In addition, in the foregoing Detailed Description, it can be seen that various features are grouped together in a single embodiment for the purpose of streamlining the disclosure. This method of disclosure is not to be interpreted as reflecting an intention that the claimed embodiments require more features than are expressly recited in each claim. Rather, as the following claims reflect,

inventive subject matter lies in less than all features of a single disclosed embodiment. Thus the following claims are hereby incorporated into the Detailed Description, with each claim standing on its own as a separately claimed subject matter.

What is claimed is:

1. A method, comprising:

obtaining a set of optimized angles of arrival for a corresponding set of radio links, wherein the set of radio links model a radio environment of a wireless unit operating at a particular location within in a radio system, and each radio link represents a different propagation path between the wireless unit and a transmitting antenna operating within the radio system, and wherein each optimized angle of arrival represents an angle of arrival of one radio link with reference to the wireless unit;

positioning a corresponding set of probe antennas, each probe antenna being positioned at a corresponding one of the set of optimized angles of arrival; and

transmitting a corresponding set of probe radio signals from the set of probe antennas.

2. The method according to claim 1, further comprising determining the optimized angle of arrival of each link by one of a mathematical model of a radio system and a channel model of a radio system.

3. The method according to claim 2, wherein the channel model of a radio system is a channel model required by a radio system operator for use in wireless unit testing.

4. The method according to claim 2, wherein the channel model is defined by a standard issued by one of 3GPP, WINNER, and CTIA.

5. The method according to claim 1, further comprising generating each probe radio signal by modifying the signal characteristics of a test signal, wherein the modification is derived from a channel model.

6. The method according to claim 1, wherein the wireless unit and the probe antennas are positioned within an anechoic chamber.

7. The method according to claim 1, further comprising deriving each optimized angle of arrival from angles of arrival of one or more sub-paths in a cluster of sub-paths of a radio link.

8. A method, comprising:

positioning a wireless unit under test at a test position within an anechoic chamber;

obtaining a set of optimized angles of arrival for a particular drop that is determined by a channel model of a radio system that includes a wireless unit and a transceiver that transmits radio signals to the wireless unit;

positioning a corresponding set of probe antennas within the anechoic chamber, each probe antenna being positioned at one of the set of optimized angles of arrival; and

performing a test using a corresponding set of probe radio signals transmitted from the set of probe antennas, wherein each probe radio signal is a modified form of a test signal, and wherein each modification is determined using the channel model.

9. The method according to claim 8, wherein the channel model of a radio system is a channel model required by a radio system operator for use in wireless unit testing.

10. The method according to claim 8, wherein the channel model is defined by a standard issued by one of 3GPP, WINNER, and CTIA.

11. The method according to claim 8, further comprising deriving an optimized angle of arrival from angles of arrival of one or more sub-paths in a cluster of sub-paths of a radio link.

.

12. An apparatus, comprising:

an anechoic chamber;

a test position for a wireless unit under test; and

a set of probe positioning devices, each probe positioning device capable of positioning one probe antenna over a range of azimuth angles and a range of elevation angles,

wherein each antenna probe of the set of probe positioning devices is set at a different one of a set of optimized angles of arrival that correspond to one set of radio links, wherein the set of optimized AoAs have been generated by a model that simulates the wireless unit under test operating in a radio system, and wherein the radio links are links representing different propagation paths between the wireless unit under test and another transceiver operating within the radio system, and wherein each optimized AoA is an angle determined by the model to optimally represent an AoA of one link with reference to the wireless unit under test.

13. The apparatus according to claim 12, wherein the range of azimuth angle and the range of elevation angles are determined from at least one radio testing standard, a geometric model of a radio system, +- 180 degrees of azimuth, and +- 180 degrees of elevation.

14. The apparatus according to claim 12, further comprising determining the optimized angle of arrival of each radio link by one of a mathematical model and a channel model.

15. The apparatus according to claim 12, further comprising a set of signal generators, each of which that generates a probe radio by modifying the signal characteristics of a test signal, wherein the modification is derived from one of a mathematical model and a channel model.

16. The apparatus according to claim 15, wherein the channel model of a radio system is a channel model required by a radio system operator for use in wireless unit testing.

17. The apparatus according to claim 15, wherein the channel model is defined by a standard issued by one of 3GPP, WINNER, and CTIA.

18. The apparatus according to claim 12, further comprising deriving each optimized angle of arrival from angles of arrival of one or more sub-paths in a cluster of sub-paths of a radio link.

Abstract of the Disclosure

A method (700, 800) and apparatus (500) for obtaining a set of optimized angles of arrival for a corresponding set of radio links (127-128, 132-133, 137-138, 142-143, 147-148, 152-153). The set of radio links model a radio environment of a wireless unit (110) operating at a particular location (111, 112, 113) within in a radio system (100). Each radio link represents a different propagation path between the wireless unit and another transmitting antenna (107) operating within the radio system. Each optimized angle of arrival represents an angle of arrival of one radio link with reference to the wireless unit. Each probe antenna of a set of probe antennas (505, 510, 515, 520, 525, 530) is positioned at a corresponding one of the set of optimized angles of arrival. A corresponding set of probe radio signals is transmitted from the set of probe antennas.

_____.

Paper 9

Measurement Uncertainty Investigation in the Multi-probe OTA Setups

Wei Fan, Istvan Szini, Michael Foegelle, Jesper Nielsen and Gert Pedersen

Accepted for publication in:
8th European Conference on Antennas and Propagation (EuCAP), April 2014

Measurement Uncertainty Investigation in the Multi-probe OTA Setups

Wei Fan[1], Istvan Szini[1,2], Michael D. Foegelle[3], Jesper Ø. Nielsen[1], and Gert F. Pedersen[1]
[1]Department of Electronic Systems, Faculty of Engineering and Science, Aalborg University, Aalborg, Denmark
[wfa, ijs, jni, gfp]@es.aau.dk
[2]Motorola Mobility Inc., Libertyville, USA
Istvan.Szini@motorola.com
[3]ETS-Lindgren, 1301 Arrow Point Drive, Cedar Park, USA
Email: michael.foegelle@ets-lindgren.com

***Abstract*—Extensive efforts are underway to standardize over the air (OTA) testing of the multiple input multiple output (MIMO) capable terminals in COST IC1004, 3GPP RAN4 and CTIA. Due to the ability to reproduce realistic radio propagation environments inside the anechoic chamber and evaluate end user metrics in real world scenarios, the multi-probe based method has attracted huge interest from both industry and academia. This contribution attempts to identify some of the measurement uncertainties of the practical multi-probe setups and provide some guidance to establish the multi-probe anechoic chamber setup. This contribution presents the results of uncertainty measurements carried out in three practical multi-probe setups. Some sources of measurement errors, i.e. cable effect, cable termination, etc. are identified based on the measurement results.**

***Index Terms*—MIMO OTA, multi-probe, anechoic chamber, measurement uncertainty, plane wave synthesis**

I. Introduction

Over the air (OTA) testing of MIMO capable terminals has attracted huge attention from both industry and academia [1], where a multi-probe anechoic chamber based method is a promising candidate. Various contributions have addressed issues related to OTA testing of MIMO capable terminals in a multi-probe anechoic chamber, i.e. channel modeling [2]–[4], validation of the implemented channel models [5], [6], end user metrics evaluation [7].

As a mandatory step for standardization, it is required to analyze the sources of errors and uncertainties in the measurements. Very few contributions have addressed the measurement uncertainties in a multi-probe OTA system. In [8], uncertainty analysis in total radiated power (TRP) and total isotropic sensitivity (TRS) is specified. However, the measurement uncertainty analysis defined for OTA testing of single antenna terminals will be not sufficient for the MIMO OTA testing, as the testing system, which includes one or several channel emulators, is more complicated. Furthermore, different figure of merits (FoMs) will be adopted for MIMO OTA testing. In [9], several sources of uncertainties and errors were listed and classified for the multi-probe setup. In recent 3GPP RAN4 meetings, measurement uncertainty evaluation of the multi-probe method has been discussed [10]. In [6], plane wave synthesis (PWS) in a practical setup was investigated and possible reasons for the deviations were briefed. In [11], measurement verification results of two channel emulation techniques, namely PWS and prefaded signal synthesis (PFS) in a practical multi-probe anechoic chamber setup were presented. Possible factors that introduce the measurements inaccuracies were discussed as well. Some deviations existed in the results and the exact causes were missing.

This paper attempts to compare and understand measurement uncertainty levels with different labs, i.e. at Aalborg university (AAU), Denmark, Motorola Mobility (MM), USA and ETS-Lindgren (ETS), USA., thus to show key aspects related to the multi-probe system setup design. Main contributions of this work are:

- Uncertainty measurements in three different practical multi-probe setups are presented. The sources of the errors that exist in the previous contributions are identified.
- Measurement results of the field synthesis for horizontal polarization are reported for the first time in the literature.

II. Multi-probe anechoic chamber setups and testing items

Figure 1 shows a simplified version of the multi-probe setup for testing a device under test (DUT). The DUT is placed on a pedestal in an anechoic chamber and surrounded by multiple probes mounted on an OTA ring. The probes are uniformly distributed located on a horizontally orientated ring with equal spacing in all the setups. The specifications of the three setups are detailed in Table I.

The main testing items of the measurement uncertainty investigations are detailed below:

a) Dipole radiation pattern measurements: The basic idea is to measure the radiation pattern of a calibration dipole which is located at the test area center. Ideally, the measured complex pattern should be constant over orientations. However, due to the system no-idealities, e.g. cable effect, dipole placement, etc. maximum gain and phase variations are up to 2dB and 10 degrees at 900MHz, and up to 1dB and 20 degrees at 2450MHz [11].

b) Turntable stability: The turntable that supports the DUT is not completely static shortly after the turntable rotating and linear sliding. As reported in the turntable stability measurement in the AAU setup in [11], the rotational movement

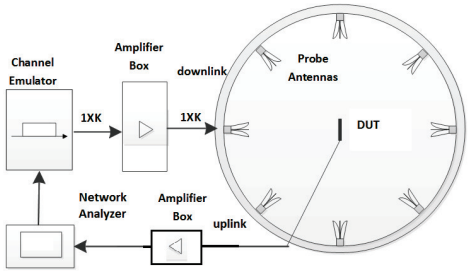

Figure 1. An illustration of the multi-probe based MIMO OTA setup. The main components are a vector network analyzer (VNA) or base station emulator (BSE), one or several radio channel emulators, an anechoic chamber, OTA probe antennas, power amplifiers (PAs) and a DUT.

Table I
SETUP SPECIFICATIONS

	AAU	MM	ETS
Chamber size	10m x 10m x 7m	3m x 3m x 2.4m	4.9m x 4.9m x 3.7m
OTA ring size	An aluminum ring with radius $R = 2$ meters. The ring is partially covered by absorbers, as shown in Fig. 2(a)	Radius $R = 1.2$ meters. Wood masts have been used to support and fix the horn antennas, as shown in Fig. 2(b)	A ring with radius $R = 2$ meters. The ring is fully covered by absorbers. The probes are loaded with absorbers, as shown in Fig. 2(c)
OTA probe	16 dual polarized horn antenna designed by AAU [12], as shown in Fig. 3(a)	8 dual polarized horn antenna designed by AAU, as shown in Fig. 2(b)	16 dual polarized Vivaldi antenna designed by ETS, as shown in Fig. 3(b)
Turntable	Polystyrene placed on top of the turntable to support the DUT, as shown in Fig. 4(a)	As shown in Fig. 4(b)	As shown in Fig. 4(c)
Channel emulator used	Two Anite Propsim F8s	Anite Propsim F16	Anite Propsim FS8 and Spirent VR5
Turntable movement	Rotational and linear slide combined movement supported	Rotational movement supported only	Rotational and linear slide combined movement supported
Cable to DUT	Cable directly connected to DUT	Choke and cartridge at various frequency bands used	Ferrite loaded cable used, as shown in Fig. 4(c)

is stable, while the linear slide movement is not stable and 20s of settling time is required. In the MM setup, the linear slide movement is not supported. In the ETS setup, both movements are supported. The turntable movement in the MM and ETS setups are stable.

c) Channel emulator stability: Signal drifting level of the channel emulator over short term and long term is investigated. Measurements showed that the signal drifting level of different channel emulators over long term and short term is negligible, and the results are not detailed in the paper.

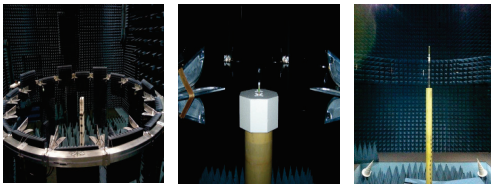

(a) OTA ring at AAU (b) Chamber at MM (c) Chamber at ETS

Figure 2. Anechoic chamber in three setups

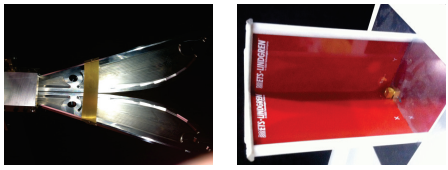

(a) Horn antenna (b) Vivaldi antenna

Figure 3. Probe antennas used in AAU/MM (left) and ETS (right).

d) System frequency flatness: Frequency flatness level is investigated in the three setups. Unflat frequency response of the OTA system can be introduced by the channel emulator, termination of the cables (probe antenna) and mismatch between the components.

e) Power Coupling between probes: Power coupling level between probes for both polarizations is investigated in the three setups. Power coupling levels between probes and between polarizations are investigated.

f) Reflection inside the chamber: The reflection level in the three setups is investigated.

g) Plane wave synthesis : Verification results of the PWS technique for vertical polarization with the AAU setup were reported in [6], [11]. In this contribution, better results are achieved with MM and ETS setups as the cable effect and turntable stability issues were addressed. Also, measurement results of the PWS for horizontal polarization are presented.

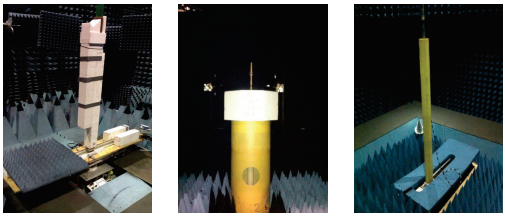

(a) Turntable at AAU (b) Turntable at MM (c) Turntable at ETS

Figure 4. Turntable in different setups

III. Measurement Results and Discussion

A. Dipole radiation pattern measurements

In [11], it is concluded that the inaccurate results of radiation pattern measurements are probably caused by cable effect or dipole placement error. The position of the calibration dipoles are carefully calibrated with the laser positioner in the three setups. In the MM setup, the cartridges and chokes for various frequency bands are used to connect to the DUT. In the ETS setup, a Ferrite loaded cable is used. Measurement results in the MM and ETS setup are shown in Figure 5 and Figure 6, respectively. Note that the gain patterns are not normalized. Measurements performed in the MM setup were without the channel emulator. The measured gain and phase pattern variation of a calibration dipole are negligible. The gain and phase pattern is quite omnidirectional, as expected. The main reason for the small variation is due to the fact that the dipole is not located in the rotation center (with an offset of around 5mm), as the phase variation follows a sinusoid curve. Measurement result in the ETS setup is shown in Figure 6. The dipole is rotated every 1^o and for every orientation 31 points separated with 1cm are sampled over the test area. The complex radiation pattern results are extracted from the measurements (samples with $r = 0$cm). The gain and phase variation, though rather small, is mainly caused by the position accuracy of the dipole. To sum up, cable effect can be minimized by use of choke and cartridge, or Ferrite loaded cable.

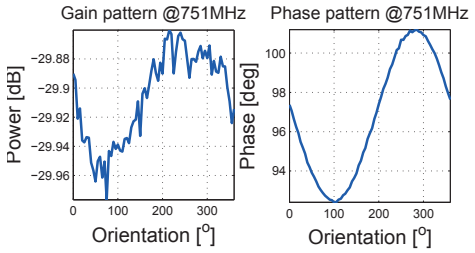

Figure 5. Gain pattern (left) and phase pattern (right) measurement results in MM setup.

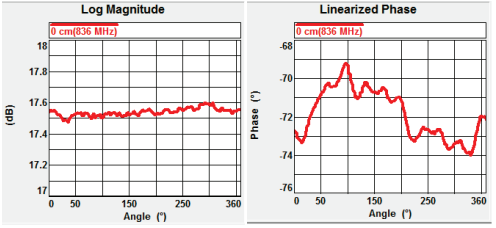

Figure 6. Gain pattern (left) and phase pattern (right) measurement results in ETS setup.

B. Ripples over frequency

In the previous measurements in the AAU setup [13], we investigated the impact of power variation over frequency on spatial correlation. Due to the nonidealities of the channel emulators, the power values are not constant over the LTE band. Also, the cable reflection can cause ripples over frequency band. To show the impact of cable reflection, a measurement was planned in the MM setup. In the first measurement, we measured the S21 of the OTA system (without the channel emulator) with one probe active and the rest terminated with 50Ω loads. In the second measurement, we performed the same measurement with the active probe and the rest non-terminated. The result is shown in Figure 7, where failure to terminate is seen to cause large ripples. The small ripples over frequency with cable terminated might be due to the cable frequency response or the mismatch between components. To investigate the mismatch between components, an additional PA of 20dB and an attenuator of 20dB were added into the system in the measurement in the ETS setup. The ripples caused by mismatch between components are up to around 0.5dB from 600MHz to 7 GHz in the ETS setup.

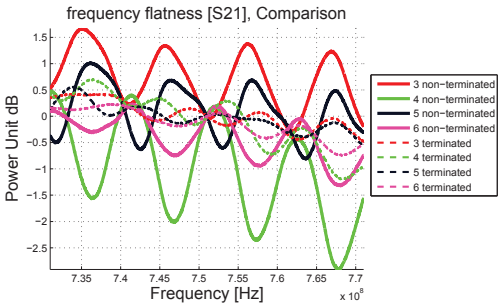

Figure 7. Frequency flatness over 40MHz measured in the MM setup. The number in the legend indicates the active horn index.

C. Power Coupling between probes

Scattering within a multi-probe setup and its impact on measurement uncertainty is investigated in [14]. It is demonstrated that the power coupling level needs to be controlled. In the previous power coupling measurements reported in [6], the cable frequency response and the PA frequency response are not compensated. Different probe antennas are investigated for the OTA systems, e.g. the horn antenna in the AAU and the MM setup, the dual-polarized Vivaldi antenna implemented in a cross form in the ETS setup. The power coupling results in the ETS setup (with cable and PA compensated) are shown in Figure 8 for the vertical polarization. The OTA probe located on the boresight direction of transmitting probe presents the maximum coupling at high frequency. The higher the frequency is, the more directive the Vivaldi antenna becomes. The power coupling will have negligible impact on the synthesized field structure.

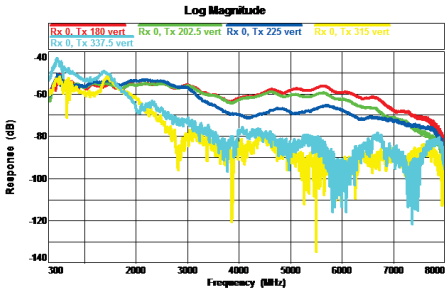

Figure 8. Power coupling between probes for the vertical polarization in the ETS setup. The value in the legend indicates the angular location of the probes.

D. Reflection inside the chamber

Measurement procedure of the reflection study was detailed in [6]. A wideband horn antenna is located in the middle of the test zone and measurements are performed in frequency domain. The frequency domain data is transformed by an inverse FFT to yield a time domain signals. Same reflection measurements were repeated in the MM and ETS setup, and no big reflections were identified in the results. To investigate the impact of a intentional reflector on the results. A metallic plate was placed in the chamber in the ETS setup. The result with an intentional reflector is shown in Figure 9. The reflection level is low as the reflector was not placed in the main lobe direction of the receive horn antenna.

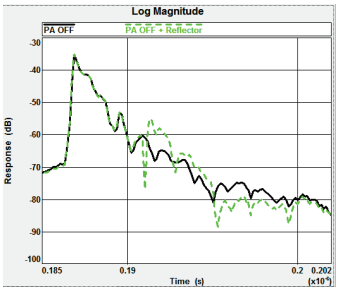

Figure 9. Reflections with/without intentional reflector inside the chamber. Rx antenna: horn

E. Plane wave synthesis

1) Target scenarios and measurement setup: In the previous PWS measurements in the AAU setup, although good agreement was achieved between the measurement and target plane wave (PW), the inaccuracy due to the cable effects, as discussed in Section III-A, was embedded in the results. In the MM setup, as linear slide movement was not supported, the DUT was offset manually with specified radius, as detailed in Table II. Vertically and horizontally polarized static PW with different angle of arrivals (AoAs) are selected as the target scenarios.

Table II
PWS MEASUREMENT DETAILS

	MM	ETS
Target scenario	A. Vertically polarized PW with AoA = 0^o	
	B. Vertically polarized PW with AoA = 22.5^o	
	C. Horizontally polarized PW with AoA = 0^o	
	D. Horizontally polarized PW with AoA = 22.5^o	
Rx antenna	Calibration dipole/magnetic loop at 751MHz	Calibration dipole/magnetic loop at 836MHz
Active OTA probes	8 OTA probes are equally spaced and fixed on the OTA ring	
Rx positions	the linear slide is rotated every 5^o with specified offsets to the rotation center ((0cm, 0.25λ, 0.35λ, 0.5λ)	the linear slide is rotated every 1^o and 31 points separated with 1cm are sampled for every orientation.

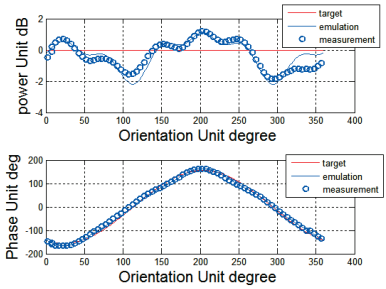

Figure 10. Comparison between the measurement, emulation and target for the power (up) and phase (down) in the MM setup for scenario B.

2) Results: An example of the measurements in the MM setup is shown in Figure 10. The measured power is normalized to its mean and the simulated phase curve is shifted to match the measured phase. The deviation between the target and emulation is due to the fact that only limited probes are used. Very good match is achieved between the measurement and emulation.

Results of the PWS measurements performed in the ETS setup are shown from Figure 11 to Figure 14. Overviews of the measured power and phase distribution over the test area for the target scenario A, B, C and D are shown in Figure 11, Figure 12, Figure 13, Figure 14 respectively. Ideally, uniform power and linear phase distribution along propagation direction are expected inside the test area. The measurement generally match with the target very well. The test area performance depends on the target channel models. As a summary, good agreement can be obtained between the measured PW and the target PW both for the vertical and horizontal polarizations.

IV. CONCLUSION

In this contribution, we presented the uncertainty measurements performed in three different multi-probe setups. Main findings of the work are:

- Cable effect will distort the radiation pattern of the DUT and hence affect the results of the measurements. By use

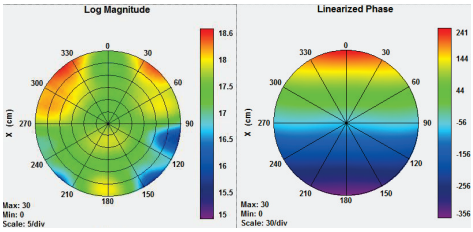

Figure 11. Measured power (left) and phase (right) distribution over test area for the target scenario A.

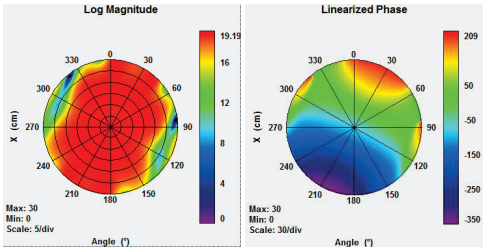

Figure 12. Measured power (left) and phase (right) distribution over test area for the target scenario B.

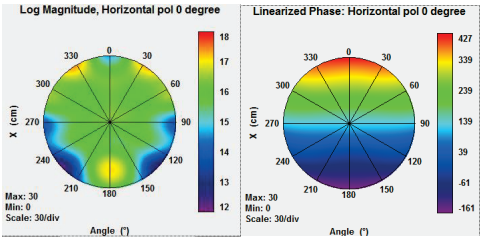

Figure 13. Measured power (left) and phase (right) distribution over test area for the target scenario C.

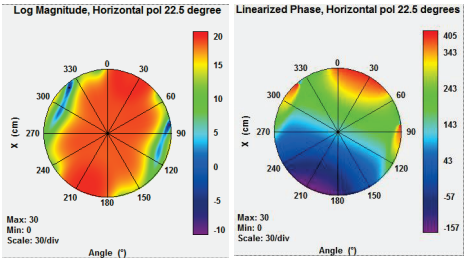

Figure 14. Measured power (left) and phase (right) distribution over test area for the target scenario D.

of a choke/cartridge or Ferrite loaded cable, the cable effect can be minimized. Field synthesis measurements demonstrated the improved results with chokes/cartridges and Ferrite loaded cables.

- Polystyrene that used to support the DUT in the AAU setup introduces instability after movement. Turntables used in the MM and ETS setup are more stable.
- Unflat frequency response of the OTA system can be introduced by the channel emulator, termination of the cables (probe antenna) and mismatch between the components.
- Good agreement between the measured plane wave and the target plane wave both for the vertical and horizontal polarizations is obtained in the MM and ETS setup.

ACKNOWLEDGMENT

This work is supported by the COST IC1004 STSM grant.

REFERENCES

[1] M. Rumney, R. Pirkl, M. H. Landmann, and D. A. Sanchez-Hernandez, "MIMO Over-The-Air Research, Development, and Testing," *International Journal of Antennas and Propagation*, vol. 2012, 2012.

[2] P. Kyösti, T. Jämsä, and J. Nuutinen, "Channel modelling for multiprobe over-the-air MIMO testing," *International Journal of Antennas and Propagation*, 2012.

[3] W. Fan, F. Sun, P. Kyosti, J. Nielsen, X. Carreno, M. Knudsen, and G. Pedersen, "3D channel emulation in multi-probe setup," *Electronics Letters*, vol. 49, no. 9, pp. 623–625, 2013.

[4] W. Fan, X. de Lisbona, F. Sun, J. Nielsen, M. Knudsen, and G. Pedersen, "Emulating Spatial Characteristics of MIMO Channels for OTA Testing," *Antennas and Propagation, IEEE Transactions on*, vol. 61, no. 8, pp. 4306–4314, 2013.

[5] W. Fan, X. Carreño, J. Ø. Nielsen, M. B. Knudsen, and G. F. Pedersen, "Channel Verification Results for the SCME models in a Multi-Probe Based MIMO OTA Setup," in *Vehicular Technology Conference (VTC Fall), 2013 IEEE*. IEEE, 2013, pp. 1–5.

[6] W. Fan, X. Carreño, J. Ø. Nielsen, K. Olesen, M. B. Knudsen, and G. F. Pedersen, "Measurement Verification of Plane Wave Synthesis Technique Based on Multi-probe MIMO-OTA Setup," in *Vehicular Technology Conference (VTC Fall), 2012 IEEE*. IEEE, 2012, pp. 1–5.

[7] X. Carreno, W. Fan, J. O. Nielsen, J. S. Ashta, G. F. Pedersen, and M. B. Knudsen, "Test setup for anechoic room based MIMO OTA testing of LTE terminals," in *Antennas and Propagation (EuCAP), 2013 7th European Conference on*, 2013, pp. 1417–1420.

[8] CTIA, "Test plan for mobile station over the air performance," *CTIA Wireless Association*, 2012.

[9] R4-126702, "Errors and Uncertainties in the MIMO OTA measurements," 2012.

[10] R4-131673, "Measurement uncertainty evaluation of multiprobe method," 2013.

[11] W. Fan, , X. Carreño, J. O. Nielsen, M. B. Knudsen, and G. F. Pedersen, "Verification of Emulated Channels in Multi-Probe Based MIMO OTA Testing Setup," in *Antennas and Propagation (EUCAP), Proceedings of the 7th European Conference on*. IEEE, 2013.

[12] O. Franek and G. F. Pedersen, "Spherical horn array for wideband propagation measurements," *Antennas and Propagation, IEEE Transactions on*, vol. 59, no. 7, pp. 2654–2660, 2011.

[13] W. Fan, J. Nielsen, X. Carreno, J. Ashta, G. Pedersen, and M. Knudsen, "Impact of system non-idealities on spatial correlation emulation in a multi-probe based mimo ota setup," in *Antennas and Propagation (EuCAP), 2013 7th European Conference on*, 2013, pp. 1663–1667.

[14] P. Hallbjorner, "Measurement uncertainty in multipath simulators due to scattering within the antenna array - theoretical model based on mutual coupling," *Antennas and Wireless Propagation Letters, IEEE*, vol. 9, pp. 1103–1106, 2010.

Paper 10

Beam-Steered Adaptive Antenna System for MIMO OTA Test Methodology Validation

Istvan Szini, Alexandru Tatomirescu, Anatoliy Ioffe, Boyan Yanakiev and Gert Pedersen

To be submitted in:
IEEE Transaction on Antenna and Propagation, March 2014

Beam-Steered Adaptive Antenna System for MIMO OTA Test Methodology Validation

Istvan Szini*, Alexandru Tatomirescu*, Anatoliy Ioffe, Boyan Yanakiev, and Gert Frølund Pedersen,
I. Szini, A. Tatomirescu (*shared first authors) and G. F. Pedersen are with the
Antennas, Propagation and Radio Networking section at the Department of Electronic Systems,
Faculty of Engineering and Science, Aalborg University, Denmark; email: {ata; ijs; gfp}@es.aau.dk.
I. Szini is with Motorola Mobility Inc., Libertyville, USA; email: Istvan.Szini@motorola.com.
A. Ioffe and B. Yanakiev and are with Intel Corporation, anatoliy.ioffe@intel.com and boyan.yanakiev@intel.com.

I. Introduction

OVER the past years, MIMO antennas have been the focus of the antenna research community. The most important feature being the linear increase in channel capacity with the number of antennas by using the uniqueness of the wireless channel in ideally rich scattering scenarios [1]–[3]. In practice the capacity improvement is dictated by the power difference and correlation of the signals in each link [4], [5].

The advantages of beam-forming in mobile communication have been proven and accepted by the community as viable solution at the base-station side. It has been discussed also for the use in MIMO scenarios and their advantages have been illustrated in [6]. As a matter a fact, the concept of smart antennas has captured the attention of researchers also in the past. However, with the recent technical advances in tuneable technologies it becomes feasible to have beam steering also on the mobile side [7]. As shown in numerous measurement campaigns, the wireless channel is directive for the duration of a packet transmission, with certain angular properties that vary from scenario to scenario [8]–[10], as used also in the standardization forums [11]. Therefore, the motivation of having antennas with steerable beams that are able to track the changes in the angular proprieties of the channel is fueled by the desire to increase the robustness of the radio link. For future communications systems (5G) this feature becomes desirable because of the high frequency of operation [12] and the inherent propagation losses.

In this paper, a MIMO antenna system for a mobile device is proposed. One of the antennas is an active antenna that can switch between four beams that cover the whole azimuth plane. The antenna will be described in the following section.

II. Proposed antenna design

For manufacturing proposes, the LTE band 7 has been chosen to illustrate, the concept although the concept can be scaled to other frequencies. The PCB size has been chosen for the ease of future measurement including external modems, in accordance to the reference antennas used in the MIMO OTA measurement campaigns [13]. At this operating frequency, the contribution to radiation from the extended ground plane is negligible therefore the conclusions remain valid also for a more realistic ground plane size.

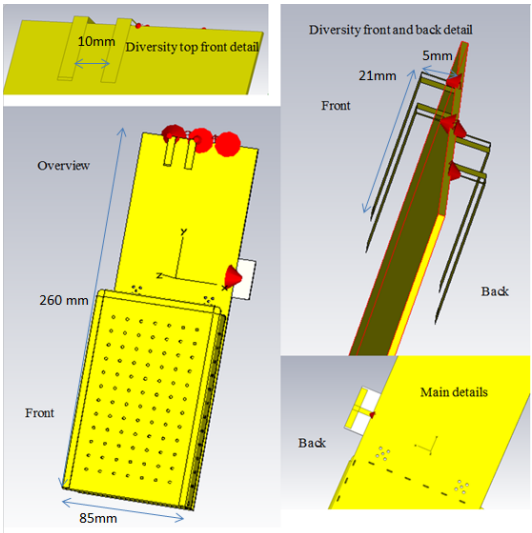

Fig. 1. The numerical model of the proposed antenna.

Simple PIFA's are used as the element of the array corresponding to the active element(diversity element). The four PIFA's are placed on each side of the PCB, two by two as illustrated in Fig. 1. Each pair of elements are fed trough a 90 degree hybrid coupler so that at each of inputs a gain pattern that covers a quarter of the azimuth space is formed, as shown in Fig. 2. The different patterns are controlled by an SP4T RF switch (HMC241LP3) which is actuated through 2 DC switches, as shown in Fig. 4. The main antenna is a top loaded monopole on the side of the PCB with the simulated gain pattern shown in Fig. 3.

III. Simulation Results

A. Simplistic Average Isotropic Assumption

The assumption of the average isotropic environment is that on the average the incoming power is equally probable

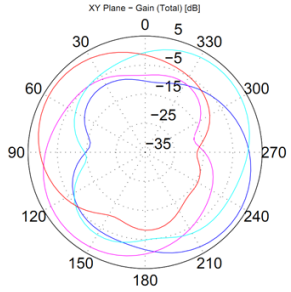

Fig. 2. Simulated Azimuth cut of the secondary antenna gain patterns.

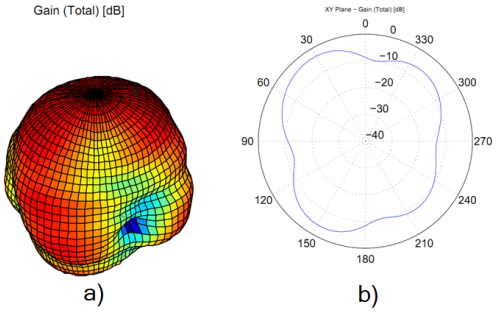

Fig. 3. Simulated Gain Patterns. a) Main antenna full gain pattern; b) Azimuth cut of the main antenna gain pattern;

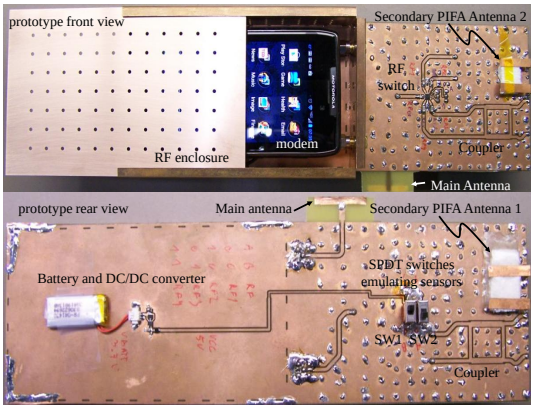

Fig. 4. Illustration of the mock-up with the RF enclosure, hybrid couplers, DC switch and RF switch.

from any direction of three dimensional space. This common assumption provides easy mathematical treatment of most problems but is no more realistic than an ideal isotropic antenna. An isotropic antenna is used extensively by antenna engineers as a theoretical concept but it is also proven theoretically not to be possible in reality. Consider the following reversal of positions we never take the average gain of an antenna and assume that because of the random use in an environment we can ignore the actual directional radiation pattern over the entire spatial domain and use an averaged out version of it. The average isotropic environment is not a realistic propagation environment but a useful mathematical abstraction to define purely antenna metrics such as efficiency for passive and TRP for active case. Therefore the isotropic properties of the antenna from Section II are shown in the Table I.

B. Realistic Environments Based on Measured Propagation Data

A far more interesting is the behavior of this antenna system in a directive environment such as SCME UMi and SCME UMa described in [14] and the environment described in [10], which we will call here AAU. First we focus on the SCME UMi and SCME UMa environments as shown in Fig. 5 and Fig. 6 respectivelly. It can be clearly seen that they are both very spatially selective. Any antenna in such environment would act as a spatial filter, some better than others of course. If we consider the environments in antenna terms we can clearly define a main lobe direction, gain, 3 dB beamwidth and side lobe level. For the UMi case the main lobe direction is around 0 degrees at about 3 dB gain, the 3 dB beamwidth is roughly 90 degrees and finally the side lobe level is about -2.5 dB. For the UMa case the corresponding values are about 60 degrees for direction at about 1 dB gain, roughly 90 degrees beamwidth and -2 dB side lobe level. If we include the cluster from around 140 degrees as part of the main lobe for the SCME UMa case, we have roughly half a hemisphere with most of the power and the other half mostly quiet. In both environments we have over 10 dB from a minimum to a maximum.

Clearly there is an opportunity to exploit these spatial characteristics and use a beam forming antenna to gain additional power. Having these considerations in mind however, it becomes clear that the performance of any antenna system would depend on orientation and only statistical analyses of the said antenna system in the environment, can provide meaningful conclusions. We performed multiple rotations of the AAS presented in Section 2 using the three Euler rotation angles as defined in [15] in the following environments:

- SCME UMi XY plane cut rotation of the AAS in the XY plane (along phi) with 5 degrees step results in 72 samples for all antenna metrics.
- SCME UMi Full 3D rotation of the AAS along all rotation angles with 30 degrees stepping equivalent to multiple 2D cuts in the model results in 864 samples for all antenna metrics.
- SCME UMa XY plane cut - rotation of the AAS in the XY plane (along phi) with 5 degrees step results in 72 samples for all antenna metrics.
- SCME UMi Full 3D rotation of the AAS along all rotation angles with 30 degrees stepping equivalent to multiple 2D cuts in the model results in 864 samples for all antenna metrics.

TABLE I
SIMULATED ISOTROPIC PROPERTIES OF THE ANTENNAS IN THE DIFFERENT DIVERSITY STATES.

Antenna	Eff. [dB]	MEG [dB]	BPR - to main (Isotropic) [dB]	Correlation – to main (Isotropic)
Main	-0.5	-3.5	-	-
Diversity state - RF 1	-2.6	-5.6	2.1	0.0
Diversity state - RF 2	-2.3	-5.3	1.8	0.0
Diversity state - RF 3	-2.5	-5.5	2	0.0
Diversity state - RF 4	-2.7	-5.7	2.2	0.0

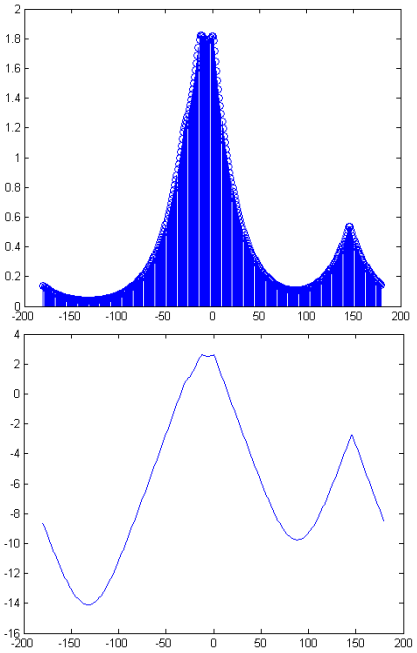

Fig. 5. SCME Uma (top linear and bottom logarithmic, normalized summed total power as a function of azimuth) .

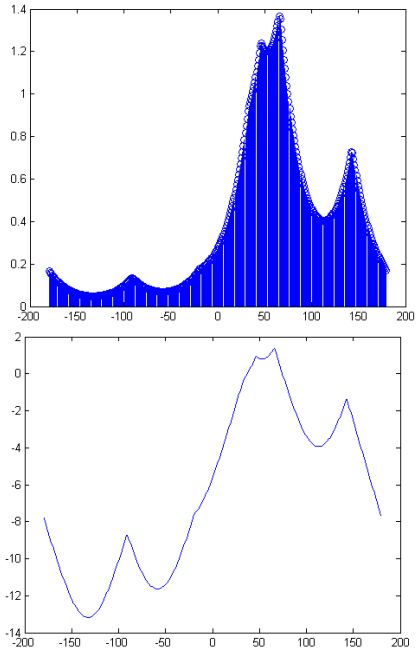

Fig. 6. SCME Uma (top linear and bottom logarithmic, normalized summed total power as a function of azimuth) .

- AAU 2D XY plane - rotation of the AAS in the XY plane (along phi) with 5 degrees step results in 72 samples for all antenna metrics.
- AAU 3D - rotation of the AAS along all rotation angles with 30 degrees stepping. results in 864 samples for all antenna metrics.

The SCME models are 2D models, which means that the environment power is only in the XY plane. Consequently all radiation pattern information in elevation is ignored. The full 3D case is achieved by multiple 2D cuts as the AAS is oriented in the three dimensional space so that various slices of the radiation pattern are evaluated together with the environment. The AAU model is published in [10] and is a full 3D power model based on measurements, much like the SCME models. In the AAU environment a 2D XY plane simply means that the AAS is only rotated in the XY plane around azimuth. Note that the antennas and the environment are still fully three dimensional and all antenna metrics are also fully three dimensional. Full 3D in the AAU environment then, means that the AAS is rotated in all possible Euler angles in the three dimensional space and of course all evaluation is done considering the full spherical radiation pattern and incoming environment power. We have used the environment parameters given in [10]. For all environments the XY plane case can be seen as a statistical sample of the larger population of the corresponding 3D case.

C. Realistic Environments Results

We begin by looking just at the Mean Effective Gain (MEG) of one state of the AAS RF1. MEG is defined in [16] and is an estimate of the power collected by an antenna in a particular propagation environment. One can think of it, and

many antenna engineers do, as the effective antenna efficiency for a particular environment. As shown in Fig. 7 we observe that under realistic conditions the antenna has a large span in the effective collected power. This of course is expected since both the antenna and the environment are directive. When the main beam of the antenna is pointing towards the main power coming from the environment the MEG is maximized and vice versa as the main lobe is directed towards the quiet zone of the environment the MEG is minimized. In all cases there is some 6 to 10 dB of difference. We can further look into the 10, 50 and 90 percent percentiles of the curves see Table II. With isotropic MEG of -5.6 dB for the RF 1 state one might be led to believe that the isotropic environment simply results in the mean of the directive environment since most mean values for the realistic environments are rather close to the isotropic value. Recall however the above consideration that the antenna and the environment both have high and low gain regions. Clearly this results in the span we see inFig. 7 but it also means that the various values are not equally probable. This is already seen by the median trending lower than the mean. A close look at the PDFs reveals precisely that. Figs. 8 to 10 clearly show that the antenna is more likely to receive either power in the lower range (hinted in the lower median value) but also it has a peak towards the high power levels. This precisely what one would expect from an antenna that covers roughly quarter of the sphere with its directive beam. Note that the isotropic value for MEG is with low probability in all cases. This means that for most of the possible orientations the antenna will receive power rather different from the average isotropic one. The similar trends are observed for all other RF states. The argument for the average isotropic environment approximating the directive one could only have been true if and only if the PDFs in Figs. 8 to 10 were Gaussian around the isotropic value. While it is possible this could be the case for some antennas it by no mean certainty as demonstrated here. Note also that branch power ratio and correlation are also functions of the incoming environment power and depend heavily on orientation. For the given realistic environments, the RF1-4 states, the correlation and BPR to the main antenna vary between 0 to 0.45 and 0 to 12 dB respectively.

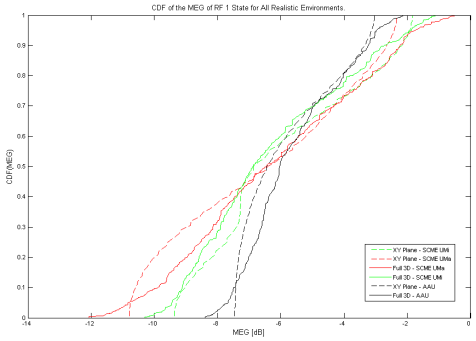

Fig. 7. MEG for RF1 State in the Various Realistic Environments .

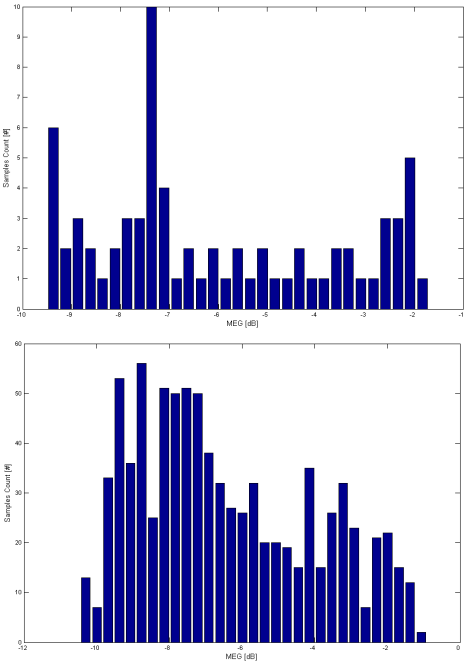

Fig. 8. PDF Statistics for the SCME UMi environment in the XY plane (top) and the Full 3D (Bottom) cases.

The considerations above are of paramount importance for the MIMO channel capacity and ultimately throughput because of the logarithmic nature of the two. Consider this very simple example with the capacity curve as a function of received SNR as shown in Fig. 11. Note that because of the logarithmic nature of the dependency a 5 dB loss or gain of SNR does not result in an equal loss or gain of capacity. Add to that non-linear dependency, the fact that BRP and correlation also change between the two states and it becomes clear that averaging the environment before the actual capacity/throughput is calculated is mathematically inconsistent. Much for the same reasons we convert the low, mid and high channel TRP values to linear scale before averaging out the TRP for a certain band. This procedure is however not straight forward for throughput, therefore the best solution is to present a realistic channel model to the DUT.

IV. Measurement Results

A. Antenna FoM measurement results

The Table III summarizes the antenna FoM measurement results, antenna 1 called secondary is the one being adapted, and antenna 2 is the main antenna.

As indicated in Table III, the antenna system has a polarization ratio near 0 dB, which is characteristic to antennas at high frequencies in small form factors. The envelope correlation is smaller than 0.1 guaranteeing uncorrelated antennas; at least at uniform incoming power; however the branch imbalance is

TABLE II
SIMULATED MEG IN [DB] OF RF1 STATE STATISTICS FOR ALL REALISTIC ENVIRONMENTS.

MEG [dB]	XY Plane - SCME UMi	XY Plane – SCME UMa	Full 3D – SCME UMa	Full 3D – SCME UMi	XY Plane – AAU	Full 3D - AAU
Mean	-5.94	-6.53	-6.23	-6.29	-5.84	-5.63
10%	-9.05	-10.62	-9.88	-9.13	-7.43	-7.50
50%	-6.86	-6.42	-6.48	-6.87	-6.45	-6.04
90%	-2.14	-2.64	-2.21	-2.73	-3.31	-3.22

TABLE III
MIMO B7 ANTENNAS FOM BASED ON 3D ISOTROPIC MEASUREMENTS @ 2655MHZ.

MIMO B7 antennas FoM based on 3D isotropic measurments @ 2655MHz					
switch state	ant. position	Total Efficiency (%)	Polarization Ratio V/H (dB)	Branch imbalance (dB)	ρe
00	Antenna 1 (secondary)	41.10	0.00	3.016	0.0014
	Antenna 2 (Main)	82.30	0.70		
01	Antenna 1 (secondary)	35.10	0.30	3.717	0.0124
	Antenna 2 (Main)	82.60	0.80		
11	Antenna 1 (secondary)	35.80	0.50	3.551	0.0186
	Antenna 2 (Main)	81.10	0.70		
10	Antenna 1 (secondary)	43.40	0.60	2.774	0.0125
	Antenna 2 (Main)	82.20	0.80		

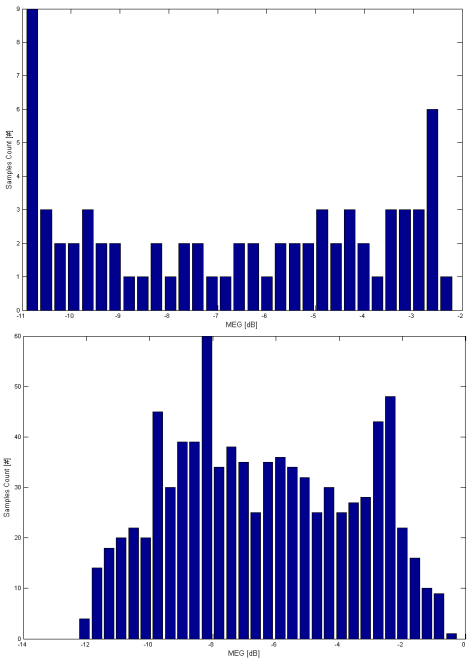

Fig. 9. PDF Statistics for the SCME UMa environment in the XY plane (top) and the Full 3D (Bottom) cases.

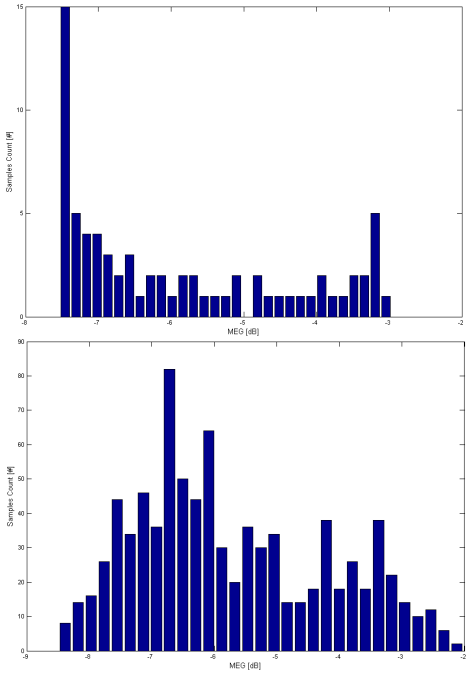

Fig. 10. PDF Statistics for the AAU environment in the XY plane (top) and the Full 3D (Bottom) cases.

near 3 dB. The following Fig. 12 shows the main antenna's radiation patterns in 3D and polar format and return loss, which is identical in all switch states. The shows the secondary antenna performance in different switch states. As indicated in Table III, the main antenna maintains the same total efficiency and radiation patterns across all four switch states. The difference in performance ¡ 0.1 dB, is within the anechoic chamber measurement uncertainty.

B. MIMO OTA absolute data throughput measurement results

The OTA measurement results are based in two test methodologies considered valid, the anechoic chamber multi-cluster

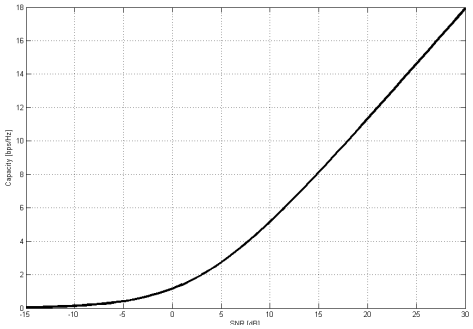

Fig. 11. Channel capacity as a function SNR not a linear function!

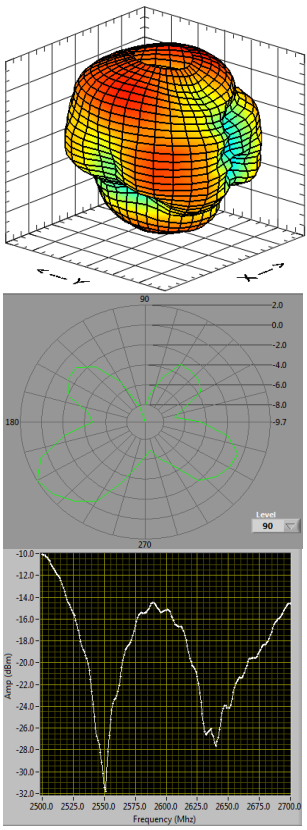

Fig. 12. Main antenna 3D, 90 degre elevation free space antenna radiation pattern and respective return loss

boundary array, and the reverberation chamber without channel emulation assistance. As indicated in the Table III, there is a branch imbalance between antennas averaging 3.3 dB, during these measurements a 3 dB series attenuator was placed between the main antenna and the DUT RF port, thus partially equalizing both antennas gain. Ideally for each tuner position a specific attenuation value should be used to equalize all antennas by the least efficient, i.e. tuner position 01 secondary antenna. However attenuators in sub-multiple values of 1 dB that could be accommodated inside the RF enclosure were not readily available. For this experiment due the lack of precise equalization of total efficiency and branch imbalance, a variation of approximately 1 dB is shown within all four switching stages. The absolute data throughput was gathered in two fundamentally different MIMO OTA test methodologies:

1) Anechoic chamber setup: The OTA test system consisted of an ETS-Lindgren AMS-8700 boundary array with eight active dual polarized antennas at a radius of 1.95 meters driven by two Spirent VR5 8 output channel emulators for 16 total output channels used to generate the applied channel model and resulting signal levels within the test volume. Two ETS-Lindgren 8-channel power amplifiers were used to amplify the outputs of the channel emulators to produce the required signal levels within the test volume. The reported measurements were captured using a Rohde & Schwarz CMW-500 as the eNodeB emulator/communication tester. The two outputs were each split and fed into the two VR5s. A separate circularly polarized conical log spiral antenna was used to provide the uplinik from the DUT. The uplink path was then fed through a pre-amplifier to provide additional downlink isolation prior to feeding the signal to the eNodeB input.

2) Reverberation chamber setup: An ETS-Lindgren AMS-7000 wireless OTA reverb test system was used to perform the average isotropic (uniform probability distribution) testing. The system consists of a compact reverberation chamber (2.00 x 1.20 x 1.50 m) with two independent stirring paddles and a DUT turntable having a lowest operating frequency of 700 MHz, connected to a Rohde & Schwarz CMW-500 as the eNodeB emulator/communication tester. The cell was selectively loaded to produce an RMS delay spread of 80 ns for the NIST model. Tests were performed using continuous stirring of all positioners for an integral number of rotations of all positioners at a fixed ratio and timed such that one long throughput measurement was performed per revolution of the slowest positioner, thus producing one average throughput measurement per power level.

The measurements on Fig. 14 shows the absolute data throughput results with the DUT at each switch state. The measurement shown in 4.4.1-6 is a compilation of the previous measurements indicating the DUT performance as the AAS was implemented, where compares the average throughput for each of the individual switch states to the average throughput determine by choosing the optimum switch state for each test position, thus replicating the effect of an intelligent algorithm adapting the antenna to the current orientation in the environment.

V. Conclusions

In the paper we present a simple AAS design capable of exploiting the directive nature of the real propagation channel modelled via the two variants of the SCME model and the AAU model. We show that:

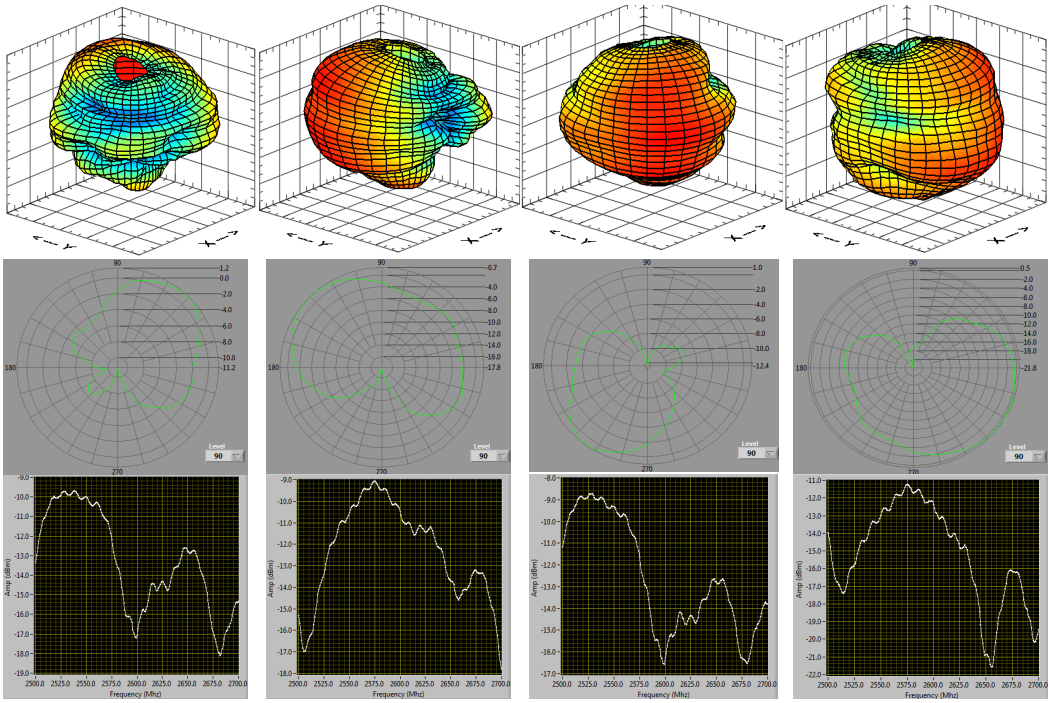

Fig. 13. Secondary antenna 3D, 90 degre elevation free space antenna radiation patterns and respective return loss, from left switch state 00, 01, 11 and 10

- 2D environments behave statistically the same as 3D environments as long as both are directive of course. The more directive an environment is the more selective is will be in the spatial domain.
- The simulation rsults of single or multiple 2D plane cuts in the SCME models result in very similar statistics see Fig. 5 and Table II but not the average isotropic values. There is no reason to expect that measuring DUTs in multiple 2D cuts in an anechoic chamber would result in different statistics. Moreover not all orientations are equally probable.
- Once again, note that because of the logarithmic nature of the dependency a 5 dB loss or gain of SNR does not result in an equal loss or gain of capacity. Add to that non-linear dependency, the fact that BRP and correlation also change between the two states and it becomes clear that averaging the environment before the actual capacity/throughput is calculated is mathematically inconsistent.
- The AAS antenna prototype radiation pattern measurements agree with design proposal and simulation results;
- The variation in absolute data throughput performance in each switch state, doesnt agree between AC and RC, while the AC test methodology has the switch state 10 as the best performer; which agrees with results shown in table Table III, the RC method has the same switch state as the worse performance, once again contradicting the concept of ranking between test methodologies;
- The simplified but realistic AAS demonstrated that while being measured in a channel model with spatial characteristics, there's an improvement in throughput vs. Sensitivity of approximately 2 dB @ 70% data throughput;
- Theres no known method to provide such AAS performance evaluation in RC, due to:
  - Lack of spatial information in the channel model;
  - Uncertainty of AoA; or multiple AoAs; for each isotropic state;
  - Uncertainty of magnitude and direction of multiple AoA in the same isotropic state;
  - Lack of realistic transition on AoA between consecutive isotropic states;
  - Dependency of RC unique features, such as:
    - Synchronism between stirrer(s) and turn table positions;
    - Relative position and shape of stirrer(s), antennas and turn table;
    - RC size;
    - Loading.

In this contribution, an active pattern antenna designed for MIMO applications has been presented. There is a good agreement between the measured results and the simulated results. Although the size of the prototype is large in order accommodate the external modem, the feasibility of having

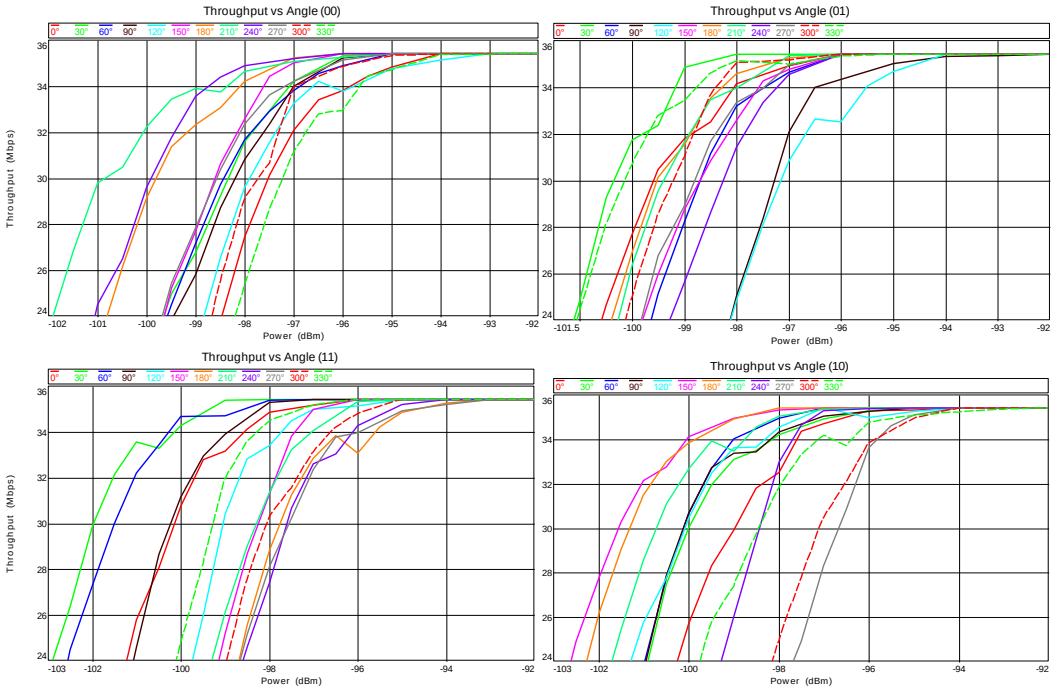

Fig. 14. Absolute data throughput, 12 DUT rotations individual curves, and average of 12 individual curves. SCME Umi, 30kph, XPR=9dB, from top left switch state 00, 01, 11 and 10

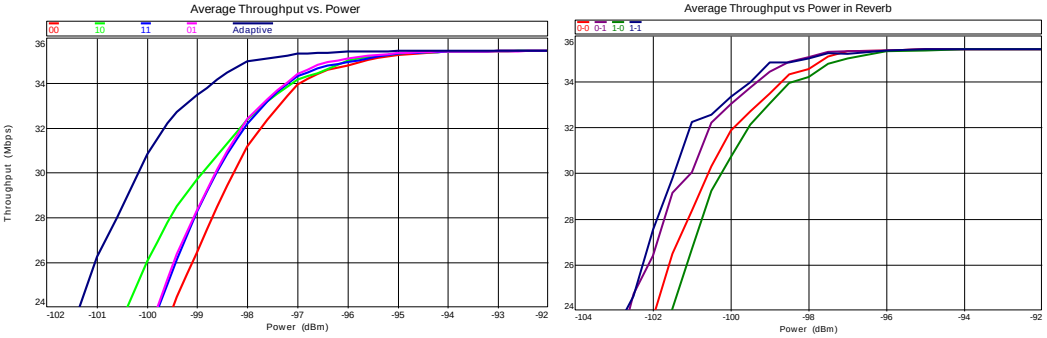

Fig. 15. Left, absolute data throughput, optimal selection of 12 DUT rotations individual curves, and average of 12 optimal individual curves. SCME Umi, 30 kph, XPR=9 dB, AAS virtually implemented (dark blue). Right, absolute data throughput, NIST (80 s RMS Delay Spread) Isotropic channel model, switch state 00 (red curve), 01 (purple), 11 (blue), 10 (green).

pattern reconfigurability in mobile phones is demonstrated.

REFERENCES

[1] R. Vaughan and J. Andersen, "Antenna diversity in mobile communications," *Vehicular Technology, IEEE Transactions on*, vol. 36, no. 4, pp. 149 – 172, nov. 1987.

[2] G. J. Foschini and M. J. Gans, "On limits of wireless communications in a fading environment when using multiple antennas," *Wireless Personal Communications*, vol. 6, pp. 311–335, 1998.

[3] H. Holma, A. Toskala, K. Ranta-aho, and J. Pirskanen, "High-speed packet access evolution in 3gpp release 7 [topics in radio communications]," *Communications Magazine, IEEE*, vol. 45, no. 12, pp. 29–35, 2007.

[4] A. Tulino, A. Lozano, and S. Verdu, "Impact of antenna correlation on the capacity of multiantenna channels," *Information Theory, IEEE Transactions on*, vol. 51, no. 7, pp. 2491–2509, 2005.

[5] A. Molisch, M. Steinbauer, M. Toeltsch, E. Bonek, and R. Thoma, "Capacity of mimo systems based on measured wireless channels," *Selected Areas in Communications, IEEE Journal on*, vol. 20, no. 3, pp. 561–569, 2002.

[6] K. Long and W.-L. Wu, "An enhanced multi-antenna solution through beamforming to 3g long-term evolution," in *Networks Security, Wireless Communications and Trusted Computing, 2009. NSWCTC '09. International Conference on*, vol. 1, 2009, pp. 112–115.

[7] M. Chryssomallis, "Smart antennas," *Antennas and Propagation Magazine, IEEE*, vol. 42, no. 3, pp. 129–136, 2000.

[8] J. Poutanen, J. Salmi, K. Haneda, V. Kolmonen, and P. Vainikainen, "Angular and shadowing characteristics of dense multipath components in indoor radio channels," *Antennas and Propagation, IEEE Transactions on*, vol. 59, no. 1, pp. 245–253, 2011.

[9] H. El-Sallabi, L. Vuoko, and P. Vainikainen, "Characterization of dissimilarity between multipath components at mobile station in microcellular environment," in *Wireless Communications and Networking Conference, 2004. WCNC. 2004 IEEE*, vol. 2, 2004, pp. 1133–1137 Vol.2.

[10] M. Knudsen and G. Pedersen, "Spherical outdoor to indoor power spectrum model at the mobile terminal," *Selected Areas in Communications, IEEE Journal on*, vol. 20, no. 6, pp. 1156 – 1169, Aug. 2002.

[11] L. Mucchi, C. Staderini, J. Ylitalo, and P. Kyöst, "Modified spatial channel model for mimo wireless systems," *EURASIP J. Wirel. Commun. Netw.*, vol. 2007, pp. 8:1–8:7, Oct. 2007. [Online]. Available: http://dx.doi.org/10.1155/2007/68512

[12] T. Rappaport, S. Sun, R. Mayzus, H. Zhao, Y. Azar, K. Wang, G. Wong, J. Schulz, M. Samimi, and F. Gutierrez, "Millimeter wave mobile communications for 5g cellular: It will work!" *Access, IEEE*, vol. 1, pp. 335–349, 2013.

[13] I. Szini, G. Pedersen, J. Estrada, A. Scannavini, and L. Foged, *Design and Verification of MIMO 2x2 Reference Antennas*, ser. I E E E Antennas and Propagation Society. International Symposium. IEEE, 2012, pp. 1–2.

[14] 3GPP, "LTE; 3gpp tr 25.996: 3rd generation partnership project; technical specification group radio access network; spatial channel model for multiple input multiple output (mimo) simulations (release 11)," 3GPP, Tech. Rep. 3GPP TS 25.996 Release 11, 2012.

[15] B. Yanakiev, J. Nielsen, M. Christensen, and G. Pedersen, "Antennas in real environments," in *Antennas and Propagation (EUCAP), Proceedings of the 5th European Conference on*, 2011, pp. 2766–2770.

[16] T. Taga, "Analysis for mean effective gain of mobile antennas in land mobile radio environments," *Vehicular Technology, IEEE Transactions on*, vol. 39, no. 2, pp. 117 –131, May 1990.